Mesangial Cell Apoptosis and Phagocytosis: The Role of Glucose and Transforming Growth Factor β-1

Tarnjit Kaur Khera

Thesis presented for the degree of

Philosophiae Doctor

May 2006

Institute of Nephrology

Cardiff University

Heath Hospital Campus,

Cardiff

CF14 4XN

UMI Number: U584041

All rights reserved

INFORMATION TO ALL USERS
The quality of this reproduction is dependent upon the quality of the copy submitted.

In the unlikely event that the author did not send a complete manuscript
and there are missing pages, these will be noted. Also, if material had to be removed,
a note will indicate the deletion.

UMI U584041
Published by ProQuest LLC 2013. Copyright in the Dissertation held by the Author.
Microform Edition © ProQuest LLC.
All rights reserved. This work is protected against
unauthorized copying under Title 17, United States Code.

ProQuest LLC
789 East Eisenhower Parkway
P.O. Box 1346
Ann Arbor, MI 48106-1346

Dedication

For Mum and Dad

Acknowledgements

I would like to thank the School of Medicine, Division of Hospital-Based Specialities, for funding this project.

I am indebted to my supervisor, Professor Aled Phillips, for his invaluable support and guidance throughout the course of my PhD and for reading drafts of this thesis. I would like to thank Professor John Williams, Professor Nicholas Topley, Dr Robert Steadman (who read the final draft of this thesis) and Dr Timothy Bowen for their help and advice in lab meetings. Last, but not least, sincere thanks to my friends and colleagues in The Institute of Nephrology, especially Dr John Martin for his advice and expert assistance through the past three years.

Publications and presentations arising from this thesis:

Publications:

'Glucose enhances mesangial cell apoptosis'. Tarnjit Khera, Stephen Riley, Robert Steadman & Aled Phillips. Lab Investigation (2006), in press.

'The role of endogenous TGF-ß1 in the binding and ingestions of apoptotic cells by mesangial cell'. Tarnjit Khera, Stephen Riley, Robert Steadman & Aled Phillips. In preparation, submitted to American Journal of Pathology.

Presentations

'Mesangial Cell Apoptosis and Phagocytosis: The role of Glucose'. Tarnjit Khera and Aled Phillips. Postgraduate Research Day, University of Cardiff College of Medicine, Nov 2003. Poster presentation

'Glucose Induced Mesangial Cell Apoptosis: Involvement of NFκB and TGFβ'. Tarnjit Khera and Aled Phillips. American Society of Nephrology, St. Louis, USA, Oct 2004. Poster presentation.

'Glucose Induced Mesangial Cell Apoptosis: Involvement of NFκB and TGFβ'. Tarnjit Khera. Postgraduate Research Day, University of Cardiff College of Medicine, Nov 2004. Oral presentation

Contents

Abbreviations

AER	Albumin Excretion Rate
AGE	Advanced Glycation End Products
APS	Ammonium Persulphate
BH	Bcl-2 homology
BMP-7	Bone morphogenic protein 7
BSA	Bovine Serum Albumin
cDNA	complementary DNA
CFSE	5-, 6- carboxyfluorescein diacetate succinimidylester
CM	Conditioned media
DAG	Diacylglycerol
DM	Diabetes Mellitus
DN	Diabetic Nephropathy
DNA	Dioxyribonucleic Acid
dNTP	deoxynucleotide triphosphate
DTT	Dithiothreitol
dTTP	deoxythymidine triphosphate
ECL	enhanced chemiluminescence
ECM	Extracellular matrix
ELISA	Enzyme linked immunosorbent assay
ERK	Extracellular signal-regulated kinases
ESRD	End stage renal disease
EMSA	Electophoretic mobility shift assay
FACS	Fluorescence Activated Cell Sorting
FADD	Fas-associated death domain protein
FCS	Foetal Calf Serum
FITC	Fluorescein Isothiocyanate
GAPDH	Glyceraldehyde-3-phosphate dehydrogenase
GBM	Glomerular basement membrane
GFAT	Glutamine: Fructose-6-phosphate amino-transferase
GFR	Glomerular filtration rate
HG	high glucose, 25mM
HRP	Horseradish Peroxidase
IAP	Inhibitor of Apoptosis Protein

IL	Interleukin
KDa	Kilo Daltons
LAP	Latency associated peptide
LTBP	latent TGFβ binding protein
MAPK	Mitogen activated protein kinase
MEKK	MAPK kinase kinase 1
Min	minutes
MPO	Myeloperoxidase
mRNA	messenger RNA
NFκB	Nuclear Factor κB
NG	normal glucose, 5mM
PBS	Phosphate buffered saline
PI	Propidium Iodide
PKC	Protein Kinase C
PMN	polymorphonuclear cells
PMSF	Phenylmethysulfonylfluoride
PS	Phosphatidylserine
PSR	Phosphatidylserine receptor
RGDS	Arg-Gly-Asp-Ser peptide
RGES	Arg-Gly-Glu-Ser peptide
RNA	Ribonucleic acid
ROS	Reactive oxygen species
RPM	Revolutions per minute
RT	Room temperature
RT-PCR	Reverse transcriptase-polymerase chain reaction
SDS	Sodium Dodecyl Sulphate
SDS-PAGE	Sodium Dodecyl Sulphate Polyacrylamide gels
S.E.	Standard Error
TGFβ	Transforming growth factor beta
TGFβRII	TGFβ receptor II
TNF	Tumour Necrosis Factor
TSP-1	Thrombospondin-1
UV	ultraviolet

CHAPTER 1: INTRODUCTION

1.1: DIABETIC NEPHROPATHY

1.1.1: Kidney structure and function

The kidneys are situated at the back of the abdominal cavity. Each kidney consists of an outer cortex and an inner medulla with conical renal pyramids. The arteries that supply the kidneys arise directly from the aorta. Within the kidneys, they branch off into the afferent arterioles in the renal cortex and deliver blood to the glomeruli. The glomeruli drain into the efferent arterioles and eventually back to the renal vein. The glomeruli, bowman's capsules and tubules make up the nephrons, the functioning units of the kidney (figure 1.1). Each kidney contains approximately one million nephrons, which drain the filtrate into the renal collecting ducts draining into the renal pelvis and ureter [1].

The kidneys have several functions, the key ones being the regulation of the amount of water in the body, the regulation of electrolytes in the blood and the elimination of waste products, the most important being those generated by the breakdown of proteins. They also control the body's acid-base balance, activate vitamin D, which is involved in bone homeostatis, and produce several hormones such as erythropoietin and angiotensin. Erythropoietin stimulates red blood cell production in the bone marrow. The kidneys help to regulate blood pressure and blood volume through the renin-angiotensin system [1].

Figure 1.1: A schematic structure of a nephron

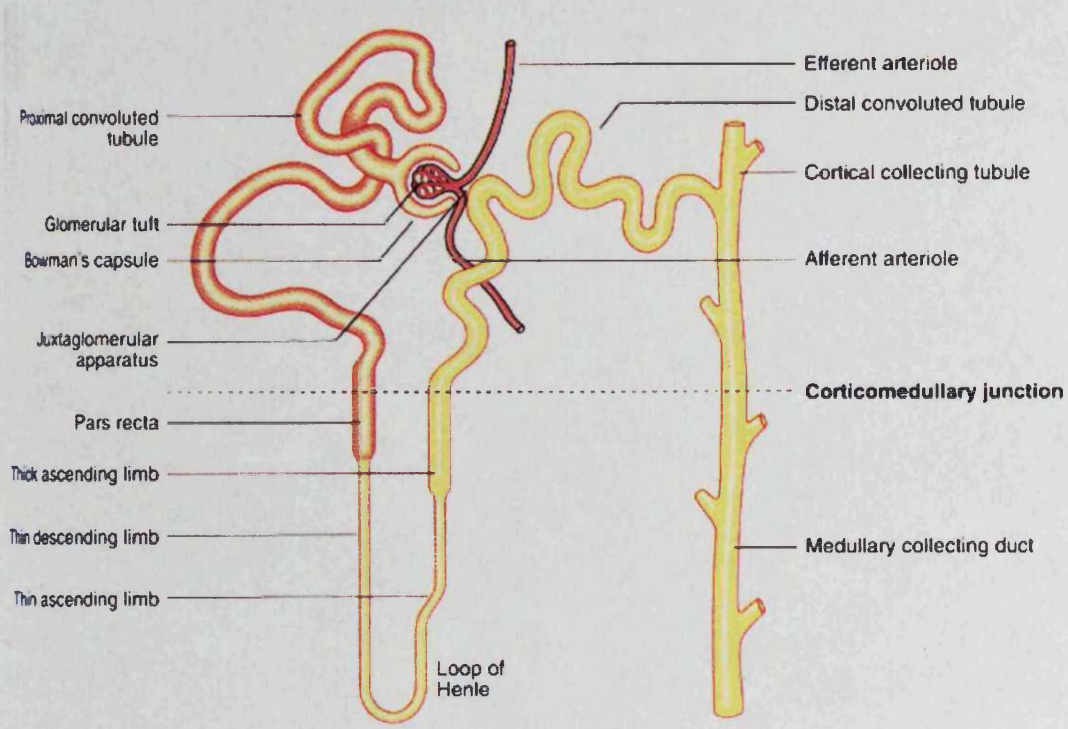

The afferent arteriole gives rise to the glomerular capillaries. They leave the glomerulus at the efferent arteriole. From the glomerulus, the proximal convoluted tube descends into the medulla where it becomes the loop of Henle with a thin descending limb and a thick ascending limb. The nephron progresses on to the distal convoluted tubule and then to the collecting tubule. This diagram was adapted from [1].

Glomerulus - structure and function

The glomerulus is responsible for ultrafiltration, a process which converts about one third of all plasma flowing through it into an almost protein-free filtrate [2]. It consists of a tuft of specialised capillaries attached to the mesangium, both of which are enclosed in the Bowman's capsule. The capillaries are supplied by an afferent arteriole and drained by an efferent arteriole. Four cell types occur within the glomerular tuft – parietal epithelial, podocyte (visceral epithelial), endothelial, and mesangial cells - and each have unique biological functions (figure 1.2).

The entire tuft of capillaries is covered by epithelial cells (podocytes), representing the visceral layer of Bowman's capsule. At the place where the afferent arteriole enters and the efferent arteriole leaves the capillary tuft, the visceral layer of Bowman's capsule becomes the parietal layer, which is a simple squamous epithelium [3].

The glomerular basement membrane (GBM) lies at the interface between the glomerular capillaries and podocyte layer of the Bowman's capsule. GBM serves as a skeleton of the glomerular tuft by supporting the capillaries and providing anchoring for the cells [3]. Its major components include type IV collagen, heparin sulphate proteoglycans and laminin. The endothelial cells, the basement membrane and the podocytes form the filtration barrier [2, 4]. The endothelial cells serve as the inner lining of the glomerular capillaries. They are fenestrated, exposing the basement membrane directly to the glomerular capillary contents [2, 4].

Figure 1.2: glomerulus structure

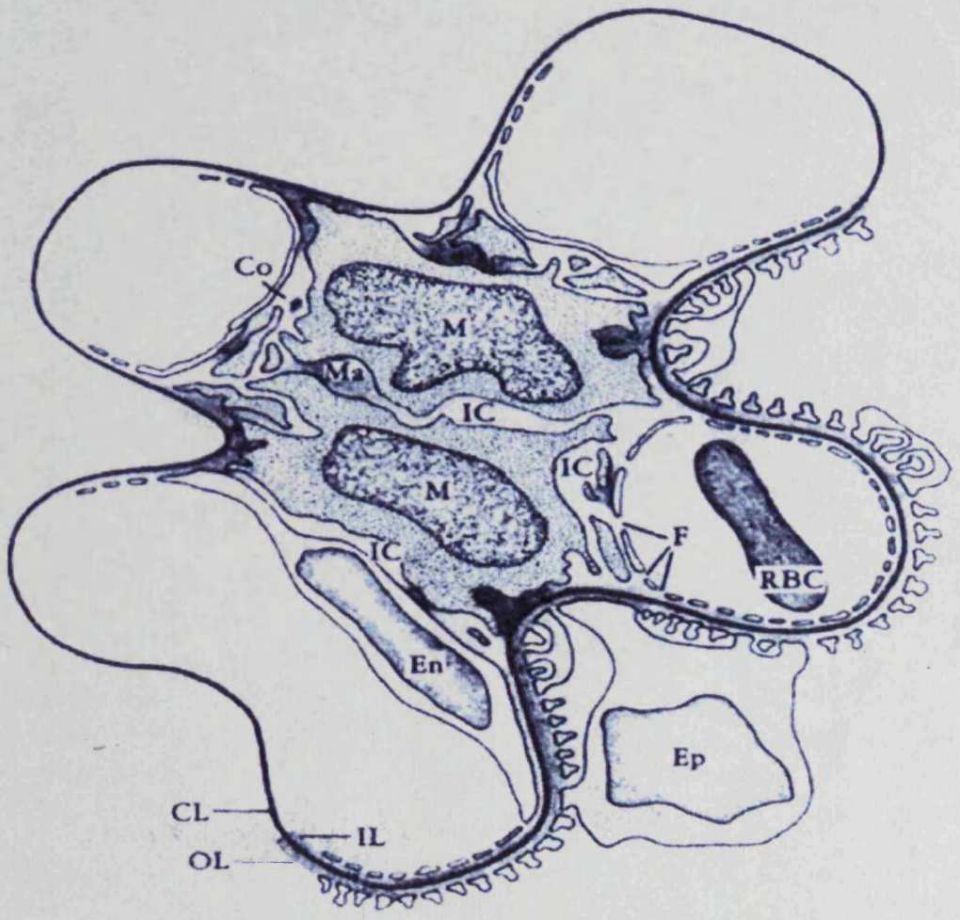

A diagram of a mesangial region surrounded by capillaries. Mesangial cells (M) are surrounded by extracellular matrix (Ma), containing intercellular channels (IC). The capillary tuft consists of a network of specialised capillaries, which are outlined by a fenestrated (F) endothelium (En). The capillary endothelium is made up of flat endothelial cells. OL, CL, and IL, outer, central and inner layers of glomerular basement membrane; Ep, epithelial cell body; RBC, red blood cell. Adapted from [5].

Podocytes

The visceral epithelial layer of the Bowman's capsule consists of highly differentiated cells, the podocytes. They play a key role in maintaining the integrity of the glomerular filtration barrier. Podocytes have a voluminous cell body that floats within the urinary space. The cell body gives rise to long primary processes that extend towards the capillaries, called foot processes. The foot processes of neighbouring podocytes regularly interdigitate with each other, leaving between them meandering slits that are bridged by an extracellular structure containing glycocalix components, fibronectin, laminin and entactin [2, 3, 6].

Mesangial cells

The mesangial cells and the mesangial matrix make up the glomerular mesangium. Mesangial cells are contractile mesenchymal cells with a high metabolic capacity, receptors for various ligands and the ability to synthesise and secrete a wide variety of cytokines and ECM molecules [5]. They are irregular in shape, with many processes extending from the cell body towards the GBM. In these processes, dense assemblies of microfilaments are found that contain actin, myosin and α-actinin. They also have many gap junctions, suggesting that they have a common origin with smooth muscle cells and resemble pericytes [3]. Mesangial cells play a crucial role in maintaining the structure and function of glomerular tufts, providing structural support for capillary loops and modulating glomerular filtration by their smooth muscle activity [7, 8].

There is evidence for a filtering function of the mesangium as well as intracellular uptake of macromolecules [9]. Mesangial cells are also phagocytic, containing some lysosomal elements and have been shown to take up particulate

tracers, e.g. ferritin and serum-coated colloidal glod particles, as well as immune complexes which may accumulate within the mesangial region [3, 9].

The mesangial matrix fills the spaces between the mesangial cells and the GBM, anchoring the mesangial cells to the GBM. Mesangial matrix is one of the two extracellular matrices in the glomerulus, the other being GBM. The mesangial matrix consists mostly of glycoproteins embedded in a hydrated, polysaccharide gel of glycosaminoglycans (proteoglycans) arranged in a lattice. This matrix extends throughout the mesangium, filling the extracellular space between adjacent mesangial cells, between endothelial and mesangial cells and between mesangial cells and the GBM [9]. The mesangial matrix provides strong, flexible support for the glomerular capillaries and creates channels for filtering and processing macromolecules [9]. The elongated cytoplasmic extensions of the mesangial cells are tightly enveloped by and connected to the mesangial matrix [9]. The mesangial matrix proteins include several types of collagens (IV, V and VI), several components of microfibrillar proteins, several glycoproteins and several types of proteoglycans [6].

1.1.2: Diabetes mellitus

Diabetes mellitus is a metabolic disorder of multiple aetiology that leads to chronic hyperglycaemia. It is associated with disturbances of carbohydrate, fat and protein metabolism resulting from defects in insulin secretion, insulin action or both [10]. It is characterised by excessive amounts of sugar in the blood and urine and inadequate production or resistance of insulin, which is responsible for the absorption of glucose into cells for their energy needs and into the liver and fat cells for storage [1].

Type I and II diabetes mellitus

Diabetes has been classified into two types, termed type I and II. Type I diabetes is an autoimmune condition that primarily causes pancreatic islet beta-cell destruction, resulting in insulin deficiency. Onset of disease is abrupt and it generally occurs in children and young adults. Type II diabetes, by comparison, is a syndrome which includes defects in insulin secretion and a variable amount of insulin resistance [11]. It usually develops gradually in adults over 40 years who are overweight and have a family history of the disease.

The past two decades have seen an increase in the number of people diagnosed with diabetes worldwide. This trend of increasing prevalence of diabetes and obesity has already imposed a huge burden on healthcare systems and this will continue to increase in the future [12-15]. Diabetic mellitus is now the most common cause of end-stage renal disease (ESRD) and diabetic nephropathy represents 18% of subjects with end-stage renal disease in the UK, with type 2 diabetes accounting for the majority of cases [12, 16]. Type II diabetes in children, teenagers and adolescents is a serious new aspect to the epidemic and an emerging public health problem [17-19]. Large proportions of patients with diabetes develop complications that result in significant morbidity and mortality.

1.1.3: Clinical diabetic nephropathy

Diabetic nephropathy is a clinical syndrome characterised by persistent albuminuria, a decline in GFR and elevated arterial blood pressure. It is a naturally progressive disease. The natural history of renal dysfunction in type I and type II diabetes is similar [20].

Early diabetes is heralded by glomerular hyperfiltraion with an absence of albuminuria and normal blood pressure. This increase in GFR is paralleled by an increase in kidney size. There is then a period of clinical 'silence' where glomerular filtration remains at the upper limit of normal and where there is normal urinary protein excretion.

The first manifestation of nephropathy is the development of microalbuminuria (albuminuria of 30-300 mg/day), indicating that glomerular damage has progressed. This occurs between 5 and 15 years after the diagnosis of diabetes and is termed incipient nephropathy; during this stage, the GFR in usually within the normal range. Generally as glomerular damage progresses, overt nephropathy develops 10 to 15 years later. During overt nephropathy, clinical albuminuria and hypertension usually develop, with a steady fall in GFR.

End stage renal failure (ESRF) is secondary to DN, occurring approximately five years after the onset of overt nephropathy. Once this develops patients need to be considered for renal replacement therapy in the form of haemodialysis, peritoneal dialysis and kidney transplantation [6, 21, 22]. DN in patients increases early mortality from cardiovascular disease approximately nine-fold [3].

The development of overt nephropathy is not linearly related to the duration of diabetes and affects only 35-50% of patients, depending on the type of diabetes. Microalbuminuria is associated with a 42% increased risk of progression to overt nephropathy [23]. Some patients with incipient nephropathy regress to normoalbuminuria [24]. The majority of diabetic patients do not develop renal failure. Although some damage does occur to their kidneys, renal function remains essentially normal until death [3].

Structural-functional relationships in diabetic nephropathy

The pathological changes seen within the kidney are similar in both type I and type II diabetes [25]. Accurate morphometric techniques have made it possible to quantify the structural changes within the diabetic kidney and to correlate these changes with renal function. The majority of data has been obtained in type I diabetic disease but some studies are available to make comparisons with type II diabetic patients [26].

Renal structural abnormalities are known to precede the development of protienuria, hypertension and reduced renal function in patients with diabetes [27]. The early stages of DN are characterised by thickening of the GBM, glomerular hypertrophy and hyperfiltration. Mesangial expansion strongly correlates to the clinical manifestations of DN such as podocyte loss and subsequent development of albuminuria [28]. Creatinine clearance correlates with both mesangial expansion and interstitial expansion, whereas proteinuria correlated only with glomerular structural changes (mesangial expansion and GBM thickening) [25]. Glomerular structural lesions and arteriolar and tubular interstitial lesion may constitute the principal cause of decline in kidney function, although continuing mesangial expansion is the main variable [20, 29, 30]. Mesangial expansion could lead to glomerular functional deterioration by restricting glomerular capillary vasculature and its filtering surface [31].

Incipient nephropathy

Incipient nephropathy develops 2-10 years after the initial changes, notably persistent renal hypertrophy. With the development of incipient nephropathy, particular structural changes are seen. The first major structural change after the onset

of type I diabetes is enlargement of the whole kidney [29]. In type I disease there seems to be an additional increase in GBM thickening as well as some evidence of preliminary mesangial expansion, with little or no glomerular enlargement [27]. The situation is less clear in type II diabetes.

Overt nephropathy

In type II diabetes, although there is no change with microalbuminuria, there is a progressive increase in GBM thickness and glomerular volume as overt nephropathy develops [32]. It is evident from the work by Mauer et al that all patients with overt DN have a marked increase in the quantity of the mesangium in the glomerulus with the mesangial volume fraction being greater than 30%. Mesangial volume fraction is a measure of the percentage of the glomerulus occupied by the mesangium (matrix and cells). In healthy subjects, the mesangium occupies around 15% of the volume of the glomerulus [30].

Pima Indians are Native American Indians with a high susceptibility to diabetes. They have therefore been used in many diabetes studies. A study in the Pima Indians demonstrated an increase in the mesangial volume fraction to 45% in subjects with impaired renal function. In addition there was a strong inverse correlation between mesangial expansion and creatinine clearance [31]. Consequently, it would seem that expansion of the mesangium out of proportion of glomerular size or volume is far more critical to the development of clinical DN than is the absolute volume of mesangium per glomerulus. With sufficient expansion, the mesangium will eventually compromise filtration surface and reduce GFR [29].

In overt nephropathy, expansion of the mesangial matrix, mesangial cell loss and glomerular sclerosis are prominent, associated with proteinuria, hypertension and

renal dysfunction [29, 33]. Increasing mesangial cell number has been documented in the incipient phase of nephropathy, with a direct correlation between mesangial cell number and AERs [34]. Mesangial cell number increases during the earlier stages of DN corresponding to an increase in glomerular volume [34, 35]. This relationship between mesangial cell number is however lost in patients with overt nephropathy and proteinuria. More recently it has been demonstrated that loss of mesangial cell through apoptosis occurs in experimental diabetic nephropathy and mesangial cell apoptosis has been demonstrated to correlate with worsening of albuminuria [36, 37]. Clinical studies in patients with type II DN report a loss of glomerular mesangial cells and podocytes that correlates with progression to diabetic glomerulosclerosis [32, 38]. Depletion of mesangial cells has been noted in segments of the glomerular tuft where expansion of the mesangial matrix has occurred [22, 39, 40]. In one study, loss of mesangial cells even correlated with significant structural changes [41].

Podocytes injury occurs after changes in mesangial cell number. Podocyte number decreased in the diabetic patients compared with controls, leading to reduction in podocyte density, causing an increase in proteinuria [28, 42, 43]. Increase in glomerular volume may be the underlying cause of foot process widening and therefore injury may be related to mesangial expansion [43]. In diabetic patients, an increase in glomerular volume would cause the podocytes to cover a larger area leading to loss of cell integrity, leakage of the filtration barrier and ultimately podocyte loss [42, 43].

From these studies it can be seen that there is a complex inter-relationship between the disease state and structural-functional changes.

1.1.5: Risk factors associated with diabetic nephropathy

The aetiology of diabetic nephropathy (DN) is multifactorial (table 1.2) [12, 44].

Table 1.2: Risk factors for the development of DN in type I and type II patients

	Type I	*Type II*
Normoalbuminuria (above median)	+	+
Microalbuminuria	+	+
Sex	*M>F*	*M>F*
Familial clustering	+	+
Predisposition to arterial hypertension	+/-	?
Increased sodium/lithium counter transport	+/-	+/-
Onset of type II diabetes before 20 yrs	+	
Glycaemic control	+	+
Hyperfiltration	+/-	?
Prorenin	+	?
Smoking	+	?
Cholesterol	+	+
Presence of retinopathy	+	+

+, present; -, not present; ?, not enough information. Table adapted from [45].

Fixed risk factors

Genetic patterns have been established with familial occurrences of DN and associated hypertension and cardiovascular diseases in family members of patients with DN. DN does not develop in all subjects but when it does, it is often in familial clusters, suggesting a genetic basis. Type II diabetes and DN is increased in several

different populations, including African-Americans, Native Americans, Mexican-Americans, Polynesians, Australian aborigines and Indo-Asians [44].

AER in families with type II diabetes is heritable and genetically correlated to blood pressure. A study by Forsblom *et al* showed that AER is an inherited trait and clusters in families of patients with type II diabetes [46]. Predisposition to high blood pressure is also a risk factor for susceptibility to nephropathy. Fogarty *et al* showed that in families with type II diabetes, UAE is a heritable trait, with heritability similar to that for blood pressure, indicating that these traits share common genetic determinants [47].

Another study in the inheritance of DN evaluating glomerular structure in families demonstrated a strong correlation between diabetic glomerular lesions among sibling pairs with long-term type I diabetes [48]. The strongest familial impact was on mesangial fractional volume, the structural parameter most closely related with renal functional abnormalities.

Modifiable risk factors

Pronounced changes in the human environment and in human behaviour and lifestyle, have accompanied globalisation and these have resulted in escalating rates of diabetes [12]. Certain environmental factors may also be associated with an increased risk of DN, including blood pressure, glucose, obesity and smoking [6].

Increased arterial blood pressure occurs early in DN, with the diastolic BP correlating with decline in GFR in type I and type II patients [45]. The importance of glycaemic control on the progression of DN has also been documented with type I and type II patients [45]. A large subset of type I diabetic patients will escape DN complications despite poor glycaemic control, whereas in the subjects susceptible to

DN complications, glycaemia is a major factor in the rate of progression of lesions [27]. Several metabolic pathways have been shown to play a role in glucose-induced microvascular lesions and glucose induced apoptosis may also contribute to hypecellularity in the glomerulus (apoptosis section 1.3).

1.1.6: Mechanism of disease

Hyperglycaemia

There is clear evidence of a positive relationship between hyperglycaemia and susceptibility to renal disease in diabetes mellitus. Increased susceptibility to long-term diabetic complications in patients with poor glycaemic control has been demonstrated [49]. In addition, strict metabolic control in the very early stages of nephropathy may delay the development of microvascular complications of diabetes [50-53]. Although the pathogenesis of type I and type II diabetes is different, the pathophysiology of microvascular complications responsible for high morbidity and mortality rates appears similar and hyperglycaemia is at least partially responsible as the underlying cause [44, 54].

In rats, mesangial lesions and albuminuria can be prevented with glycamic control. In contrast, GBM thickening can be prevented, but not reversed, if plasma glucose levels are returned to normal [29]. Numerous *in vitro* studies have suggested that elevated concentrations of glucose modify mesangial cell function. Mesangial cells are prone to hyperglycaemia-induced cell stress and injury [44, 55]. Exposure of mesangial cells to high glucose levels also promotes transcriptional activation of type IV collagen and fibronectin genes, and increased the synthesis of their respective proteins [56-58]. There is also evidence that in addition to increased synthesis of

ECM components, glucose may also decrease degradation of matrix components which may also contribute to ECM accumulation in the diabetic state [59].

Glucose signalling in mesangial cells in diabetic nephropathy has been reviewed by Haneda et al, 2003. Glucose entering the cells is normally metabolised by the glycolytic pathway but in the presence of excessive glucose, it is metabolised by various pathways and activates various signalling pathways (figure 1.4). In mesangial cells cultured under high glucose conditions, there is an increase in the entry of glucose in the polyol pathway, the dacylglycerol synthetic pathway and the hexosamine pathway [54].

Figure 1.4: Glucose-induced signalling pathways in a mesangial cell

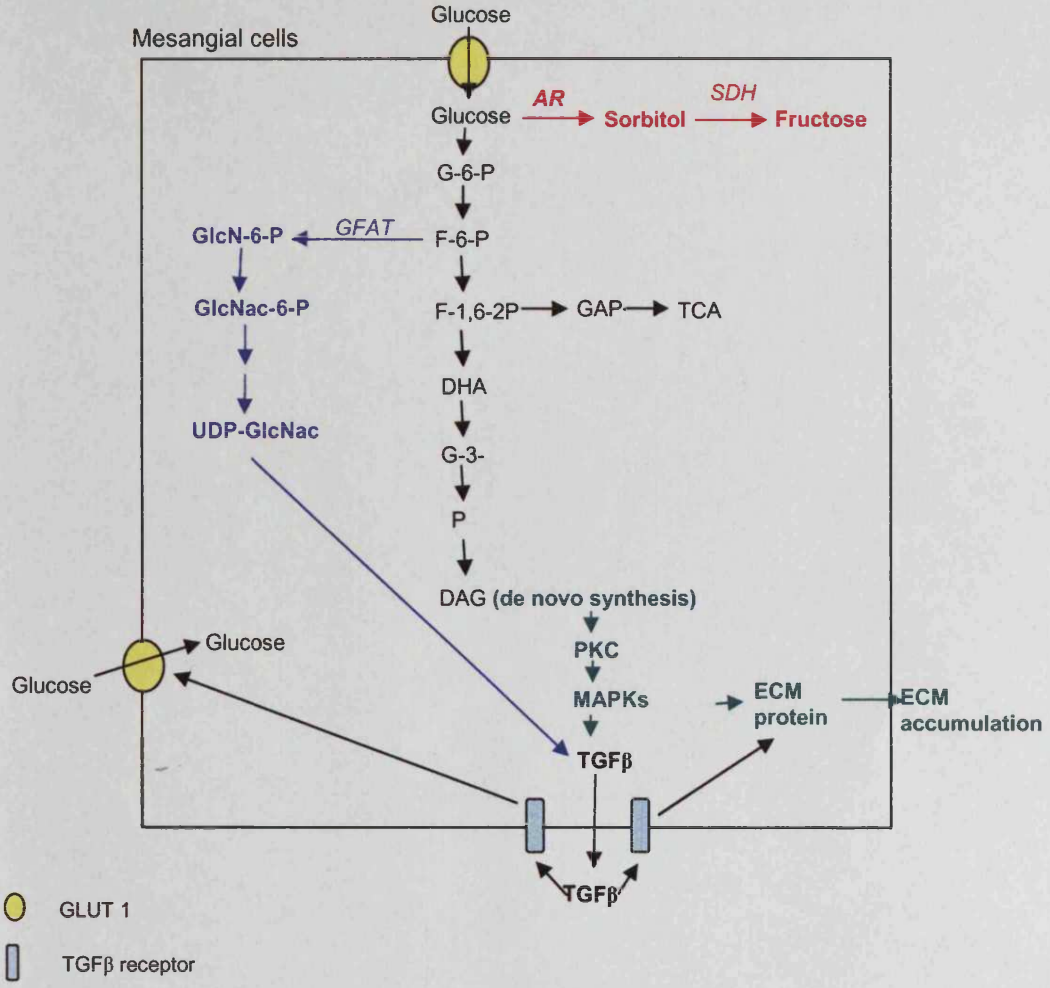

Glucose that enters the cells will be metabolised mainly by the glycolytic pathway (black), however, in the presence of excessive glucose, it is metabolised by various pathways. The polyol pathway is shown in red, the PKC pathway is green and the hexoamine pathway in blue.

G-6-P, glucose-6-phosphate; F-6-P, fructose-6-phosphate, F-1,6-2P, fructose-1, 6-biphosphate; GAP, glyceraldehydes-3-phosphate; DHAP, dihydroyacetone phosphate; G-3-P, glycerol-3-phosphate; PA, phosphatidic acid; DAG, diacylglycerol; AR, aldose reductase, SDH, sorbitol dehydrokinase; GFAT, glutamine:fructose-6-phosphate-aminotransferase; GlcN-6-P, glucosamine-6-phosphate; GlcNac, N-acetylglucosamine-6-phosphate; UDP-GlcNac, uridine-5-diphosphate-N-acetylglucosamine.

The diagram was adapted from [60].

Polyol pathway

Generation of polyols that occurs in hyperglycaemia has been suggested as a cause of some of the complications of diabetes. In tissues where glucose uptake is independent of insulin, such as the lens, retina and kidney, chronic hyperglycaemia results in increased tissue levels of glucose. The excess glucose is subsequently reduced to sorbitol by aldose reductase [6, 61]. Under normal physiological conditions, only a small amount of glucose is handled through this pathway; however, significant increases from 3-30% can be seen in the diabetic state. Aldose reductase is present in the papilla, glomerular epithelial cells, distal tubular cells and mesangial cells of the kidney [3]. Cellular accumulation of sorbitol has been documented to happen selectively in tissues predisposed to developing diabetic complications, including the kidney [62, 63]. GBM width was increased by diabetes and decreased by sorbinil (an aldose reductase inhibitor) in rats with streptozocin-induced diabetes [63].

A five-year study in dogs with an aldose reductase inhibitor prevented diabetic neuropathy, but did not prevent retinopathy or capillary basement membrane thickening in the retina, kidney and muscle [64]. A clinical trial in humans has shown a similar affect, with aldose reductase inhibition limiting progression of neuropathy [65]. Blockade of the polyol therefore appears to limit progression of diabetic neuropathy, but may not affect progression of the other complications of diabetes, including nephropathy.

PKC pathway

PKC, a family of serine-threonine kinases, has at least eleven isoforms. It is involved in various vascular functions such as vascular permeability, contractility, cell

proliferation, ECM synthesis and signal transduction for hormones and growth factors. High glucose leads to elevated DAG levels, causing activation of PKC.

Many of the adverse effects of hyperglycaemia have been attributed to PKC activation, which regulates various functions including contractility, bloodflow, cell proliferation and vascular permeability [6]. PKC activation has a role in the increase in fibronectin production seen in mesangial cells exposed to elevated glucose concentrations [66] and induces TGFβ1, fibronectin and type IV collagen upregulation in the glomeruli of diabetic rats [67]. PKC antagonism was found to benefit the db/db mouse model of DN [68]. Treatment with a PKCβ inhibitor prevented the initial increase in GFR, partially correcting albuminuria and ameliorating mesangial expansion.

Hexosamine pathway

In the hexosamine pathway, fructose-6-phosphate is diverted from glycolysis by its conversion to glucosamine-6-phosphate by the enzyme glutamine: fructose-6-phosphate aminotransferase (GFAT). In the kidneys, GFAT is expressed in tubular epithelial cells but not glomerular cells. In contrast, in patients with DN, GFAT is expressed in glomerular epithelial and mesangial cells, indicating that GFAT expression may be induced by diabetes [69]. Shunting of excess intracellular glucose into the hexosamine pathway might cause several manifestations of diabetic complications. In cultured mesangial cells, the hexosamine pathway lead to increased TGFβ1 induction and increased ECM production [70-72]. Activation of the hexosamine pathway by hyperglycaemia may alter gene expression and protein function, thus contributing to the pathogenesis of DN [61].

Inhibition of GFAT has been shown to abrogate high glucose-induced TGFβ1 overexpression and subsequent effects on mesangial cell proliferation and matrix production through decreasing glucosamine metablolites in mesangial cells [60].

Reactive oxygen species

High glucose induces intracellular ROS directly via glucose metabolism and auto-oxidation and indirectly through the formation of AGEs. ROS mimic the effects of glucose and upregulate TGFβ1, plasminogen activator inhibitor-1 and ECM proteins by glomerular mesangial cells, thus leading to mesangial expansion [73]. The different mechanisms of glucose-induced damage all lead to superoxide production by mitochondria [61]. ROS activate other signalling molecules such as PKC and MAPKs and transcription factors such as NFκB, AP-1 and SP-1 leading to transcription of genes encoding cytokines, growth factors and ECM proteins. Also, various antioxidants inhibit mesangial cell activation by high glucose and ameliorate features of DN [73].

AGEs

Chronic hyperglycaemia can lead to glycation of proteins leading to irreversible cross-linking and the formation of AGEs. AGEs have been shown to be increased in the serum of patients with DN and have been localised to glomeruli. They have been suggested to mediate a variety of cellular actions including expression of adhesion molecules involved in mononuclear cell recruitment, cell hypertrophy, ECM synthesis and inhibition of nitric oxide synthesis [61].

Diabetic patients with ESRD have markedly increased levels of AGEs in their serum compared to diabetic controls without renal involvement [61, 74].

Accumulation of AGEs is characteristic of DN, particularly in the mesangium [75]. The prevention of AGE formation as well as inhibition of AGE-induced crosslinks has been shown to prevent the occurrence of albuminuria and lessen mesangial expansion [6, 76].

TGFβ

Several manifestations of DN may be a consequence of altered production and/or response to cytokines and TGFβ is one such factor because it promotes renal cell hypertrophy and regulates production of ECM molecules. Several studies have demonstrated that TGFβ expression is elevated in the kidneys of animals with diabetes [77-81]. There is a close similarity between the actions of TGFβ and high ambient glucose on the growth and ECM metabolism of renal cells [82]. Both glucose and glucose generated AGEs stimulate production of TGFβ *in vitro* in a variety of cell types [83].

1.2: Transforming Growth Factor β

1.2.1: Introduction

TGFβ and related factors are multifunctional cytokines that regulate growth, differentiation, adhesion and apoptosis of various cell types. More than thirty proteins have been identified as members of the TGFβ superfamily, which includes TGFβs, activins, and BMPs [84, 85]. TGFβ is secreted as a homodimeric protein and regulates numerous cellular responses such as proliferation, differentiation, migration and apoptosis [85, 86].

TGFβ isoforms

In the kidney, TGFβ1 is the most highly expressed, being present mainly in tubular epithelial cells and to a lesser extent in the glomerulus [87, 88]. TGFβ3 follows a similar pattern of expression but in lesser amounts [82]. TGFβ2 is restricted mostly to the juxtaglomerular apparatus, co-localising with rennin staining [82]. TGFβ1 is generally considered to be the predominant form involved in renal disease, with the roles of TGFβ2 and TGFβ3 being less clear. Although all three isoforms of TGFβ have been shown to have fibrogenic effects on renal cells, the effects of TGFβ2 and TGFβ3 may be partially mediated by TGFβ1 [89].

TGFβ activation

TGFβ exists commonly as a homodimer bound to its latency-associated peptide and must be activated to exhibit its biological effects (figure 1.4) [84, 90, 91]. Activation of latent TGFβ *in vivo* may be controlled by the action of plasmin to cleave the latency-associated peptide from the active TGFβ dimer [82]. TGFβ can also be activated by ROS generation, TSP-1 [92, 93] and αvβ6 integrin [94-98]. Glucose upregulates TSP-1 expression in mesangial cells, leading to increased TSP-1 mediated TGFβ1 activation [99, 101]. TSP-1 activates TGFβ by altering the conformation of latent TGFβ [102]. L-TGFβ1 has been shown to co-localise with CD36, the TSP-1 receptor. Since TSP-1, not TGFβ1, is the natural ligand for CD36, this suggests that TSP-1 forms a complex with CD36 and L-TGFβ [103].

TSP-1 is a glycoprotein released by a number of cells including mesangial cells, although only 11% of the cells expressed TSP-1 at the cell surface, the vast majority had an intracellular pool [104, 105]. It mediates a variety of processes related to wound repair, including the induction of apoptosis and recruitment of macrophages

[106-108]. TSP is a trimeric adhesive molecule of ~450kD capable of binding to a wide range of macromolecules and many cell types [105, 109-111]. TSP has been implicated as a 'molecular bridge' mediating adhesive interactions between activated platelets and other cells [112, 113].

Figure 1.4: Schematic representation of TGFβ1 precursor processing

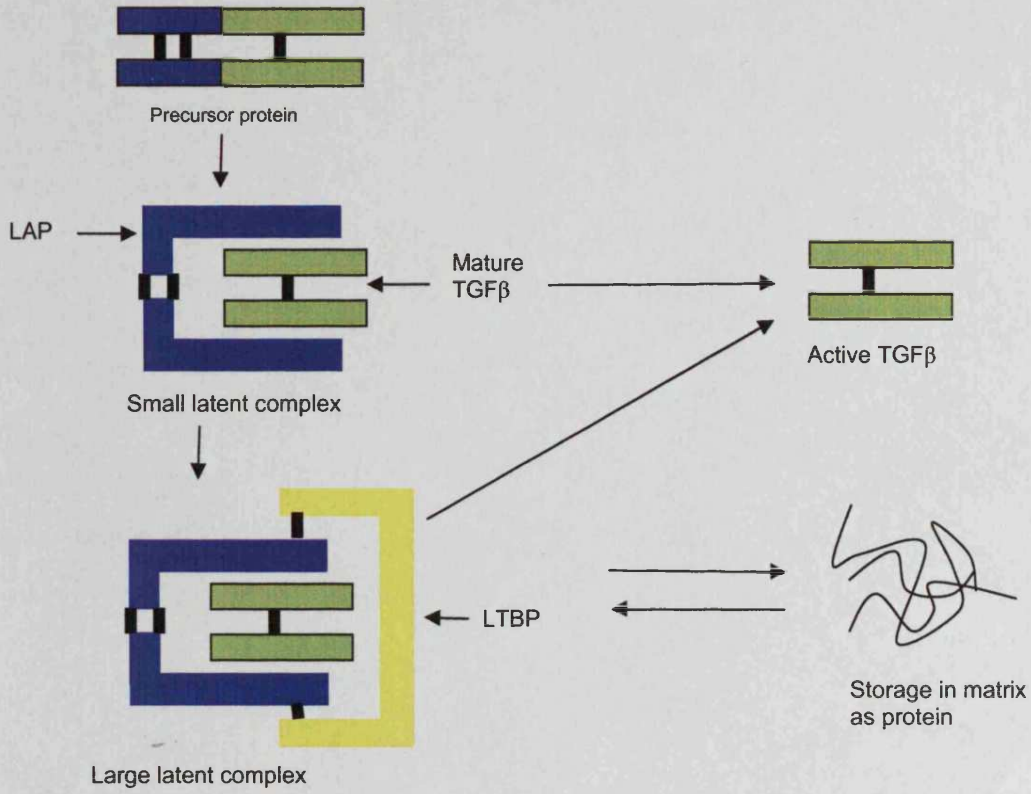

TGFβ is secreted in a latent form composed of three proteins from two genes [114]. The product of one gene, after processing, becomes TGFβ and latency associated peptide (LAP). LAP binds to TGFβ, rendering it latent and thereby preventing TGFβ from binding to its receptor. The product of the other gene is LTBP, which loosely forms a large complex with LAP and TGFβ [114]. LTBP binds to the latent TGFβ complex within 15 minutes after synthesis and plays a critical role in the assembly and secretion of the latent TGFβ [90, 91].

1.2.2: TGFβ signalling

TGFβ1 signalling occurs through type I and type II serine/threonine kinase receptors [85]. Each member of the superfamily binds to a characteristic combination of type I and II receptors [82, 85]. Ligand binding induces assembly of type I and II receptors into complexes, within which type II phosphorylates type I [82, 85]. In the absence of ligand, type I and II receptors exist as homodimers at the cell surface [115]. Activated type I receptor phosphorylates receptor regulated Smads (R-Smads: Smad2, Smad3, Smad5 and Smad8) and activated R-Smads form heteromeric complexes with Smad4 [85]. These complexes accumulate in the nucleus where they control gene expression in a cell-type specific and ligand dose-dependent manner through interactions with transcription factors, co-activators and co-repressors [85]. Inhibitory Smads (I-Smads: Smad6 and Smad7) act in an opposing manner to R-Smads and antagonise signalling [85]. They were originally shown to compete with R-Smads for binding to activated type I receptors and thus to inhibit the phosphorylation of R-Smads [85].

In contrast to the other Smads, which are generally regulated by post-translational modifications, the expression of the Smad7 gene is induced by TGFβ itself. Smad7 mRNA was induced by TGFβ1 within one hour in murine mesangial cells [116, 117]. Overexpression of Smad7 is a highly effective method of blocking at least some mesangial cell effects of TGF-β1 [116]. It binds to the ligand-activated RI and interferes with the phosphorylation of substrate Smads [117]. An upregulation of Smad7 mRNA upon TGFβ treatment in the cells suggests that Smad7 participates in a negative-feedback loop which regulates the length and intensity of the signalling [118].

Besides Smad-mediated transcription, TGFβ activates other signalling cascades, including MAPKs. Studies using Smad4-deficient cells, or dominant negative Smads, support the possibility of MAPK activation that is independent from Smads [115]. In addition, mutated TGFβ type I receptors, defective in Smad activation, activate p38 MAPK signalling in response to TGFβ.

1.2.3: Role in diabetic nephropathy

Circulating levels of TGFβ are increased in type II diabetes, correlating with blood glucose levels [119, 120]. TGFβ is an important mediator of the high glucose induced effect on mesangial cells [121, 122]. Studies by Wolf, et al demonstrated a biophasic growth response of mesangial cells when they were cultured in high glucose concentration; initially there was stimulation of replication followed by a sustained inhibition after longer incubation periods [123]. High glucose increases TGFβ1 mRNA and protein levels in cultured mesangial cells. The factors that mediate increased renal TGFβ activity involve hyperglycaemia and the intermediary action of other potent mediators such as angiotensin II, thromboxane, endothelins and PDGF [124].

Cell culture experiments have revealed that the effects of high glucose on renal proximal tubular cells and glomerular mesangial cells are mediated by autocrine production and activation of TGFβ [82]. Several studies have demonstrated that TGFβ expression is elevated in the kidneys of animals with insulin-dependent diabetes [82]. The actions of TGFβ on renal cells to induce hypertrophy [125-127] and stimulate ECM production, features that are characteristic of diabetic kidney disease, also predict that this growth factor may be involved in the pathogenesis of the disease. In the kidney, TGFβ promotes tubuloepithelial cell hypertrophy and regulates the

glomerular production of almost every known molecule of ECM [82]. TGFβ expression is also elevated in the glomerulus of patients with DN [128, 129].

The ability of TGFβ to enhance matrix synthesis underlies its important role in healing wounds. On the other hand, excess production of the cytokine may cause irreversible tissue fibrosis in a host of disease states [82]. In mesangial cells, TGFβ increases the production of type I and type IV collagens, fibronectin and proteoglycans [130].

The Smad family of proteins is the predominant signal inducer of TGFβ signalling. In *db/db* and STZ mice kidneys, nuclear localisation of Smad3 and expression of TGFβ ligand and its receptor were shown to be increased [131, 132]. Neutralisation of TGFβ activity could prevent the progression of renal failure in diabetic mice, preventing the increase in plasma creatinine concentration and decreasing expansion of the mesangial matrix [133].

1.2.4: TGFβ and Apoptosis

NFκB

NFκB is a molecule involved in cell survival, but can be pro-apoptotic under some circumstances [134-137]. It belongs to a family of transcription factors recognised by the κB enhancer element [138]. NFκB is normally held in the cytoplasm of unstimulated cells in an inactive form bound to an inhibitory protein, IκB [85, 118, 138-141]. Phosphorylation of IκB by the IKK complex leads to ubiquitination and degradation of IκB, which unmasks a nuclear targeting sequence on the NFκB molecule [139-142]. This promotes the translocation of NFκB from the cytoplasm to the nucleus where it becomes an active transcription factor [142]. Different dimers bind with diverse affinity to the variety of κB sites in DNA, resulting

in subtle cell and gene-specific modulations of gene expression. NFκB dimers do not promote gene transcripton by themselves, but as part of a complex of several co-activators such as CBP or AP-1 [141].

TGFβ can either promote or inhibit NFκB activation depending on the cell line [143-145]. Treatment of intestinal cells with TGFβ1 resulted in suppression of NFκB p65 accumulation in the nucleus and increased transcripts and protein levels of IκB, the NFκB inhibitor [146]. Smad7, however, maintained high NFκB activity by blocking the effects of TGFβ1. Decreasing Smad7 expression using an antisense oligonucleotide allowed endogenous TGFβ1 to up-regulate IκBα and lower NFκB accumulation in the nucleus [146].

The Smad7 promoter is also regulated by NFκB since expression of the p65 subunit was able to inhibit the Smad7 promoter activity and this inhibition could be reversed by co-expression of IκB [118]. TGFβ can reduce NFκB activity by inducing increased transcription of its inhibitor, IκBα [145]. Smad7 inhibits the survival factor NFκB, providing a potential mechanism whereby Smad7 potentiates cell death [147].

Activation of p38 MAPK and caspase-3 is required for TGFβ-mediated apoptosis, but not for apoptosis induced by Smad7 in podocytes, although Smad7 may act as an amplifier of TGFβ-induced apoptosis in podocytes [148]. TGFβ1 induced apoptosis in podocytes is associated with increased Bax protein synthesis and caspase-3 activity [148].

Role of p38 MAPK in apoptosis

p38 is a member of the MAP kinase superfamily, which is activated by stress signals and implicated in cellular processes involving inflammation and apoptosis [149-152]. Chronic exposure of human mesangial cells to high glucose activates the

p38 MAPK pathway via ROS generation and PKC activation [153-155]. TGFβ1 induced p38 MAPK activation is required for the TGFβ1 mediated apoptosis in mammary epithelial cells [156].

When trophic factors are removed, apoptosis increases and p38 MAPK activity is elevated [157, 158]. Selective blockade of p38 MAPK prevents apoptosis [157], also, inhibition of p38 MAPK and overexpression of kinase-inactive p38 MAPK significantly attenuated cell death induced by high glucose in endothelial cells in epithelial cells [159]. Caspase inhibitors significantly attenuated the sustained phosphorylation of p38 MAPK induced by high glucose. Phosphorylation of p38 MAPK occurred downstream of the caspase pathway mediated by MEKK1. An increase in the Bax to Bcl-2 ratio leads to cytochrome c release, caspase-3 activation, phosphorylation of p38 MAPK by MEKK1 and cell death [159].

TGFβ1 has been shown to induce Bax gene transcription and mitochondrial translocation of Bax protein leading to release of cytochrome c from mitochondria and subsequent activation of caspase-3 in liver epithelial cells [160]. TGFβ may be stimulating p38 MAPK signalling to induce Bax protein synthesis and mitochondrial translocation, leading to caspase-3 activation.

P38 MAPK kinase may function both upstream and downstream of caspases in the apoptotic response and involvement of p38 MAPK in apoptosis is cell type and stimulus dependent [161-163]. Most inflammatory cytokines are regulated by NFκB and recently it has been found that p38 MAPK regulates NFκB-driven gene expression [86, 164].

1.3: APOPTOSIS AND CELL CLEARANCE

1.3.1: Introduction

Apoptosis is an evolutionarily conserved, 'programmed' form of cell death, which does not incite an inflammatory response as opposed to necrosis, a process by which injury to the cell leads to release of intracellular contents. Apoptosis plays a central role in development, homeostatis and in many diseases [165, 166]. Virtually every cell type appears to be programmed to undergo apoptosis by default unless it receives a constant and sufficient supply of survival signals, which may be provided by soluble mediators such as hormones and cytokines or by contact with ECM or other cells [167]. Survival signals from the cell's environment and internal sensors for cellular integrity normally keep a cell's apoptotic machinery in check. In the event that a cell loses contact with its surroundings or sustains irreparable internal damage, the cell initiates apoptosis [168].

Apoptosis is characterised by DNA fragmentation, chromatin condensation, membrane blebbing, cell shrinkage and formation of apoptotic bodies [169, 171, 172]. These are the result of an ordered series of biochemical events within the dying cell, caused by activation of a family of cysteine proteases called caspases. Changes in the concentrations of the cell survival and cell death proteins lead to caspase activation [173, 174]. Caspases act on multiple intracellular targets, such as I^{CAD} (leading to DNA fragmentation), cell survival proeteins (e.g. Bcl-2) and lamins (contributing to chromatin condensation) [172]. This leads to characteristic changes such as endonuclease-mediated internucleosomal chromatin cleavage (DNA laddering) and plasma membrane alterations, including exposure of the anionic phospholipid phosphatidylserine [175-177].

A critical event during programmed cell death appears to be the acquisition of plasma membrane changes that allow phagocytes to recognise and engulf these cells before they rupture [176]. The plasma membrane of a healthy cell generally exhibits an asymmetric distribution of its major phospholipids. PS externalisation is an early and widespread event during apoptosis of a variety of cell types, regardless of initiating stimulus. Redistribution of PS during apoptosis may precede the nuclear condensation and cell shrinkage events also seen during this process [176].

Apoptotic cell death occurs in two phases: first a commitment to cell death where the balance between cell survival and cell death proteins tips in favour of cell death and caspases are activated (caspase activation is an irreversible change). This is followed by an execution phase, during which caspases cleave specific proteins, characterised by dramatic stereotypic morphological changes in cell structure [178].

1.3.2: Dysregulation in disease

Apoptosis and disease

In healthy tissues, the elimination of cells by apoptosis (which leads to rapid and inconspicuous clearance of intact dying cells by phagocytes) counterbalances cell birth by mitosis, so the two processes maintain the normal number of cells. Abnormal control of apoptosis is implicated in many human diseases, including Alzheizmers, Huntingtons, ischaemic damage, autoimmune disorders and several forms of cancer and is recognised to play an important role in regulating renal cell number in health and disease [179].

Kidney disease

Inappropriate engagement of apoptosis contributes to the progression of renal diseases such as polycystic kidney disease, mediating the loss of 'desirable' cells and

the eventual development of the hypocellular endstage kidney [180]. However, in some disease states, such as glomerulonephritis, apoptosis leads to resolution of injury [180]. Tight regulation of apoptosis is therefore essential for the maintenance of healthy tissues.

Diabetes

In glomerular core preparations from rats with experimental DM and in mesangial cells in culture there is a mild rise in replication during the early phase after exposure to high glucose concentrations but longterm cell culture in high glucose leads to downregulation of the anti-apoptotic proteins (bcl-2 and bcl-xL) and upregulation of the pro-apoptotic proteins (bax) [181]. The late phase of DN is characterised by the loss of resident glomerular cells [182]. Apoptosis of glomerular cells correlated with expansion of the mesangial matrix and with worsening of albuminuria. Consistent with this, caspase-9 cleavage was elevated only in diabetic rat kidneys [37]. High glucose can also lead to apoptosis in kidney cells via oxidative stress [183].

Mesangial cells

Apoptosis in cultured human mesangial cells can be triggered by stimuli known to trigger apoptosis in other cell types, such as deprivation of growth factors or exposure to inhibitors of protein synthesis [184]. Several recent studies show that high glucose induces mesangial cell apoptosis [37, 182, 185]. High glucose promotes apoptosis in mesangial cells by increasing intracellular ROS generation. This has been reported to change the Bax:Bcl-2 ratio in favour of apoptosis and lead to cytochrome c release from mitochondria and caspase-3 activaton [182]. In kidney cells, high glucose has been shown to downregulate Bcl-2 and Bax mRNA expression and increasing Bax mRNA expression [181].

1.3.3: Apoptosis pathways

Two pathways of cell death have been elucidated: a pathway that is directly activated by death receptors and a pathway that involves the mitochondria (figure 1.5). Signal transduction pathways initiated at the cell surface by death receptors are mediated by adaptor complexes that lead to caspase activation. The signal transduction pathways that activate mitochondria are less well understood. One class of stimulus that activates the mitochondrial pathway is cell stress, i.e. uv radiation, serum/growth factor withdrawal, addition of chemicals such as cycloheximide or etoposide [186].

Figure 1.5: Apoptosis pathways

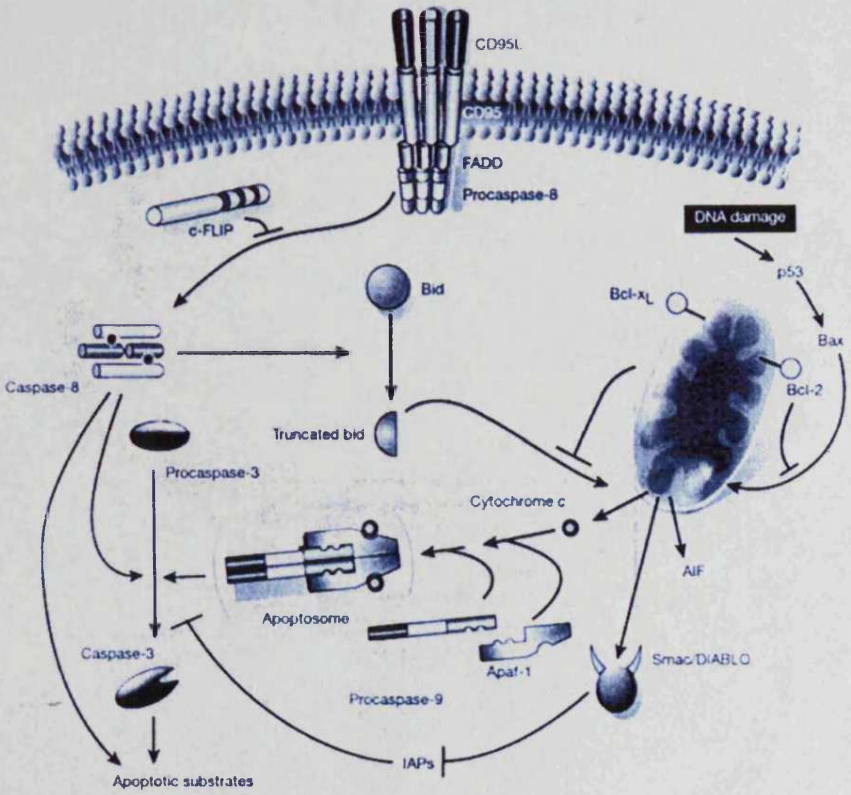

The death-receptor pathway is triggered by members of the death-receptor superfamily (e.g. CD95 and TNF receptor I). Binding of CD95 ligand to CD95 induces receptor clustering apoptotic signalling. The receptor recruits, via FADD, multiple procaspase-8 molecules, which results in caspase-8 activation.

The mitochondrial pathway involves apoptosis via serum-deprivation and DNA damage. Pro-apoptotic signals direct the pro-apoptotic proteins to the mitochondria, where they can mitochondrial membrane disruption. Cytochrome c, which is usually found within mitochondria, leaks out during apoptosis and activates caspase-9.

Both pathways converge upon caspase-3. Cross-talk between the two pathways can occur via Bid, a pro-apoptotic protein. Adapted from [173].

Death receptors

Death receptors – cell surface receptors that transmit apoptosis signals initiated by specific 'death ligands' – play a central role in apoptosis. These receptors can activate caspases within seconds of ligand binding, causing an apoptotic demise of the cell within hours [168]. Death receptors belong to the TNF receptor superfamily, which is defined by similar, cysteine-rich extracellular domains [168].

The role of mitochondria

The mitochondrion is a pivotal decision centre – it controls life and death by releasing death-promoting factors into the cytosol [187]. The pro-survival proteins seem to maintain organelle integrity [174, 188, 189]. The key function of Bcl-2 family members seems to be to regulate the release of pro-apoptotic factors, in particular cytochrome c, from the mitochondrial intermembrane compartment into the cytosol [173]. Bcl-2 acts *in situ* on mitochondria to prevent the release of cytochrome c and thus caspase activation [173, 188]. Addition of pro-apoptotic Bcl-2 family members to isolated mitochondria is sufficient to induce cytochrome c release, whereas overexpression of anti-apoptotic Bcl-2 family members will prevent it [173, 174, 188, 190-192].

Cytochrome c, a component of the mitochondrial electron transfer chain, is released from mitochondria during apoptosis [193, 194, 187]. Its release, which occurs following a variety of death stimuli, has been shown to activate Apaf-1, which in turn activates caspase-9 and caspase-3 [195-198]. Concurrent with cytochrome c, Smac/Diablo, a 25kDa mitochondrial protein, is released from mitochondria into the cytosol during apoptosis [173, 193]. Smac/Diablo binds to IAP family members and neutralises their anti-apoptotic activity [173]. Although cytochrome c activates Apaf-

1, its absence only attenuates apoptosis [235]. Since the level of total caspase activity is markedly lower in the absence of the apoptosome (a complex formed when ctyochrome c, Apaf-1 and pro-caspase-9 bind), it must be an amplifier of the caspase cascade rather than a critical initiator [200].

1.3.4: Apoptosis – The key players

Bcl-2 family

The Bcl-2 family has over 15 members and includes both pro- and anti-apoptotic molecules but I will concentrate on just four – two cell survival (Bcl-2 and Bcl-xL) and two cell death (Bcl-xS and Bax) proteins - because previous work has examined changes in expression of these molecules in the kidney [174, 181, 182, 200, 201].

Bcl-2 family members possess up to four conserved BH domains designated BH1, BH2, BH3 and BH4 which correspond to α-helical segments [174, 188, 202] (figure 1.6). Most pro-survival members, which can inhibit apoptosis, contain at least BH1 and BH2 and those most similar to Bcl-2 have all four BH domains [188]. Deletion and mutagenesis studies suggest that the amphipathic α-helical BH3 domain serves as a critical death domain in the pro-apoptotic members [174, 203].

Many Bcl-2 family members also contain a hydrophobic domain, which is essential for its targeting to membranes such as the mitochondrial outer membrane [174, 200]. An additional characteristic of the members of this family is their ability to form homo- and heterodimers, suggesting neutralising competition between these proteins [174, 188, 202, 204, 205]. Mutagenesis studies also established that the BH1, BH2 and BH3 domains strongly influence homo- and hetero-dimerisation [188]. Coalescence of the α-helices in its BH1, BH2 and BH3 regions creates an elongated

hydrophobic cleft, to which a BH3 amphipathic α-helix can bind [188]. The presence of an anti-apoptotic molecule such as Bcl-2 or Bcl-xL can inhibit the activation of Bax following a death signal [174]. The ratio between the two subsets helps determine, in part, the susceptibility of cells to a death signal [204]. Bax also heterodimerises with Bcl-xL, amongst other anti-apoptotic Bcl-2 family members suggesting that the susceptibility to apoptosis is determined by multiple competing dimerisations in which Bax may be a common partner [39].

Figure1.6: BH domains

The Bcl-2 family has been classified into three functional groups, I, II and III.

Group I: These are charcaterised by four short conserved BH domains, BH1-BH4. They also possess a C-terminal hydrophobic tail, which localises the proteins to the outer surface of the mitochondria. All members of this group are anti-apoptotic, e.g. Bcl-2 and Bcl-xL.

Group II: Members of this group include Bax. They have a similar structure to group I proteins but lack the BH4 domain.

Group III: This group consists of a large and diverse collection of proteins whose only common feature is the presence of the BH3 domain.

Adapted from [173].

The Bcl-2 family is regulated by cytokines and other death/survival signals at different levels. Several pro-survival genes are induced transcriptionally by certain cytokines [188, 206, 207].

Anti-apoptotic proteins

The anti-apoptotic proteins are integral membrane proteins found in the mitochondria, ER or nuclear membrane [189, 200, 208, 209]. Bcl-x transcripts are alternatively spliced into a long (bcl-xL) or short (Bcl-xS) form, which lacks the transmembrane domain [210]. Bcl-xL is normally located in both the cytosol and the mitochondria [211, 212].

These anti-apoptotic proteins can form membrane channels in the mitochondrial membrane [213], maintaining a decreased mitochondrial membrane potential and therefore preventing mitochondrial swelling following apoptotic stimuli [214]. One theory as to how the Bcl-2 family would control the swelling of mitochondria relates to a proposed channel entitled the permeability transition pore (PTP) [174, 202, 215]. Membrane-inserted helices from two or more Bcl-2/Bcl-xL molecules should associate to form a ring that creates an aqueous lumen but the number of molecules associating to form the channel is not known [202]. Opening of the PTP involves the opening of a large channel in the inner membrane of the mitochondrian results in mitochondrial depolarisation, uncoupling of oxidative phosphorylation and swelling of the mitochondria. This occurs almost universally during apoptosis [174, 194, 202].

The BH4 region of these proteins is required for pro-survival activity [216]. The BH1 and BH2 domains of Bcl-2 and Bcl-xL are required for it to heterodimerise with Bax (and other pro-apoptotic molecules), suppressing apoptosis [39]. Cleavage

of the amino terminus of Bcl-xL and Bcl-2 (predicted to expose their BH3 domain surface) can convert them into pro-apoptotic molecules [174].

Pro-apoptotic proteins

A large fraction of the pro-apoptotic proteins localise to cytosol or cytoskeleton prior to a death signal [217, 174]. Bax is a pro-apoptotic protein that can become integral mitochondrial membrane protein, where it can permeabilise the outer mitochondrial membrane, allowing efflux of proteins that lead cell death [174, 200]. Following a death signal, the pro-apoptotic members undergo a conformational change that enables them to target and integrate into membranes, especially the mitochondrial outer membrane [174]. Bax is predominantly a cytosolic monomer in healthy cells but during apoptosis it undergoes conformational changes at both termini, translocates to the outer mitochondrial membrane and oligomerises [200, 212]. This leads to the release of proteins such as cytochrome c from the mitochondria. Bax may induce apoptosis alone or by forming heterodimers with Bcl-xL, inhibiting its ability to maintain mitochondrial membrane potential. [204, 218, 219]. Bcl-xS, an alternatively spliced form of Bcl-x, acts directly as a dominant interfering Bcl-2 and Bcl-xL antagonist, favouring apoptosis [220].

Constitutively active pro-apoptotic Bcl-2 members may be transcriptionally activated. To avoid toxicity in healthy cells they would by transcriptionally silent, but in response to selected death stimuli cells would initiate their transcription. In select settings, Bax appears to be transcriptionally responsive [221].

Caspases

Caspases participate in a cascade that is triggered in response to proapoptotic signals and culminates in cleavage of a specific set of proteins, resulting in apoptosis [172, 178]. They are synthesised as inactive proenzymes (zymogens) comprising an N-terminal peptide (prodomain) together with one large and one small subunit, which heterodimerise upon being processed [172]. In apoptosis, caspases function in both cell disassembly (effectors), leading to the typical morphological changes seen during apoptosis and in initiating this disassembly in response to proapoptotic signals (initiators), activating and amplifying the apoptosis signal [172]. Initiator caspases are activated at the apex of the apoptosis signal (examples of these as caspase-8 and caspase-9). Caspase-8 is associated with apoptosis involving death receptors and caspase-9 is involved in death induced by cytotoxic agents [172]; whereas caspase-3 is one of the key executioners of apoptosis and its activation results in the morphological changes associated with apoptosis, including chromosome condensation, cell membrane blebbing and DNA fragmentation [201].

Caspase-8

Procaspase-8 and, only in humans, procaspase-10 are activated by receptor aggregation at the plasma membrane [222]. When death receptors of the TNF family are engaged by their cognate ligands, these procaspases are recruited by the adaptor FADD to the aggregated receptor, where their high local concentration promotes autocatalysis [172, 178, 222].

Caspase-9

A conformational change in Apaf-1, induced by cytochrome c from damaged mitochondria, allows it to recruit procaspase-9, forming an 'apoptosome' which

activates caspase-9 [172, 173, 198, 200]. Caspase-9 then processes and activates caspase-3 and -7 [200].

Caspase-3

Pro-caspase 3 appears to have both cytosolic and mitochondrial distributions [174]. An increase in Bax or a decrease in Bcl-2 alters the balance between these two proteins and has an effect on caspase-3 mediated apoptosis [201]. Its activation results in the phenotype of apoptosis including chromosome condensation, cell membrane blebbing and DNA fragmentation [201]. Caspase-3 activated by cell death signals may be via the mitochondrial or death receptor routes.

NFκB

Active NFκB is present as a homodimer or heterodimer of five subunits – p65/RelA, c-Rel, Rel-B, p100/p52 and p105/p50 [141]. The most abundant form of NFκB is a heterodimer of p50 and p65/RelA subunits, in which the p65/RelA subunit contains the transcriptional activator domain [117]. All of these proteins share a highly conserved Rel homology region (RHR), which is required for interaction with other members of the family, DNA binding and IκB protein binding and it also contains a nuclear localisation sequence [141]. The subunit p50 lacks the transactivation domain so is therefore unable to promote transcriptional activity and is considered to mediate transcriptional repression. Conversely, p65/RelA is a potent transcriptional activator [141].

Inhibition of NFκB activation stimulates apoptosis regardless of the injury pathway responsible for NFκB activation [142]. NFκB controls an anti-apoptotic mechanism upstream of caspase-3 activation and mitochondria [223]. Furthermore, the two main subunits of NFκB, p50 and p65 are also substrates for caspase-3 [224].

NFκB is involved in anti-apoptotic genomic response, although the putative anti-apoptotic genes that are activated by NFκB in response to apoptotic stimuli (e.g. TNFα) remain to be identified [138]. *Bcl-2* and *Bcl-x* are among the target genes of NFκB [225]. The presence of the NFκB site has been demonstrated in the promoters of human *bcl-2* and *bcl-x*. The *Bcl-x* gene promoter contains a putative consensus sequence for NFκB responsive activation. Upregulation of transcription of the Bcl-x promoter in mammalian brain cells in culture resulted from being transfected with NFκB p50 and p65 [226].

1.3.5: Phagocytosis

Apoptotic cells are swiftly recognised and ingested by phagocytic cells before release of toxic contents, *in vivo*. Phagocytosis requires distinguishing features on the surface of the apoptotic cells and recognition and tethering molecules on the surface of the phagocytic cells, as well as the cytoskeletal and other cellular machinery involved in engulfment. The recognition of apoptotic cells by phagocytes involves signals on the apoptotic cell that differentiate it from normal-self cells and receptors for these signals on the phagocytosing cell, such as PS exposure. In a number of tissues it has been observed or estimated that apoptotic cells are ingested and degraded so rapidly that they are only visible for 1-2 hours [175, 184].

Mesangial cells have the capacity to participate in clearance of neutrophils undergoing apoptosis, in keeping with previous reports of apoptotic cell uptake by other 'semi-professional' phagocytes, such as epithelial and tumour cells [227].

Phagocytic receptors

Apoptotic cells express 'eat me' receptors on their surface [228]. These signals include molecules that newly appear on their cell surface, such as externalised PS, and existing molecules such as altered surface sugar residues, which during the process of apoptosis are altered by oxidation processes and modifications in sugar chains or surface charges [229]. Ligands expressed on the apoptotic cell that signal phagocyte recognition are poorly understood. Many receptors have been implicated in phagocytosis (figure 1.7).

Macrophages have been shown to use a wide repertoire of receptors to phagocytose apoptotic cells. The precise receptor involved seems to be dependent on the species and activation state of the macrophage as well as the type of apoptotic cell being phagocytosed [138].

Figure 1.7: Proteins implicated in the phagocytosis of apoptotic cells

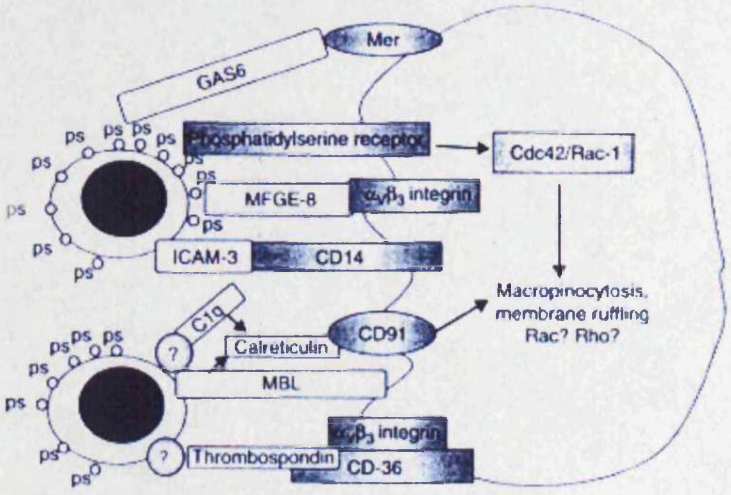

This diagram shows the molecules that have been implicated in phagocytosis of apoptotic cells. The apoptotic cells are shown on the left and the phagocyte on the right. Adapted from [228].

CD14 on the phagocyte can bind to ICAM-3 on the apoptotic cell to facilitate engulfment [228, 231]. Mer, which is implicated in the recognition of apoptotic thymocytes, may act through an interaction with Gas-6, which binds to phosphatidylserine on the surface of apoptotic cells [232]. The mannose-binding lectin (MBL) and surfactant proteins A and D enhance the uptake of apoptotic cells. MFG-E8 is secreted from activated macrophages binds to apoptotic cells and brings them to phagocytes for engulfment [233]. Complement has also been implicated to have a role in phagocytosis [234]. There are also receptors that inhibit engulfment, such as CD47 on the surface of erythrocytes or CD31, which functions as a 'don't eat me' signal [228, 235, 236].

CD36/TSP-1/αvβ3 mechanism

Introduction

A lot of research suggests that this mechanism is important in cell uptake by macrophages as well as being the key mechanism for mesangial cells [104, 230, 237-239]. CD36 is thought to act in co-ordination with the vitronectin receptor, αvβ3, by forming a bridge via thrombospondin to the apoptotic cell; the ligand on the apoptotic cell is unknown. It has been postulated that TSP-1 is bound to an unknown ligand on the apoptotic neutrophils, acting as a bridge between the apoptotic cell and the CD36/αvβ3 complex on the macrophage [237].

Macrophages

A complex consisting of TSP-1, its receptor CD36 and the integrin αvβ3 has been shown to be instrumental in macrophage phagocytosis of apoptotic neutrophils, with TSP-1 binding to both CD36 and αvβ3 [237]. Other studies have shown that macrophages also use this complex to phagocytose apoptotic neutrophils and eosinophils [230, 238]. TSP-1 has been implicated in adhesion between platelets and monocytes by forming molecular bridges with CD36 and other integrin receptors [240].

Mesangial cells

Mesangial cell phagocytosis of apoptotic neutrophils also involves an αvβ3/TSP-1 mediated mechanism [104, 239]. Cultured mesangial cells are capable of synthesising and secreting TSP-1 but apoptotic neutrophils did not express TSP-1, αvβ3 or CD36 on their surface [104], therefore another unknown molecule, a receptor on the apoptotic cell, must be involved. TSP-1 binds to apoptotic neutrophils specifically and 'bridges' the apoptotic neutrophils to αvβ3 on the mesangial cell surface. The RGDS (Arg-Gly-Asp-Ser) tetrapeptide can block the CD36/αvβ3

pathway but RGDS was incapable of reducing binding or phagocytosis of late apoptotic cells (cells expressing more a larger amount of phosphatidylserine on their surface but have not yet lost their membrane integrity) cells by human mesangial cells [241]. This suggests that cells in late apoptosis may be phagocytosed by a different mechanism.

Importance of phosphatidylserine

A major change in apoptotic cells is the translocation of phosphatidylserine from the inner to the outer leaflet of the plasma membrane [242, 243]. Loss of phospholipids asymmetry and PS expression is required for phagocyte engulfment of apoptotic cells and imply a critical role for PS recognition in the uptake process [242]. Apoptotic cells that failed to lose phospholipid asymmetry and that did not express PS externally were not phagocytosed by macrophages or fibroblasts, even though they showed other morphological apoptotic changes such as DNA fragmentation and caspase-3 activity [242].

Inhibition of phosphatidylserine-mediated recognition of apoptotic cells significantly reducing binding of late apoptotic U937 cells by human mesangial cells [241, 244]. Phagocytic cells deficient in wildtype PSR were defective in removing apoptotic cells [245]. Macrophages depend on the PS exposed on the surface of apoptotic lymphocytes for recognition and phagocytosis and they recognise cells in the very early stages of apoptosis via cell surface PS [246, 247].

PS may not bind directly to the PS receptor but rather indirectly via the bridging molecule Annexin I, an intracellular protein, which during apoptosis translocates from the cytosol to the PS-rich plaques in the outer leaflet of the plasma membrane [248].

Another PS binding bridging protein that has recently been described is protein S, which is known to bind to receptors of the Mer receptor-tyrosin kinase family [249].

Hoffman and colleagues have demonstrated that the vast majority of 'eat me' signals mediate tethering of apoptotic cells to the engulfing cell but only little internalisation. Ligation of the PS receptor alone induced neither attachment nor uptake. Engagement of both PS receptor and other phagocytic receptors converted the tethering mediated by PSR to internalisation [229, 236, 249, 250]. This suggests that other receptors (such as αvβ3/TSP-1/CD36, for example) are required for binding but PSR may be required for internalisation. The addition of antibodies to receptors such as CD36 or αvβ3 facilitated the tethering of erthocytes to macrophages, but did not promote engulfment.

When the erythrocyte was coated with PS and tethered to a macrophage, however, the erythrocyte was rapidly phagocytosed. Thus, PS exposure is sufficient to drive the engulfment of tethered cells. These findings support the idea that apoptotic cells can be tethered by multiple mechanisms and suggest a signalling role for the PSR in the activation of engulfment [228].

1.2.5: Role of TGFβ in cell clearance

The process of apoptotic cell clearance actively suppresses the initiation of inflammation and immune responses, in part through release of anti-inflammatory cytokines [251-253]. Phagocytosis of apoptotic cells by macrophages is associated with the production of anti-inflammatory cytokines such as IL-10 and TGFβ, *in vivo* and *in vitro*, resulting in an anti-inflammatory effect and suppression of the pro-inflammatory mediators, e.g. IL-1α, IL-8 and TNF-α [247, 252, 254].

TGFβ1 secretion upon ingestion of apoptotic cells appeared to require PS on the apoptotic cells since this effect could be reproduced by instillation of PS-containing liposomes as well as PS-expressing apoptotic cells [253, 254]. Kruosaka and colleagues argue that the production of anti-inflammatory cytokines during co-culture with apoptotic cells maybe physiologically irrelevant because cells at a very early stage of phagocytosis may be quickly phagocytosed without any adverse effects *in vivo* [247]. They examined secretion of pro-inflammatory cytokines IL-1α, IL-1β, IL-6, IL-8 and TNF-α and anti-inflammatory cytokines IL-10 and TGFβ. Of these, they found that after co-culturing macrphages with cells in the early stages of apoptosis, only IL-10 and TGFβ increased [247, 255].

1.4: SUMMARY

Mesangial expansion is strongly linked to the clinical manifestations of DN. Increasing mesangial cell number has been documented in incipient nephropathy but in overt nephropathy there is a loss of mesangial cells. This later loss of cells occurs through apoptosis and correlates to worsening albuminuria.

Hyperglycemia plays a major role in diabetes and has been shown to induce apoptosis in various cell types, including mesangial cells. In addition, high glucose increases TGFβ1 expression, a cytokine that is an important mediator of the high glucose effects. TGFβ1 is known to inhibit cell growth and can cause cell death in various cell types.

In vivo, apoptotic cells are rapidly cleared via phagocytosis by neighbouring cells before they release their toxic contents. Mesangial cells are sem-professional phagocytes that are able to ingest apoptotic cells via the αvβ3/TSP-1/CD36 mechanism. In other phagocytic cells, this uptake can induce secretion of anti-

inflammatory cytokines such as TGFβ1 and phosphatidylserine exposure on the apoptotic cell has been implicated in this response.

The aims of this project were the following:

1. The role of glucose in mesangial cell apoptosis: Various methods were used to quantify apoptosis. The effect of high glucose on survival factors such as NFκB, Bcl-2 family and caspase-3 were determined and the apoptotic pathway mediated by high glucose determined.

2. TGFβ1 as a regulator of glucose and apoptosis: The amount of latent and active TGFβ1 secreted by cells in high glucose was quantified and the apoptosis pathway mediated by TGFβ1 was examined.

3. The effects of high glucose on mesangial cell clearance of apoptotic cells and its effect on TGFβ1 generation: Apoptotic neutrophils were used to study the effects of mesangial cells to apoptotic cells. The effect of TGFβ1 on phagocytosis was determined. Binding of apoptotic cells to mesangial cells lead to increased TGFβ1 secretion and the receptors involved in this response were investigated.

CHAPTER 2: METHODS

2.1 TISSUE CULTURE

2.1.1: Mesangial Cells

Mesangial cell derivation

The rat mesangial cell line used in this thesis was in use in our department. The primary rat mesangial cells were originally established from collagenase treated glomeruli. The glomeruli were isolated from Wistar rats under sterile conditions and the preparation was separated by serial sieving – the glomeruli being collected on a 53 μm sieve. Tubular contamination of the original culture was less than 1% as assayed by phase contrast microscopy. Intact glomeruli were washed 3 times with PBS and resuspended in bacterial collagenase 750u/ml. These were then incubated for 30 min at 37°C in order to digest the glomeruli, releasing the epithelial cell from the core fragments. The suspensions were then centrifuged at 50xg for 5 min at 4°C and the cores washed x3 with PBS. The cores were finally resuspended in RPMI-1640 supplemented with 20% FCS, plated in 25cm flasks and incubated in a humidified atmosphere. Cells grew out of the explants after 3-4 days and reached confluence by day 14. The cells were identified as mesangial cells by staining for Thy 1 and the presence of intracellular myosin fibrils as well as significant collagen IV and fibronectin. The cells were also negative for Factor VIII excluding the possible contamination of endothelial cells. . In most instances the cell preparation failed to replicate in culture for more than approx 10 passages – in one instance however the cell culture continued to replicate indefinitely – and example of "spontaneous transformation" on vitro as has been reported [Cancer Res. 2005 Apr 15;65(8):3035-9. Erratum in: Cancer Res. 2005 Jun 1;65(11):4969]. These cells were therefore available for use in this study. They were characterised as mesangial cells in order to

confirm their identity (see below) and used in the rat cell experiments described in this work. As transformed cells they have the advantages and disadvantages described for all such lines. They allow direct comparison between different experiments without concern about different sources and restrict the need for the continuous sacrifice of fresh animals. They do however suffer the disadvantages of all such lines in that it is impossible to know which if any of their functions have been altered to induce immortality in vitro. These cells have been used by others in the lab and have been shown to have the same characteristics as primary human cells [Martin, J et al. KI (1989) 39:790-801; Martin, J et al KI (1994) 46:877-885; Martin, J et al JI (1986) 137:525-529].

Mesangial cell characterisation

A spontaneously transformed rat mesangial cell line (RMC) was used for all experiments. These cells were characterised as mesangial cells before use. The mesangial cells were cultured on 8-well chamber slides until 50% confluent. The medium was removed and the cells washed x3 in PBS before fixation in a 1:1 ratio mixture of acetone:methanol (Sigma) at room temperature for 5 mins. The cells were washed and incubated with the primary antibody (figure 2.1) at RT for 3 hrs. The primary antibodies were diluted 1 in 80 in PBS containing 1% BSA. The cells were washed in PBS and incubated with the secondary antibody (anti-mouse FITC conjugated) at RT for 1 hr, diluted in PBS, a 1 in 80 dilution. The cells were washed x3 in PBS and viewed. Light microscopy showed large stellate cells with many irregular cytoplasmic projections. In long-term culture, mesangial cells pile up and formed 'hillocks'. The mesangial cells failed to stain for cytokeratin, a marker for

endothelial cells. Mesangial cells stained for actin and desmin, which supported a mesanchymal and myogenic origin. Macrophages stain negative for desmin, distinguishing them from mesangial cells [9] (figure 2.1).

Mesangial cell culture

Cells were cultured in a 1:1 ratio of DMEM without glucose (Life Technologies, Paisley, UK) and RPMI 1640 (5.5mM glucose final concentration) with supplements - 5μg/ml insulin (Sigma-Aldrich Co Ltd, Gillingham, UK), 5μg/ml transferrin (Sigma-Aldrich), 5ng/ml sodium selenite (Sigma-Aldrich), 10U/ml penicillin (Life Technologies), 10μg/ml streptomycin (Life Technologies) and 2mM L-glutamine (Life Technologies) - and 10% FCS (Autogen Bioclear UK Ltd, Calne, UK). The cells were cultured in either 5.5mM glucose medium (normal glucose control) or 25mM glucose medium (high glucose). The high glucose medium was prepared by adding 1.802g D-glucose (Sigma-Aldrich) to 500mls of normal glucose medium and sterile filtering once the glucose dissolved. Fresh growth medium was added to the cells every 3 to 4 days until confluent.

Subculture

Confluent cell monolayers for passage were sub-cultured using the following method. Growth medium was removed and the cells were treated with 10 ml trypsin/EDTA (GIBCO/BRL Life Technologies, Paisley, UK) diluted 2:1 with PBS (GIBCO/BRL). After 5-10 min incubation at room temperature (RT), cells were detached from the flask with gentle agitation, followed by addition of 5mls FCS to neutralize the protease activity. The cell suspension was transferred to a 50ml centrifuge tube (Greiner Bio-One Ltd) and the cells were pelleted by centrifugation

(Mistral 3000i, Sanyo) at 1500 rpm at 4°C for 7 min. After removing the supernatant, the cells were suspended in 30ml fresh supplemented medium containing 10% FCS and seeded into 3 new T75 cm^2 tissue culture flasks (Falcon, Becton Dickinson, Oxford, UK).

Freezing

Excess mesangial cells were stored in liquid nitrogen. Cells for freezing were removed from a confluent T75 cm^2 flask with trypsin and pelleted by centrifugation as described above for subculturing. After centrifugation, the cells were resuspended in 3mls of freezing mixture (10% v/v DMSO (Sigma-Aldrich), 30% v/v FCS and 70% v/v 5.5mM glucose culture medium) and 1.5mls was aliquoted into cytotubes (Nunc A/S, Denmark). These tubes were stored at -80°C overnight before storage in liquid nitrogen.

Cells taken out of liquid nitrogen were thawed in a 37°C water bath and added to 50mls culture medium in a 50ml tube. This was centrifuged at 1500rpm, 4°C, 7mins and the cells were resuspended in 10mls of culture media containing 10% FCS and transferred into a T75 cm^2 flask.

Figure 2.1: Mesangial cell characterisation

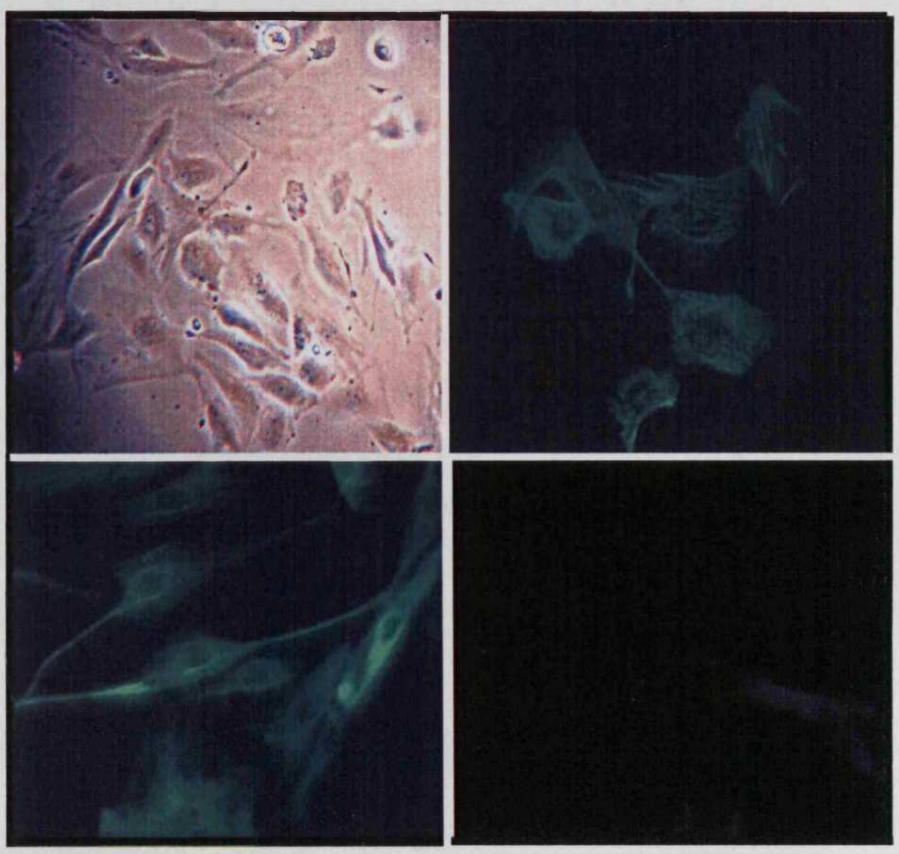

Upper left: Mesangial cells in cuture. Light microscopy shows large stellate or spindle-shaped cells with many irregular cytoplasmic projections (x125 magnification).

Upper right: Mesangial cells stained for smooth muscle actin with a mouse anti α-smooth muscle actin antibody (Daco, Denmark), x600 magnification.

Lower left: Mesangial cells stained for desmin with a mouse anti-desmin antibody (Daco), x600 magnification.

Lower right: Mesangial cells stained for cytokeratin with a mouse anti-cytokeratin antibody (Daco), x600 magnification.

2.1.2: Neutrophils

Isolation of Neutrophils

30-120mls of blood was taken from healthy volunteers at a time using 50ml syringes. The blood was sedimented in 13mls tubes (Sarstedt, Germany) by adding 5mls blood to 1ml 6% Dextran-70 (Baxter) and seven drops anticoagulant (76mM citric acid, 169mM sodium citrate, pH 5.6, filter sterilise) at 37°C for one hour. The plasma layer was pooled into new 13ml tubes and these were centrifuged (300g, 8mins) in a minifuge T. After discarding the supernatant, the cells were washed in PBS and centrifuged again. The supernatant was discarded and the cells resuspended in 5mls of PBS. This cell suspension was layered onto Ficoll (Amersham Biosciences) to separate the neutrophils from other white blood cells by Ficoll density gradient centrifugation (400g, 35mins). The supernatant was discarded and the cells washed in PBS and centrifuged. Any contaminating red blood cells were removed by lysing with water (3mls, 20seconds), then restoring osmolarity by filling the tubes with PBS, and centrifuging (300g, 8mins). The cells were washed in PBS once more. Cell number was determined with a Coulter Counter (Beckman Counter). 20µl of the PMN cell suspension was added to 20mls of Isoton (Beckman, UK) and mixed by inversion. Two background readings were taken on the Coulter Counter followed by two readings to obtain a cell count. The following formula was used to calculate the number of cells/ml:

(Average PMNs count – average background count) x 1000 = cells/ml

High neutrophil (PMN) yield was determined by cytospin preparations. 20µl of cells and 80µl of PBS were added to each chamber of a cyto-centrifuge (Cytopsin 4, Thermo Shandon). The cells were adhered onto the microscopic slides by

centrifuging at 1000g for 10mins. The slides were allowed to air-dry overnight and were then stained using a Quick III Haematology stain kit (Astral Diagnostics). The cells were first fixed in a solution of 100% methanol for 45 seconds and then dipped in solution I (an eosin solution, red tones) for 45 seconds followed by another 45 seconds staining in solution II (a basophilic solution, blue tones). The cells that had a purple nucleus, red granules and a pink cytoplasm were identified as neutrophils (100%).

In order to assess the impact of isolation and overnight aging on neutrophil activation cell surface expression of CD18 in fresh isolated and aged neutrophils was assessed by flow cytometry (figure 2.2). Activated PMNs also became clumped in culture, therefore any PMN preparations that became clumped were discarded.

Figure 2.2: CD-18 expression of aged and fresh PMNs

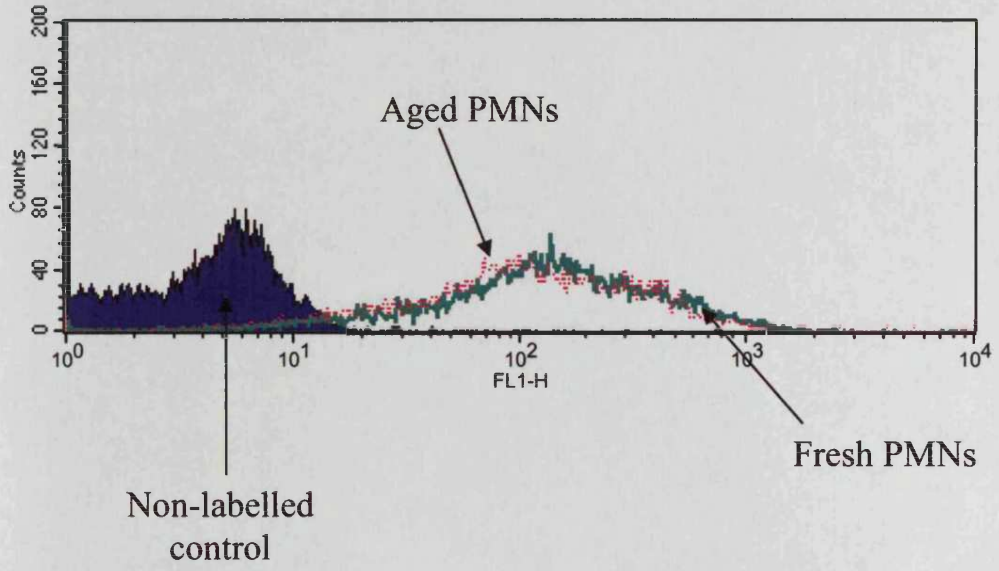

Fresh and aged PMNs were incubated in FACS buffer with the primary mouse anti-CD18 antibody (1:1000 dilution, diluted in FACS buffer) for 30 minutes at 4°C. The cells were washed in PBS and incubated with the secondary anti-mouse-FITC conjugated antibody (1:100 dilution) for 30 minutes at 4°C. They were then centrifuged as above, washed x3 in PBS, resuspended in FACS buffer and analysed by flow cytometry. The non-labelled cells were incubated with the secondary antibody only. The histogram shows a typical result from three separate experiments.

2.2: APOPTOSIS

2.2.1: Annexin-v/Propidium Iodide FACS analysis

Annexin-V is a Ca^{2+} dependent phospholipids-binding protein that has high affinity for phosphatidylserine (PS). It binds to phosphatidylserine when it is exposed on the outer membrane of cells during the early stages of apoptosis and therefore can be used to study apoptotic cells. In contrast, Propidium Iodide enters the cell when membrane integrity is lost, thus distinguishing apoptotic cells from necrotic cells.

Apoptosis in mesangial cells was induced in 6-well plates (Falcon) by serum depriving the cells for up to 72 hours. After induction of apoptosis, the medium was removed and the cells washed in PBS. Trypisn was added to the wells to detach the mesangial cells and form a single-cell suspension. After ten minutes, the trypsin was neutralised by addition of 100µl FCS. The cell suspension was then pipetted into a 1.5 ml eppendorf and centrifuged (centrifuge 5415R, Eppendorf) at 1600rpm, 4°C for 7mins. The cells were resuspended in PBS and centrifuged again. Following the wash in PBS, the cells were stained for PI and annexin-v-FITC. They were resuspended in 100µl of the reaction mixture made up of 90µl distilled water, 10µl 10x binding buffer (100mM HEPES (Life Technologies), 1.5M NaCl, 50mM KCl, 10mM $MgCl_2$ and 18mM $CaCl_2$, pH 7.4), 5µl annexin-V conjugated to FITC (Pharmingen, UK) and 5µl propidium iodide (PI, Pharmingen UK). The samples were incubated in the dark for 20 minutes at room temperature, centrifuged, followed by a wash in PBS and resuspended in 500µl 1x binding buffer.

The samples were analysed immediately by flow cytometry (FACSCalibur, Becton Dickinson, Oxford, UK). The viable cells were annexin-V/PI negative, cells

in early apoptosis were annexin-v positive and PI negative and cells in late apoptosis/necrosis were annexin-V/PI positive. Figure 2.3 shows a typical scatter plot.

Figure 2.3: Typical scatter plot – annexin-V/PI

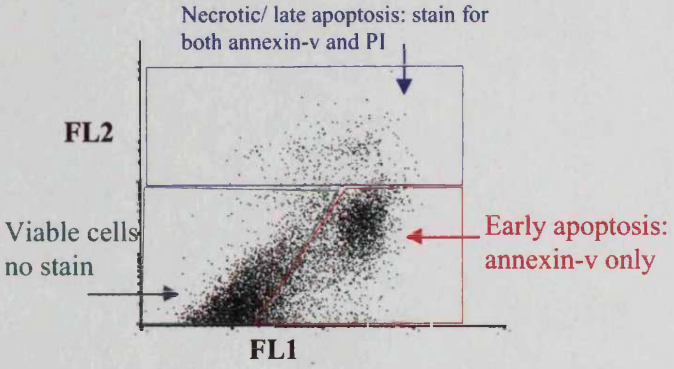

This figure shows a typical scatter plot after staining the cells for annexin-V-FITC and PI. Cells cultured in normal glucose medium containing 10% serum were used as controls. Three distinct regions were chosen as shown in the figure. The population of cells in the lower left-hand corner did not stain for annexin-V or PI and were therefore described as viable (green). The population to the right stained for annexin-V (measured on the FL1 axis) and were therefore in early apoptosis (red). Any cells above these sections were described as being in late apoptosis/necrotic (blue) because they stained for PI, measured on the FL2 axis. These regions were copied onto the scatter plots for the induced cells and the % of cells in early apoptosis is shown graphically in the results sections. Ten thousand cells were analysed per sample.

2.2.2: Analysis of mitochondrial membrane potential

Disruption of the mitochondrial transmembrane potential is one of the earliest intracellular changes following the onset of apoptosis. The DePsipher kit (RnD Systems Europe Ltd) can be used as a marker of mitochondrial activity. The green dye, 5,5', 6, 6'-tretrachloro-1,1'3,3'-tetraethylbenzimidazolyl carbocyanine iodide, exists as a monomer at low membrane potential; however, it aggregates at higher membrane potentials and once aggregated it produces a red-orange fluorescence. Thus, the emission of fluorescence following addition of this dye can be used to follow changes in mitochondrial membrane potential as a result of apoptosis.

Apoptosis in mesangial cells was induced in 6-well plates and the cells were trypsinised as described in the previous section. The cell suspension was centrifuged in a 1.5ml eppendorf at 1600rpm, 4°C for 7mins, resuspended in PBS and centrifuged again. This was followed by suspension in 1ml of diluted DePsipher solution (5,5', 6, 6'-tretrachloro-1,1'3,3'-tetraethylbenzimidazolyl carbocyanine iodide, R&D Systems Europe Ltd) and incubated at 37°C, 5% CO_2 for 30 minutes in the dark. The samples were washed twice in PBS, resuspended in PBS and analysed immediately by flow cytometry. Figure 2.4 shows a typical scatter plot. The non-induced cells (cells cultured in normal glucose medium containing 10% serum) were used as controls. These controls were used to set up the two regions on the scatter plot and the % of cells in early apoptosis is shown graphically in the results sections.

Figure 2.4: Typical scatter plot - DePsipher

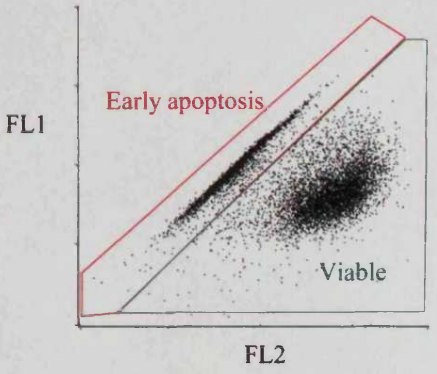

This figure shows a typical scatter plot after addition of 5,5', 6, 6'-tretrachloro-1,1'3,3'-tetraethylbenzimidazolyl carbocyanine iodide. The non-induced control was used to create the regions. Two distinct regions were chosen as shown in the figure. The population of cells in lower region produced a red-orange fluorescence, since the mitochondrial membrane potential was high and the cells were viable (green region). The upper region shows the population of cells that fluoresced green because the cells were in apoptosis and therefore the mitochondrial membrane potential was low (red region). Ten thousand cells were analysed per sample.

2.2.3: Quantification of Caspase-3 activity

Caspase-3, a cytoplasmic protein, is the most downstream protease which mediates apoptosis. A commercially available caspase-3 assay (BD Biosciences) was used to measure the amount of caspase-3 in cell lysates. After induction of apoptosis, the medium was removed and the cells washed in PBS. Following quantification of cell number using the alamar blue assay (described later), the cells were scraped into 1ml of PBS and pipetted into a 1.5ml eppendorf for centrifugation at 1300rpm, 4°C for 7mins. This was followed by suspension in 50µl chilled lysis buffer (a component of the Caspase-3 assay) to release cytoplasmic proteins, incubation on ice for 20mins, 10 seconds of vortexing the samples and centrifuging again (13000rpm, 10mins, 4°C). The supernatant was placed into fresh 500µl tubes. Fifty µl 2x Reaction buffer/ DTT mix and 5µl caspase-3 substrate (DEVD-pNA) were then added to each tube. Active caspase-3 cleaves the DEVD-pNA, leading to release of pNA and this causes the solution to turn yellow. The intensity of the colour determines the concentration of the active caspase-3 in the sample. The tubes were incubated for 1hr in a 37°C water bath. A pNA standard curve was generated (figure 2.5) using a range of pNA concentrations and the samples were read at 405nm in a plate reader (BMG Labtechnologies Ltd, Aylesbury, UK).

Figure 2.5: pNA standard curve

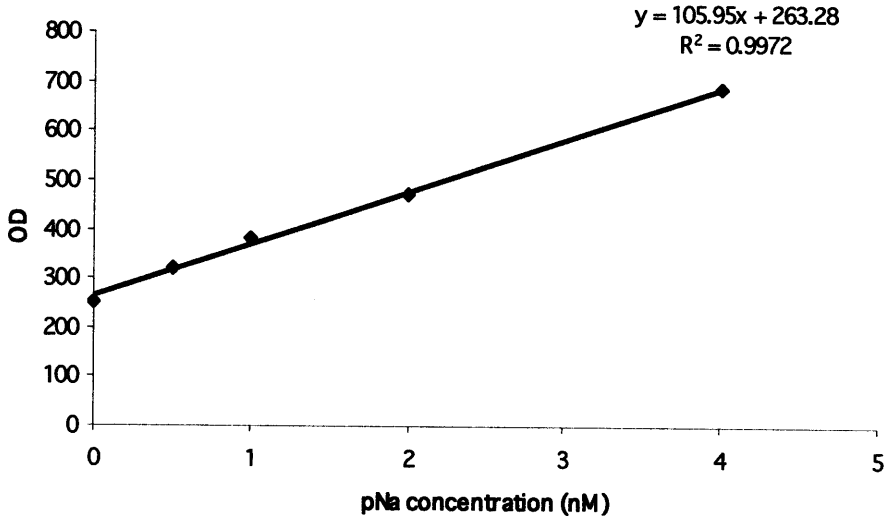

2.2.4: Induction of Apoptosis in Neutrophils

Apoptotic neutrophils were used to study the functional consequences of mesangial cell contact with apoptotic cells. Apoptosis was induced by 'aging' the neutrophils [235, 256]. After isolation, they were incubated overnight in DMEM medium (containing glucose) and 10% FCS in a 6-well plate in a 37°C, 5% CO_2 incubator (Iteraeus Instruments). Per $50x10^6$ neutrophils, 10mls of medium was used for the overnight incubation. The amount of apoptosis was assessed by FACS analysis using annexin-V and propidium iodide (PI) staining, as described for mesangial cells (figure 2.6).

Figure 2.6: Aging neutrophils induces apoptosis

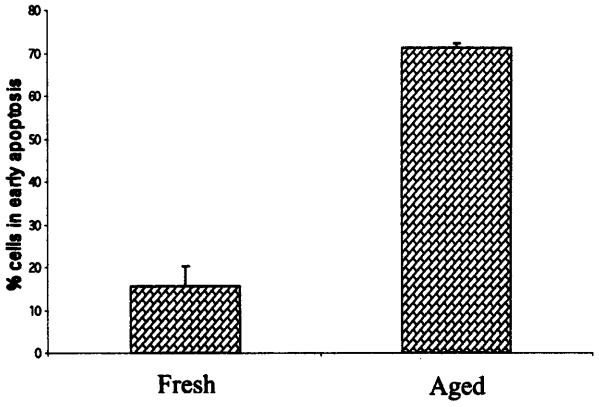

After isolation, apoptosis in fresh and aged PMNs was quantified by annexin v-FITC/PI labelling and flow cytometry analysis. There was over a three-fold increase in apoptotic cells. The results are presented graphically showing the percentage of cells that were in early apoptosis (annexin v-FITC positive and PI negative). The mean result is plotted, ± S.E., n =3. Data from all volunteers gave a similar result, therefore data from one volunteer is shown.

The % of cells that were in necrosis were as follows:

Fresh PMN – 6.17±3.35

Aged PMN – 10.29±5.8%.

2.3: PHAGOCYTOSIS

2.3.1: Microscopic analysis of phagocytosis

The mesangial cells were cultured in 8-well chamber slides. They were grown to confluence in 5mM glucose medium, followed by culture in serum free medium containing 5mM or 25mM glucose for 48 hours. Aged neutrophils were then added to the mesangial cells for 3 hours, either in the presence of 5mM or 25mM glucose. After 3 hours of co-culture, the media was removed and any remaining PMNs were washed three times in PBS using a Pasteur Pipette to gently agitate the solution. The cells were then fixed in 100% ice-cold methanol for 20mins. This was removed, followed by three washes in PBS. The ingested neutrophils were stained for myeloperoxidase (MPO) for 10 mins using a MPO stain made up of a 1:1 ratio of 1.25mg dianisidine and 0.05% H_2O_2. They were washed again in PBS and viewed under a light microscope using a x125 magnification [257].

2.3.2: FACS analysis to quantify phagocytosis of apoptotic cells using CFSE-labelled aged neutrophils

CFSE labelling of aged neutrophils

Isolated neutrophils were labelled with 5-, 6- carboxyfluorescein diacetate succinimidylester (CFSE, Molecular Probes), a fluorescent green dye [239]. CFSE is an amine-reactive reagent which can passively diffuse into cells. It is colourless and nonflourescent until its acetate groups are cleaved by intracellular esterases to yield highly fluorescent, amine-reactive fluorophores [258]. Once incorporated into cells, it remains there even through cell division.

After aging the neutrophils overnight and determining cell number, the cells were put into 13 ml tubes and centrifuged at 1500rpm, 4°C for 7 mins. The cells were then resuspended in 10mls of PBS per $30x10^6$ PMNs with 20µl of CFSE (stock 5mM in DMSO) (figure 2.7). After 10 mins incubation in the dark at room temperature, the uptake of the fluorescent cell stain was inhibited by addition of 200µl FCS (figure 2.8). The cells were centrifuged as before, and resuspended in 5mM glucose medium without FCS for co-culture experiments.

Co-culture of labelled PMNs with mesangial cells

The labelled neutrophils were co-cultured with mesangial cells for three hours, either in the presence or absence of FCS. The media was then removed and the PMNs washed off with gentle agitation in PBS, using a Pastuer pipette, three times. 600µl of PBS and 100µl of trypsin was then added to each well and the plates gently agitated. This was to detach the mesangial cells from the plate and to dislodge any bound PMNs. After ten minutes, the trypsin was neutralised by adding 100µl of FCS. The cell suspension was then centrifuged in a 1.5ml eppendorf at 1600rpm, 4°C for 7mins. The cells were resuspended in PBS and analysed for phagocytosis immediately by flow cytometry.

Analysis of phagocytosis by flow cytometry

Ten thousand cells, in total, were analysed per sample (figure 2.9). The x-axis was set up to measure cell size (mesangial cells are larger than PMNs) and the y-axis was set up to measure green flouresecence (only PMNs labelled, therefore any 'labelled' mesangial cells have ingested PMNs).

Figure 2.7: CFSE labelling of aged PMNs

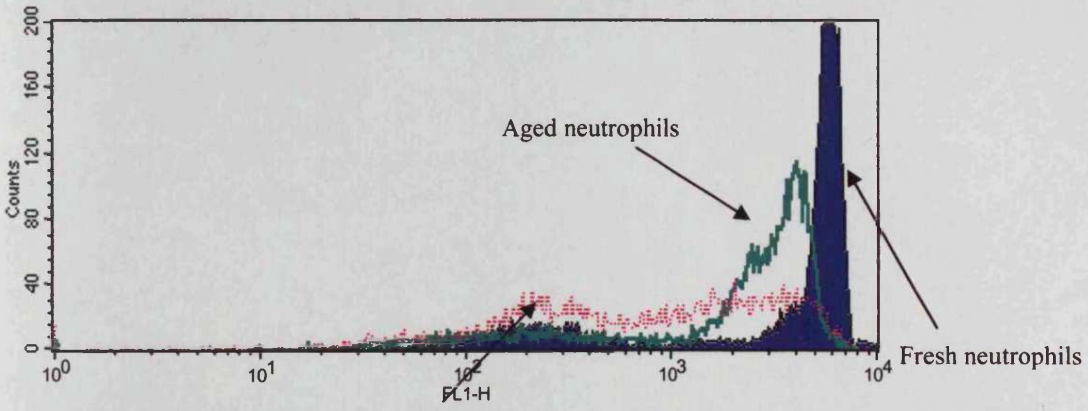

Neutrophils labelled while fresh and then aged.

Isolated PMNs were labelled with CFSE and dye uptake was analysed by flow cytometry.

Purple: Isolated PMNs were labelled while fresh.

Green: Isolated PMNs were labelled after aging overnight.

Red: Isolated PMNs were also labelled while fresh, followed by aging overnight.

Aged and fresh PMNs stained for CFSE. Therefore, for all of the experiments, the PMNs were labelled after aging overnight.

Figure 2.8: Serum inhibits uptake of CFSE in mesangial cells

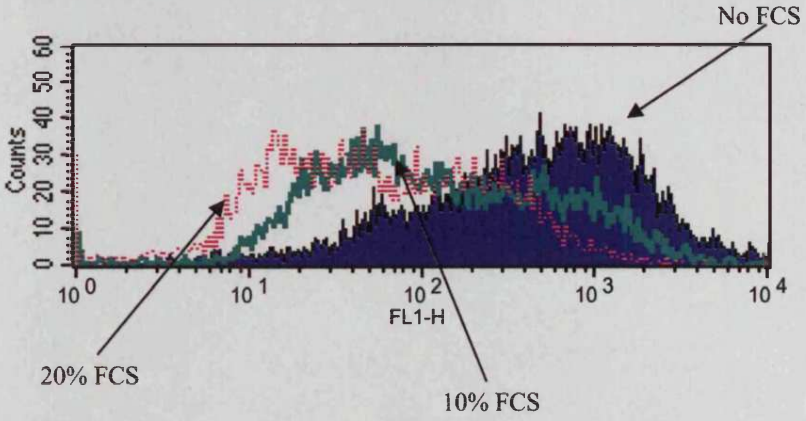

Mesangial cells were grown to confluence, serum-deprived for 48 hours, followed by addition of CFSE to the medium. Various doses of FCS were also added to the mesangial cells at this point. After 3 hours, the medium was removed and the mesangial cells washed in PBS, trypsinized and CFSE uptake examined by flow cytometry. FCS inhibited the uptake of CFSE by mesangial cells in a dose-dependent manner. Therefore, phagocytosis experiments were carried out in the presence of serum, unless otherwise stated.

Figure 2.9: FACS analysis of CFSE-labelled PMNs to quantify phagocytosis

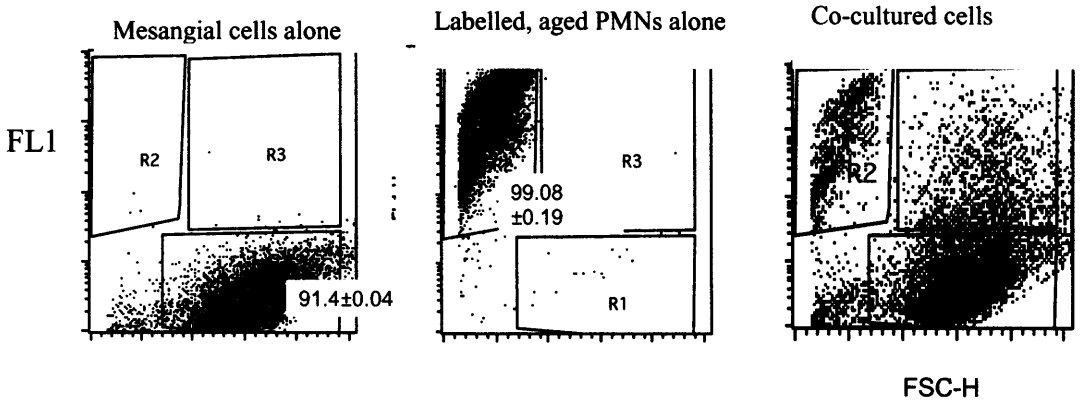

To quantify phagocytosis, aged PMNs were labelled with CSFE and co-cultured with mesangial cells. FACS analysis was used to quantify phagocytosis. Mesangial cells were larger than neutrophils (size measured on the x-axis, FSC) and not labelled (CFSE-fluorescence measured on the y-axis, FL1). Trypsin treatment disloged any bound PMNs [227] and these lone PMNs can be seen in region 2 in the plot showing co-cultured cells. Taken together, this suggests that any fluorescent mesangial cells (R3) must have ingested PMN(s). In the results section, the % phagocytosed cells (cells in R3) is represented graphically.

2.4: WESTERN BLOT

2.4.1: Principles of Western Blot

A Western blot separates a complex mixture of proteins on basis of size by SDS-PAGE. The proteins are then transferred onto a membrane (i.e. nitrocellulose membrane) by electroblotting, during which a sandwich of gel and membrane is immersed in buffer between two electrodes and transferred by passing an electric current. The membrane is then probed for the protein(s) of interest using specific antibodies. In order to visualise the protein of interest, the blot is incubated with an enzyme-linked secondary antibody (conjugated to HRP). Enhanced chemiluminescence (ECL) is then used to detect the proteins of interest. In the presence of hydrogen peroxide and the chemiluminescent substrate luminal, HRP oxidises the luminal producing light. The light emission can be detected by exposing the blot to photographic film (figure 2.10). Band intensities can be detected on ECL film, showing the relative concentrations of the protein of interest in the samples [259].

Figure 2.10: Immunodetection of proteins

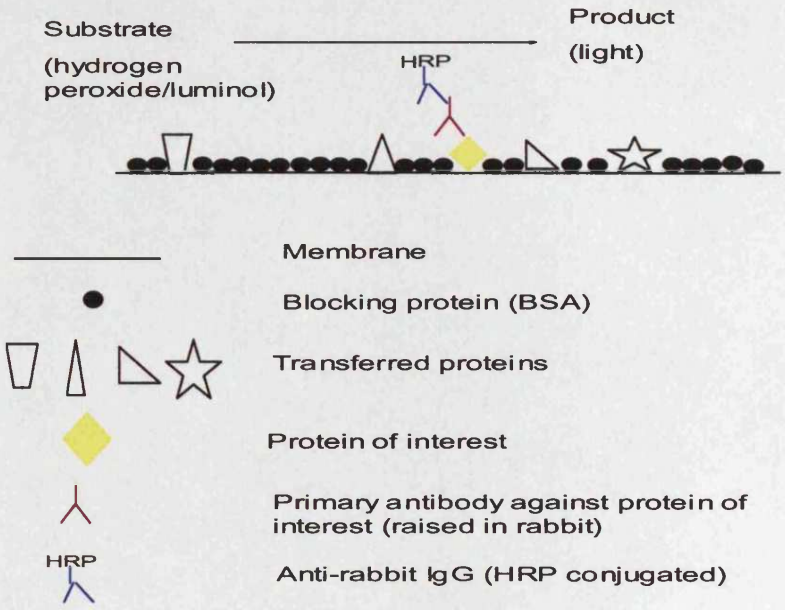

The primary antibody detects the protein of interest and the enzyme-linked secondary antibody detects the primary antibody. HRP oxidises luminal in the presence of hydrogen peroxide to produce light [adapted from 259].

2.4.2: Cytosolic Protein Extraction

At the end of experiments, the media was removed and the cells washed once in PBS and then scraped into 1.5ml cold PBS and centrifuged at 1600rpm, 4°C for 7mins to pellet the cells. The supernatant was discarded and the cells were resuspended in 100µl of NP40 cell lysis buffer (0.5% NP-40 in TBS,5mM EDTA, 1mM PMSF, pH 7.5 plus protein inhibitor cocktail), vortexed for 10 seconds and then incubated on ice for 20mins. The cells were vortexed again for 10 seconds and centrifuged at 13000rpm, 4°C for 3 minutes to pellet the cell debris. The supernatant was transferred to a sterile eppendorf and stored at -20°C.

2.4.3: Bradford Assay

Proteins were quantified to ensure equal loading of the prepared proteins by measuring protein concentration using the Bradford assay. This assay is based on the observation that absorbance of Coomassie Brilliant Blue shifts from 465nm to 595mn when protein binding to the dye occurs. A standard curve of Bovine Serum Albumin (Sigma-Aldrich) was prepared for each assay, over the range 0-2000µg/ml. 5µl aliquots of samples and standards were added to 250µl aliquots of 20% v/v Bradford Reagent (Bio Rad) in H_2O in triplicate in a clear 96-well plate and their absorbance read at 570nm in a plate reader after 10 minute incubation at room temperature. If the sample readings fell outside the standard curve, the dilution was adjusted as appropriate and the assay repeated. Cell extracts were diluted so that the protein concentration fell within the range of the standards used for this assay; typically this meant a 4-fold dilution.

2.4.4: Western Blot

Sample preparation and electrophoresis

Confluent, growth arrested mesangial cells were grown in T25 cm^2 flasks as required for each experiment. At the end of the time point the medium was removed and total protein was extracted as described earlier. 100μg of protein from each sample was mixed with reducing buffer (3x RB: 60mM Tris, 30% glycerol, 3mM EDTA, 3% SDS, 0.01% bromophenol blue, 15% β-mercaptoethanol, pH 6.8) and then heated to 95°C in the waterbath for 10 minutes to denature the proteins. The samples were loaded into the wells of a 10% SDS-PAGE gel prepared as table 2.1, adjacent to 15μl of dye-conjugated protein standards (See Blue Plus Two, Invitrogen). Gels were electrophoresed in discontinous vertical mini-gel apparatus using 1xRunning Buffer (3g Tris, 14.4g Tris, 1g SDS, 1L H_2O, pH 8.3) at 150V for 1hr.

Table 2.1: Composition of SDS-polyacrylamide gels

	Gel:	*Stacking*	*10%*	*12%*
H_2O (ml)		6.1	4.0	3.35
Tris pH8.8, 1.5M (ml)		-	2.5	2.5
Tris pH6.8, 0.5M (ml)		2.5	-	-
10% SDS (μl)		100	100	100
40% Bis-acrylamide (ml)		1.3	3.34	4.0
10% APS (μl)		50	50	50
Temed (μl)		10	5	5

Transblotting

The gel was removed from the casting plates and placed on PVDF transblotting membrane (Hybond ECL, Amersham) pre-wetted with transfer buffer (14.4g glycine, 3g Tris, 200mlo methanol, 800ml H_2O). Blot and gel were sandwiched in an inner layer of filter paper and an outer layer of plastic wire wool before electroblotting at 120V for 90 minutes in chilled transfer buffer. Successful transfers were confirmed by the appearance of the protein standards on the membranes.

Blocking, primary and secondary antibodies

Following transfer, the membrane was blocked for one hour in 5% w/v non-fat milk/0.2% Tween-20 in TBS (1.21g Tris, 4g NaCl, 500ml H_2O, pH 7.6) before washing over 30 minutes in 0.2% Tween-20 in TBS. The primary antibody was diluted to the titre recommended by the manufacturer (table 2.2) in 5% BSA/0.2% Tween-20 in TBS to a volume of at least 20ml. The membrane was incubated in the primary antibody overnight at 4°C. Following x4 washes in TBS/0.2%Tween over 30 minutes, secondary antibody was diluted in 5% w/v BSA/TBS-0.2%Tween and added for one hour at room temperature.

Table 2.2: Western blot antibodies and their dilutions

Primary antibody	Dilution
Smad7 antibody	1:500
Actin antibody	1:100
Caspase-3	1:250
Bcl-2	1:50
Bax	1:200
TGFβRII	1:200
c-myc-tag	1:200
Secondary antibody	**Dilution**
Anti-goat-HRP	1:20000
Anti-mouse-HRP	1:10000
Anti-rabbit-HRP	1:20000

All antibodies were purchased from Santa Cruz Biotechnolgy, except Caspase-3 (Cell Signalling), TGFβRII (Abcam) and c-myc-tag (Sigma).

Detection

Following a further x4 washes in TBS-Tween over one hour, the blot was developed using the ECL chemiluminescence system (Amersham) according to the manufacturer's instructions. The blot was dabbed dry on filter paper and 1ml each of Reagents A and B (HRP and luminal, Amersham Biosciences) were mixed and applied to the blot by pippetting. After exactly one minute, excess reagent was removed with filter paper, the blot wrapped in clingfilm and exposed immediately to chemiluminescence photographic film (Amersham). Five minutes and 15 minutes films were developed and further exposure times were determined on the basis on the appearance of these films.

Stripping and Reprobing

To determine the concentrations of different proteins on the same membrane, the blots were stripped of primary and secondary antibodies by immersion in Stripping Buffer (20g SDS, 7.57g Tris/HCl, 100mM β-mercaptoethanol, 1L H_2O, pH 6.7) for 30 minutes at 55°C followed by washes in TBS-0.2% Tween-20 over one hour before blocking and probing as above with a different set of antibodies.

2.5: QUANTIFICATION OF TGFB1

2.5.1: Enzyme-linked Immunosorbent Assay

TGFβ1 concentrations were determined using a commercially available ELISA development kit (RnD Systems Europe Ltd). The kit contains paired anti-TGFβ1 antibodies for capture and detection and TGFβ1 standards. High protein binding 96-well plates (Immulon 4, Dynex Technologies) were coated with TGFβ1 capture antibody (mouse anti-TGFβ1, 2μg/ml in PBS) overnight at room temperature. Wells were washed three times with wash buffer (0.5mls Tween-20 in 1L PBS) using a plate washer (Denley Wellwash 4, Thermo Life Sciences) at this and each subsequent step. The plate was incubated for one hour at room temperature with block buffer (for one plate - 1.5ml Tween-20, 1.5g sucrose, 30ml PBS) then washed before addition of TGFβ1 standards (recombinant human TGFβ1) and acid activated cell culture supernatant samples. A low pH activated the TGFβ1 by releasing the active molecule from the TGFβ1 binding protein; therefore the concentration of total TGFβ1 was measured. Cell culture supernatant samples were acid activated according to the kit instructions: 20μl 1M HCl was added to each 100μl sample and the samples were

incubated for 10 minutes at room temperature. The samples were neutralised with 20µl 1.2M NaOH/0.5M HEPES. The pH of the samples following neutralisation was checked with pH indicator paper to make sure it was in the desired range for the assay of 7.0-7.5. Following addition of standards and samples, plates were covered and incubated for 2 hours at room temperature, then washed three times with wash buffer. Detection antibody (biotinylated chicken anti-human) was added at 300ng/ml in reagent diluent (for one plate – 0.7g BSA in 50mls wash buffer) and the plate incubated for 2 hours at room temperature, then washed. Streptavidin-Horseradish Peroxidase (0.5% v/v in reagent diluent) was added to each well and the plate incubated in the dark for 20 minutes, then washed. Substrate solution (1:1 H_2O_2 solution and tetramethylbenzidine, RnD Systems) was added to the wells and the plate incubated for 20 minutes in the dark before addition of the stop solution (1M H_2SO_4). The plate was read immediately at 450nm. Recombinant human TGFβ1 was prepared in fresh tissue culture medium according to the kit instructions to provide a standard curve ranging from 0-2000pg/ml. The TGFβ1 concentrations were normalised to cell number, which was determined by the alamar blue assay, as described below.

2.5.2: TGF-ß1 bioactivity

Activity of TGF-ß1 was examined by determining the luciferase activity of HK-2 cells transiently transfected with a Smad-responsive promoter construct. Transfection is the process of bringing foreign DNA into cells and monitoring protein expression. DNA transfection is essential for studying gene function and regulation. Common transfection techniques include calcium phosphate co-prepipitation, microinjection, electroporation, the use of viral vectors and cationic liposome mediate transfection methods (i.e. FuGENE 6 and GeneJuice). FuGENE 6 Transfection

Reagent (Roche Diagnostics Ltd, Lewes, UK) is a lipid-based transfection reagent that complexes with DNA and transports it into the cell. GeneJuice (Novagen) is a non-lipid based reagent composed of a non-toxic cellular protein and a polyamine.

HK2 cells were transfected with the SMAD-responsive promoter and the β-galatosidase promoter, which was used to normalise the results for transfection efficiency, a validated method [260].

HK2 cell culture

HK2 cells are a proximal tubular cell line, transformed using human papilloma virus 16 E6/E7 genes. These cells were used in the TGFβ1 bioactivity experiments. Cells were cultured in a 1:1 mixure of Dulbecco's Modified Eagle's Medium and Ham's F12 supplemented with 10% FCS, 20mM HEPES, 2mM L-glutamine, 5μg/ml insulin, 5μg/ml transferrin, 5ng/ml sodium selenite and 0.4μg/ml hydrocortisone. Fresh growth medium was added to the cells until confluent. The subculturing and cell freezing protocols were the same as for mesangial cells.

TGFβ1 Bioactivity

Conditioned medium was generated by culturing mesangial cells under serum free conditions in either 5mM or 25mM D-glucose for 72 hours. Subsequently either untreated conditioned medium or conditioned medium subjected to 10 cycles of freeze-thawing were added to HK2 cells transfected with the Smad reporter construct 24 hours prior to determining luciferase activity. Repeated cycles of freeze-thawing of samples are well established *in vitro* mechanisms of activation of latent TGF-ß1 [261].

2.5.3: Alamar Blue Assay

The alamar blue assay (Biosource UK Ltd) was used to determine cell number. The assay incorporates an oxidation-reduction indicator that both fluoresces and changes in colour in response to chemical reduction of growth medium resulting from cell growth and therefore gives a measure of viable cell number. The REDOX indicator is minimally toxic to living cells and is therefore suitable for use to establish a growth curve and the cytotoxic effects of some compounds and cytokines. Data may be collected using either fluorescence-based or absorbance-based instrumentation. In all experiments, fluorescence was monitored at 544nm excitation wavelength and 590nm emission wavelength using a Fluostar Optima Meter.

In order to be certain there was a linear relationship between cell number and Alamar Blue fluorescence, a standard curve for mesangial cells was performed for culturing in 6- and 24- well plates (Figure 2.11). Mesangial cells were removed from a confluent T75 cm^2 flask by trypsining as described for subculturing. Cell number was determined using a Coulter Counter and a range of different cell numbers was plated. The volume in each well was standardised to 1ml in a 6-well plate and 0.5ml in a 24-well plate with culture medium and 10% Alamar Blue. The cells were returned to the incubator for one hour, after which 100µl aliquots of each well were quantified in duplicate in a 96-well plate for alamar blue fluorescence.

The cell medium was removed and stored. It was replaced with fresh medium containing 10% alamar blue (1ml in a 6-well plate and 0.5ml in a 24-well plate). After one hour, 100µl aliquots of medium were pipetted in duplicate into a 96-well plate, with media containing no alamar blue as the blank.

Figure 2.11: Alamar blue standard curves

A) 6-well plate

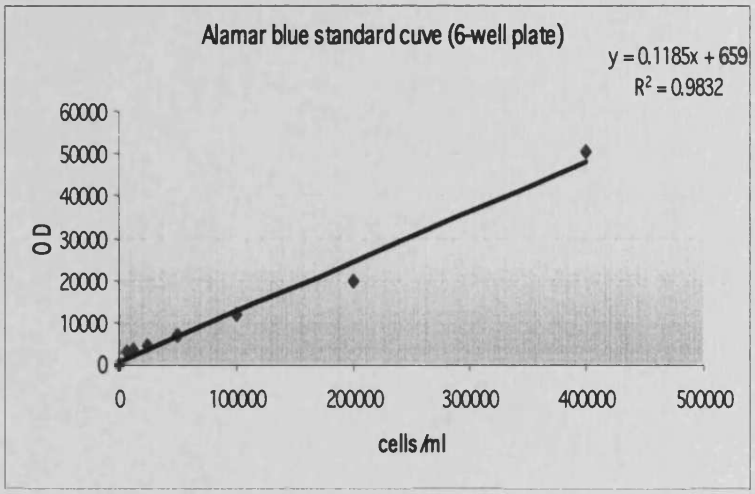

B) 24-well plate

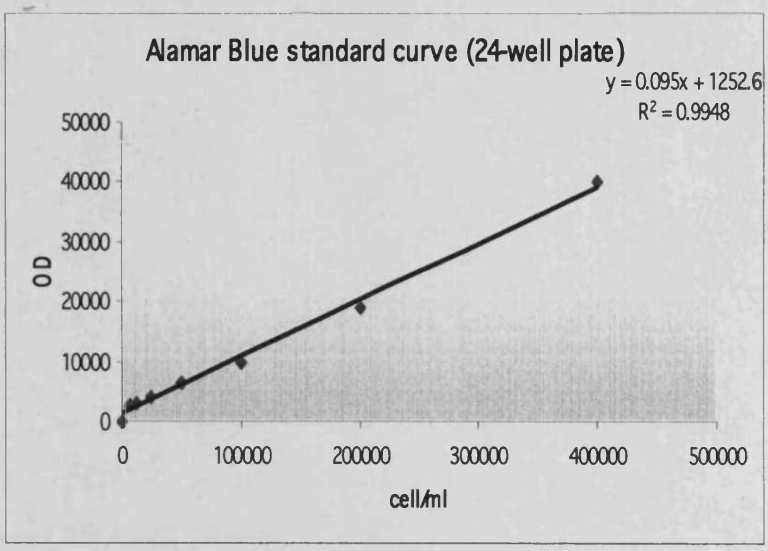

2.6: NFκB ACTIVATION

2.6.1: Introduction to the electrophoretic mobility shift assay

The electophoretic mobility shift assay (EMSA) determines the binding interaction between DNA and DNA binding proteins, such as the interaction of transcription factors with regulatory regions. The assay is based on the observation that complexes of protein and DNA migrate more slowly through a non-denaturing polyacrylamide gel than unbound DNA oligonucleotides. Addition of antibodies which recognise the binding protein(s) produces an even slower migration than the original DNA-protein complex.

2.6.2: Nuclear protein extraction

The cells were grown in T75 cm^2 tissue culture flasks as required for the experiments. They were then washed in PBS, scraped off into 1.5ml cold PBS using a cell scraper, and transferred in to a 1.5ml eppendorf for centrifugation at 13000rpm, 4°C for 10 seconds. The cells were resuspended in 400µl of ice-cold Buffer A (10mM HEPES-KOH, 1.5mM $MgCl_2$, 10mM KCl, 0.5mM DTT, 0.2mM PMSF, pH 7.9), incubated on ice for 10 minutes, vortexed for 10 seconds to disrupt their plasma membranes and then centrifuged for 10 seconds at 13000rpm. The pellet was resuspended in 100µl ice-cold Buffer C (20mM HEPES-KOH, 25% glycerol, 420mM NaCl, 1.5mM $MgCl_2$, 0.2mM EDTA, 0.3mM DTT, 0.2mM PMSF, pH 7.9), incubated on ice for 20 minutes and vortexed for 10 seconds to disrupt the nuclear membrane before centrifugation for 10 seconds at 13000rpm. The supernatant

(nuclear extract) was transferred to a fresh 1.5 ml eppendorf and stored at -20°C. The Bradford assay was used to determine protein concentration in the extracts.

2.6.3: Electrophoretic Mobility Shift Assay

Preparing the probe

An oligonucleotide containing the consensus motif for NFκB was prepared by annealing the two sequences:

5' CGA AGT TGA GGG GAC TTT CCC AGG C 3'

3' TCA ACT CCC CTG AAA GGG TCC G AGC 5'

Complementary single-stranded oligonucleotides were purchased from Invitrogen, each containing a CGA sequence tagged on at the 5' end. This was annealed to its complementary sequence, creating a three-base overhang. The overhangs were then filled in using the Klenow reaction and a radiolabelled nucleotide (dTTP-[^{32}P], Amersham Biosciences). A 1μg/μl stock of each strand was prepared in sterile water. A mixture of 10μl (from 1μg/μl stock) of each strand, 10μl 1M NaCl and 70μl sterile water was prepared, heated to 95°C for 5minutes and then allowed to cool at room temperature.

The annealed oligonucleotide (10ng/μl stock) was labelled with dTTP-[^{32}P]. A labelling reaction mix was prepared consisting of 2.5μl oligonucleotide stock (25ng/ml, Promega), 1.0μl non-labelled dNTPs (2.5mM x3), 5μl 10x Klenow buffer (Promega), 5μl 1M NaCl and 32.5μl distilled water. 3μl of dTTP-[^{32}P] was then added to the labelling reaction mix along with 1μl of the Klenow fragment of DNA polymerase I (2U/μl, Promega). The labelling reaction was incubated at room temperature for 20mins and the reaction stopped by the addition of 2μl EDTA (0.5M,

pH 8.0) and 50µl STE buffer (100mM NaCl, 10mM Tris-Cl and 1mM EDTA, pH 8.0). The radiolabelled probe was cleaned of any excess radioactivity using ProbeQuant G-50 micro columns (Amersham Biosciences).

Protein/probe binding reaction

A binding reaction mix was made up of 4µl 5x binding buffer (1µl 0.1M PMSF, 0.5µl 1M DTT, 10µl acetylated BSA (Sigma)) and 89µl 5x reaction buffer (50µl 1M HEPES, 250µl 1M KCl, 500µl 100% glycerol and 90µl water), 5µg nuclear protein extract, 1µl poly dI/dC (Amersham Biosciences) and the total volume made up to 18µl with distilled water. This mixture was incubated at room temperature for 10 minutes, 2µl of the [^{32}P]-labelled oligonucleotide probe was then added and the mix incubated for a further 20minutes.

EMSA gels

The samples were loaded onto a non-denaturing 6% polyacrylamide gel (for two mini-gels: 14.75mls water, 5mls 40% acrylamide stock, 2.5mls 5xTBE, 2.5mls 50% glycerol, 250µl 10% ammonium persulphate and 20µl TEMED). The gel had been pre-run at 300V for 30mins in 0.5% TBE (54g Tris-base, 27.5g boric acid, 20ml 0.5M EDTA and 1L H2O, pH 8.0) at 4°C. The samples were electrophoresed at 90V for 3-5 hours in 0.5% TBE at 4°C. Following electrophoresis, the gel was dried using a BioRad vacuum gel dryer for one hour at 70°C, and the dried gel exposed to an X-ray film (Hyperfilm, Amersham Biosciences) at -70°C for 6-48 hours.

Supershifts

To determine which subunits of NFκB were involved, supershift assays were carried out. When a specific antibody binds to the protein, it retards the movement of the DNA-protein complex through the resolving gel. Supershifts were carried out using antibodies specific to the five different subunits of NFκB (p65, p50, p52, c-Rel and RelB). 10 μg of the desired antibody (Santa Cruz Biotechnology Inc, Santa Cruz, CA, USA) was incubated with 5 μg of nuclear protein for 20 min at RT prior to the addition of the radiolabelled probe as per EMSA method. Samples were then run down a 4% non-denaturing acrylamide gel at 100 V for 6 hr at 4°C. Gels were then dried and exposed as described above.

2.7: RNA EXTRACTION AND ANALYSIS

2.7.1: Introduction

RT-PCR can be used to determine the relative concentration of specific mRNA present in the cell. The extracted RNA is converted into complementary DNA (cDNA) by reverse transcription. Random hexamers were used for the reverse transcriptase step. They randomly anneal to the RNA and provide a free 3'-hydroxyl group for reverse transcriptase, which is used as a starting point (figure 2.12). The cDNA is then used directly in PCR and specific primers can be used to amplifiy particular sections of genes of interest. The products of PCR are run on an agarose gel.

Figure 2.12: Reverse Transcription

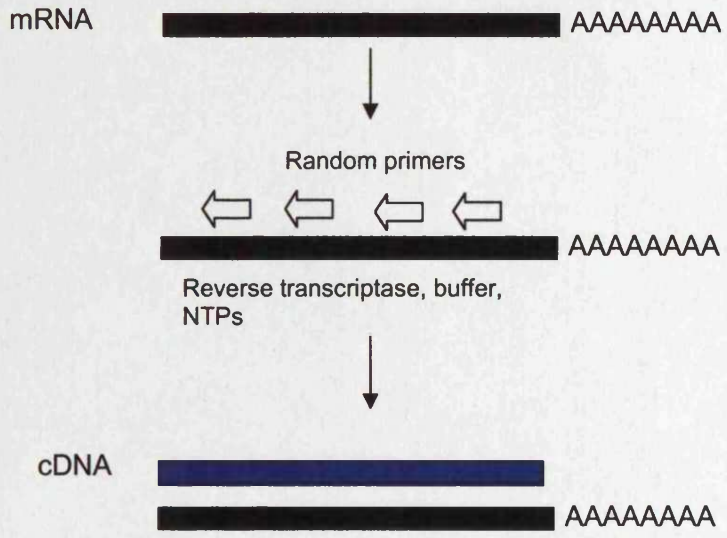

A diagram showing cDNA formation from mRNA [adapted from 259].

2.7.2: Cell lysis and RNA extraction

Total RNA was extracted from cells with 1ml of Tri-Reagent (Sigma) per well of 6-well plate and 0.2ml chloroform (Sigma) was added to induce phase separation. The thin, white middle layer contained DNA and the lower pink layer contained proteins. The sample was inverted to mix, incubated on ice for 5 minutes and then centrifuged at 13000rpm for 30 minutes at 4°C. The upper aqueous layer containing the RNA was removed and added to 0.5ml of ice-cold isopropanol and incubated overnight at -20°C to induce RNA precipitation. The samples were centrifuged (Hawk 15/05, Sanyo) at 13000rpm for 30 minutes at 4°C to pellet the RNA. The supernatant was discarded and the pellet washed by resuspending in 0.5ml 70% cold ethanol, followed by centrifugation at 13000rpm for 20 minutes at 4°C. After aspiration of the ethanol, the pellet was air dried for 1 hour in a fume hood before being dissolved in 10µl sterile water.

Measurement of RNA quality and quantity

RNA was quantified by its UV absorbance at 260nm. One µl of RNA was diluted in 99µl of sterile water and absorbance was measured in a Beckman DU 64 single beam spectrophotometer (Beckman Instruments). RNA purity was confirmed by an OD 260:280 ratio greater than 1.5. Where necessary, the purity and integrity of the RNA was confirmed by electrophoresis of 1µg samples in a 1% agarose gel containing ethidium bromide. RNA was quantified using the following equation:

$(A^{260}x100x40)/1000 =$ (A) µg/µl of RNA

1/ (A) = (B) µl for one µg RNA

2.7.3: Reverse Transcription-Polymerase Chain Reaction

Reverse Transcription

Purified RNA samples diluted to 1µg of RNA in a total volume of 10µl made up with sterile water were used for cDNA synthesis. The reaction mixture contained 1µl random hexamers (100µM, Pharmacia Biosystems), 5µl dNTPs (2.5mM, Invitrogen), 2µl 10xPCR Buffer (Applied Biosystems), 2µl Dithiothreitol (100mM, GIBCO) and 1µg RNA in sterile 0.2ml PCR tubes. The reverse transcription program was performed in a GeneAmp PCR System 9700 Thermocycler (PE Applied Biosystems), with incubation for 5 minutes at 95°C followed by rapid cooling on ice. Once cool, 1µl Superscript Reverse Transcriptase (200U/µl), Gibco) and 1µl RNAsin (400U/µl, Promega) were added per tube. The samples were returned to the cycler and annealed at 25°C for 10 minutes, followed by cDNA synthesis at 42°C for 60 minutes and finally sample denaturation at 95°C for 5 minutes. The resulting single stranded complementary DNA (cDNA) was stored at -20°C until PCR amplification.

Polymerase Chain Reaction

The PCR reaction mix (final volume 50µl) was prepared as follows: 2µl cDNA was added to 48µl master mix: 36.25µl sterile water, 1.25µl of each primer (listed in table 2.3) in pair (20mM), 4µl dNTPs, 5µl PCR 10x buffer and 0.25ul Taq Polymerase (10U/µl amplitaq gold, Applied Biosystems). PCR amplification was carried out using a GeneAmp PCR System 9700 thermocycler. PCR reactions were performed over a range of cycle numbers to ensure that the samples were assessed in the linear phase of product amplification. The PCR programme used was as follows:

1) Pre-PCR: 94°C, 10 mins → 72°C, 10mins

2) **X** cycles: 94°C, 40seconds → 55°C, 1minute → 72°C, 1 minute

3) Post-PCR: 94°C, 40seconds → 60°C, 10 minutes → 4°C, ∞

The final range of cycle number for experimental samples was 30-35 and 26 for the housekeeping gene, β-actin. The negative control consisted of a reaction containing water instead of cDNA (-PCR).

Table 2.3: RT-PCR Primers

Primer		Sequence	Product size
Smad 7	F	5' CCA ACT GCA GAC TGT CCA GA 3'	430bps
	R	5' AAC CAG GGA ACA CTT TGT GC 3'	
Bcl-x	F	5' GCG GTA CCG GAG AGC AT 3'	Bcl-xL 395bps
	R	5' TGA AGA GTG AGC CCA GCA GAA 3'	Bcl-xS 206bps
Caspase-3	F	5' TGC GGT ATT GAG ACA GAC AG 3'	359bps
	R	5' AAC ATG CCC CTA CCC CAC TC 3'	
Bax	F	5' ATC ATG GGC TGG ACA CTG GAC TTC 3'	155bps
	R	5' ATG GTG AGC GAG GCG GTG AGG AC 3'	
Bcl-2	F	5' TCC TTC CAG CCT GAG AGC AAC C 3'	491bps
	R	5' GAC AGC CAG GAG AAA TCA AAC AGA 3'	
TSP-1	F	5' AAC CAG GCC GAC CAC GAT AAA GAT 3'	446bps
	R	5' TAC CCG AAA ACA AAG CCA GCA TAG 3'	
B-actin	F	5' GGA GCA ATG ATC TTG ATC TT 3'	204bps
	R	5' CCT TCC TGG GCA TGG AGT CCT 3'	
PSR	F	5' CTG AAT TCA AAC CCC TGG A 3'	146bps
	R	5' TAC CGT CTT GTG CCA TAC C 3'	

RT-PCR gels

10μl of amplified cDNA was mixed with 3μl Orange G loading buffer and separated by electrophoresis on a 1.5% agarose gel (Flowgen Instruments Ltd,

Sittingbourne, UK) in 50ml 1x TAE buffer. Ethidium bromide (5µl of 1mg/ml, Sigma) was added to the molten gel prior to casting. 123 base pair ladder (Invitrogen) was run alongside the samples to confirm that PCR products were of the expected size. The gel was run at 100V until the loading buffer had run the full length of the gel. PCR products were visualised under ultraviolet light and digital images were captured and analysed (Chemidoc System and Model 620 video densitometer, BioRad). All of the reactions generated a single product of the expected size and the negative controls did not give detectable products in any of the experiments performed.

2.8: TRANSFECTION

2.8.1: Plasmid preparation

A range of plasmids were acquired for these experiments (table 2.4):

Table 2.4: Plasmids

Plasmid	*Source*	*Other information*
Smad2 DN	A kind gift from Dr. Wrana, Toronto, Canada.	REs*: SalI and XbaI
Smad3 DN	A kind gift from Dr. Wrana, Toronto, Canada.	REs*: ClaI and XbaI
Smad7 OE	A kind gift from Dr. Wrana, Toronto, Canada.	REs*: EcoRI and XbaI Insert 2.9kb
Empty pCMV5 vector	A kind gift from Dr. Wrana, Toronto, Canada.	Control for Smad-2, -3 and -7 vectors.
B-galactosidase	Promega	Constitutively active control plasmid
CAGA	Dr. Aristidis Moustakos	4 Smad binding elements – luciferase construct. TGFβ1 responsive plasmid.

*RE: restriction enzymes

Plasmids from other investigators were received dried onto filter paper. The spot containing the plasmid was excised and rehydrated in 50µl sterile water. 5µl of this

solution was added to 40µl of competent E.coli (JM109 strain, Promega) and left on ice for 30 minutes and then placed in a 42°C waterbath for 45 seconds. It was incubated on ice again for a further 5 minutes. 150µl of liquid SOC medium (2g tryptone, 0.5g yeast extract, 0.05g NaCl, 1ml 250mM kCl, 50ml H_2O, autoclave and adjust pH to 7.0, add 0.36g glucose, 0.5ml 2M $MgCl_2$ and adjust volume to 100ml) was added to the tube and the cells were incubated at 37°C in an orbital shaker (220rpm) for 1.5 hours. The bacteria were grown on YT (16g bacto-tryptone, 10g yeast extract, 5g NaCl, 16g agar 1L H_2O, autoclave) agar plates containing 100µg/ml carbenicillin overnight. A single colony was picked and grown in 5ml liquid YT medium and carbenicillin (final concentration 100µg/ml) in a sterile tube overnight in the orbital shaker at 37°C, 220rpm. To make sure that the bacteria from that colony had been transformed, the plasmid was extracted and purified using the Miniprep kit (QIAGEN). The DNA was digested with specific restriction enzymes and the product run on a 1.5% agarose gel to check for digested DNA.

The bacteria were grown in 50 ml YT medium and carbenicillin in a 500ml flask overnight in the orbital shaker at 37°C. The plasmid was then extracted and purified using the Midiprep kit (QIAGEN). Plasmid DNA was diluted to a stock concentration of 1µg/µl in sterile water and stored at -20°C before use in experiments. Stocks of bacteria transformed with each plasmid were prepared in 30% glycerol/70% LB medium (10g bacto-tryptone, 5g yeast extract, 10g NaCl, 1L H_2O, autoclave) and stored at -70°C until needed. When required, 20µl was added to 50ml YT medium containing carbenicillin overnight in the orbital shaker as above.

2.8.2: Transient transfection

HK2 cells

HK-2 cells from a confluent T75 cm^2 flask were collected by trypsin treatment. After resuspension of the cells in 50 ml growth medium (supplemented with 10% FCS), they were plated out into 6-well plates, 2ml of the cell suspension per well. Cells were then grown to approximately 70% confluence prior to transfection.

Transient transfection of HK-2 cells was performed using FuGENE 6. Initial characterisation experiments determined that a ratio of 3 µl FuGene to 1 µg DNA was optimal for transfection into HK-2 cells seeded in 6-well plates [260]. With the cells at 70% confluence, the growth medium was removed and the cells were washed twice with PBS. They were then transfected with 1 µg of the required promoter construct, and 1 µg of the β-galactosidase vector. The β-galactosidase vector was used to determine transfection efficiency. The transfection was carried out in serum-free HK2 medium for 24 hours. After this time, the medium was replaced with conditioned medium from the mesangial cells for 24 hours.

Mesangial cells

Transient transfection of mesangial cells was performed using the mixed lipofection agent Fugene 6 as described above for HK2 cells. Another method using GeneJuice transfection reagent was also used for mesangial cells. The cells were grown to 60% confluence prior to transfection. A 3:1 ratio of GeneJuice to plasmid was used to a total volume of 100µl per well. GeneJuice was incubated in serum-free media a RT for 5minutes in a 1.5ml eppendorf, followed by addition of 1µg of plasmid for 10minute incubation at RT. 100µl of this mixture was added to 2ml of

medium containing 10% FCS in each well. This was incubated for 8hrs, after which time the medium was removed and serum-free media was used to induce apoptosis. Apoptosis was quantified using flow cytometry and transfection efficiency was checked by Western Blot (the plasmids contained a c-myc-tag).

2.8.3: Reporter gene analysis

Reporter gene analysis

The media was removed and the cells were washed with PBS before the addition of 500 µl of Reporter lysis buffer (Promega) per well. The cells were then incubated at RT for 15 min with gentle agitation, to detach the cell monolayer. The remaining adhered cells were detached using a cell scraper, and the cell suspensions were transferred to 1.5 ml centrifuge tubes, followed by vortexing for 10 seconds.

Luciferase activity was measured using the Bright-Glo luciferase assay kit (Promega). In the luciferase assay system, the functional enzyme is created immediately upon translation and the assay is rapid, reliable and easy to perform. Firefly luciferase is a 61kDa monomer that catalyses the oxygenation of beetle luciferin, producing light. Fifty µl of each sample was transferred to a white 96-well luminometric plate. Fifty µl of Bright-Glo was added to each sample and the luminescence of each sample recorded for 10 seconds using a luminometer (FLUOSTAR Optima, BMG Labtechnologies GmbH, Offenburg, Germany).

B-galactosidase assay

The β-galactosidase plasmid is constitutively active and can therefore be used to correct the results for transfection efficiency. Fifty µl of cell lysate was added to 2x

buffer assay in duplicate and this was incubated at room temperature for 30minutes. The buffer assay contains the substrate *O*-nitrophenyl-β-*D*-galactopyranoside (ONPG, Sigma-Aldrich). During the incubation, the β-galactosidase hydrolyses the colourless substrate to *o*-nitrophenyl, which is yellow. The reaction was then blocked with 100µl 1M Na2CO3 per well and the absorbances read with a plate reader at 420nM.

2.9: Statistical analysis

Mann-Whitney Test

The Mann-Whitney was used to calculate significance for all data. This is non-parametric test used to compare two independent groups of sampled data. Unlike the parametric t-test, the Mann-Whitney does not make assumptions about the distribution of the data (e.g., normality). This, like many non-parametric tests, uses the ranks of the data rather than their raw values to calculate the statistic. Since this test does not make a distribution assumption, it is not as powerful as the t-test (http://www.texasoft.com/winkmann.html).

CHAPTER 3:
THE ROLE OF GLUCOSE IN MESANGIAL CELL APOPTOSIS

CHAPTER 3: THE ROLE OF GLUCOSE IN MESANGIAL CELL APOPTOSIS

3.1: Introduction

There is clear evidence of a positive relationship between hyperglycaemia and susceptibility to renal disease in diabetes mellitus [49]. A direct role for glucose in diabetic nephropathy has been suggested by cell culture studies showing glucose can induce cell hypertrophy, ECM synthesis and TGFβ1 production in a variety of cell types [6]. Numerous *in vitro* studies have suggested that elevated concentrations of glucose modify mesangial cell function [12, 44, 55].

Increasing mesangial cell number has been documented in the incipient phase of nephropathy, with a direct correlation between mesangial cell number and AERs [34]. This relationship between mesangial cell number is however lost in patients with overt nephropathy and proteinuria. In overt nephropathy, expansion of the mesangial matrix, mesangial cell loss and glomerular sclerosis are prominent [29, 33]. Loss of mesangial cells through apoptosis occurs in experimental DN and correlates with worsening of albuminuria [36, 37].

Altering glucose concentration may regulate cell number, although its effects on apoptosis are cell-specific. High glucose causes cell death in many cell types – myocardial cells [262], preimplantation blastocysts [263], neural tubular cells [264], endothelial cells [265], retinal microvasular cells [266] and Schwann cells in development [267]. However, it has also been reported to inhibit cell death through

protein kinase C in vascular smooth muscle cells [268]. Several studies have shown that high glucose induces mesangial cell apoptosis [37, 182, 185]. In kidney cells, high glucose has been shown to downregulate Bcl-2 and Bcl-x mRNA expression and increase Bax mRNA expression [181].

The transcription factor NFκB is a critical immediate early response gene involved in modulating cellular responses and NFκB plays a complex role in apoptosis since it has been found to depend on the cell type. Some studies have implicated NFκB in promoting apoptosis in certain cells [136, 137]. Conversely several reports provide convincing evidence that NFκB is involved in inhibition of apoptosis [223, 269-271]. Recent studies have demonstrated that activating NFκB prior to injury was anti-apoptotic only following stimuli dependent on tyrosine kinase activation of IκBα, but not IKK-dependent serine phosphorylation of IκBα. This therefore suggests that cell fate may be not only be dependent on the cell type but also on the pathway mediating regulation of NFκB [142].

Therefore, the aim off the work described was to study the effect on high glucose on mesangial cell apoptosis and to investigate the pathway involved. The aims of this chapter were to:

1. Use various methods to quantify apoptosis induced by serum deprivation.
2. The effect of 25mM glucose on mesangial cell apoptosis induced by serum deprivation.
3. The effect of serum-deprivation and 25mM glucose on Bcl-2, Bax and Bcl-x mRNA and protein expression.
4. The effect of serum-deprivation and 25mM glucose on NFκB activity.

5. The effect of NFκB inhibition on mesangial cell apoptosis and the mechanism.

3.2: Results

3.2.1: Serum withdrawal induced apoptosis in mesangial cells

Mesangial cells were cultured in either 5mM or 25mM glucose medium containing 10-0% FCS for 72 hours. Apoptosis was quantified by measuring phosphatidylserine exposure on the mesangial cells (figure 3.1). A dose-dependent increase in apoptosis was seen when the concentration of FCS in the culture medium was decreased. This increase in apoptosis was more pronounced in cells cultured in high glucose medium at all concentrations of FCS, except 10%.

Therefore, this result suggests that upon removal of serum, mesangial cells are prone to apoptosis and cells cultured under 25mM glucose conditions are more sensitive to cell death-inducing stimuli.

Figure 3.1: Apoptosis induced by serum withdrawal is augmented by high glucose

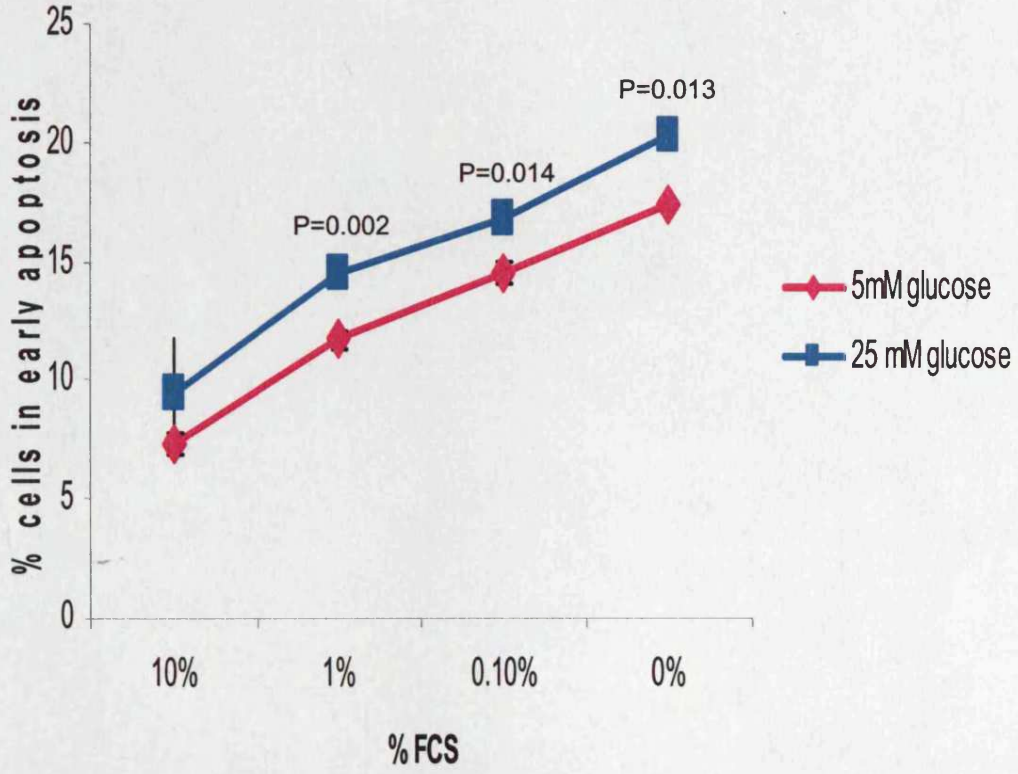

Rat mesangial cells were grown to confluence, followed by growth in 5mM D-glucose or 25mM D-glucose, containing the appropriate amount of FCS for 72 hours. Apoptosis was quantified using the annexin-v/PI flow cytometry assay. The mean % of cells in early apoptosis is plotted ± S.E., n=3 and * denotes significance. The corresponding FACS plots are shown below.

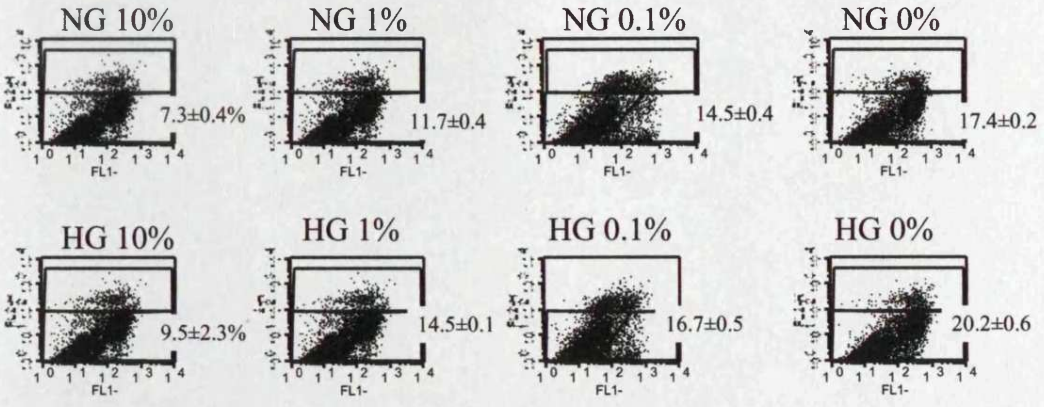

3.2.2: 25mM D-glucose augmented mesangial cell apoptosis induced by serum deprivation

To determine the effect of high glucose concentration on mesangial cell survival, confluent mesangial cells were cultured in serum-free medium containing 5mM or 25mM D-glucose for up to 72hrs. The effect of elevated glucose concentrations on apoptosis was established using three different methods to quantify and confirm apoptosis.

Apoptosis confirmed by measuring phosphatidylserine exposure at the cell surface: Apoptotic cells were identified by exposure of phosphatidylserine at the cell surface using annexin V conjugated to fluorescein isothiocyanate (FITC), in conjunction with propidium iodide (PI) to distinguish apoptotic cells (Annexin V-FITC positive, PI negative) from necrotic cells (Annexin V-FITC positive, PI positive) (figure 3.2).

Using this method, there was an increase in apoptotic cells cultured in 5mM glucose medium for up to 72 hours. This increase was more prominent, however, in cells cultured in 25mM glucose medium. Exposure of mesangial cells to 25mM D-glucose under serum free conditions for 72 hours led to a significant increase in the number of cells in early apoptosis as compared to cells exposed to 5mM D-glucose for the same time (29.1±0.05% apoptosis in cells cultured in 25mM glucose, compared to 21.9±1.05 in cells cultured in 5mM glucose, $p=0.002$).

The effects of high glucose are specific: To distinguish between specific glucose-mediated effects and non-specific osmolar effects, mesangial cells were cultured in serum-free media containing 5mM D-glucose, L-glucose (made up of 5mM D-

glucose and 20mM L-glucose) or 25mM D-glucose for 72 hours (figure 3.3). Addition of L-glucose increased osmolarity outside the cell, but not inside and has been used as an osmolar control in the past [Singh & Crook, Am J Physiol Renal Physiol (2000) 279:F646-F654]. L-glucose cannot be metabolised by cells. These results showed that there was no increase in apoptosis with L-glucose, compared with 5mM D-glucose. This suggests that the increase in cell death is not an osmolar effect of glucose.

Quantification of apoptosis by measuring mitochondrial membrane disruption: Cellular energy produced during mitochondrial respiration is stored as an electrochemical gradient across the mitochondrial membrane, creating a mitochondrial transmembrane potential. Disruption of this potential is one of the first intracellular changes following the onset of apoptosis. DePsipher^{TM} is a lipophilic cation (5,5', 6, 6'-tretrachloro-1,1'3,3'-tetraethylbenzimidazolyl carbocyanine iodide) which can be used as a mitochondrial activity marker. This method was also used to detect early apoptosis (figure 3.4).

By DePsipher flow cytometry assay, exposure of mesangial cells to 5mM glucose led to an 1.5-fold increase in apoptosis at 48 hours, compared to 0 hours. After 72 hours, the increase in apoptosis compared to 0 hours was 1.25-fold. Culturing the mesangial cells in high glucose amplified this affect. After culturing the cells in high glucose, the increase in apoptosis was 2.8-fold, compared to 0 hours and a 1.8-fold increase in apoptosis after 72 hours. Cells cultured in 25mM glucose had a significantly higher number of apoptotic cells compared to cells cultured in 5mM glucose at the 48 hours ($p=0.04$) and 72 hours ($p=0.029$) time-points.

Quantification of apoptosis by measuring caspase-3 concentration: A commercially available caspase-3 assay was used to measure the amount of active caspase-3 (figure 3.5). Caspase-3 in the most downstream execution enzyme involved in apoptosis. Activation of capase-3 is controlled by proteolytic cleavage of the inactive, full-length protein by other caspases. The increase in caspase-3 activity in cells cultured in 25mM glucose is first apparent at 48 hours where there was a 2.1-fold increase in apoptosis in cells cultured in 25mM glucose compared to a 1.6-fold increase with 5mM glucose. The differences become statistically significant at 72 hours where there is a 2-fold increase in caspase-3 activity with 25mM glucose compared to a 1.5-fold increase with 5mM glucose ($p=0.003$).

The caspase-3 western blot was another method of measuring the concentration of active caspase-3 (figure 3.6). In the mesangial cells cultured in 25mM glucose medium, there was significantly more active caspase-3 compared to the mesangial cells. These differences were clear after 48 hours of cell culture in 25mM glucose, when the cleaved products of caspase-3 became visible..

Both of these results suggest that mesangial cells cultured in high glucose have higher levels of active caspase-3 and therefore undergo more apoptosis compared to mesangial cells cultured under normal glucose conditions.

In conclusion, all three methods of quantifying apoptosis suggest that cells cultured in 5mM glucose undergo apoptosis in a time-dependent manner when deprived of serum. Culturing mesangial cells in 25mM glucose augments this effect.

Figure 3.2A: Flow cytometry analysis of phosphatidylserine exposure (rat cells)

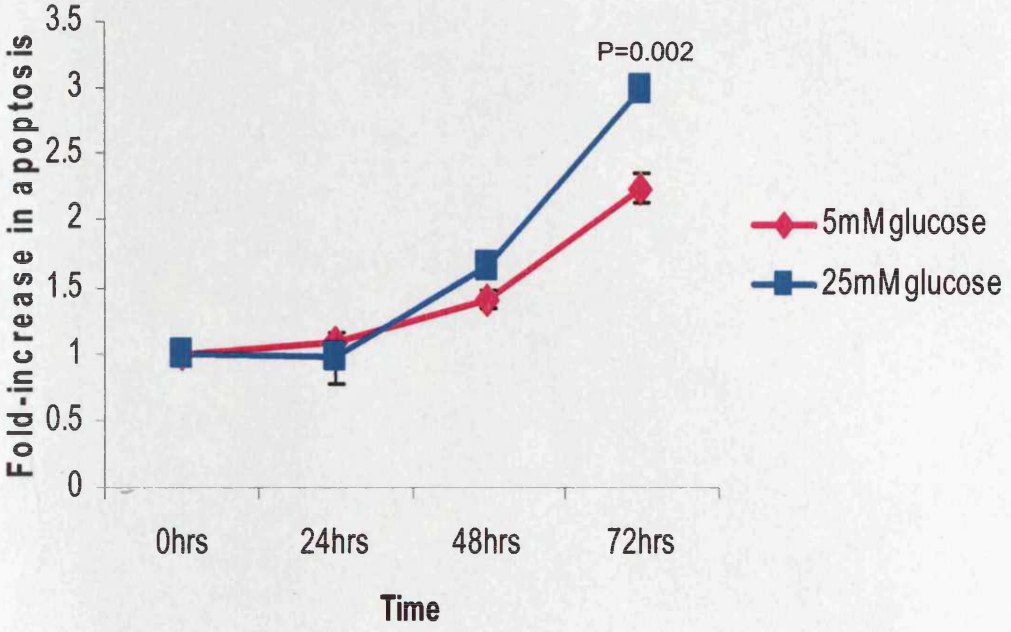

Mesangial cells were grown to confluence and, subsequently, apoptosis was induced by serum-deprivation either in the presence of 5mM D-glucose or 25mM D-glucose. At the time points indicated, apoptotic cells were identified by flow cytometry using annexin V conjugated to fluorescein isothiocyanate (FITC), in conjunction with propidium iodide (PI) to distinguish apoptotic cells (Annexin V-FITC positive, PI negative) from necrotic cells (Annexin V-FITC positive, PI positive). The figure shows the results presented graphically as the fold-increase of cells in early apoptosis, compared to 5mM glucose at 0 hrs (cells cultured in 5mM glucose medium containing 10% F|CS), and represent the mean ± S.E. of 6 individual experiments * denotes significance.

The corresponding FACS plots are on the next page.

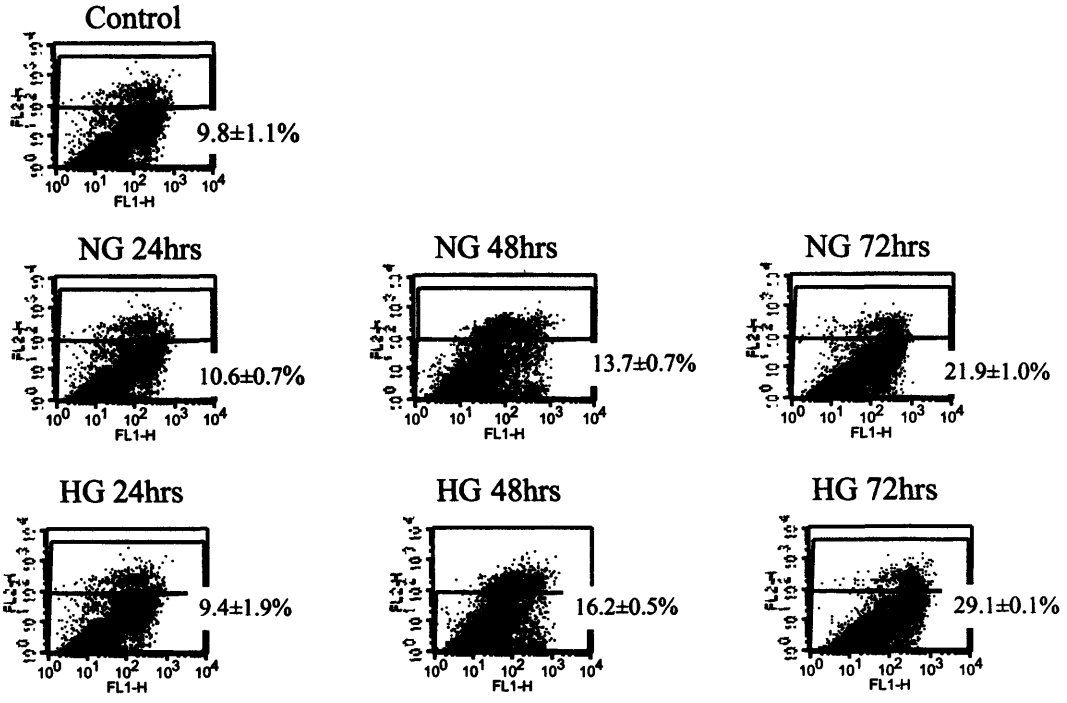
Control
9.8±1.1%
NG 24hrs
10.6±0.7%
NG 48hrs
13.7±0.7%
NG 72hrs
21.9±1.0%
HG 24hrs
9.4±1.9%
HG 48hrs
16.2±0.5%
HG 72hrs
29.1±0.1%
FL1-H

Figure 3.2B: Flow cytometry analysis of phosphatidylserine exposure (primary human cells)

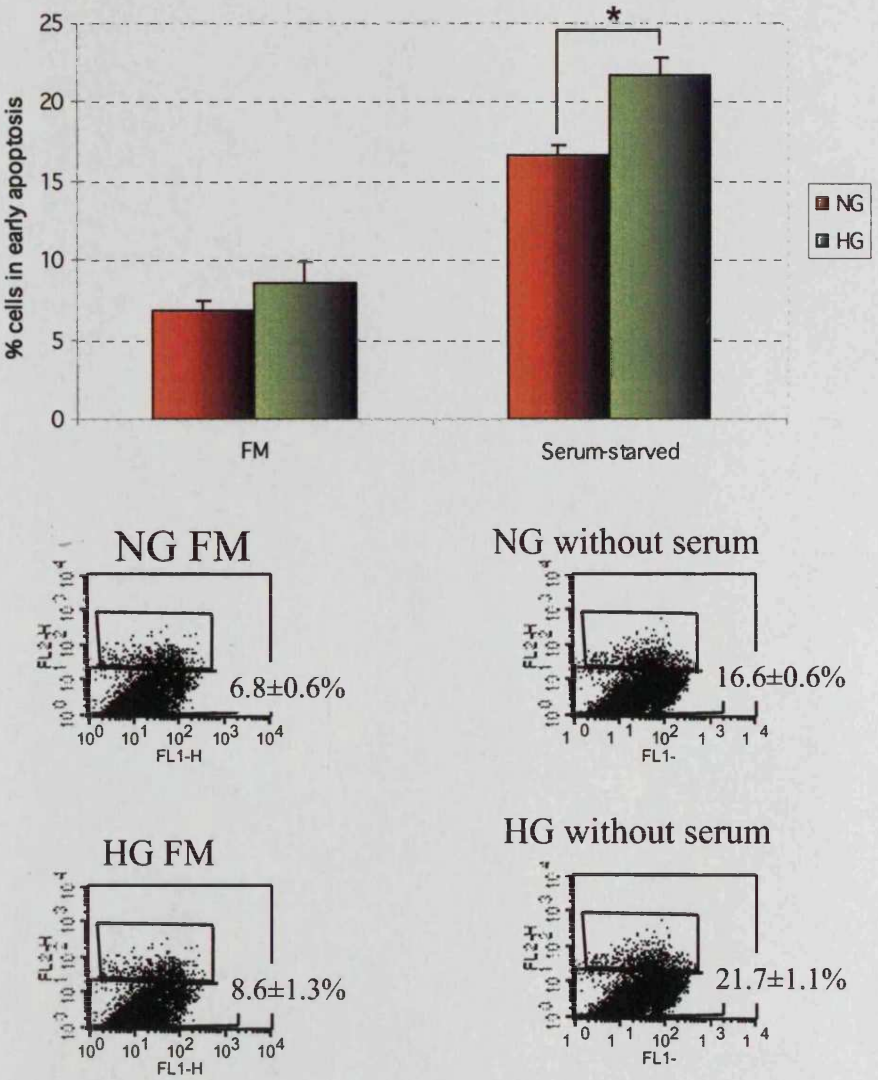

Mesangial cells were grown to confluence and, subsequently, apoptosis was induced by serum-deprivation either in the presence of 5mM D-glucose or 25mM D-glucose for 72hrs. The control cells were cultured in media containing serum (FM). The apoptotic cells were identified by flow cytometry using annexin V conjugated to fluorescein isothiocyanate (FITC), in conjunction with propidium iodide (PI) to distinguish apoptotic cells (Annexin V-FITC positive, PI negative) from necrotic cells (Annexin V-FITC positive, PI positive). The figure shows the results presented graphically as the fold-increase of cells in early apoptosis and represent the mean ± S.E. of 3 individual experiments * denotes significance. The corresponding FACS plots are shown below the graph.

Figure 3.3: L-glucose has no effect on apoptosis

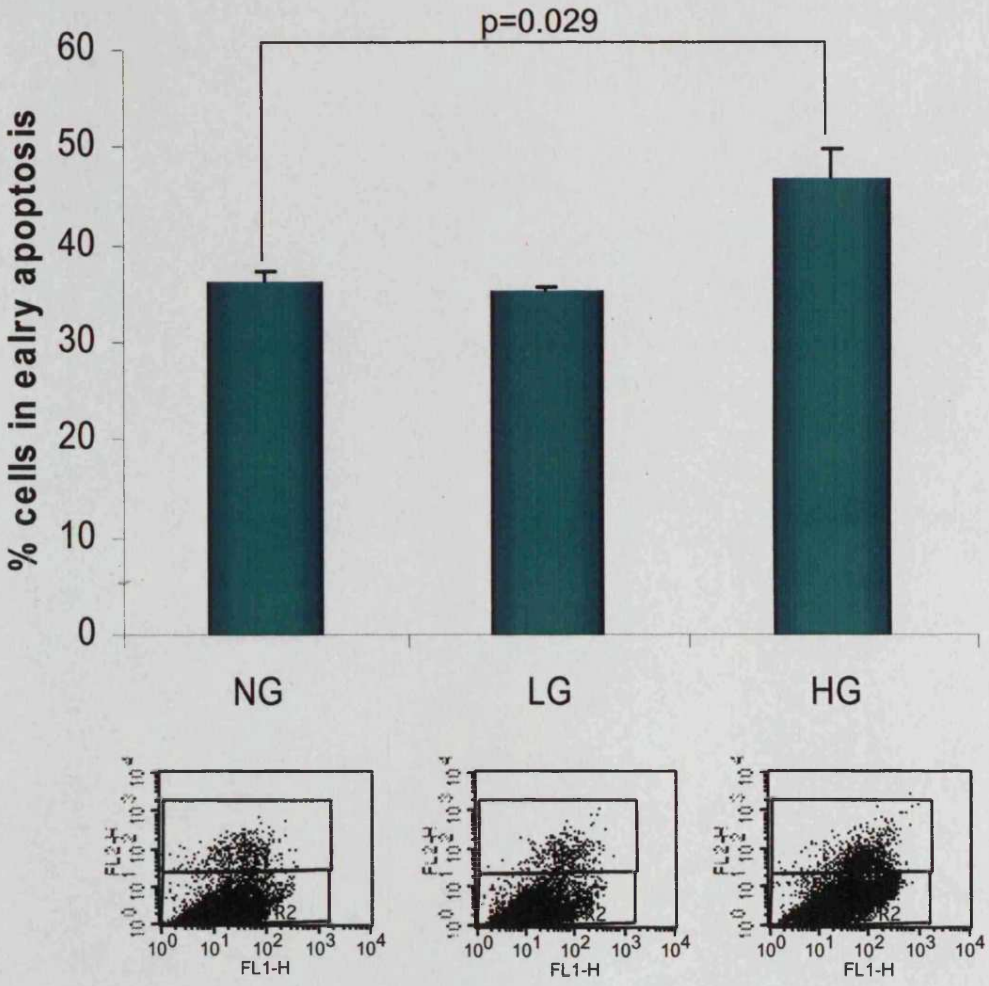

Mesangial cells were grown to confluence and, subsequently, apoptosis was induced by serum-deprivation either in the presence of 5mM D-glucose (NG), 25mM L-glucose (LG) (made up by adding L-glucose to 5mM D-glucose medium to obtain a final concentration of 25mM glucose) or 25mM D-glucose (HG) for 72 hours. Apoptotic cells were identified by flow cytometry using annexin V-FITC, in conjunction with PI. The figure shows the results presented graphically as the % of cells in early apoptosis and represent the mean ± S.E. of three individual experiments * denotes significance. Below the graph are the corresponding FACS plots.

Figure 3.4: Measuring changes in the mitochondrial membrane potential

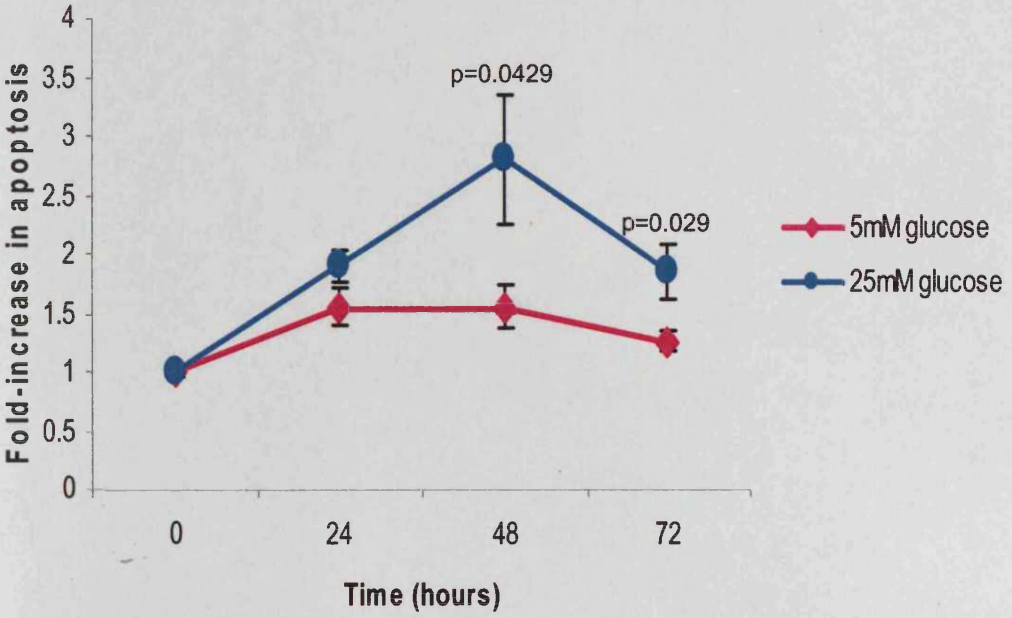

Rat mesangial cells were grown to confluence and then apoptosis induced by serum-deprivation either in the presence of 5mM D-glucose or 25mM D-glucose. At the time points indicated, apoptotic cells were identified by flow cytometry using the DePsipher flow cytometry assay. The results are presented graphically as a fold-increase in apoptosis, compared to 5mM glucose at 0 hours (cells cultured in 5mM glucose containing 10% FCS) and represent the mean ± S.E. of 6 individual experiments * denotes significance. The corresponding FACS plots are shown on the next page.

Control

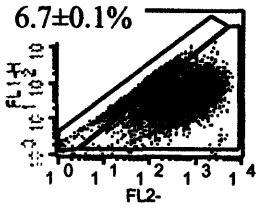

NG 24hrs

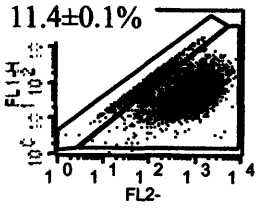

NG 48hrs

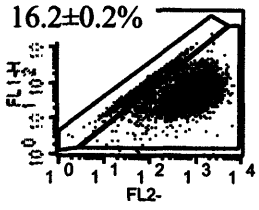

NG 72hrs

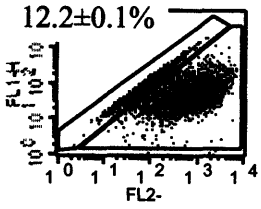

HG 24hrs

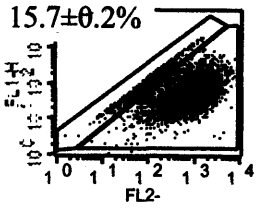

HG 48hrs

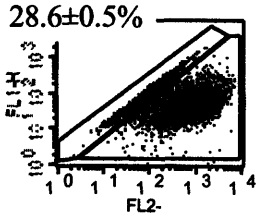

HG 72hrs

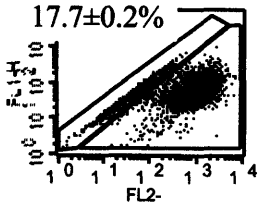

Figure 3.5A: Quantification of active Caspase-3 (rat cells).

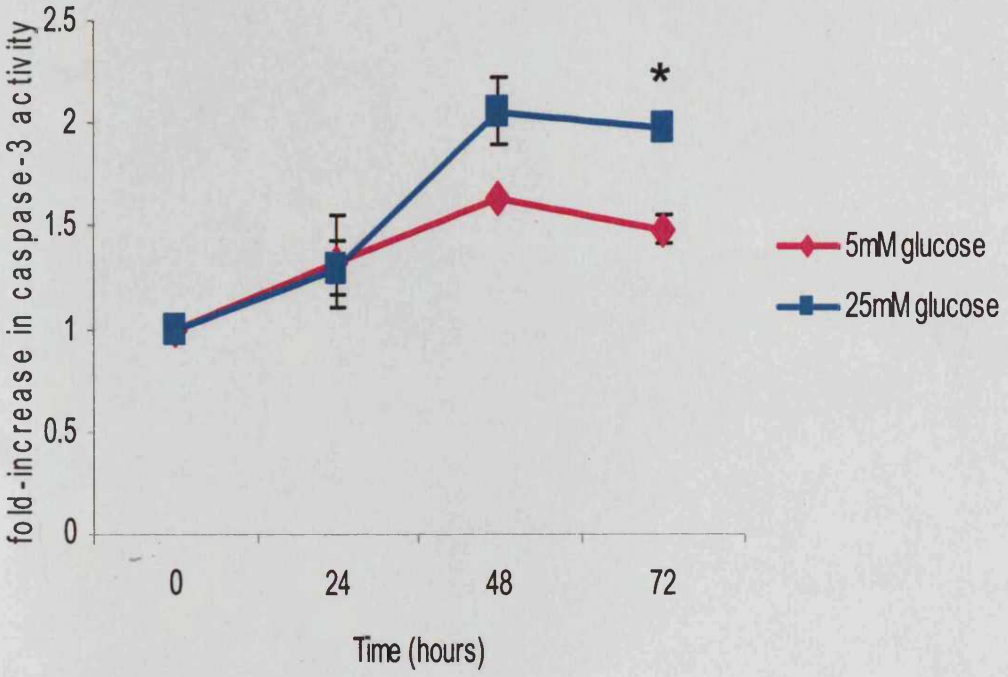

Apoptosis was induced by serum-deprivation either in the presence of 5mM D-glucose or 25mM D-glucose. At the time points indicated, the amount of active caspase-3 was measured in a rat mesangial cell line using the caspase-3 assay. The mean results are plotted graphically ± S.E., n=3 and * denotes significance.

Figure 3.5B: Quantification of active Caspase-3 (primary human cells).

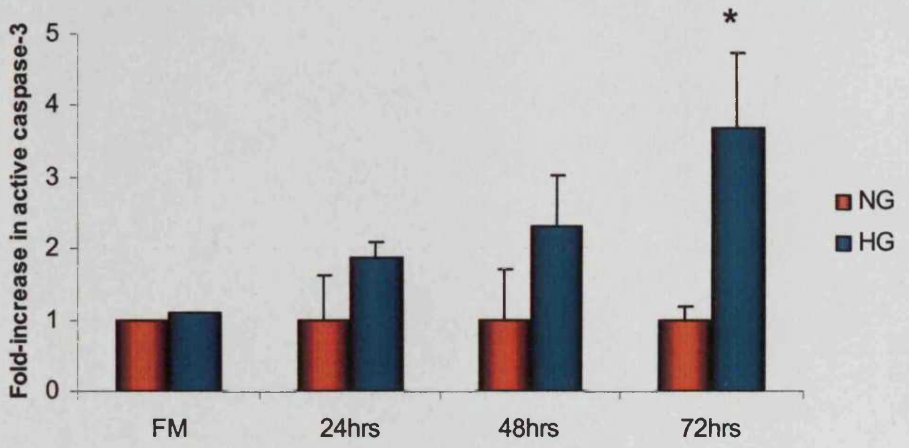

Apoptosis was induced by serum-deprivation either in the presence of 5mM D-glucose or 25mM D-glucose. At the time points indicated, the amount of active caspase-3 was measured in a primary human mesangial cells using the caspase-3 assay. The mean results are plotted graphically ± S.E., n=3 and * denotes significance.

Figure 3.6: Western blot analysis showed mesangial cells cultured in 25mM glucose express increased amounts of caspase-3

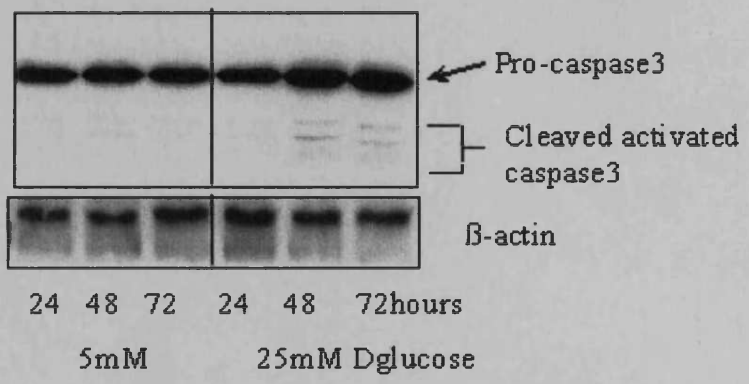

Apoptosis was induced by serum-deprivation either in the presence of 5mM D-glucose or 25mM D-glucose. At the time points indicated, the amount of active caspase-3 was measured in a rat mesangial cell line using Western blot analysis. Western blot analysis showed expression of the full length, inactive caspase-3 protein (35kDa) and the cleaved, active protein. 100µg of protein was loaded per well. Equal loading of gels was confirmed by re-probing the membranes for β-actin. This figure shows a typical result of three experiments.

3.2.3: Glucose induced apoptosis – Role of the Bcl-2 family

Culturing mesangial cells in serum-free 5mM glucose media lead to apoptosis and this effect was augmented by high glucose. To determine if the mechanism for both pathways was the same, the expression of the Bcl-2 protein family was studied.

Bcl-2:Bax ratio

The bax:bcl-2 ratio has been shown to be a critical factor in activating caspase-3 [272]. To examine the potential mediators of glucose induced apoptosis, the relative mRNA expression of the Bcl-2 related proteins, Bcl-2 and Bax was analysised. Confluent cells were exposed to either 25mM D-glucose or 5mM D-glucose under serum free conditions for up to 72hours. Total mRNA was isolated at the indicated time points and Bcl-2 and Bax mRNA expression examined by RT-PCR (figure 3.7A).

Under serum free conditions, no change in Bax mRNA expression was seen. In contrast, serum deprivation in mesangial cells cultured in 5mM glucose led to a reduction in Bcl-2 expression. The decrease in Bcl-2 mRNA expression was significantly more pronounced when cells were exposed to 25mM D-glucose at all time-points. The mesangial cells cultured in full medium contained the highest amount of bcl-2 mRNA expression.

Consequently there was a significantly greater increase in the Bax:Bcl-2 mRNA ratio in the cells exposed to 25mM D-glucose as compared to those exposed to 5mM D-glucose (figure 3.7B). After 72 hours, there was a two-fold increase in the Bax:Bcl-2 mRNA ratio in cells cultured in 25mM glucose compared to 5mM glucose. In all

experiments, the housekeeping gene ß-actin was used to ensure equal loading of the gels.

The changes in Bcl-2 and Bax protein expression were also measured by western blot (figure 3.8). There was no change in Bax protein expression. The membrane was then stripped and re-probed for Bcl-2. Despite trying two different anti-Bcl-2 antibodies at various dilutions (the most concentrated being 1:10), neither worked. The ratio between the Bcl-2 and Bax proteins could therefore not be determined. Previous reports have shown that there is no difference between Bax and bcl-2 mRNA and protein expression [272].

Changes in Bcl-x expression

The Bcl-x gene gives two products – Bcl-xL and Bcl-xS, a shorter, alternatively spliced form. Bcl-xL is a cell survival factor whereas Bcl-xS is a pro-apoptotic protein. The mRNA expression of the Bcl-x proteins was measured by RT-PCR (figure 3.9). There was no change in Bcl-xL expression over 72 hours and no difference between cells cultured in 5mM glucose and 25mM glucose. The Bcl-xS product was not detectable at 33 or 35 cycles.

These results suggest that the Bcl-x gene may not have a role in mesangial cell apoptosis induced by serum-deprivation over 72 hours.

Figure 3.7: High glucose reduces Bcl-2 mRNA expression

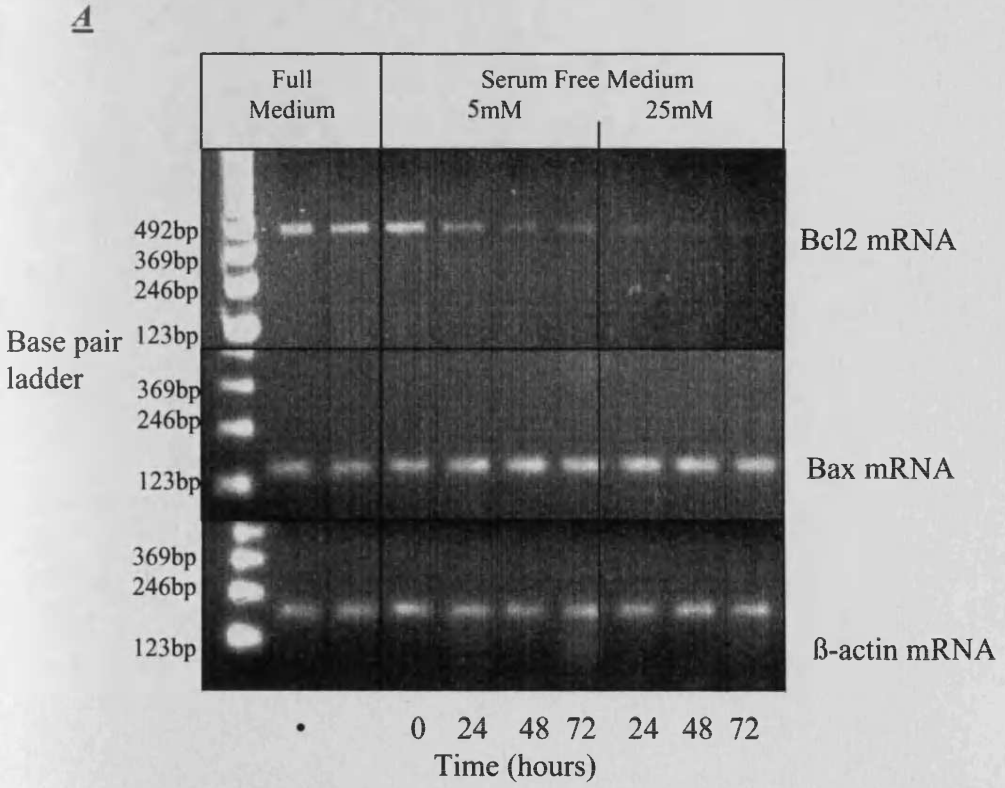

Mesangial cells were grown to confluence. Subsequently apoptosis was induced by serum-deprivation either in the presence of 5mM D-glucose (NG) or 25mM D-glucose (HG). At the time points indicated total RNA was isolated and RT-PCR performed. Ethidium bromide stained PCR products were separated on a 3% agarose gel. For Bcl2 and Bax, amplification was performed for 33 cycles. PCR amplification for ß-actin (lower panel) was performed for 26 cycles.

B

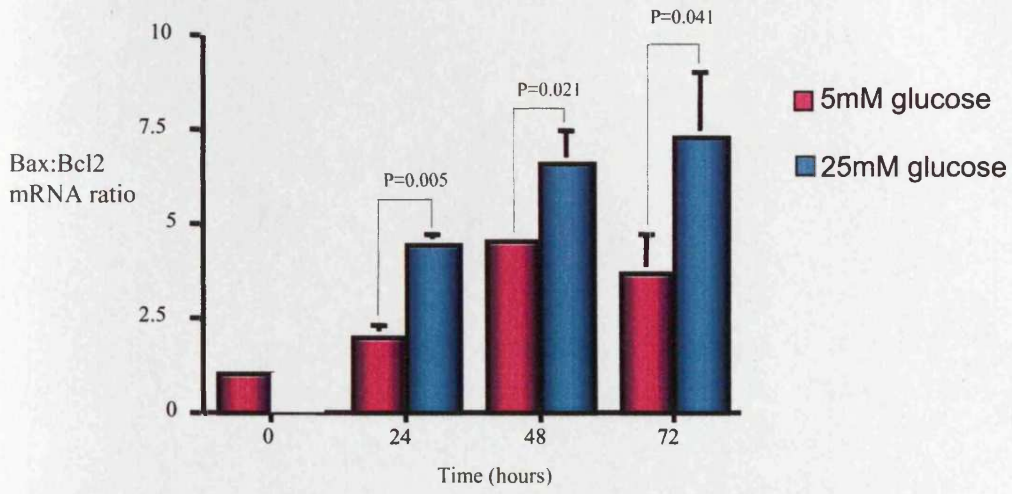

Scanning densitometry of three individual experiments was performed, and the results expressed as the mean ± S.E. ratio of Bcl2:Bax mRNA corrected at each time point for the house keeping gene ß-actin.

Figure 3.8: Bax and Bcl-2 protein expression in mesangial cells deprived of serum

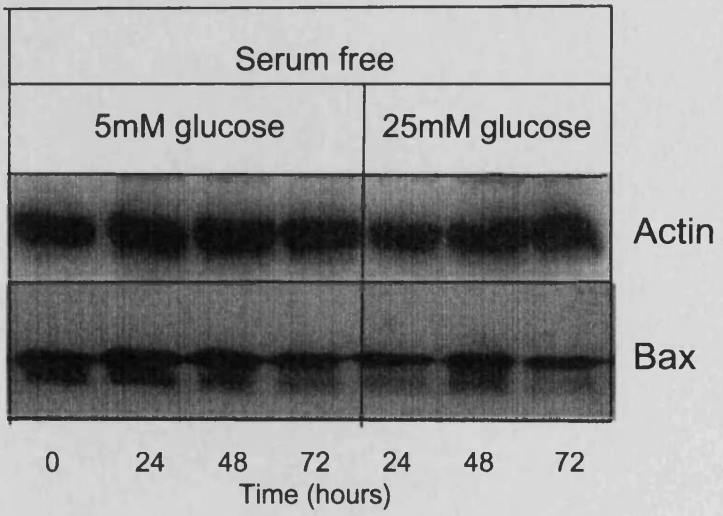

Mesangial cells were grown to confluence. Subsequently apoptosis was induced by serum-deprivation either in the presence of 5mM D-glucose or 25mM D-glucose. At the time points indicated cytoplasmic protein was isolated and Western blot analysis performed. One hundred μg of protein was loaded for each sample and the gel probed for Bcl-2 protein, Bax protein and β-actin to ensure equal loading.

Figure 3.9: Serum-deprivation in mesangial cells does not cause changes in Bcl-x expression in mesangial cells

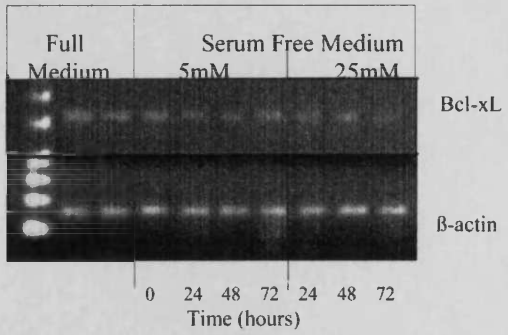

Mesangial cells were grown to confluence. Subsequently apoptosis was induced by serum-deprivation either in the presence of 5mM D-glucose or 25mM D-glucose. At the time points indicated total RNA was isolated and RT-PCR performed. Ethidium bromide stained PCR products were separated on a 3% agarose gel. For Bcl-x amplification, 33 cycles were performed. PCR amplification for ß-actin (lower panel) was performed for 26 cycles.

3.2.4: Effects of caspase-8 and caspase-9 inhibition

There are two pathways to apoptosis – the death receptor pathway and the mitochondrial pathway. The death receptor pathway involves caspase-8 activation and the mitochondrial pathway involves caspase-9 activation. Both pathways then merge upon caspase-3 activation.

Apoptosis in mesangial cells was induced by 72 hours serum-deprivation and the effect of caspase-9 and caspase-8 inhibitors was determined (figure 3.10). The caspase-8 inhibitor had no effect on apoptosis. However, the caspase-9 inhibitor decreased apoptosis from 33.6% to 24.3% ($p = 0.026$). This suggests that serum-deprivation lead to apoptosis via mitochondrial disruption, agreeing with other reports [37, 182, 272] and also with figure 3.3, which shows that serum deprivation increases mitochondrial membrane disruption.

Figure 3.10: Apoptosis induced by serum deprivation involves caspase-9

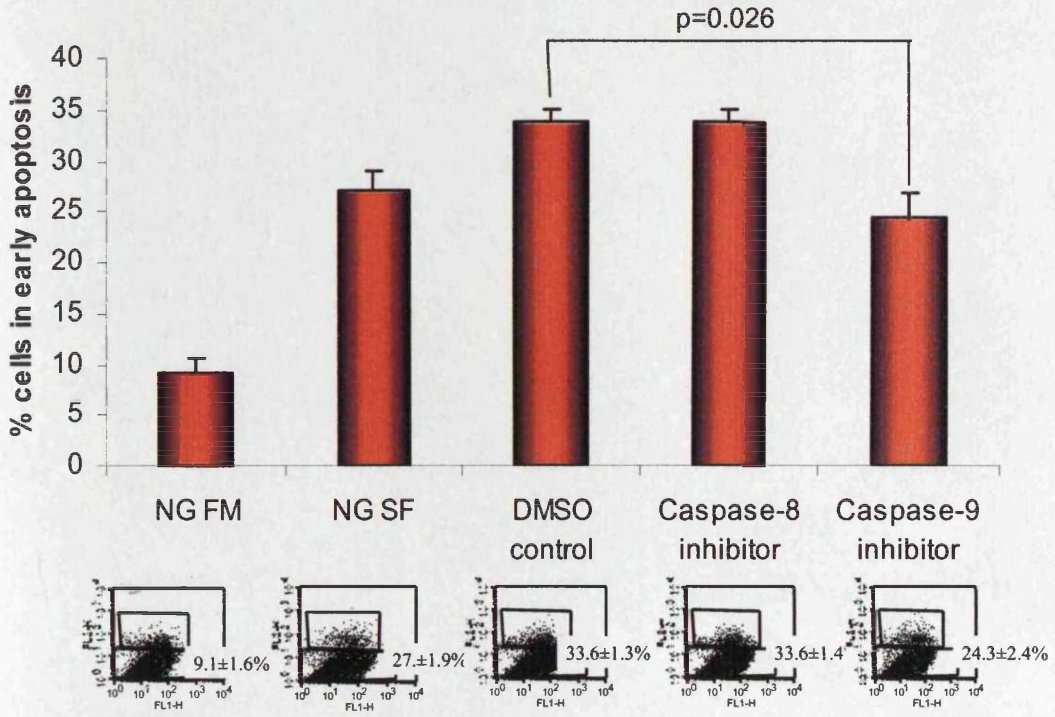

Apoptosis was induced by serum-deprivation in the presence of 5mM D-glucose for 72hrs. Either the 100μM caspase-8 or -9 inhibitor (both from Calbiochem, UK) were added during this time. The stock caspase inhibitors were made up in DMSO, therefore DMSO was used as a control. The control cells were incubated in 5mM full-medium (NG FM) or 5mM glucose serum-free medium for 72 hours (NG SF). Subsequently apoptotic cells were identified by flow cytometry using annexin V conjugated to fluorescein isothiocyanate (FITC), in conjunction with propidium iodide (PI) to distinguish apoptotic cells from necrotic cells. The mean results are expressed graphically ± S.E., n=3 * denotes significance. The corresponding FACS plots are also shown.

3.3.5: Increased apoptosis is associated with reduced activation of NFκB

There is strong evidence implicating a role for the transcription factor NF-kappa B as a cell survival factor [134]. Furthermore, diminished nuclear translocation of NF-kappa B has been associated with impaired mesangial cell survival [135]. A recent study also showed that high glucose-induced mesangial cell apoptosis was induced by NFκB [182].

25mM glucose reduces NFκB activity in mesangial cells: To determine whether NFκB is involved in glucose-induced apoptosis, gel shift assays were performed with nuclear proteins and an NFκB site-specific probe. Nuclear proteins from mesangial cells cultured in serum-free, 5mM glucose media exhibited decreased binding to the NFκB DNA oligonucleotide after 48 hours, which was further reduced by exposure to 25mM D-glucose at all time-points (figure 3.11A). The second band was due to non-specific binding of the probe.

A control gel was also run, comparing binding of the radiolabelled probe (lane 1) and excess cold probe (lane 2). No band is visible in lane 2, suggesting that the radiolabelled probe is specific for NFκB.

The p65 subunit of NFκB is involved in mesangial cell survival: Supershift analysis was performed to determine which NFκB subunits were involved. Antibodies against the five NFκB subunits were used and the antibodies against the p65 subunit retarded movement of the protein-DNA complex through the gel (figure 3.12). Therefore the p65 subunit is involved in mesangial cell survival.

These results suggest that NFκB is a survival factor in mesangial cells and that serum-depriving the cells reduced its activity. Addition of 25mM glucose augmented this effect.

3.2.6: NFκB inhibition mimics the effects of high glucose

SN50 inhibits NFκB activation: The cell permeable NFκB inhibitor peptide SN50, which inhibits translocation of NFκB to the nucleus, was used to further investigate the role of NFκB in glucose induced mesangial cell apoptosis. Inhibition of NFκB nuclear translocation with SN50 was confirmed by gel shift assay (Figure 3.13).

Inhibition of NFκB increases the Bax:Bcl-2 ratio: Following inhibition of NFκB nuclear translocation, Bax:Bcl-2 mRNA ratio was examined by RT-PCR (figure 3.14A). There was a decrease in Bcl-2 mRNA expression and no change in Bax with the addition of SN50 (in serum free, 5mM D-glucose medium). This led to a time-dependent increase in the Bax:Bcl-2 mRNA ratio which was greater than that seen following addition of serum free medium alone (figure 3.14B). The increase in the Bax:Bcl-2 ratio was significant after 6 hours treatment with 10μM SN50.

NFκB inhibition decresed Bcl-xL mRNA expression: Mesangial cells were grown to confluence and then cultured in 5mM glucose medium containing either 10μM or 20μM SN50 for 72 hours. The controls were mesangial cells cultured in full medium and in serum-free medium containing either 5mM or 25mM glucose. Inhibition of NFκB did lead to a dose-dependent decrease in Bcl-xL and a dose-dependent increase in Bcl-xS (figure 3.15).

Inhibition of NFκB leads to caspase-3 acitvation: Mesangial cells were cultured in serum-free 5mM medium either in the presence or absence of SN50 for 72 hours. The amount of caspase-3 was determined by Western blot analysis (figure 3.16). Inhibition of NFκB lead to increased caspase-3 activation compared to the control.

Inhibition of NFκB increases mesangial cell apoptosis: Mesangial cells were cultured in serum-free 5mM glucose medium either in the presence or absence of 10μM SN50. Addition of SN50 led to a significant increase in mesangial cell apoptosis (Figure 3.17) as assessed by flow cytometry using annexin V/PI as described above, compared to the addition of serum free medium.

Inhibition of NFκB mimics the effects of 25mM glucose, causing a decrease in bcl-2 mRNA levels with no change in bax mRNA levels, increasing apoptosis. Inhibition of NFκB also decreased Bcl-xL mRNA expression and increased Bcl-xS mRNA expression.

Figure 3.11: High glucose decreases NFκB activity

A)

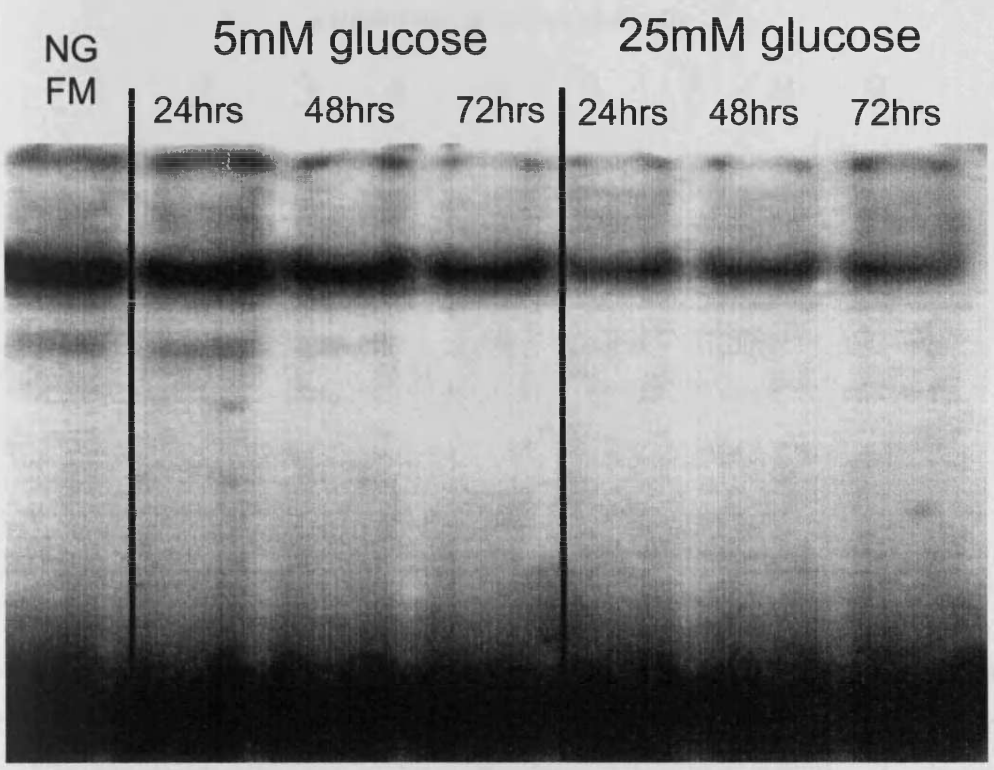

Confluent monolayers of mesangial cells were exposed to either complete medium together with 10%FCS (full medium), serum free medium in the presence of 5mM D-glucose) or serum free medium in the presence of 25mM D-glucose for up to 72hours. Subsequently nuclear proteins were prepared and gel shift assays were performed using an NFκB site-specific probe.

Below (B), is the control gel. Lane 1: radiolabelled NFκB probe was added to the nuclear protein preparations. Lane 2: cold NFκB probe was added for 20 mins, followed by addition of the radiolabelled probe for 20 mins. The full gel is shown, the free probe was run off the gel.

B)

Figure 3.12: The p65 NFκB subunit is involved in apoptosis induced by serum withdrawal in mesangial cells

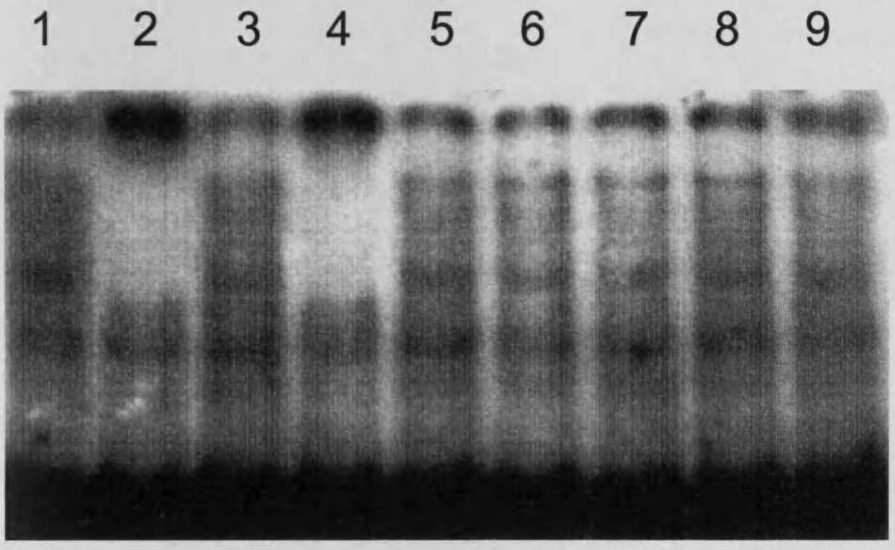

Confluent monolayers of mesangial cells were exposed to 5mM complete medium. Subsequently nuclear proteins were prepared and gel shift assays were performed using an NFκB site-specific probe. To determine which NFκB subunits were involved, supershift analysis was performed using antibodies to the five different NFκB subunits. The following antibodies were used: lane 1 – no antibody control, lane 2 – p65, lane 3 – p50, lane 4 – p65 and p50, lane 5 – p52, lane 6 – c-Rel, lane 7 – RelB, lane 8 – actin (control) and lane 9 – stat1 (control).

Figure 3.13: SN50 inhibits NFκB

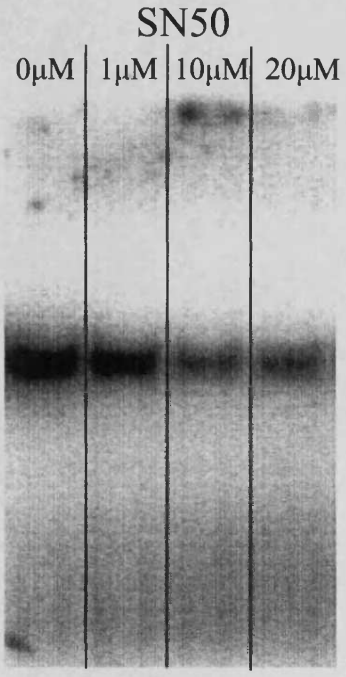

The role of NFκB was further examined by the use of the cell permeable NFκB inhibitor peptide SN50 (Merck Biosciences Ltd, Nottingham, UK). Mesangial cells were incubated with various concentrations of SN50 under serum free conditions for 72hours. Inhibition of NF-kappa B nuclear translocation was confirmed by gel shift assay.

Figure 3.14: Inhibition of NFκB decreases Bcl-2 mRNA expression

A

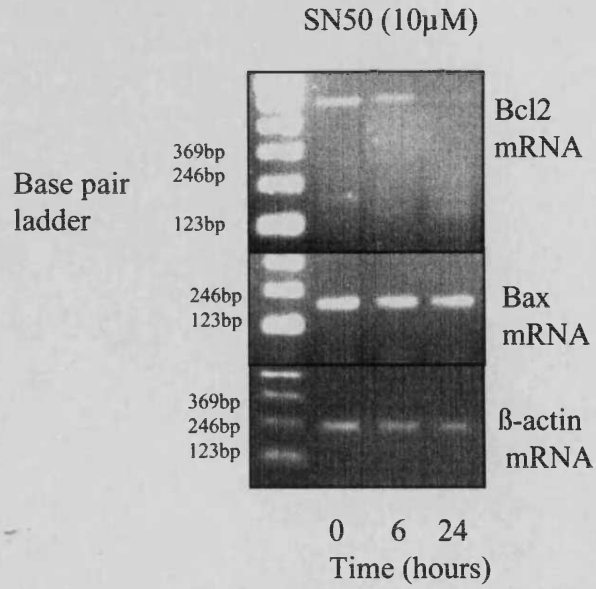

Mesangial cells were grown to confluence, followed by culture in serum-free 5mM glucose medium containing SN50 for 6 or 24 hours. In the control experiment, the mesangial cells were cultured in serum-free 5mM glucose medium for 48 hours. Subsequently, total RNA was isolated and RT-PCR preformed. Ethidium bromide stained PCR products were separated on a 3% agarose gel. For Bcl-2 and Bax, amplification was preformed for 33 cycles. PCR amplification for β-actin was preformed for 26 cylces.

B

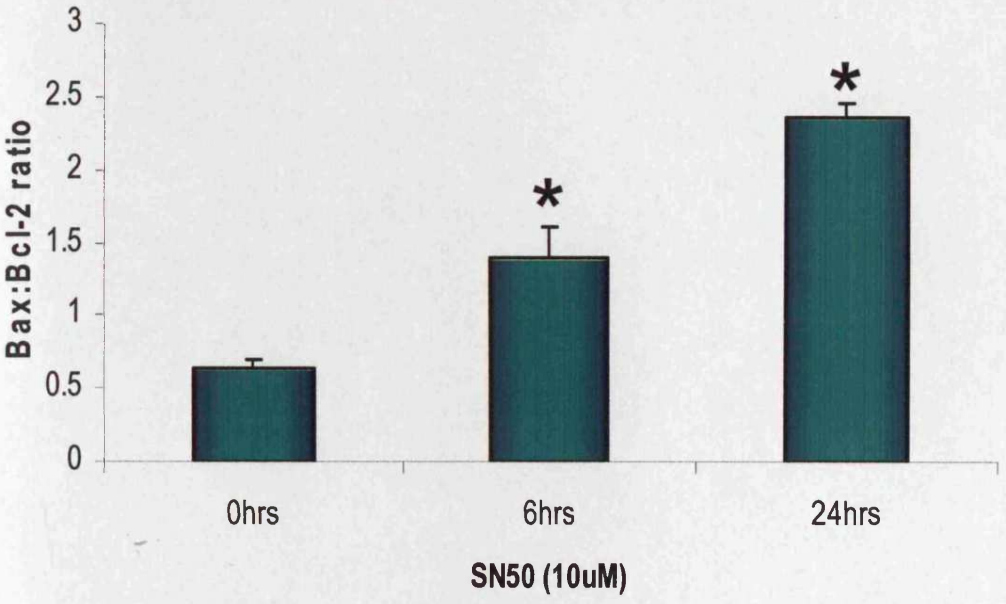

Scanning densitometry of three individual experiments was performed and the results expressed at the mean±S.E. ratio of Bax:Bcl-2 mRNA corrected at each time-point for the house-keeping gene, β-actin, $p<0.05$.

Figure 3.15: Effect of NFκB inhibition on Bcl-x mRNA expression

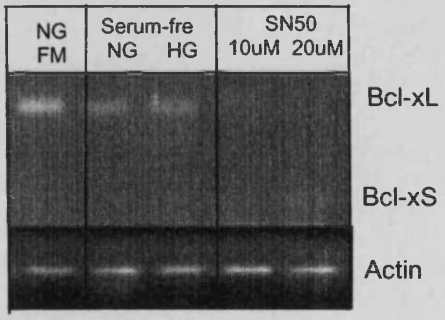

Mesangial cells were grown to confluence, followed by culture in serum-free 5mM glucose medium containing either 10μM or 20μM SN50 for 72 hours. In the control experiment, the mesangial cells were cultured in serum-free 5mM glucose medium, 25mM glucose medium or full medium for 72 hours. Subsequently, total RNA was isolated and RT-PCR preformed. Ethidium bromide stained PCR products were separated on a 3% agarose gel. For Bcl-2 and Bax, amplification was preformed for 33 cycles. PCR amplification for β-actin was preformed for 26 cylces.

Figure 3.16: Inhibition of NFκB leads to caspase-3 activation in mesangial cells

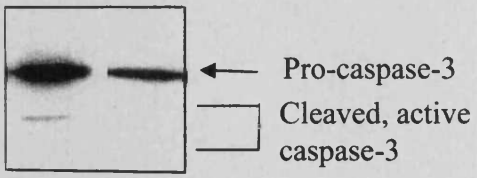

SN50 control

Mesangial cells were incubated either in the presence or absence of 10μM SN50 under serum free conditions for 72hours. Quantity of active and pro-caspase in cytoplasmic preparations of mesangial cells was determined by Western blot. The caspase-3 antibody detects full-length caspase-3 (35kDa) and cleaved caspase-3 (17kDa).

Figure 3.17: Inhibition of NFκB induces mesangial cell apoptosis

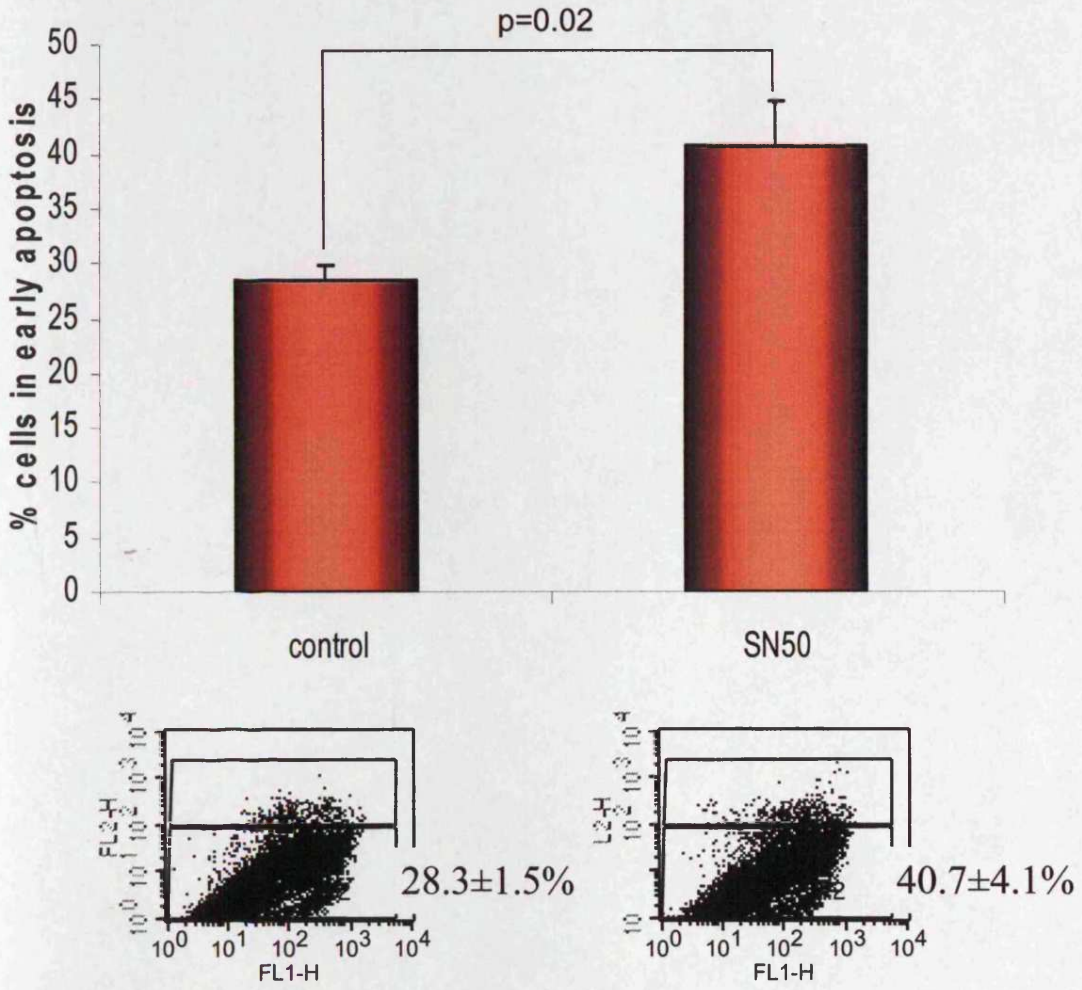

Confluent monolayers of mesangial cells were incubated in the presence or absence of 10μM SN50 in 5mM glucose, serum-free medium for 72hours. Subsequently apoptotic cells were identified by flow cytometry using annexin V-FITC, in conjunction with PI. Results are presented graphically as the % of cells in early apoptosis and represent the mean ± S.E. of three individual experiments* denotes significance. The corresponding FACS plots are also shown.

3.3: Discussion

The late phase of diabetic nephropathy is characterised by loss of resident glomerular cells, a process which correlates with the decline in GFR [273]. Mesangial cell death by apoptosis is known to be involved in the resolution of glomerular hypercellularity following injury suggesting that apoptosis may be a homeostatic mechanism regulating the glomerular cell population [274]. It is also clear that apoptosis plays a pathological role leading to deletion of mesangial cells associated with progressive glomerular sclerosis [275].

In the current study, numerous different methodological approaches were used to demonstrate that elevated glucose concentration induces the pro-apoptotic pathway activated by serum deprivation in renal mesangial cells. All of the methods used showed that high glucose augmented the effect of serum-depletion on mesangial cell apoptosis.

Other methods of quantifying apoptosis are also available, although I did not use them due to time constraints. Hoescht staining is another way of assessing apoptosis. Hoescht 33342 is readily taken up by cells during the initial stages of apoptosis and selectively stains nuclei of apoptotic cells fluorescent blue. Viable cells have evenly stained nuclei, while nuclei from apoptotic cells show condensed or fragmented morphology. Fluorescent microscopy can then be used to count the cells and calculate the % of cells in apoptosis. DNA fragmentation that occurs during apoptosis produces DNA strand breaks and the TUNNEL (terminal deoxynucleotidyl transferase dUTP nick end labelling) assay is a method that detects DNA nucks in apoptotic cells. Commercial TUNNEL assays can be used to quantify the % of apoptotic cells.

Exposure of cells to 25mM glucose in the presence of 10% FCS inhibited apoptosis, probably because FCS contains many growth factors. Serum-deprivation lead to disruption of the mitochondrial membrane, capase-9 activation, followed by caspase-3 activation and the morphological changes seen during apoptosis, i.e phosphatidylserine exposure. Furthermore, growth of mesangial cells under conditions of elevated glucose lead to decreased mRNA expression of Bcl-2, with no change in Bcl-xL and Bax mRNA expression. An alteration in the Bax:Bcl-2 ratio is known to activate caspase-3 [272]. All of these changes were more pronounced in mesangial cells cultured under 25mM glucose conditions, suggesting the same pathway is involved.

Yang et al showed that the ratios of Bax to Bcl-2 mRNA and protein were significantly increased in apoptotic mesangial cells and this correlated with upregulated caspase-3 activity [272]. High glucose has also been reported to promote apoptosis in mesangial cells by increasing intracellular ROS generation. This has been shown to increase the Bax:Bcl-2 ratio in favour of apoptosis and lead to cytochrome c release from mitochondria and caspase-3 activation [182]. Ideally, the mRNA data should be collaborated with protein data but the Bcl-2 antibodies for Western blot did not work. If time had not been limited, I could have quantified Bcl-2 and Bax protein levels with ELISA kits.

Mesangial cell culture in 5mM glucose, serum-free media lead to decreased NFκB levels and this was augmented with culture in 25mM glucose. The difference in NFκB levels between cells cultured in 5mM or 25mM glucose was apparent after 24 hours. Inhibition of NFκB increased the Bax:Bcl-2 ratio in favour of apoptosis after 6 hours. NFκB inhibition also decreased the cell survival protein Bcl-xL and increased

expression of the pro-apoptotic protein Bcl-xS after 72 hours treatment. In contrast, there was no difference in mRNA expression of Bcl-xL in mesangial cells cultured in 5mM or 25mM glucose after 72 hours. This difference could be because inhibition of NFκB had a greater effect on apoptosis and the cells were further along in the apoptosis pathway.

Although figure 3.13 shows that addition of SN50 led to decreased NFκB activation, a further experiment using a control for SN50, could have been carried out. If time had not been limiting, the effects of SN50 and SN50M, an inactive control for SN50 which does not have an effect on NFκB translocation (Calbiochem), could have been compared. The EMSA method could have been used to compare the effects of SN50 and SN50M on NFκB activation.

In conclusion, serum-deprivation in mesangial cells leads to decreased NFκB activity, an increase in the Bax:Bcl-2 ratio, disruption of the mitochondrial membrane potential, activation of caspase-9, activation of caspase-3 and then the morphological changes seen during apoptosis. In mesangial cells, apoptosis induced by serum deprivation via this pathway is augmented by culturing the mesangial cells in 25mM glucose.

In vivo, mesangial cells are exposed to plasma but not serum [Mene 1989]. Under these serum-free conditions in diabetic patients, the mesangial cells in the glomerulus probably undergo increased apoptosis. This could lead to the mesangial cell loss associated with proteinuria, hypertension and renal dysfunction in overt nephropathy.

CHAPTER 4:

THE ROLE OF TGFβ1 IN MESANGIAL CELL APOPTOSIS

CHAPTER 4: THE ROLE OF TGFB$_1$ IN MESANGIAL CELL APOPTOSIS

4.1: Introduction

Previous studies have demonstrated that glucose induced alterations in mesangial cell function may be mediated by the pro-fibrotic cytokine TGF-ß1. Elevated glucose leads to transcriptional activation of TGFβ1 [276, 277]. Furthermore, many glucose mediated alterations in mesangial cell function are mediated by autocrine activation of TGFβ1 [125]. Glucose also stimulates TGF-ß type II receptor expression in mesangial cells [278], which enhances sensitivity of mesangial cells to the effects of TGF-ß [279].

Smad7 has been shown to induce sensitisation of cells to different forms of cell death and increases TGFβ1-mediated apoptosis in epithelial cells [147]. In addition to the SMAD signalling intermediates, numerous other pathways of signal transduction, such as MAP kinase and Rho GTPases, have been identified following TGF-ß1 receptor activation [280-286]. In podocytes, activation of p38 MAP kinase and caspase-3 was required for TGF-ß mediated apoptosis [148]. Similarly in renal tubular epithelial cells, TGF-ß1 signalling potentiates apoptosis by a Smad independent p38 MAP kinase-dependent mechanism [287]. In contrast, stimulation of hepatocytes by TGF-ß leads to Smad-dependent expression of GADD45b (an immediate-early response gene for TGF-ß), which through p38 MAP kinase, triggered apoptosis [289]. Rat fibroblasts grown in the presence of serum have undetectable amounts of p38 MAPK activity. Removal of serum leads to markedly elevated

apoptosis and p38 MAPK activity, which is inhibited by growth factors [157]. Inhibition of p38 MAPK inhibited the effect of high glucose induced apoptosis, although there was no apparent change in total p38 [159]. Phosphorylation of p38 MAPK was found to be downstream of the bax-caspase pathway [159].

These data suggest that Smad and non Smad p38 MAP kinase pathways may act independently or synergistically to mediated TGF-ß1 apopotic effects in a cell specific manner.

We therefore sought to determine the role of glucose induced TGF–ß1 in induction of mesangial cell apoptosis and its relationship with suppressed NFκB nuclear translocation. The aims of this chapter were:

1. To determine the effect of TGFβ1 on NFκB activation and Bcl-2, Bax and Bcl-x expression and caspase-3 expression.
2. The effect of recombinant TGFβ1 and the TGFβ1-neutralising antibody on mesangial cell apoptosis.
3. Quantification of TGFβ1 secretion by mesangial cells cultured in 5mM and 25mM glucose.
4. Study mesangial cell sensitivity to TGFβ1.

4.2: Results

4.2.1: TGFβ1 mimicked the effects of high glucose

TGFβ1 inhibited NFκB activation in mesangial cells: The mesangial cells were cultured in 5mM glucose containing 1ng/ml TGFβ1 for up to 24 hours. In the control, the cells were cultured in 5mM glucose without TGFβ1 for 48 hours. Stimulation of

mesangial cells under serum free conditions with recombinant TGF-ß1, led to a significant reduction in nuclear translocation of NFκB (Figure 4.1). This decrease was apparent after 6 hours of TGFβ1 treatment, with a further decrease after 24 hours.

TGFβ1 increased the Bax:Bcl-2 ratio: Mesangial cells were grown to confluence, followed by incubation in serum-free 5mM glucose media containing recombinant TGFβ1 for up to 24 hours (figure 4.2). In the control, mesangial cells were cultured in serum-free 5mM glucose media for 48 hours. Subsequently, mRNA expression of Bax and Bcl-2 was quantified.

As in chapter 3, Bax mRNA expression stayed constant. After 6 hours incubation with TGFβ1, there was no decrease in Bcl-2 expression, although there was a significant decrease after 24 hours (a 2.2-fold increase in the Bax:Bcl-2 mRNA ratio).

Effect of TGFβ1 on Bcl-2 and Bax protein expression: To investigate the effect of TGFβ1 on the protein expression of Bcl-2 and Bax, Western blot analysis was performed (figure 4.3). Changes in the Bcl-2:Bax ratio at the protein expression level could not be determined because the Bcl-2 antibody did not work well and the bands were not clear enough for densitometry.

TGFβ1 decreased Bcl-xL expression: The effect of TGFβ1 on Bcl-x expression at the mRNA level was also investigated (figure 4.4). Mesangial cells were cultured in 5mM glucose containing either 10pg/ml or 1ng/ml of TGFβ1 for 72 hours. In the control experiments, the cells were cultured in full-medium, 5mM glucose or 25mM

glucose without TGFβ1. Both concentrations of TGFβ1 mediated a decrease in Bcl-xL expression, favouring apoptosis, similar to effect of inhibiting NFκB (chapter 3).

These results suggest that TGFβ1 mimics the effects of high glucose by inhibiting NFκB and increasing the Bax:Bcl-2 ratio. TGFβ1 and NFκB inhibition have similar effects on Bcl-xL mRNA expression.

Figure 4.1: TGFβ1 inhibits NFκB activity

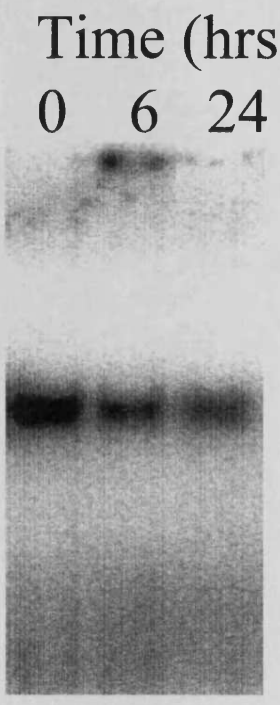

Confluent monolayers of mesangial cells were exposed to serum-free medium in the presence of 1ng/ml recombinant TGF-ß1 for up to 24 hours. In the control, mesangial cells were cultured in 5mM glucose without TGFβ1 for 48 hours. Subsequently nuclear proteins were prepared and gel shift assays were performed using an NFκB site-specific probe.

Figure 4.2: TGFβ1 increased the Bax:Bcl-2 ratio in mesangial cells

<u>A</u>

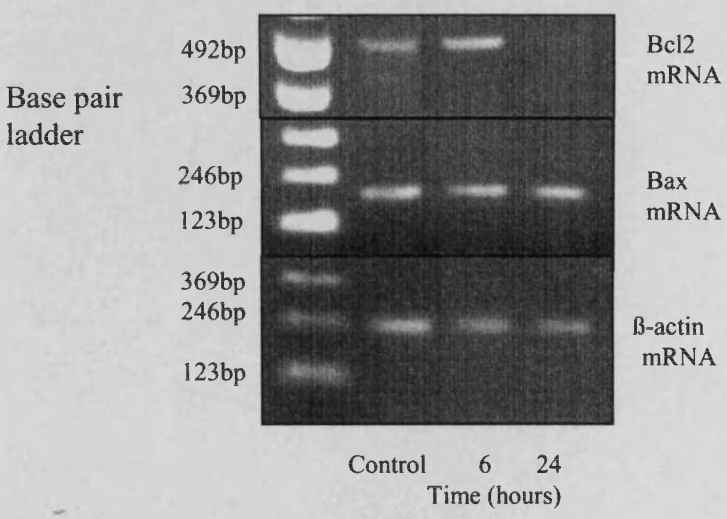

Mesangial cells were incubated with serum free medium with a glucose concentration of 5mM, either alone for 48 hours or in the presence 1ng/ml of recombinant TGFβ1 for up to 24 hours prior to isolation of total RNA. Ethidium bromide stained PCR products were separated on a 3% agarose gel. For Bcl2 (upper panel), Bax (middle panel) amplification was performed for 33 cycles. PCR amplification for ß-actin (lower panel) was performed for 26 cycles.

B

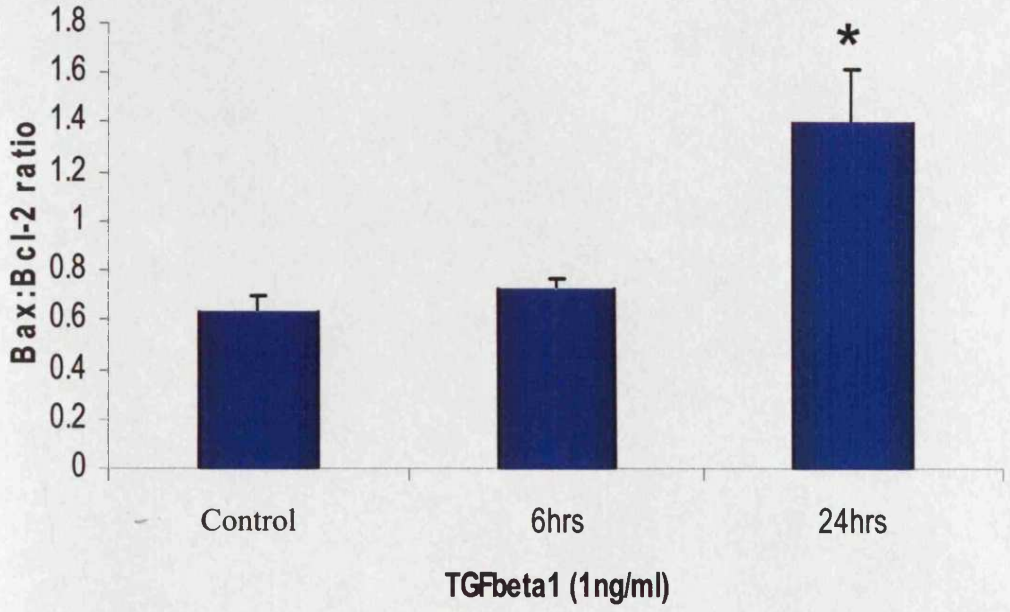

Scanning densitometry of three individual experiments was performed, and the results expressed as the mean ± S.E ratio of Bcl2:Bax mRNA corrected at each time point for the house keeping gene ß-actin. Results represent mean ± S.E. of three individual experiments, * denotes $p<0.05$ compared to control.

Figure 4.3: Protein expression of Bcl-2 and Bax

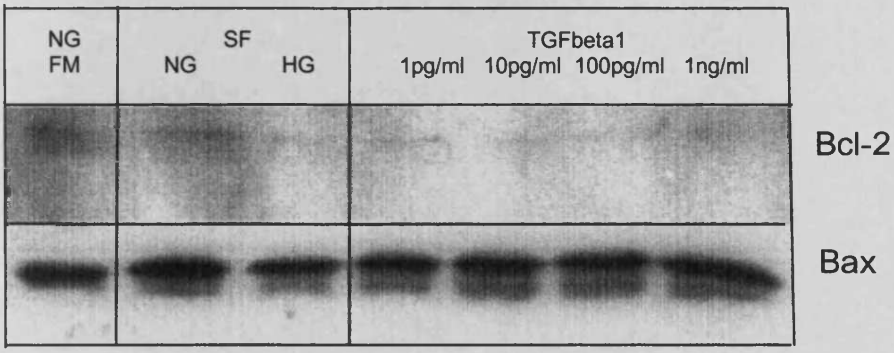

Mesangial cells were grown to confluence, followed by growth in serum-free medium for 72 hours in the presence of various doses of TGFβ1. The control cells were cultured in full-medium, 5mM glucose medium or 25mM glucose medium for 72 hours. Western blot analysis was performed to determine the changes in the Bcl-2 and Bax protein levels. 100μg of protein was loaded per well.

Figure 4.4: Effect of TGFβ1 on Bcl-x expression in mesangial cells

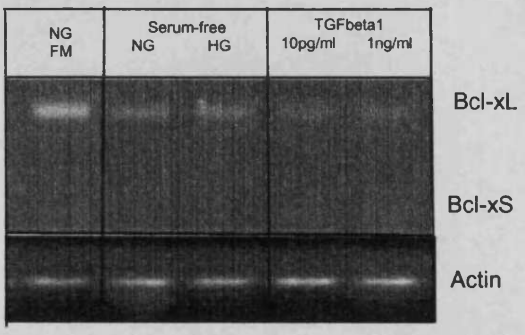

Mesangial cells were incubated in serum free medium with a glucose concentration of 5mM, either alone or in the presence of either 10pg/ml or 1ng/ml of recombinant TGFβ1 for 72hours prior to isolation of total RNA. RT-PCR performed as described in materials and methods. Ethidium bromide stained PCR products were separated on a 3% agarose gel. For Bcl-x (upper panel), amplification was performed for 33 cycles. PCR amplification for ß-actin (lower panel) was performed for 26 cycles.

4.2.2: TGFβ1 induced apoptosis in mesangial cells

Effects of recombinant TGFβ1: The effect of TGFβ1 on mesangial cell apoptosis was also studied. Addition of recombinant TGF-ß1 led to a significant increase in mesangial cell apoptosis as assessed by flow cytometry using annexin V/PI (Figure 4.5). A 43% increase in apoptosis was observed after addition of 1ng/ml of TGFβ1 for 72 hours (an increase from 28.3±1.5 to 40.5±1.8).

Recombinant TGFβ1 activated caspase-3: Mesangial cells were grown in 5mM glucose containing various doses of TGFβ1 for 72 hours. In the controls, mesangial cells were cultured in 5mM or 25mM glucose without TGFβ1 for 72 hours. Addition of 100pg/ml recombinant TGFβ1 lead to an increase in latent and active caspase-3 (figure 4.6).

High glucose-induced apoptosis can be inhibited by neutralising TGFβ: The role of TGF-ß1 in glucose induced mesangial cell apoptosis was further examined by blockade of TGF-ß1 function. Addition of a blocking antibody (10μg/ml) to TGF-ß1 significantly attenuated glucose induced apoptosis (Figure 4.7). Neutralising TGFβ1 decreased apoptosis by 11% from 34.4±2.9 to 30.5±0.7. 10μg/ml of the control antibody IgG had no affect on apoptosis.

Taken together, these results suggest that TGFβ1 increases apoptosis in mesangial cells and high glucose-induced mesangial cell apoptosis and this can be inhibited by neutralising TGFβ1.

Figure 4.5: TGFβ1 induces apoptosis in mesangial cells

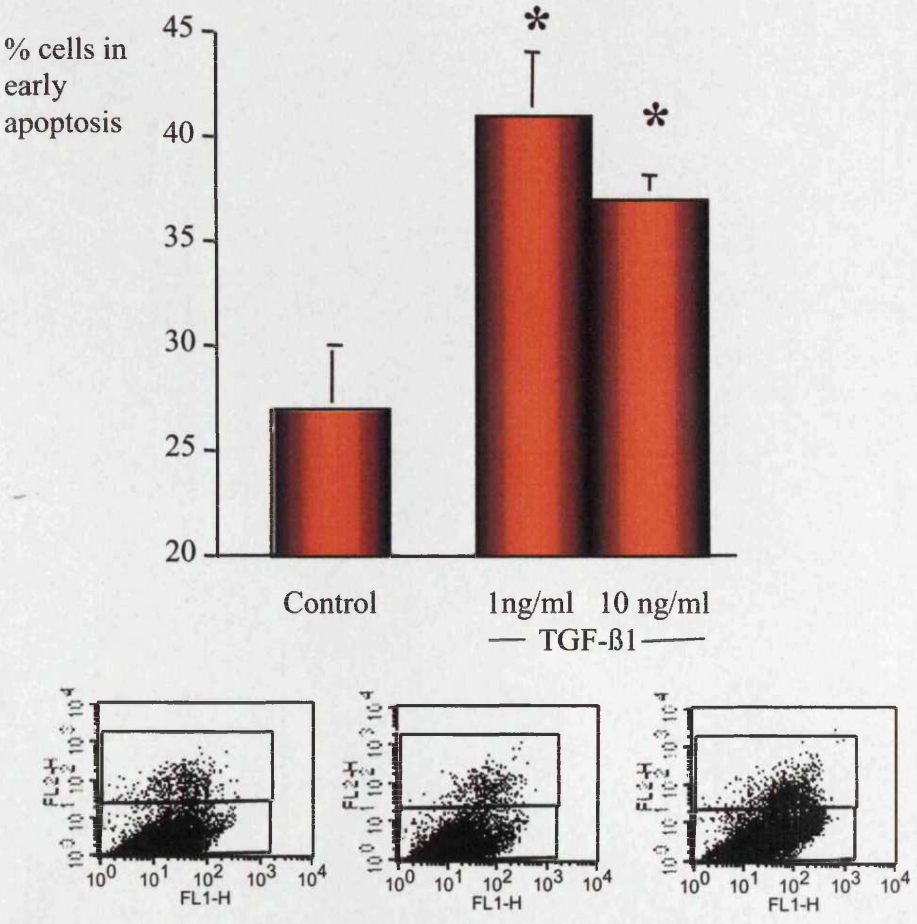

Confluent mesangial cell monolayers were incubated with either serum free medium, or serum free medium in the presence of increasing doses of recombinant TGF-ß1 and the role of TGF-ß1 in glucose induced apoptosis was examined. Apoptotic cells were identified by flow cytometry using annexin V and propidium iodide cell surface staining. Results represent mean ± S.E. of three individual experiments, * denotes $p<0.05$ compared to control. The corresponding FACS plots are also shown.

Figure 4.6: TGFβ1 induces caspase-3 activation

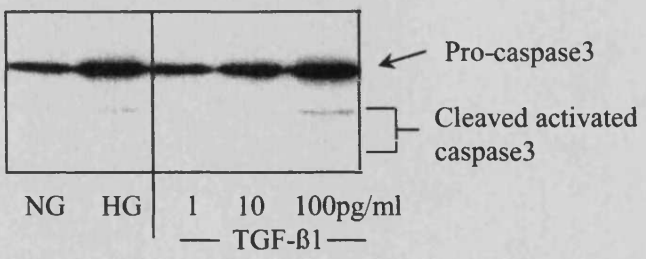

Confluent mesangial cell monolayers were incubated with either serum free medium, or serum free medium in the presence of increasing doses of recombinant TGF-ß1 prior to cytoplasmic protein extraction. One hundred μg of protein was loaded for Western blot analysis and probed for the full-length pro-enzyme and the cleaved, active caspase-3.

Figure 4.7: The TGFβ1-neutralising antibody attenuates apoptosis

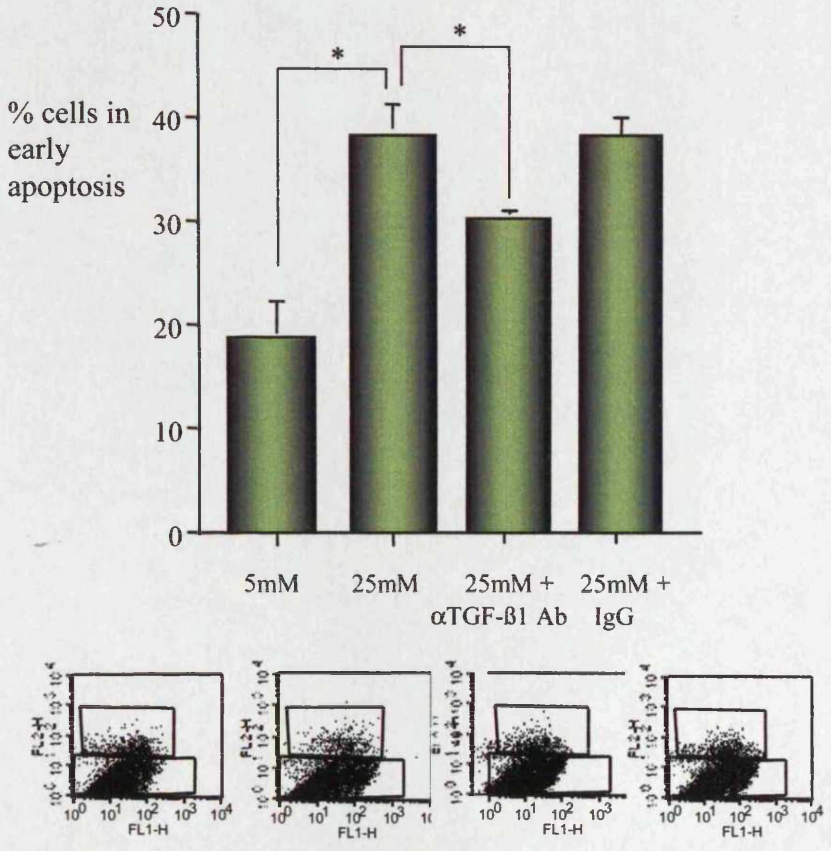

Confluent monolayers of mesangial cells were also incubated with either 5mM D-glucose, 25mM D-glucose or 25mM D-glucose in the presence of 10µg/ml of blocking antibody to TGF-ß1 (or 10µM IgG in the control) (R&D Systems). Apoptotic cells were identified by flow cytometry using annexin V and propidium iodide. Results represent mean ± S.E. of three individual experiments, * denotes significance. The corresponding FACS plots are also shown.

4.2.3: TGFβ1 induces mesangial cell apoptosis via p38 MAPK

To study the apoptosis pathyway mediated by TGFβ1 in mesangial cells, the role of the Smad proteins and p38 MAPK was studied.

Smad proteins

Effect of smad inhibiton on mesangial cell apoptosis: Mesangial cells were transfected with a Smad2 dominant-negative (DN), Smad3 DN, Smad7 over-expression (OE) or an empty vector prior to addition of 1ng/ml TGFβ1 for 72 hours. Apoptosis was quantified by annexin-v/PI flow cytometry (figure 4.8A) and transfection efficiency was verified by Western blot analysis for the c-myc tag, which was present in all of the vectors (figure 4.8B).

There was no change in apoptosis because the transfection process did not work, c-myc-tag expression did not change. Transfection was tried several times using two different chemical methods –FUGENE 6 and Genejuice – but I was still unable to successfully transfect the mesangial cells.

Smad7 protein expression in mesangial cells: Smad7 is a negative regulator of TGFβ1 activity and has been implicated in TGFβ1 induced apoptosis [147]. Therefore, changes in Smad7 protein expression were studied by Western blot (figure 4.9). Over 72 hours there was no change in Smad7 expression in mesangial cells cultured in 5mM or 25mM glucose.

These experiments gave inconclusive results.

P38 MAP Kinase

Activation of p38 MAP kinase has also been implicated as a mediator of pro-apototic effects of TGF-ß1 [289].

Inhibition of p38MAP kinase activity decreased apoptosis induced by TGFβ1: Mesangial cells were cultured in 5mM glucose containing 1ng/ml TGFβ1 for 72 hours, either in presence or absence of 3000ng p38 inhibitor, SB203580 (a chemical inhibitor, Sigma) (figure 4.10). The inhibitor decreased mesangial cell apoptosis induced by TGFβ1, a decrease from 41.3±4.6 to 21.3±2.7 (a 48% decrease in apoptosis).

Inhibition of p38 MAPK inhibited high glucose-induced apoptosis: The effect of the p38 MAPK inhibitor on high glucose-mediated apoptosis was also investigated (figure 4.11). Mesangial cells were cultured in 25mM high glucose, either in the presence of absence of 3000ng SB203580, for 72 hours. The controls were mesangial cells cultured in full-medium or 5mM glucose for 72 hours. Inhibition of p38 MAP Kinase also inhibited high-glucose mediated apoptosis (a 37% decrease in apoptosis).

Taken together, these results suggest that TGFβ1-mediated mesangial cell apoptosis involves the p38 MAP Kinase pathway. Also, high glucose-induced mesangial cell death is mediated by TGFβ1 and this pathway involves p38 MAPK.

Figure 4.8: Role of the Smad pathway in mesangial cell apoptosis

A

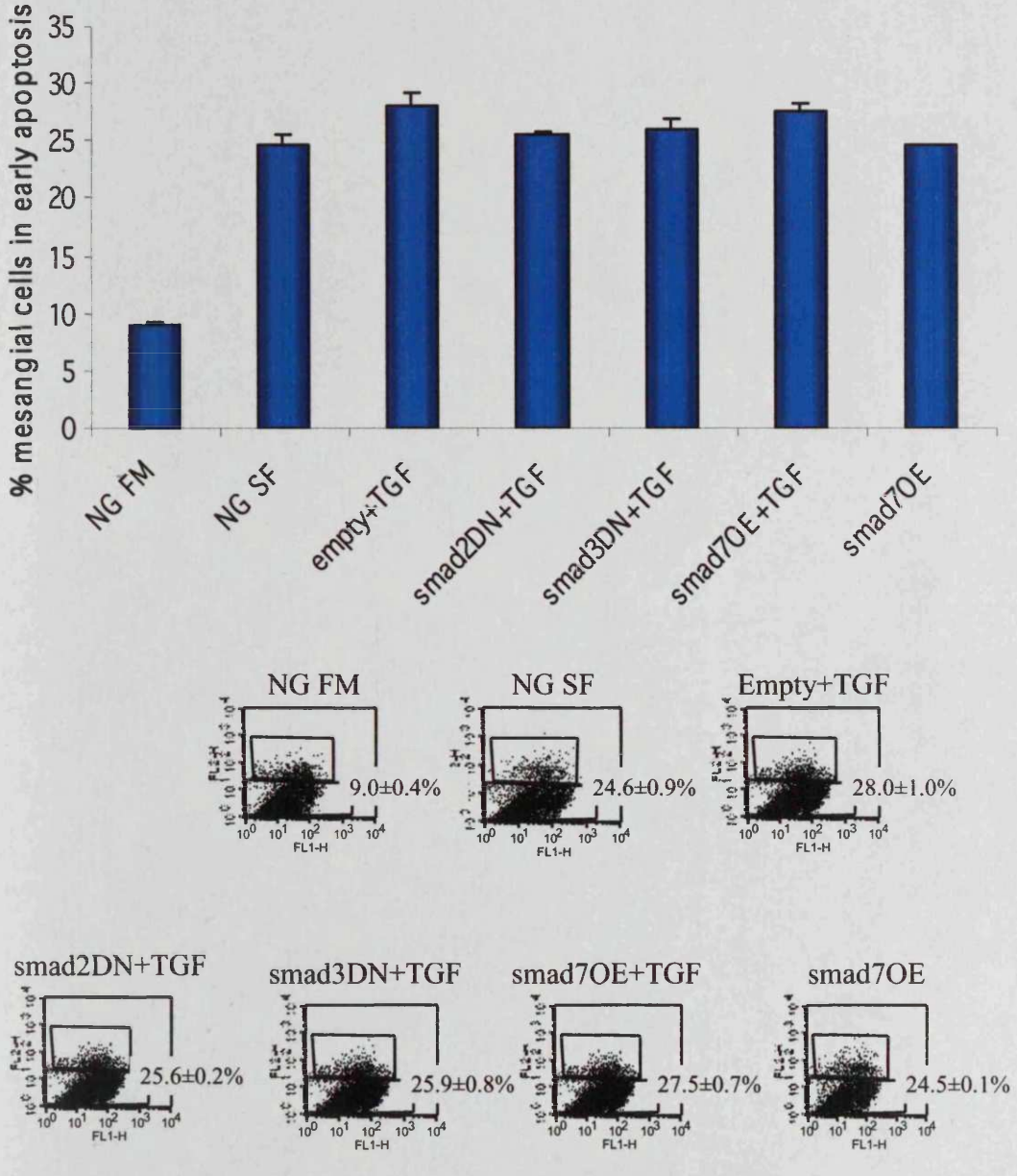

Confluent monolayers of mesangial cells were transfected with an empty, Smad2 dominant-negative (DN), smad3 DN or a Smad7 over-expression (OE) vector and then incubated with 1ng/ml TGF-ß1 for 72hours. The controls were full medium, NG serum-free and NG with TGFβ1, 72 hours. Apoptotic cells were quantified using annexin-v/PI and analysed by flow cytometry (A). Results represent mean ± S.E. of three individual experiments, and the Mann-Whitney U-test was used to calculate significance. The corresponding FACS plots are also shown.

B

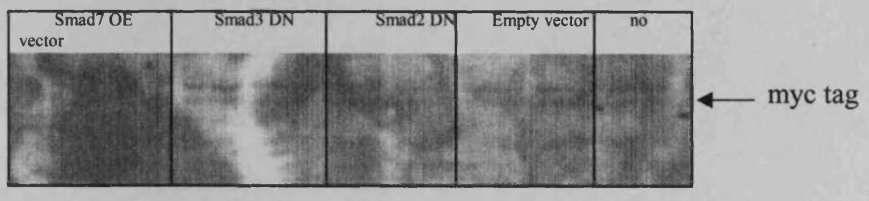

Transfection efficiency was tested by Western blot analysis of the c-myc tag in the cells (B).

Figure 4.9: Effect of high glucose on smad7 protein expression

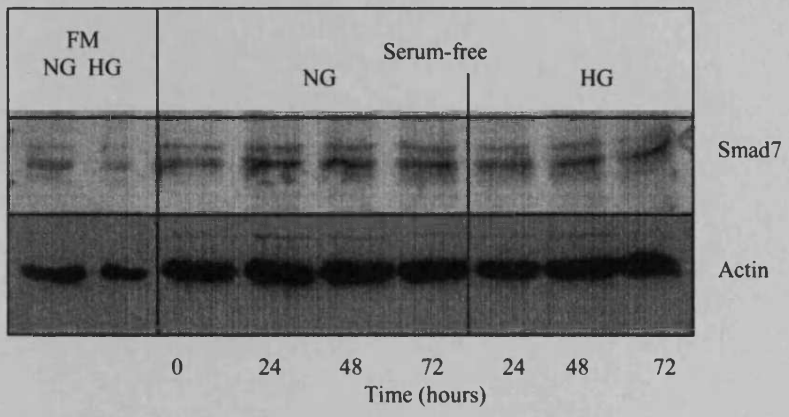

Mesangial cells were grown to confluence. Subsequently apoptosis was induced by serum-deprivation either in the presence of 5mM D-glucose or 25mM D-glucose. At the time points indicated cytoplasmic protein was isolated and Western blot analysis performed for Smad7 protein expression. Actin was used as a control for loading equal amounts of protein per well.

Figure 4.10: Effect of p38 MAPK inhibition on apoptosis induced TGFβ1

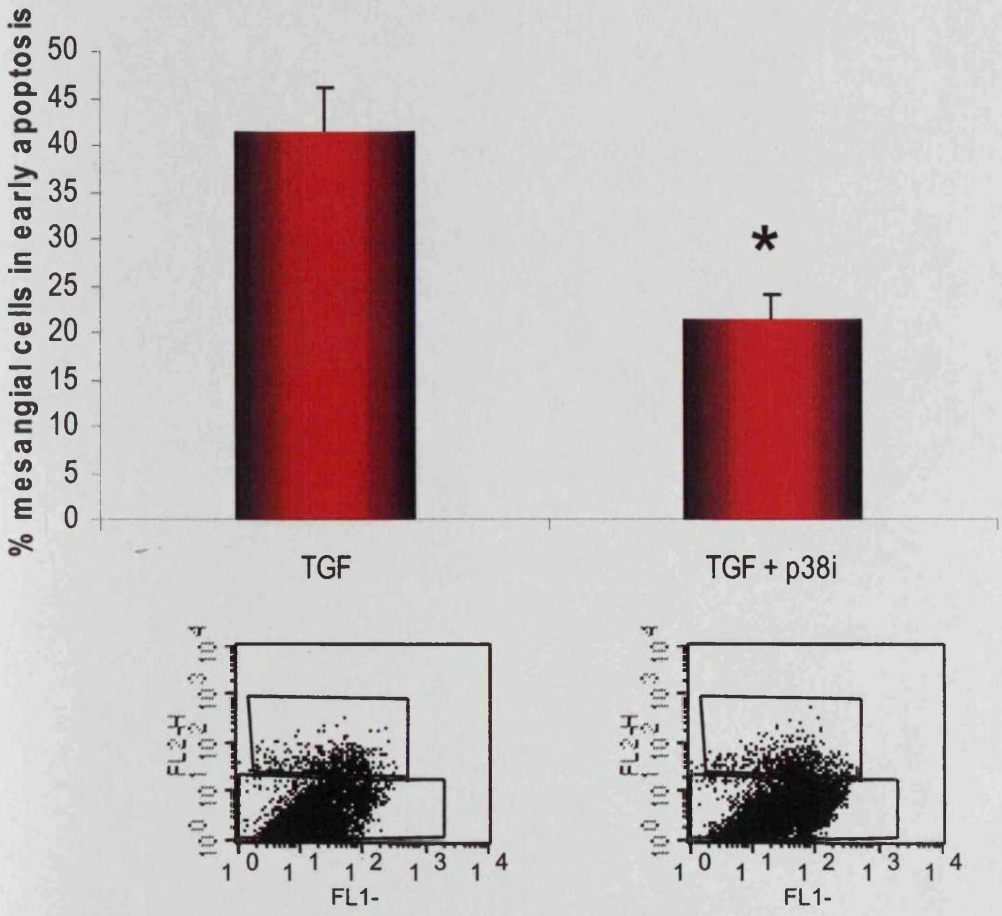

Confluent monolayers of mesangial cells were incubated with 1ng/ml TGF-ß1 under serum free conditions, or 1ng/ml TGF-ß1 in the presence of 3000ng of the chemical inhibitor of p38 MAP kinase (p38i), SB203580, for 72hours. Apoptotic cells were identified by flow cytometry using annexin V and propidium iodide. Results represent mean ± S.E. of three individual experiments, and * denotes $p<0.05$. The corresponding FACS plots are also shown.

Figure 4.11: Inhibition of p38 MAPK decreases glucose induced apoptosis

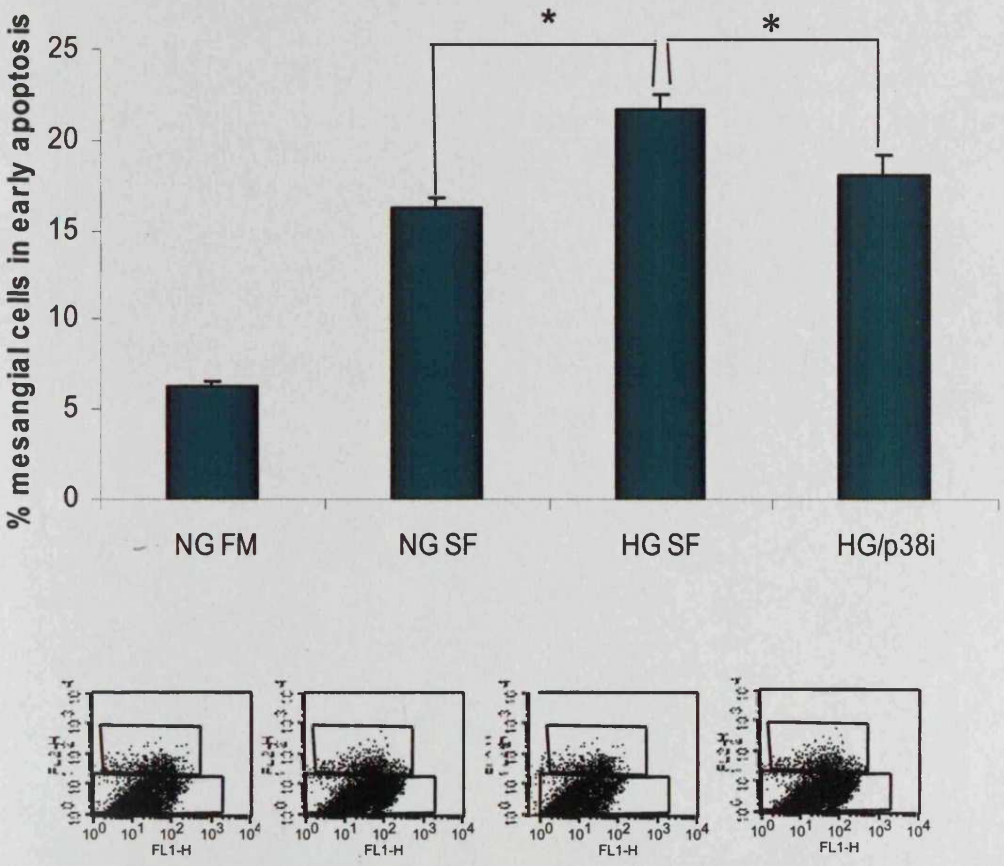

Confluent monolayers of mesangial cells were incubated in full medium, 5mM or 25mM D-glucose under serum free conditions, or 25 mM D-glucose in the presence of 3000ng p38 MAP kinase inhibitor SB203580 for 72hours. Apoptotic cells were identified by flow cytometry using annexin V and propidium iodide. Results represent mean ± S.E. of three individual experiments, and * denotes $p<0.05$. The corresponding FACS plots are also shown.

4.2.4: Elevated glucose concentration increased TGF-ß1 secretion

The amount of TGFβ1 secreted by mesangial cells cultured in 5mM and 25mM glucose was determined.

High glucose conditions induced TGFβ1 secretion in mesangial cells: Mesangial cells were cultured in 5mM or 25mM glucose for up to 72 hours and TGFβ1 concetration was assessed by ELISA (figure 4.12).

Under serum free conditions, maintenance of mesangial cells in the presence of 25mM D-glucose led to an increase in total TGFβ1. There was approximately a two-fold increase in total TGFβ1 production by mesangial cells from 24 to 72 hours and a significant difference between cells cultured in 25mM glucose and 5mM glucose was observed after 48hrs (1965.7±99.4pg/ml vs 1611.1±48.4pg/ml).

High glucose induced secretion of active TGFβ1 in mesangial cells: Confirmation of the active nature of TGF-ß1 was sought by addition of conditioned medium from mesangial cells exposed to either 5mM D-glucose or 25mM D-glucose for 72 hours to HK2 cells transiently transfected with the Smad responsive promoter-luciferase construct.

Addition of recombinant TGFβ1 to these transfected HK2 cells lead to a marked increase in luciferase activity (figure 4.13A).

There was also a significant increase in luciferase activity of the promoter construct following addition of 25mM compared to 5mM D-glucose conditioned medium (Figure 4.13B).

In vitro activation of latent TGF-ß1 was performed by repeated cycles of freeze thawing of the samples. Addition of freeze-thawed conditioned media from mesangial cells cultured in 5mM glucose lead to a significant increase in Smad responsive promoter activity. In contrast, repeated cycles of freeze thawing of 25mM D-glucose conditioned medium did not increase luciferase activity compared to that seen following addition of untreated 25mM D-glucose conditioned medium.

These data therefore confirm that high glucose induces TGFβ1 secretion in mesangial cells and following addition of 25mM D-glucose the increase in TGF-ß1 was of its active form.

Figure 4.12: Cells cultured in 25mM D-glucose secrete more TGFβ1.

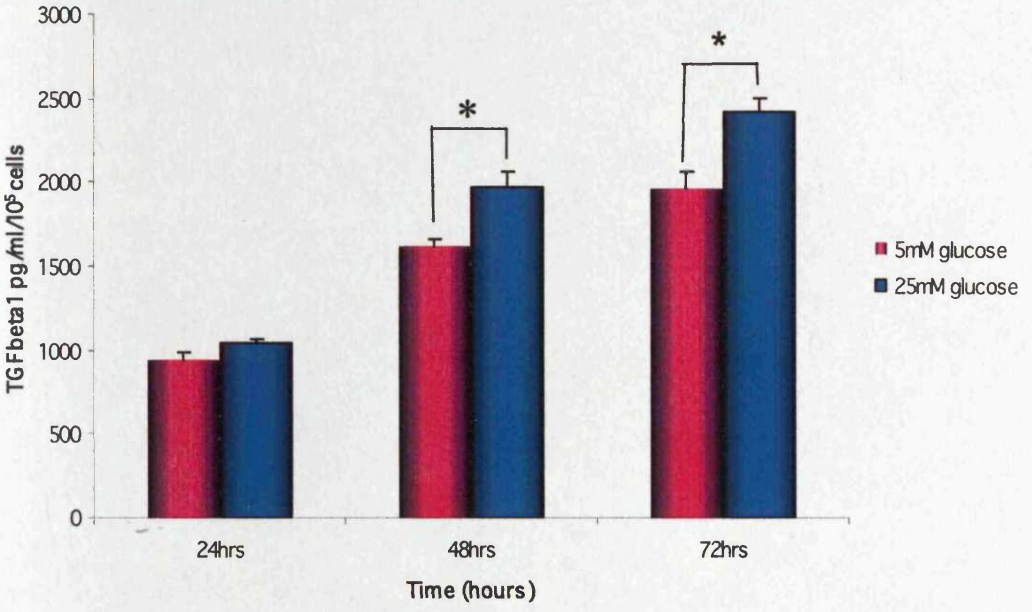

Confluent mesangial cells were incubated under serum free conditions with either 5mM D-glucose (NG) or 25mM D-glucose (HG) for up to 72hours. At the time points indicated cell culture supernatant was collected and TGF-ß1 quantified by ELISA. Total TGF-ß1 was determined following activation of latent TGF-ß1 by acid activation of supernatants. Results represent mean ± S.E. of three individual experiments, * denotes $p<0.05$

Figure 4.13: TGFβ1 bioactivity

A

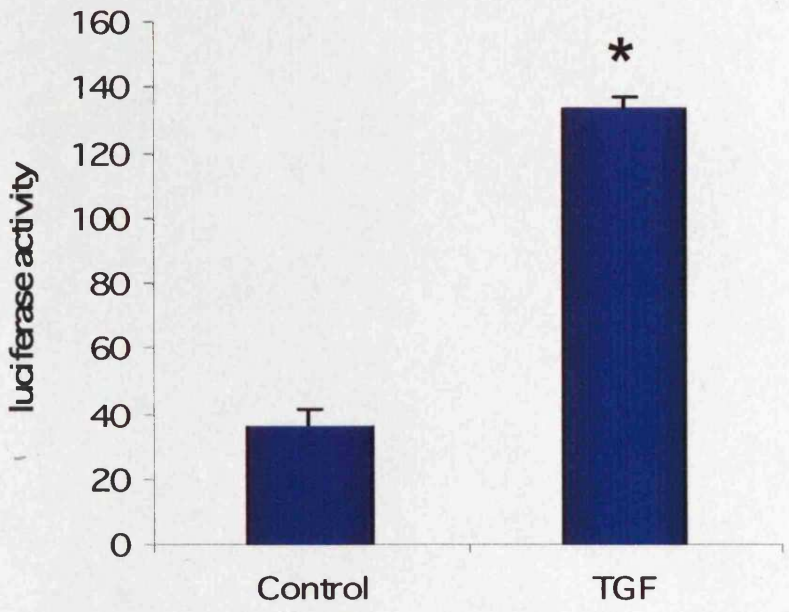

One ng/ml of TGFβ1 (R&D Systems Europe Ltd, Abingdon, UK) was added to HK2 cells that had been transfected with a Smad responsive promoter-luciferase construct for 24 hours prior to quantifying luciferase activity. In control experiments, serum-free culture medium alone was added to the transfected cells (5mM). Results represent means ± S.E. of three individual experiments and * indicates $p < 0.05$.

B

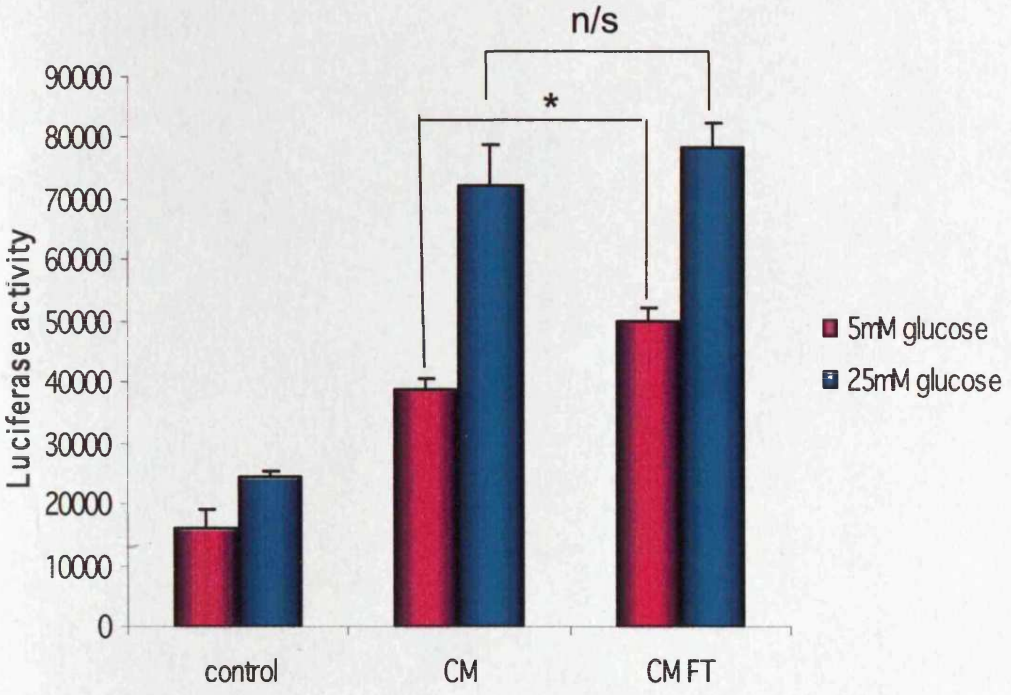

Conditioned medium (CM) collected from mesangial cells exposed to either 5mM D-glucose (5CM) or 25 mM D-glucose (25CM) for 72 hours was added to transfected HK-2 cells. In addition to latent TGF-ß1, conditioned medium from either 5mM D-glucose (5CM FT) or 25mM D-glucose (25CM FT) were subjected to 10 cycles of freeze thawing prior to addition to transfected cells. In control experiments, culture medium alone was added to the transfected cells (containing either 5mM or 25mM glucose). Luciferase activity was quantified 24 hours after the addition of conditioned medium. Results represent means ± S.E. of three individual experiments and *denotes $p<0.05$.

4.2.5: High glucose induced TGFβ1 sensitivity in mesangial cells

There is a significant difference in TGFβ1 secretion between mesangial cells cultured in 5mM and 25mM glucose after 48 hours. High glucose-induced apoptosis can be inhibited by the TGFβ1 neutralising antibody and p38 MAPK inhibition. However, high glucose treatment decreases NFκB activity and increases the Bax:Bcl-2 ratio within 24 hours (chapter 3). This implies that the early effects of high glucose-induced apoptosis are not caused by increase TGFβ1 secretion by mesangial cells cultured in 25mM glucose. Therefore the effect of mesangial cell sensitivity after culture in high glucose was studied.

High glucose induced sensitivity to TGFβ1 in mesangial cells: Mesangial cells were transfected with the Smad-responsive promoter and then incubated in either 5mM or 25mM glucose containing 1ng/ml TGFβ1 for 24 hours prior to assessment of luciferase activity (figure 4.14). In the control, mesangial cells were incubated in 5mM glucose without TGFβ1 to measure baseline luciferase activity. TGFβ1 treatment increased luciferase activity significantly in mesangial cells cultured in 25mM glucose compared to 5mM glucose (an 18.6% increase).

Effect of high glucose on TGFβRII expression: Mesangial cells were cultured in 5mM or 25 mM glucose, without serum, for up to 72 hours. Subsequently, TGFβRII expression was assessed by Western blot (figure 4.15). There was no change in expression of TGFβRII.

These results suggest that culuring mesangial cells in high glucose induces sensitivity to TGFβ1, although there seems to be no change in TGFβRII expression.

Figure 4.14: High induces TGFβ1 sensitivity in mesangial cells

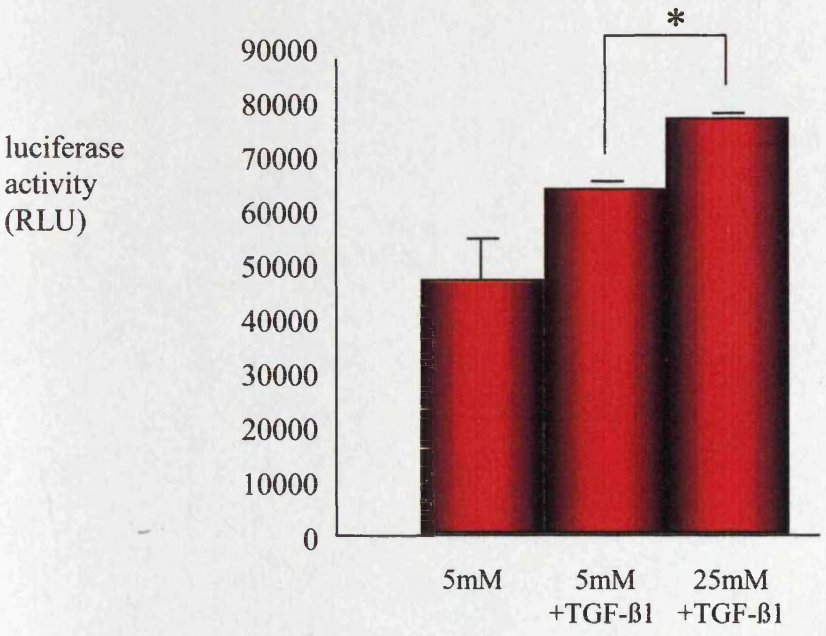

Mesangial cells were grown to 50% confluence and then transfected overnight with the Smad-responsive promoter and the β-galactosidase plasmid (used as a control for transfection efficiency). Subsequently, the media was changed to 5mM or 25mM glucose containing 1ng/ml TGFβ1 for 24 hours. In the control, the cells were cultured in 5mM glucose without TGFβ1 to assess baseline promoter activity. Luciferase activity was then quantified. Results represent means ± S.E. of three individual experiments and * denotes $p<0.05$.

Figure 4.15: High glucose does not affect TGFβRII expression

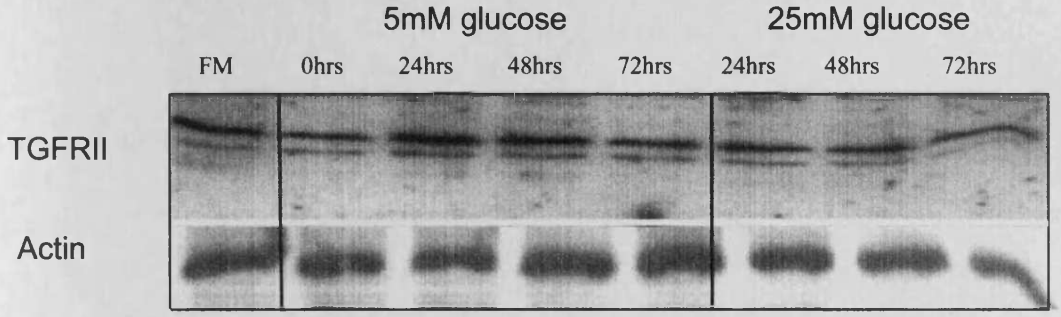

Mesagial cells were grown to confluence, followed by growth in serum-free media contatining 5mM or 25mM glucose for up to 72 hours. In the controls, the cells were cultured in full medium. Western blot analysis was performed to assess expression of TGFβ1 receptor II (TGFRII). The membrane was reprobed for actin to ensure equal loading.

4.3: Discussion

Numerous studies have demonstrated that TGFß1 mediates many of the effects of glucose on mesangial cell function. Elevated glucose leads to transcriptional activation of transforming growth factorβ1 [276, 277]. Furthermore glucose mediated alteration in mesangial cell function in response to glucose is mediated by autocrine activation of transforming growth factor beta [125]. TGFβ1 has been shown to increase apoptosis in murine mesangial cells by increasing Bax expression and suppresing Bcl-2 expression and therefore leading to activation of caspase-9 [290].

In the current study I have demonstrated that addition of recombinant TGF-ß1 mimics the effects of glucose both by inhibiting NFκB activation and also increasing the Bax:Bcl-2 ratio in favor of enhanced cell death by apoptosis. Addition of TGFβ1 also lead to a decrease in Bcl-xL mRNA expression, mimicking the effect of NFκB inhibition. Furthermore, inhibition of TGFß1 action using a blocking antibody abrogated 25mM D-glucose induced apoptosis, confirming the central role of TGF-ß1 in this response.

The data presented clearly demonstrate that inhibition of p38 MAP kinase using the chemical inhibitor SB203580 prevented both TGF-ß1 and glucose induced apoptosis, thus supporting a role for this pathway in mediating glucose stimulated TGF-ß1 dependent apoptosis in mesangial cells. The role of Smad proteins in TGFβ1 mediated apoptosis needs more work because the results are inconclusive. A different transfection method could have been used (i.e. viral transfection). If it increased transfection efficiency, apoptosis could have been quantified after transfection with the Smad2DN, Smad3DN and Smad7OE plasmids.

Although I confirmed increased generation of bio-active TGFβ1 in mesangial cells exposed to elevated concentrations of glucose, the delayed time course suggests that stimulation of *de novo* synthesis is unlikely to be the mediator of the effects of elevated ambient glucose on apoptosis. TGFβ1 decreased NFκB activity within 6 hours, whereas cell culture in high glucose lead to a significant increase in TGFβ1 secretion after 48 hours. It is more likely that this is mediated by enhanced sensitivity to TGFβ1 signalling. Although the expression of the TGFβRII did not change over 72 hours, cells cultured in high glucose showed increased smad-responsive signaling upon addition of TGFβ1.

In conclusion, I have demonstrated that glucose induced mesangial cell apoptosis is mediated by autocrine stimulation by TGF-ß1 and the p38 MAP kinase pathway. This leads to inhibition of nuclear translocation of NFκB and suppression of Bcl2 expression.

TGFβ1 is an important mediator of diabetic nephropathy. It exerts its effects via downstream signalling molecules such as Smad2, Smad3, ERK and p38 MAP kinase [114]. *In vivo*, mesangial cells exposed to high glucose secretion increased concentrations of TGFβ1, leading to fibrosis, and are also more sensitive to the effects of TGFβ1. In the glomeruli of diabetic rats there is a progressive increase in TGFβ1 mRNA and protein expression [128]. TGFβ1 is the mediator of high glucose-induced mesangial cell apoptosis which occurs during overt nephropathy.

CHAPTER 5:
GLUCOSE AND THE HANDLING OF APOPTOTIC CELLS

CHAPTER 5: GLUCOSE AND THE HANDLING OF APOPTOTIC CELLS

5.1: Introduction

Mesangial cell loss through apoptosis occurs in experimental diabetic nephropathy [193] and in clinical studies in patients with diabetic nephropathy, a loss of mesangial cells correlates with progression to diabetic glomerulosclerosis [32, 38, 41]. *In vivo,* apoptotic cells are rapidly recognised and ingested by phagocytic cells, macrophages and mesangial cells, before release of toxic contents. Necrotic cells, however, lose their membrane integrity, releasing their contents, leading to inflammation. Engulfment of apoptotic cells is thought not only to remove them from the tissues but also to provide protection from local damage resulting from release or discharge of pro-inflammatory contents [291].

In a number of tissues it has been observed that apoptotic cells are ingested and degraded so rapidly that they are only visible for 1-2 hours [175, 184]. Mesangial cells have a role in particulate clearance in the glomeruli [227] and the capacity to phagocytose does seem compatible with this property, emphasising the 'cleansing' function of the cell. Mesangial cells are semi-professional phagocytes that have the capacity to ingest apoptotic cells such as apoptotic neutrophils [227]. Resolution post nephritis is known to involve phagocytosis of apoptotic neutrophils by mesangial cells [274].

The recognition of apoptotic cells by phagocytes involves changes in expression of molecules on the apoptotic cell surface, such as exposure of phosphatidylserine [229]. Ligands expressed on the apoptotic cell that signal phagocyte recognition are poorly understood, although many have been implicated. Two of the most widely studied molecules are the phosphatidylserine receptor and the αvβ3/CD36/TSP-1 mechanism.

Apoptotic cells that did not express phosphatidylserine externally were not phagocytosed by macrophages or fibroblasts [242] and phagocytic cells deficient in wild-type phosphatidylserine were defective in removing apoptotic cells [245]. Mesangial cell phagocytosis of apoptotic U937 cells can be inhibited when the phosphatidylserine-mediated mechanism is reduced by addition of phospho-L-serine [241, 244].

A second mechanism is αvβ3/CD36/TSP-1 and macrophages have been reported to use this mechanism to ingest apoptotic cells. TSP-1 forms a bridge between the two cells by binding to an unidentified ligand on the apoptotic cell and αvβ3/CD36 on the phagocytic macrophage [237]. Mesangial cells also use this mechanism to ingest apoptotic neutrophils [104, 239] and inhibition of αvβ3 and TSP-1 can reduce phagocytosis of apoptotic cells by mesangial cells [257].

The process of apoptotic cell clearance actively suppresses the initiation of inflammation and immune responses, in part through release of anti-inflammatory cytokines [251-253]. Phagocytosis of apoptotic cells by macrophages is associated with the production of anti-inflammatory cytokines such as IL-10 and TGFβ1 *in vivo* [247, 254, 292].

Particularly interesting from the point of view of this thesis is that phagocytosis of apoptotic cells induces TGFβ1 secretion in macrophages. The results in chapters 3 and 4 showed that high glucose induced mesangial cell apoptosis was mediated by high glucose induced increased sensitivity to TGFβ1 and increased TGFβ1 secretion. Although hyperglycaemia has been implicated in mesangial cell apoptosis, the relationship between hyperglycaemia and mesangial cell handling of apoptotic cells has not been characterised.

Since mesangial cells are semi-professional phagocytes and apoptotic mesangial cells are not seen in a hypocellular diabetic kidney, the role of high glucose in mesangial cell clearance was studied. Aged PMNs were used as a model of apoptotic cells in this study. The aims of this chapter were therefore:

1) To examine the effect of elevated glucose concentration on engulfment of apoptotic cells and define the mechanism by which this occurs.
2) To examine the functional consequences of interaction between mesangial cells and apoptotic cells with particular emphasis on TGFβ1 generation, which has been implicated as a critical factor promoting renal injury in diabetes.

5.2: Results

5.2.1: High glucose increased mesangial cell ingestion of apoptotic cells

MPO staining of apoptotic cells to determine phagocytosis: To determine the effect of high glucose concentration on mesangial cell phagocytosis, confluent mesangial cells were cultured in 5mM or 25mM D-glucose for 48 hours prior to the addition of aged neutrophils. The ratio of aged neutrophils to mesangial cells was 2:1, giving an

excess of aged neutrophils. The two cell types were co-cultured in either the presence or absence of 10% FCS. After 3 hours of co-culture, the neutrophils were removed with gentle agitation using a Pasteur pipette and the mesangial cells were washed in PBS. The mesangial cells were fixed and the ingested neutrophils were stained for MPO. Only the neutrophils contained MPO, therefore this method could be used to distinguish between the two cell types (see methods section).

Mesangial cells cultured with aged neutrophils in the presence of 10% FCS ingested more PMNs (figure 5.1). Also, mesangial cells cultured in 25mM glucose phagocytosed more apoptotic cells compared to mesangial cells cultured in 5mM glucose, in the presence of 10% FCS.

There were three limitations to using this method to quantify phagocytosis of apoptotic cells. By light microscopy, it was difficult to see each mesangial cell and therefore difficult to count the number of neutrophils per mesangial cell. The aged neutrophils may not have been phagocytosed, just bound to the surface of the mesangial cell. There may also have been different numbers of mesangial cells per field, as glucose induces mesangial cell hypertrophy [293].

Quantification of phagocytosis by flow cytometry: Mesangial cells were cultured in either 5mM or 25mM glucose prior to addition of aged neutrophils. Aged neutrophils were labelled with CFSE before co-culture with mesangial cells in either the presence of 5% or 10% FCS (validation in methods chapter). The apoptotic cells were washed off after 3 hours of co-culture by gentle agitation with a Pasteur pipette and then the mesangial cells were treated with trypsin to remove them from the plate and to form a

single cell suspension. Trypsin treatment also dislodged any remaining bound neutrophils. Phagocytosis was quantified by assessing mesangial cell fluorescence by flow cytometry as described in the methods section. This method was much more robust and reproducible than staining the ingested apoptotic neutrophils for MPO and therefore used for all the remaining experiments to quantify phagocytosis.

Effect of serum on phagocytosis: In macrophages, serum is required for internalisation of apoptotic cells and only binding of apoptotic cells has been reported to occur in the absence of serum [239, 249, 294]. The presence of serum is also known to increase phagocytosis in mesangial cells [227, 249].

Mesangial cells were cultured in either 5mM or 25mM glucose. Aged neutrophils were then added in the presence of 5% or 10% serum (figure 5.2). Serum increased phagocytosis of aged PMNs by mesangial cells cultured under both conditions. Under 5mM glucose conditions, phagocytosis increased from 30.8±3.1% to 35.6±0.3% when the concentration of FCS was increased. Under 25mM glucose conditions, phagocytosis increased from 41.2±1.0% in 5% FCS to 45.7±0.3% in 10% FCS. At both concentrations of FCS, mesangial cultured in 25mM glucose phagocytose more aged PMNS compared to mesangial cells cultured under 5mM glucose conditions.

Effect of high glucose on phagocytosis: Mesangial cells cultured in high glucose ingested more aged PMNs compared to mesangial cells cultured in normal glucose in a time-dependent manner (figure 5.3). This difference was apparent after 48 hours (21% phagocytosis in 5mM glucose compared to 24% phagocytosis in 25mM glucose). After 72 hours, the amount of phagocytosis was still significantly different

between mesangial cells cultured in 5mM and 25mM glucose, but was no greater than at 48 hours. Therefore mesangial cells were cultured in normal or high glucose for 48 hours for all remaining experiments.

Taken together, these results show that mesangial cells cultured in 25mM glucose ingest more apoptotic cells and that a component of serum is required for phagocytosis. For all of the remaining experiments, the flow cytometry method was used to quantify phagocytosis.

Figure 5.1: MPO-staining of ingested apoptotic cells

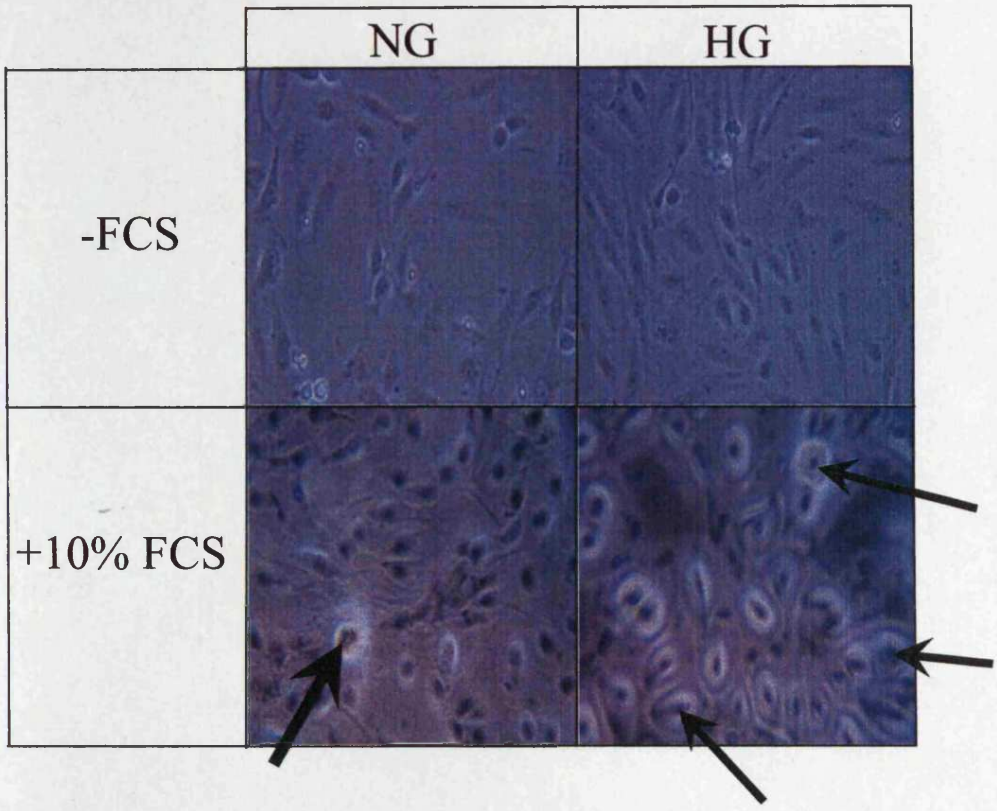

Mesangial cells were grown to approximately 70% confluence and then cultured in the presence of either 5mM D-glucose (NG) or 25mM D-glucose (HG) in the absence of FCS for 48 hours, followed by co-culturing with aged PMNs for 3 hours in either the presence or absence of 10% FCS. The cells were fixed and stained for MPO and the ingested PMNs viewed with a light microscope (x125 magnification).

⟶ = ingested aged PMNs.

Figure 5.2: Serum increases phagocytosis

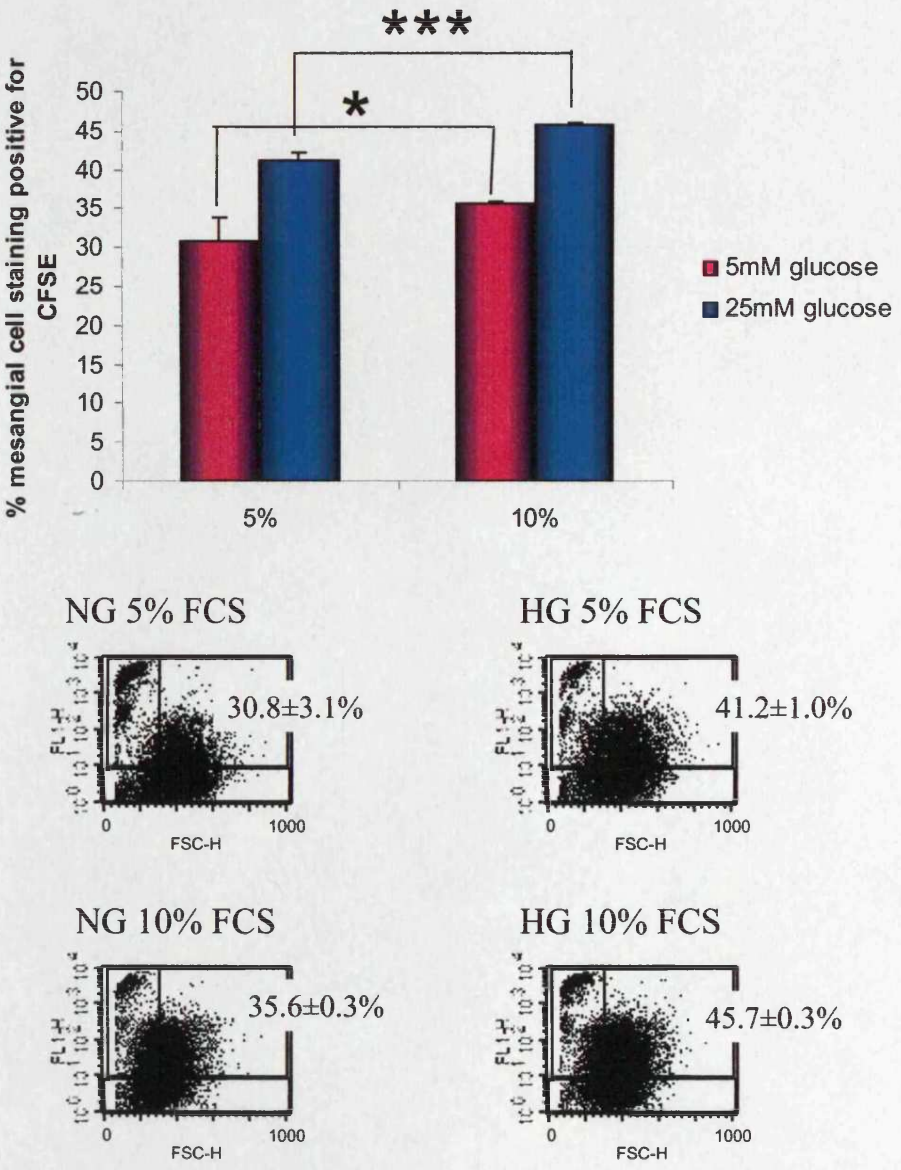

Rat mesangial cells were grown to confluence, followed by growth in serum free media containing 5mM or 25mM glucose for 48 hours. Aged, CFSE-labelled PMNs were then co-incubated with the mesangial cells (a 2:1 ratio of apoptotic cells to mesangial cells) in media containing 5% or 10% FCS for 3 hours prior to quantification of phagocytosis by flow cytometry. The mean result of three individual samples is expressed, ± S.E, * denotes $p < 0.05$ and *** denotes $p < 0.001$. The corresponding FACS plots are also shown.

Figure 5.3: High glucose increases phagocytosis

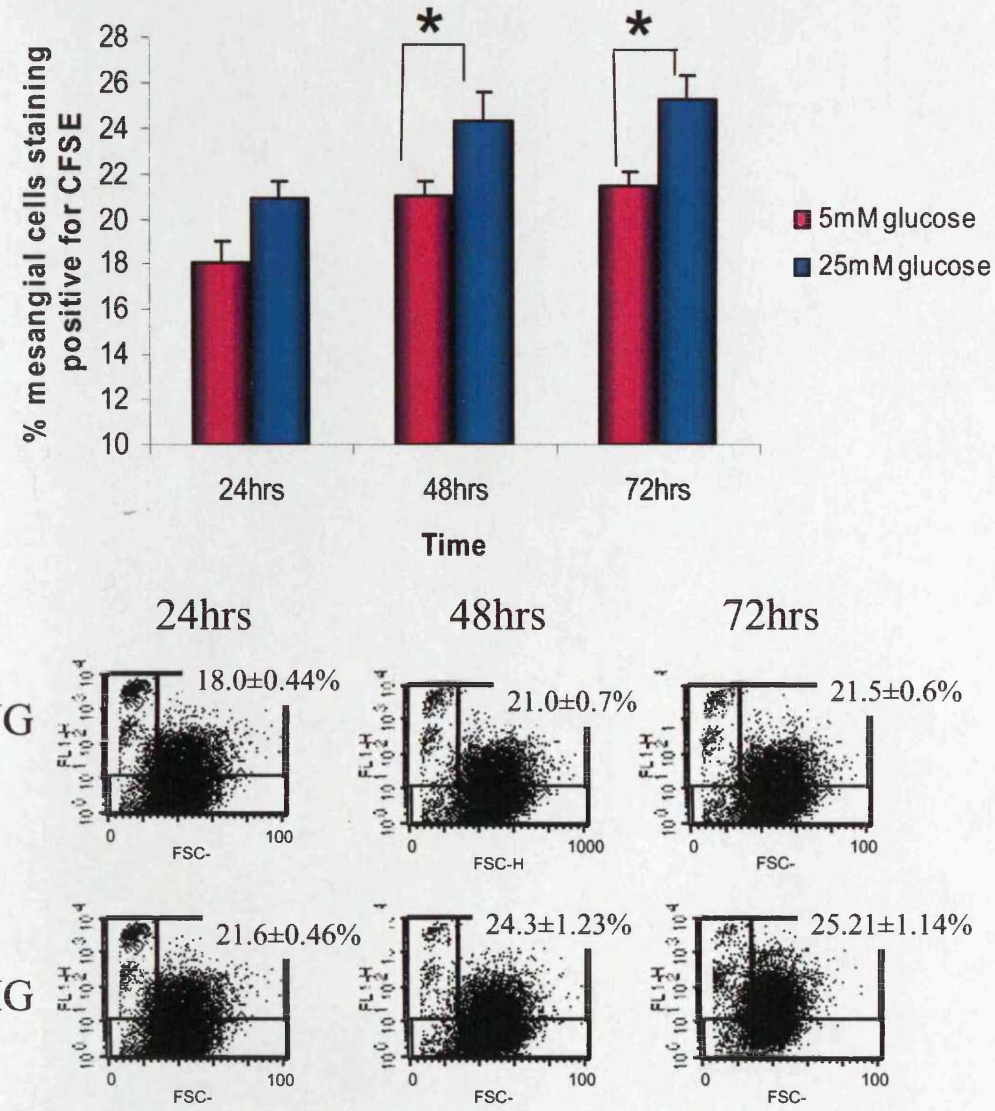

Rat mesangial cells were grown to confluence, followed by growth in serum free media containing 5mM or 25mM glucose for up to 72 hours. Aged, CFSE-labelled PMNs were then co-incubated with the mesangial cells (a 2:1 ratio of apoptotic cells to mesangial cells) in media containing 10% FCS for 3 hours prior to quantification of phagocytosis by flow cytometry. The mean result of six individual samples is expressed, ± S.E. and * denotes $p < 0.05$. The corresponding FACS plots are also shown.

5.2.2: The effect of TGFβ1 on phagocytosis

High glucose increased phagocytosis of aged PMNs and mesangial cells cultured under high glucose conditions secreted more TGFβ1 compared to normal glucose. Mesangial cells cultured under high glucose conditions were also more sensitive to the effects of TGFβ1 (chapter 4 results). The effect of TGFβ1 on phagocytosis was therefore determined. Initially, mesangial cells were cultured in 5mM glucose for 48 hours prior to the addition of apoptotic neutrophils in the presence or absence of recombinant TGFβ1 (figure 5.4). Under these experimental conditions, TGFβ1 did not influence phagocytosis of aged PMNs.

Since TGFβ1 did not have a direct effect on phagocytosis, the effect of TGFβ1 pre-treatment on mesangial cells was investigated (figure 5.5). Addition of recombinant 1ng/ml TGFβ1, 48 hours prior to PMN addition, to mesangial cells cultured in normal glucose lead to a 23-34% increase in phagocytosis. Mesangial cells cultured in high glucose ingested more cells compared to normal glucose (55.4% phagocytosis in 25mM glucose vs 47.6% phagocytosis in 5mM glucose). Also, addition of the anti-TGFβ antibody to mesangial cells cultured in high glucose for 48 hours lead to a 21% decrease in phagocytosis (55.4% ingestion without antibody and 43.6% ingestion with antibody).

These results suggest that TGFβ1 increases phagocytosis and the effects of high glucose are mediated by TGFβ1.

Figure 5.4: Effect of TGFβ1 on phagocytosis when added at the same time as apoptotic PMNs

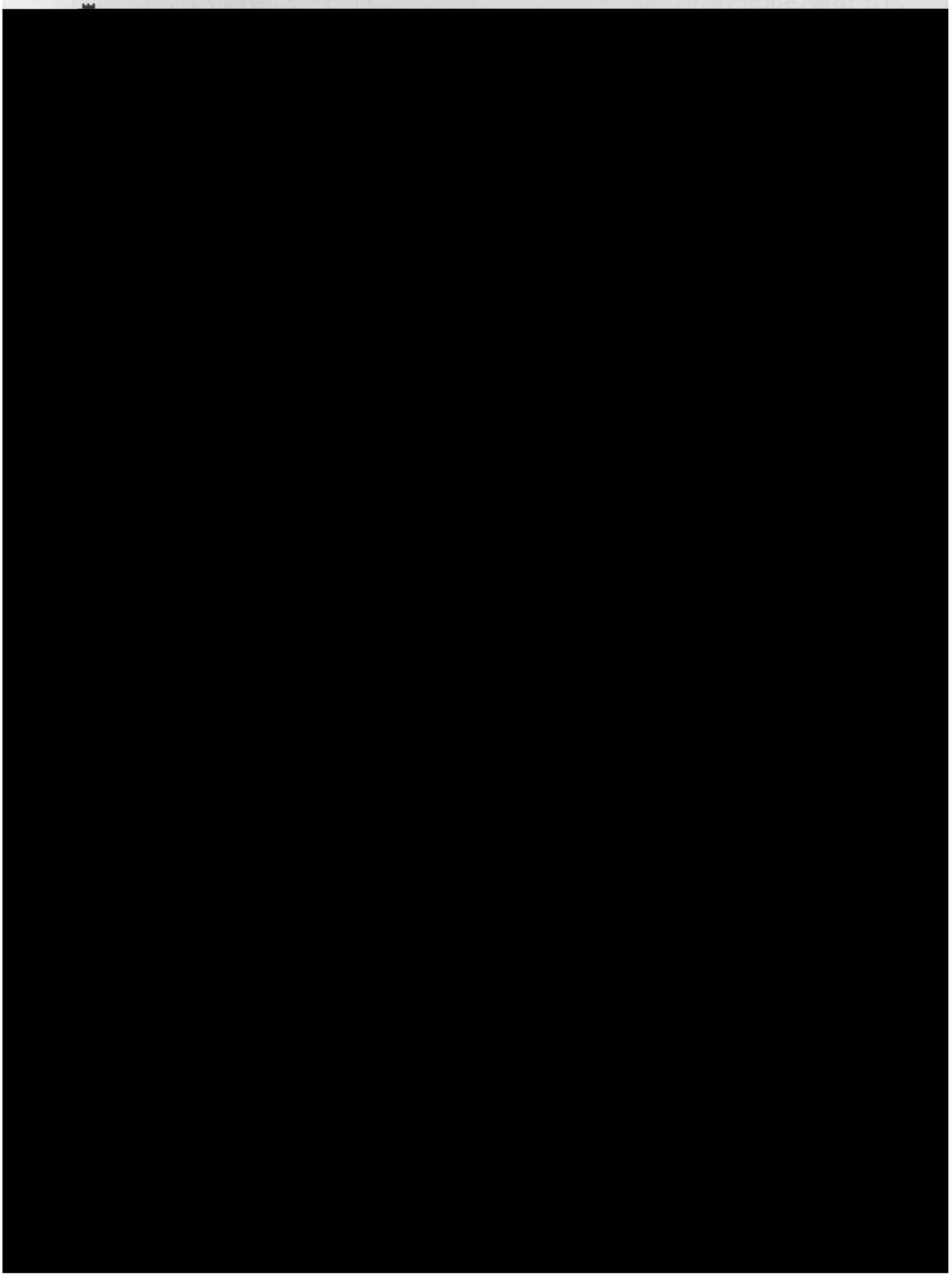

Figure 5.5: Effect of TGFβ1 pre-treatment on mesangial cell phagocytosis

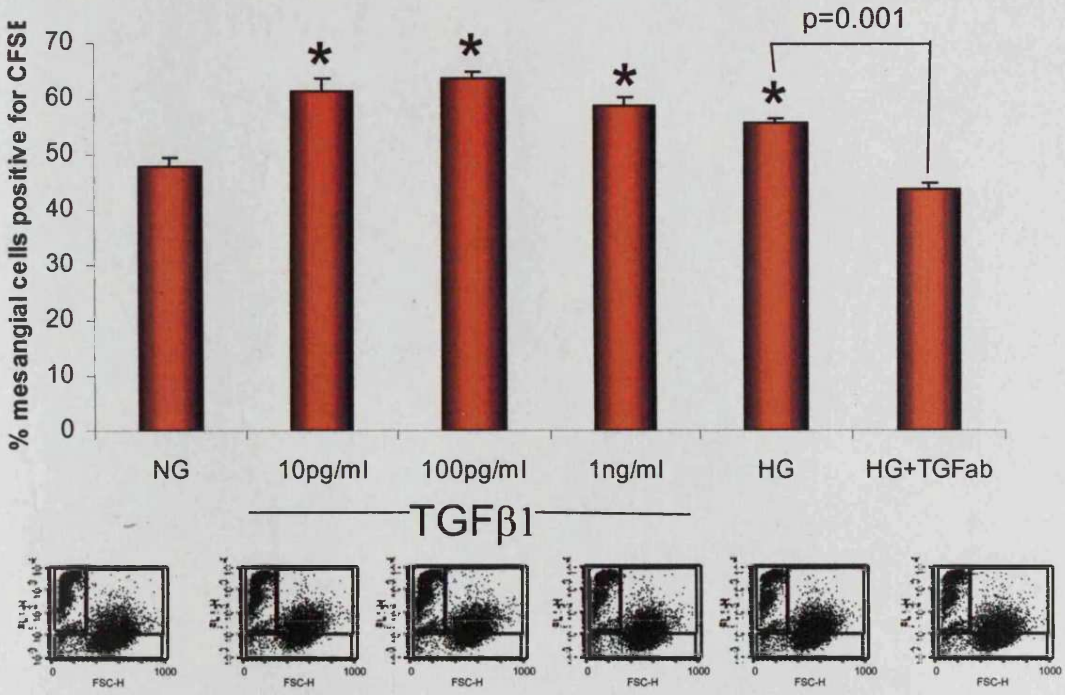

Rat mesangial cells were grown to confluence in 5mM glucose, followed by growth in serum free media containing 5mM (NG) or 25mM (HG) glucose for 48 hours. TGFβ1 was added to cells cultured in 5mM glucose for 48 hours. The TGFβ antibody (20μg/ml) was added as indicated to cells cultured in 25mM glucose. Aged, CFSE-labelled PMNs were then co-incubated with the mesangial cells (a 2:1 ratio of apoptotic cells to mesangial cells) for 3 hours prior to quantification of phagocytosis by flow cytometry. The mean result of three individual samples is expressed, ± S.E. and * denotes $p < 0.05$ compared to NG. The corresponding FACS plots are also shown.

5.2.3: Involvement of the phosphatidylserine receptor

The phosphatidylserine receptor is molecule which has been implicated in phagocytosis of apoptotic cells [245, 246, 248]. The role of this receptor in mesangial cell phagocytosis was therefore investigated. The effect of high glucose on expression of PSR at the mRNA level was studied using specific oligonucleotide primers (figure 5.6). The mesangial cells were cultured in 5mM or 25mM glucose for 48 hours, without serum prior to RNA extraction. PCR revealed a single band of 146 bps, the expected product size. Addition of 25mM D-glucose, however, did not alter PSR mRNA expression.

The effect of blocking the phosphatidylserine receptor using *O*-phospho-L-serine, a soluble form of phosphatidylserine, was used to determine the role of PSR in mesangial cell phagocytosis (figure 5.7). Addition of *O*-phospho-L-serine had no effect on mesangial cell phagocytosis of apoptotic PMNs, suggesting that in this experimental system PSR is not involved.

Figure 5.6: PS receptor mRNA expression

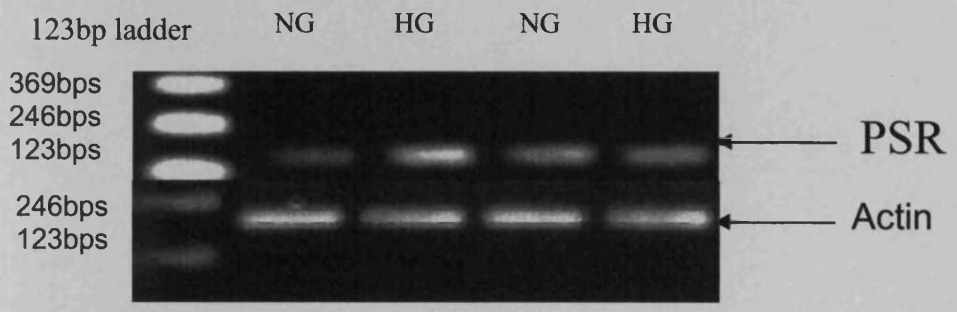

Mesangial cells were grown to confluence followed by serum-deprivation for 48 hours in either 5mM glucose (NG) or 25mM glucose (HG) medium. RNA was extracted for RT-PCR analysis of PSR expression, 35 cycles amplification. Ethidium bromide stained PCR products were separated on a 3% agarose gel.

Figure 5.7: Effect of blocking PSR on phagocytosis

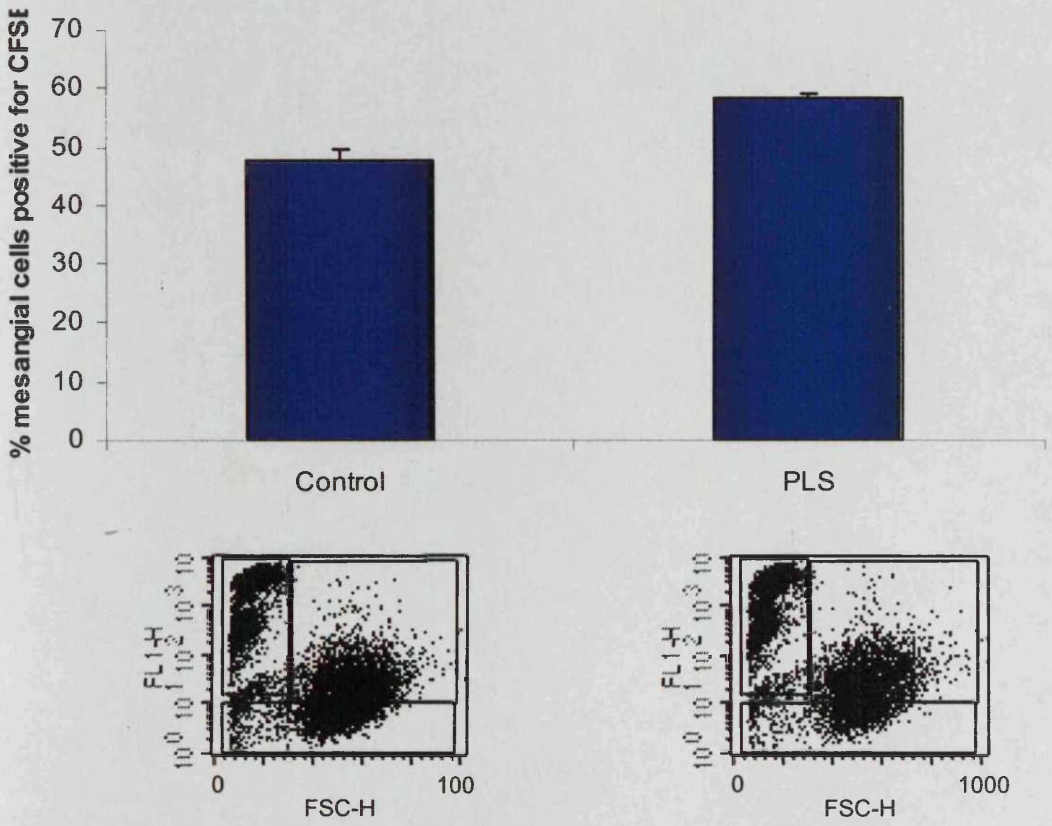

Rat mesangial cells were grown to confluence, followed by growth in serum free media containing 5mM (NG) glucose for 48 hours. 30 minutes before the addition of aged PMNs, the phospho-L-serine (PLS, 1mM) was added to cells, as indicated. In the control experiment (control), PLS was not added to the mesangial cells. Aged, CFSE-labelled PMNs were then co-incubated with the mesangial cells (a 2:1 ratio of apoptotic cells to mesangial cells) for 3 hours prior to quantification of phagocytosis by flow cytometry. The mean result of three individual samples is expressed, ± S.E. The corresponding FACS plots are also shown.

5.2.4: Involvement of the CD36/αvβ3/TSP-1 mechanism in phagocytosis

The CD36/αvβ3/TSP-1 mechanism has been implicated to have a role in macrophage [230, 237, 238, 242, 292] and mesangial cell phagocytosis [257]. To study the role of CD36/αvβ3/TSP-1 in mesangial cell phagocytosis, two strategies of inhibiting this mechanism were used (figure 5.8). Firstly, the RGDS peptide (Arg-Gly-Asp-Ser) was used to inhibit phagocytosis. The RGDS peptide binds to integrins such as αvβ3, and inhibits the phagocytosis mechanism. It can also bind to other integrins which recognise the RGD motif, such as α5β1, αIIbβ3 and most α5-containing integrins. RGES (Arg-Gly-Glu-Ser) is the control peptide. In the second method, a TSP-1 neutralising antibody was used to inhibit phagocytosis via this mechanism.

Effect of the αvβ3/TSP-1/CD36 mechanism on phagocytosis: In mesangial cells cultured in 5mM glucose, the RGDS peptide decreased phagocytosis from 35.6% to 25.6%, a 28% decrease. The TSP-1 neutralising antibody decreased ingestion to 30.1%, a 15% decrease. Both the RGDS peptide and TSP-1 neutralising antibody in combination decreased phagocytosis from 35.6% to 25.6%, a 28% decrease. The control peptide, RGES did not affect mesangial cell phagocytosis of aged PMNs.

In mesangial cells cultured in 25mM glucose, there was also a decrease in phagocytosis, although it was only significant when both RGDS and the antibody to TSP-1 were added in combination. Ingestion decreased from 45.7% to 35.1%, a 23% decrease in mesangial cells cultured in high glucose.

These results suggest that the αvβ3/CD36/TSP-1 mechanism is involved in mesangial cell phagocytosis of aged neutrophils.

Effect of high glucose on TSP-1 mRNA expression: Since the inhibition of apoptotic cell ingestion is more marked in mesangial cells cultured in normal glucose, high glucose may have been increasing the expression of one or more factors involved in this mechanism. Therefore, the effect of high glucose on TSP-1 mRNA expression was determined by RT-PCR (figure 5.9). High glucose did not induce changes in TSP-1 expression at the mRNA level over 72 hours.

Figure 5.8: Effect of blocking αvβ3/CD36/TSP-1 on phagocytosis

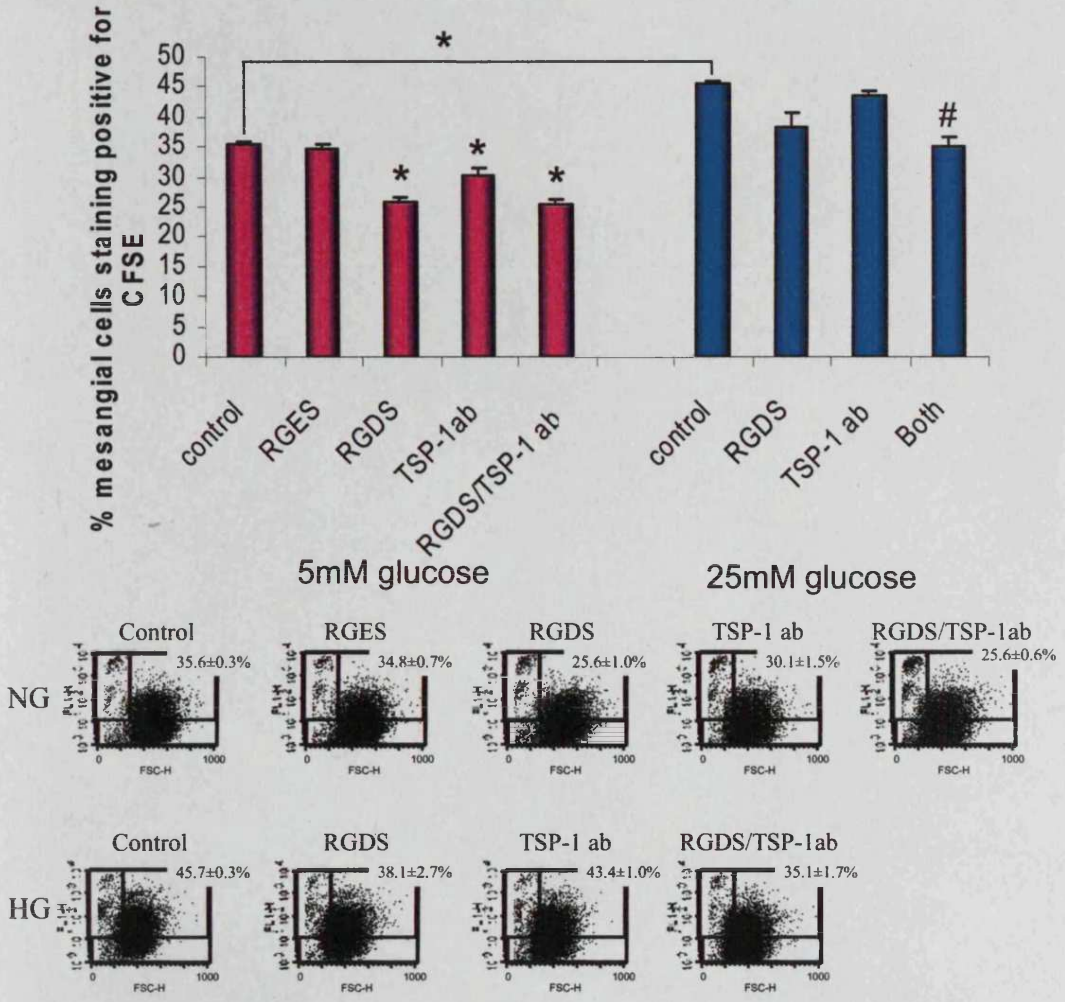

Rat mesangial cells were grown to confluence, followed by growth in serum free media containing 5mM or 25mM glucose for 48 hours. 30 minutes before the addition of aged PMNs, the RGES (100μM) peptide, RGDS (100μM) peptide and the TSP-1 neutralising antibody (7μg/ml) were added to cells, as indicated. Aged, CFSE-labelled PMNs were then co-incubated with the mesangial cells (a 2:1 ratio of apoptotic cells to mesangial cells) for 3 hours prior to quantification of phagocytosis by flow cytometry. The mean result of three individual samples is expressed, ± S.E., * and # denoting $p < 0.05$; * is used to show significance compared to the NG control and # denotes significance compared to the HG control. The corresponding FACS plots are also shown.

Figure 5.9: Effect of HG and TGFβ1 on TSP-1 mRNA expression

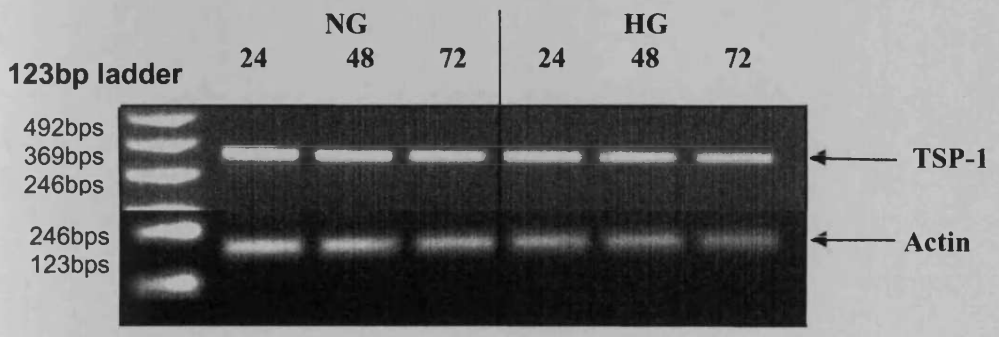

Mesangial cells were grown to confluence prior to serum-deprivation for 24-72 hours in either normal or high glucose. RNA was extracted for RT-PCR analysis of TSP-1 expression, 26 cycles amplification. Ethidium bromide stained PCR products were separated on a 3% agarose gel.

5.2.5: Binding of apoptotic cells induces TGFβ1 secretion

Ingestion of apoptotic cells alters macrophage function [247, 254] and may also have a similar affect on mesangial cell function. TGFβ1 secretion increased in macrophages that had ingested apoptotic cells. Therefore, the effect of co-culturing mesangial cells with apoptotic PMNs on TGFβ1 secretion was determined.

Co-culture with aged neutrophils induces TGFβ1 secretion in mesangial cells: Mesangial cells were cultured in normal or high glucose for 48 hours, prior to the addition of either fresh or aged neutrophils for 3 hours before measuring TGFβ1 secretion (figure 5.10). Addition of fresh neutrophils lead to a significant increase in TGFβ1 concentration (from 683±55.8 pg/ml to 4267±501.4 pg/ml, p=0.002). Addition of aged neutrophils lead to a significantly greater increase, rising to 6501±512.2 pg/ml. A ten-fold dilution in the concentration of PMNs lead to a decrease in TGFβ1 secretion, showing this was a dose-dependent response of neutrophils.

Culturing mesangial cells in 25mM glucose lead to a significant increase in TGFβ1 secretion, compared to mesangial cells cultured in 5mM glucose (an increase from 683±55.8 pg/ml to 1246.6±69.5 pg/ml, p=0.003). This increase was much smaller than the effect of either fresh or aged PMNs and the effect of PMNs was not influenced by glucose. Therefore, this increased secretion of TGFβ1 was an effect of neutrophils binding to mesangial cells, not glucose concentration.

TGFβ1 secreted by mesangial cells and neutrophils: In the control experiments, mesangial cells were cultured in 5mM glucose for 48 hours prior to quantifiying

TGFβ1 by ELISA. The concentration of TGFβ1 secreted by fresh and aged PMNs was also measured (figure 5.11). Mesangial cells secreted significantly greater amounts of TGFβ1 than either aged and fresh neutrophils.

Phagocytosis of apoptotic cells is not required for TGFβ1 secretion: Mesangial cells require serum for phagocytosis of apoptotic cells and without serum, only binding occurs [239, 294]. Figure 5.2 shows also showed that serum increased ingestion of apoptotic neutrophils in mesangial cells. As a result, co-culturing mesangial cells with aged PMNS in the presence of serum would lead to increased phagocytosis of apoptotic cells. Mesangial cells and neutrophils were co-cultured either in the presence or absence of 10% FCS (FCS contained 12.08ng/ml TGFβ1, therefore in media containing 10% FCS the cells were exposed to 604pg TGFβ1) to determine the effects of phagocytosis of apoptotic cells on TGFβ1 secretion. There was no significant difference in TGFβ1 secretion between cells co-cultured in the presence or absence of serum (figure 5.12). Therefore, phagocytosis was not required for TGFβ1 secretion by mesangial cells and this was independent of internalisation.

Binding of aged PMNs to mesangial cells induces TGFβ1 secretion: Two methods were used to study if cell binding is required for increased TGFβ1 secretion. Firstly, to determine if cell binding was required to induce TGFβ1 secretion or whether a secreted molecule in the media was required, the effect of conditioned media from aged PMNs on mesangial cells was investigated (figure 5.13). Aged neutrophils were cultured in 5mM glucose media for 24 hours to generate the conditioned media. This conditioned media from PMNs was added to the mesangial cells for 3 hours and

TGFβ1 secretion was quantified. Conditioned media from aged PMNs contained a low amount of TGFβ1 and did not increase TGFβ1 secretion in mesangial cells.

In the second method, tissue culture inserts were used to keep the two cell types apart during the co-culture step (figure 5.14). The insert inhibited cell-cell contact between mesangial cells and the neutrophils, but allowed any soluble factors that were secreted into the media to mix. There was no change in TGFβ1 secretion when the insert was present.

These results show that cell binding is required to induce TGFβ1 secretion in mesangial cells.

Apoptotic cells induce secretion of active TGFβ1 in mesangial cells: TGFβ1 is generated in a latent form which may be activated by proteolytic processing of the latent complex [156, 295], and also conformation change of the latent complex, which may be mediated by integrin binding [98].

The results so far compared the concentrations of total TGFβ1. A TGFβ1 ELISA was not sensitive enough to determine the concentration of active TGFβ1, therefore the TGFβ1 bioassay method was used. For the TGFβ1 bioassay, conditioned media were added to HK2 cells transfected with a Smad-responsive promoter construct. The conditioned media was prepared from mesangial cells that were cultured in 5mM glucose or 25mM glucose for 48 hours before co-culture with aged PMNs for 3 hours. In the controls, conditioned medium was taken from mesangial cells and aged PMNs (figure 15).

In the control mesangial cell cultures, without PMNs, there was some active TGFβ1 and this was increased with high glucose (from 392.8 units of luciferase activity to 513.1 units). There was over two-fold increase in luciferase activity in the presence of apoptotic cells (an increase from 392.8units to 926units in 5mM glucose) but there was no significant difference between normal and high glucose. Conditioned media from aged PMNs (labelled PMN media) contained very a low concentration of active TGFβ1.

These results suggest that binding of apoptotic cells to mesangial cells induced secretion of active TGFβ1, with no significant difference between cells cultured in normal and high glucose. This is consistent with previous data on TGFβ1 secetion.

All of these results taken together suggest that binding of aged neutrophils to mesangial cells induced TGFβ1 secretion in mesangial cells and there was no difference between cells cultured in 5mM or 25mM glucose. Binding alone, not phagocytosis, was sufficient to induce TGFβ1 secretion. The presence of apoptotic cells increased the amount of latent and active TGFβ1 secreted by the mesangial cells.

Figure 5.10: Aged PMNs induce TGFβ1 secretion upon binding in mesangial cells

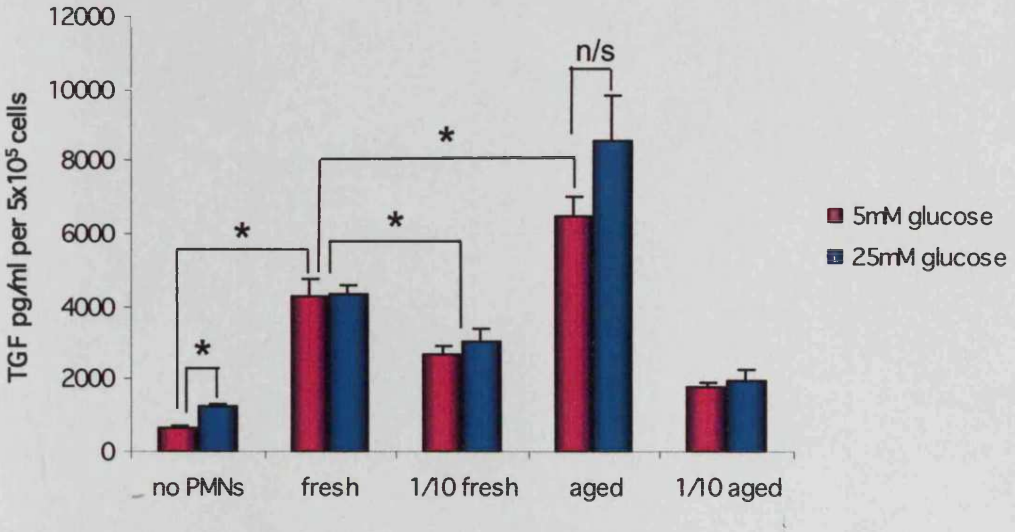

Rat mesangial cells were grown to confluence, followed by growth in serum free media containing 5mM or 25mM glucose for 48 hours. Aged or fresh PMNs were then co-incubated with the mesangial cells (a 2:1 ratio of apoptotic cells to mesangial cells) in media containing no FCS for 3 hours. Two different doses of PMNs were incubated with mesangial cells giving a 2:1 ratio of apoptotic cells to mesangial cells and a 1/10 dilution of this concentration. After the three hours incubation, the PMNs were washed off and the media changed to normal glucose without FCS for 48 hours. The amount of TGFβ1 secreted into this media was then quantified by ELISA. The mean result of three individual samples is expressed, ± S.E and * denotes $p < 0.05$.

Figure 5.11: Neutrophils do not secrete TGFβ1

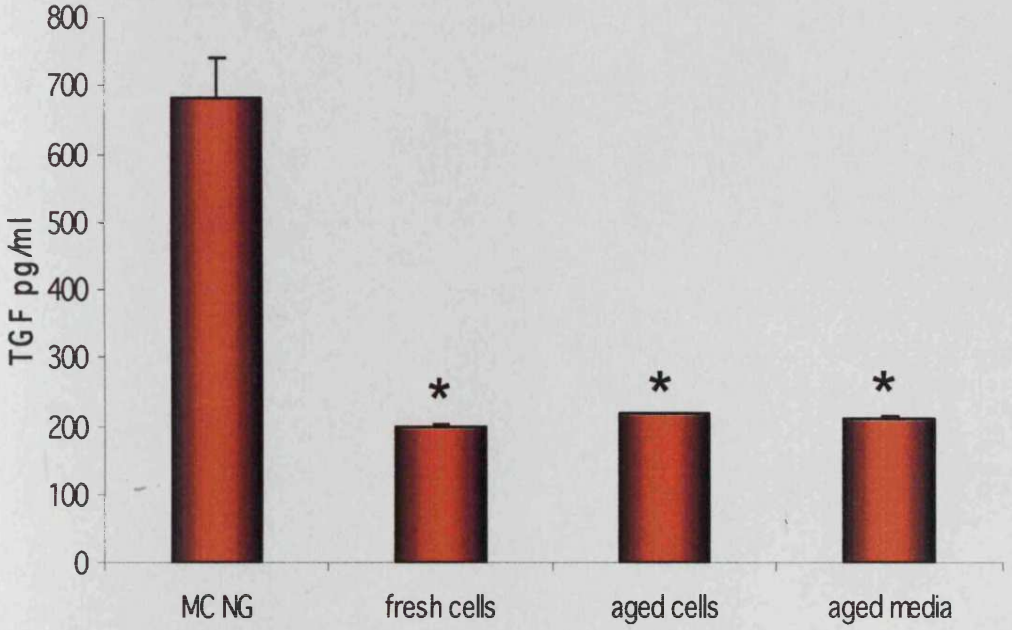

Rat mesangial cells were grown to confluence, followed by growth in serum free media containing 5mM glucose (NG) for 48 hours. The media was changed again to NG without FCS for 48 hours for the mesangial cells (MCs) and the concentration of TGFβ1 in this media was measured.

The amount of TGFβ1 secreted by fresh neutrophils was measured over 3 hours (fresh cells).

The amount of TGFβ1 secreted by aged neutrophils over 3 (aged cells, 3 hours) and 24 hours was also measured (aged cells, 24 hours).

The concentration of TGFβ1 secreted into the media was then quantified by ELISA. The mean result of three individual samples is expressed, ± S.E and * denotes $p < 0.05$ compared to MC NG.

Figure 5.12: Binding, not ingestion, leads to TGFβ1 secretion in mesangial cells

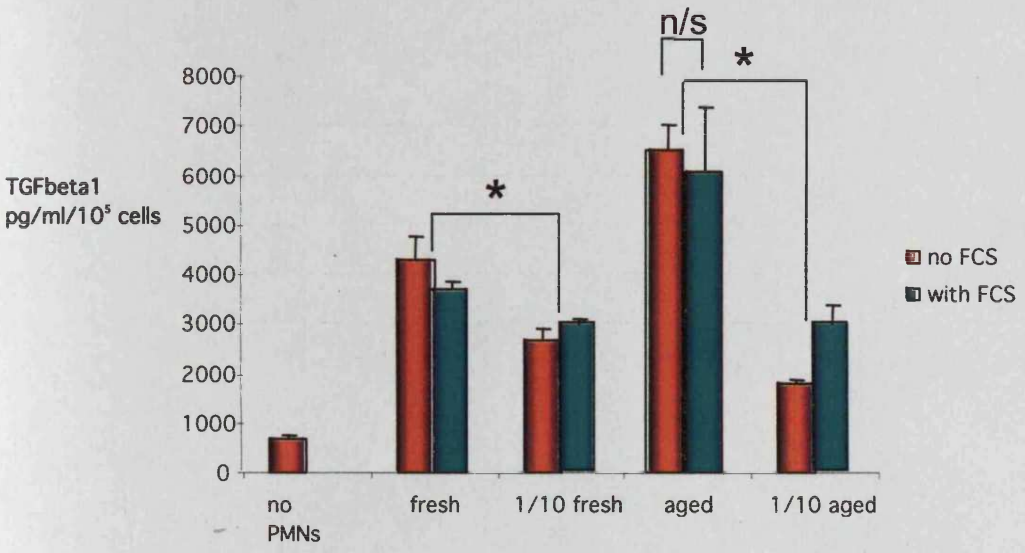

Rat mesangial cells were grown to confluence, followed by growth in serum free media containing 5mM or 25mM glucose for 48 hours. Aged or fresh PMNs were then co-incubated with the mesangial cells (a 2:1 ratio of apoptotic cells to mesangial cells) in media containing either 0% or 10% FCS for 3 hours. Two different doses of PMNs were incubated with mesangial cells giving a 2:1 ratio of apoptotic cells to mesangial cells and a 1/10 dilution of this concentration. After the three hours incubation, the PMNs were washed off and the media changed to 5mM glucose without FCS for 48 hours. The amount of TGFβ1 secreted into this media was then quantified by ELISA. The mean result of three individual samples is expressed, ± S.E. and * denotes significance.

Figure 5.13: Conditioned media from aged PMNs did not induce TGFβ1 secretion in mesangial cells

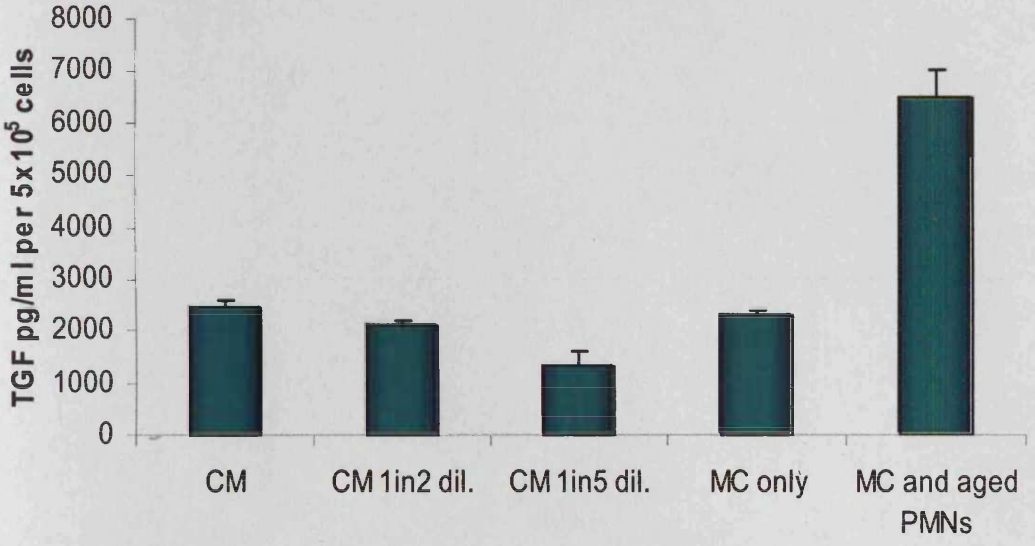

Rat mesangial cells were grown to confluence, followed by growth in serum free media containing 5mM glucose for 48 hours. Conditioned media from aged PMNs was collected after 24 hours. This conditioned media was then added to the mesangial cells for 3 hours at different dilutions (concentrated – CM, 1in2 dilution – CM 1in2 dil. - and 1in5 dilution – CM 1in5 dil.).

The negative control was mesangial cells cultured alone and the positive control was mesangial cells co-incubated with aged PMNs for 3 hours.

After the three hours, the media changed to 5mM glucose without FCS for 48 hours. The amount of TGFβ1 secreted into this media was then quantified by ELISA. The mean result of three individual samples is expressed, ± S.E

Figure 5.14: Binding of aged PMNs to mesangial cells is required for TGFβ1 secretion

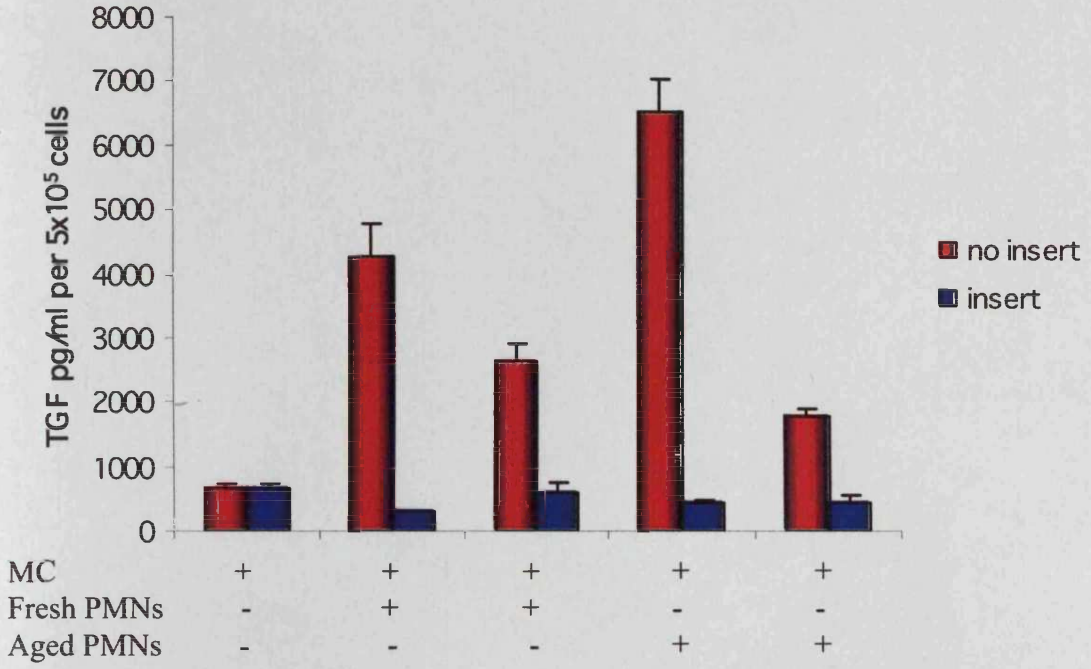

Rat mesangial cells were grown to confluence, followed by growth in serum free media containing 5mM glucose for 48 hours. PMNs were co-incubated with the mesangial cells (a 2:1 ratio of PMNs to mesangial cells) in media containing no FCS for 3 hours. The cells were co-cultured either in the presence or absence of a tissue culture inserts. Two different doses of PMNs were incubated with mesangial cells giving a 2:1 ratio of apoptotic cells to mesangial cells and a 0.2:1 ratio (a 1/10 dilution of this concentration). In the control experiments, mesangial cells were incubated alone, without PMNs.

After the three hours incubation, the PMNs were washed off and the media changed to NG without FCS for 48 hours. The amount of TGFβ1 secreted into this media was then quantified by ELISA. The mean result of three individual samples is expressed, ± S.E

Figure 5.15: Binding of apoptotic cells induces activation of TGFβ1 in mesangial cells

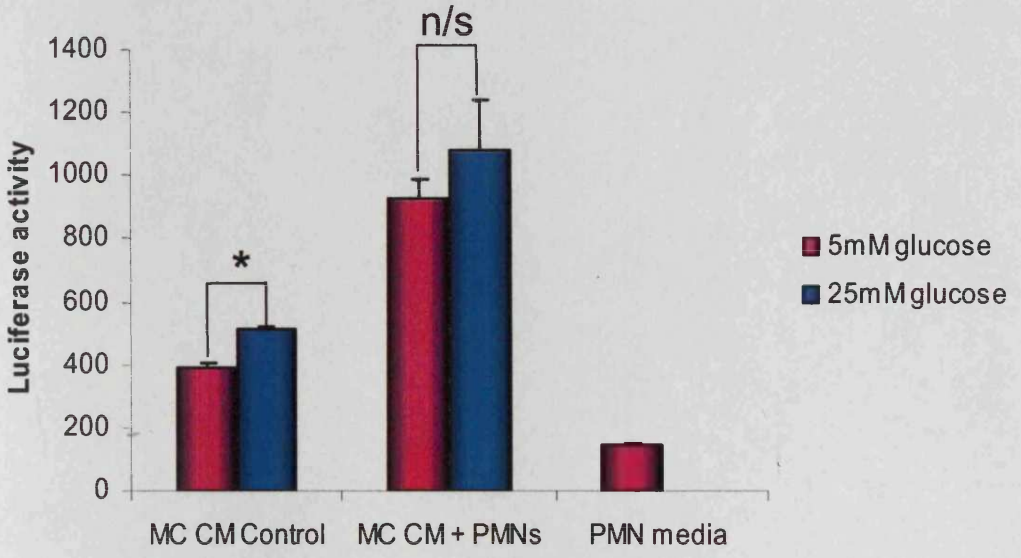

Conditioned media (CM) was prepared as follows:

Rat mesangial cells were grown to confluence, followed by growth in serum free media containing 5mM or 25mM glucose for 48 hours. Aged PMNs were then co-incubated with the mesangial cells (a 2:1 ratio of apoptotic cells to mesangial cells) in media containing no FCS for 3 hours (MC CM + PMNs). In the control, mesangial cells were incubated alone, without PMNs (MC CM control). Media from aged PMNs was also used as a control (PMN media).

After the three hours incubation, the PMNs were washed off and the media changed to normal glucose without FCS for 48 hours.

This conditioned medium was added for 24 hours to Smad-responsive vector transfected into HK2 cells, prior to measuring luciferase activity. The mean result of three individual samples is expressed, ± S.E. and * denotes significance.

5.2.6: ICAM-1 cross-linking did not induce TGFβ1 secretion in mesangial cells

Previous published work from this laboratory has shown that ICAM-1 cross-linking increased TGFβ1 secretion [296]. In proximal tubular cells, binding of unstimulated monocytes increased TGFβ1 secretion, which was dependent on ICAM-1-CD18 binding, implicating ICAM in the pathogenesis of interstitial injury [296]. In fibroblasts, direct contact of leukocytes with ICAM-1 led to cell activation and further upregulation of ICAM-1 [297]. This raises the possibility that increased TGFβ1 secretion upon addition of PMNs to mesangial cells may be dependent on ICAM-1. Therefore, the expression of CD18 on PMNs and ICAM-1 on mesangial cells was studied.

CD18 expression in PMNs and ICAM-1 expression in mesangial cells: Flow cytometry confirmed expression of CD18 on aged and fresh PMNS (figure 5.16) and the presence of ICAM-1 on mesangial cells (figure 5.17).

ICAM-1 cross-linking did not induce TGFβ1 secretion in mesangial cells: Since mesangial cells expressed ICAM-1 and aged PMNs expressed CD18, the effect of ICAM-1 cross-linking on TGFβ1 secretion in mesangial cells was investigated (figure 5.18). In contrast to proximal tubular cells, ICAM-1 cross-linking did not lead to changes in TGFβ1 secretion in mesangial cells. This suggests that CD18-ICAM is unlikely to be leading to TGFβ1 secretion in mesangial cells.

Figure 5.16: CD18 expression in neutrophils

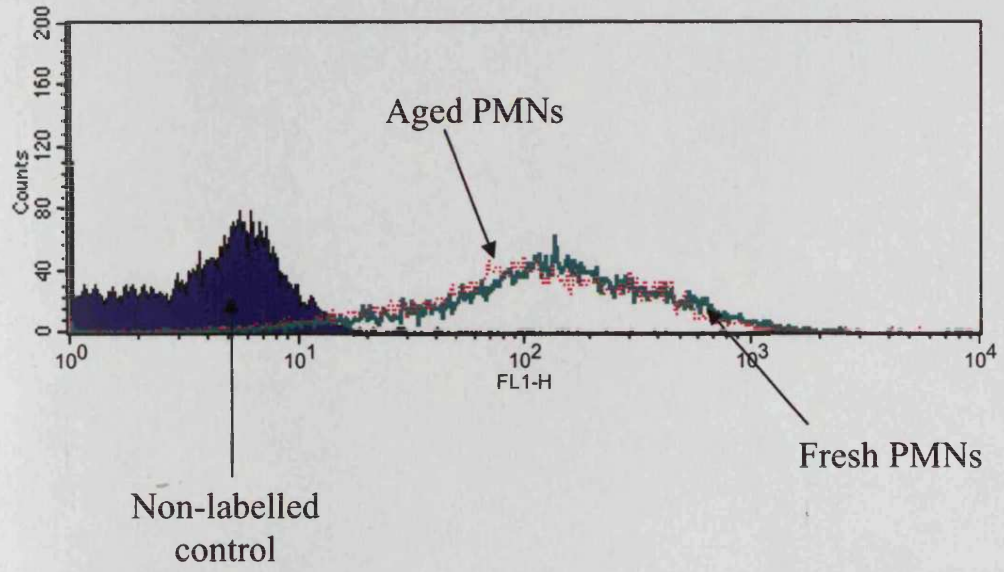

Fresh and aged PMNs were incubated in FACS buffer with the primary mouse anti-CD18 antibody (1:1000 dilution, diluted in FACS buffer) for 30 minutes at 4°C. The cells were washed in PBS and incubated with the secondary anti-mouse-FITC conjugated antibody (1:100 dilution) for 30 minutes at 4°C. They were then centrifuged as above, washed x3 in PBS, resuspended in FACS buffer and analysed by flow cytometry. The non-labelled cells were incubated with the secondary antibody only. The histogram shows a typical result from three separate experiments.

Figure 5.17: ICAM-1 expression in mesangial cells

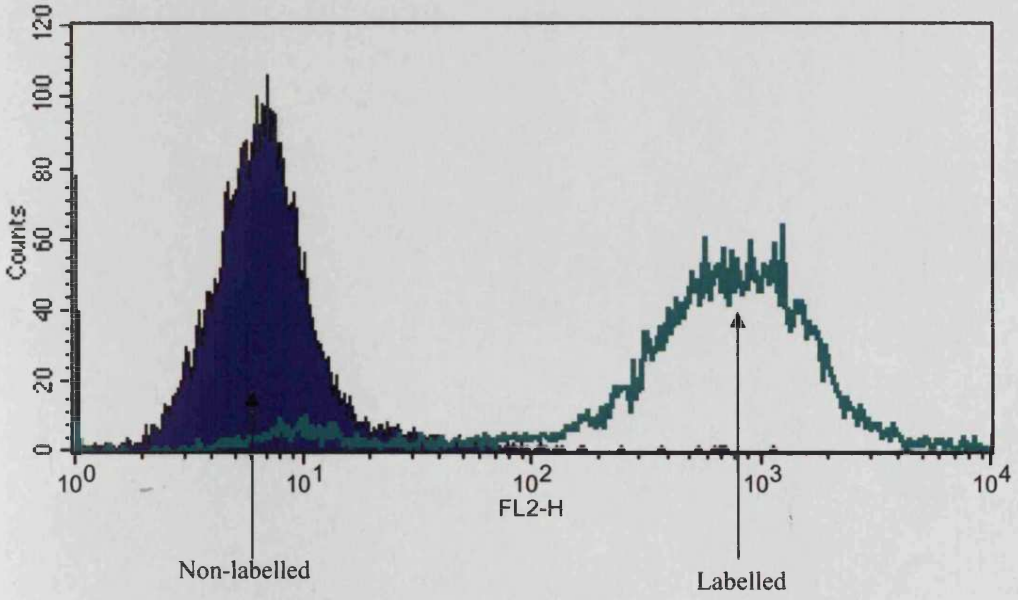

The mesangial cells were grown to confluence, followed by serum deprivation in 5mM glucose media for 48 hours. The medium was removed and the cells were washed with PBS before trypsinisation. They were placed in 1.5ml eppendorfs and centrifuged (1600rpm, 4°C, 7 mins), followed by two washes in PBS. The cells were incubated in FACS buffer with the FITC-conjugated anti-ICAM-1 antibody (1:200 dilution) for 30 minutes at room temperature. They were then centrifuged as above, washed x3 in PBS, resuspended in FACS buffer and analysed by flow cytometry. The non-labelled cells were incubated with a control anti mouse IgG antibody. The histogram shows a typical result from three separate experiments.

Figure 5.18: ICAM-1 cross-linking did not induce TGFβ1 secretion in mesangial cells

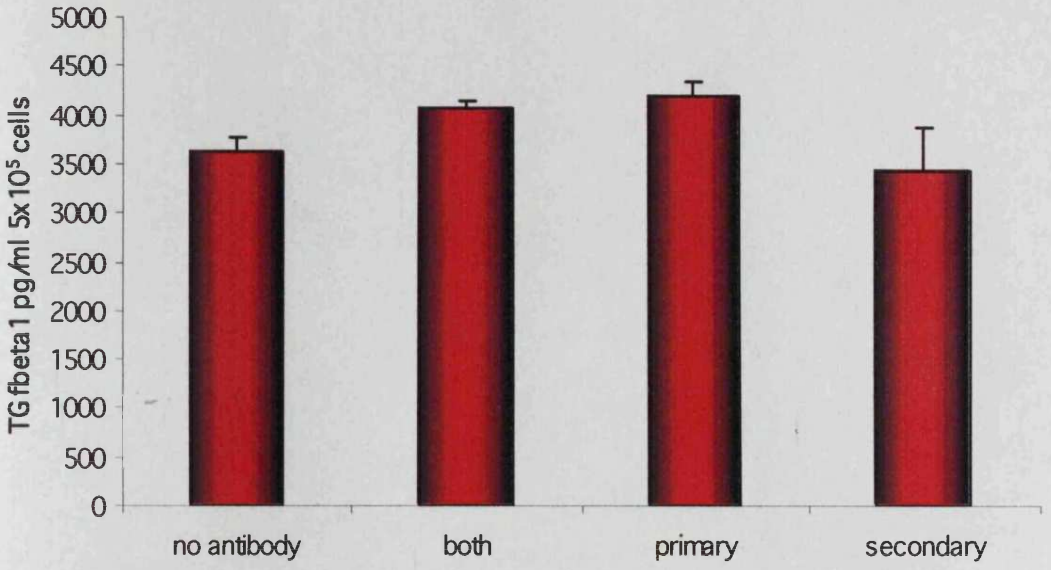

Rat mesangial cells were grown to confluence, followed by growth in serum free media containing 5mM (NG) glucose for 24 hours. The primary antibody (1ug/ml) containing the Fab portion was added to the cells for one hour, the cells were washed and the secondary cross-linking antibody (1μg/ml) was added for 24 hours. After this incubation, the antibody was washed off and the media changed to NG without FCS for 48 hours. The amount of TGFβ1 secreted into this media was then quantified by ELISA [297]. The mean result of three individual samples is expressed, ± S.E.

5.2.7: Involvement of the CD36/αvβ3/TSP-1 mechanism

The role of CD36/αvβ3/TSP-1 in TGFβ1 secretion was also studied. The mesangial cells were cultured in 5mM or 25mM glucose for 48 hours, prior to co-culture with aged PMNs. Thirty minutes before co-culture, the RGDS peptide, RGES peptide and the TSP-1 neutralising antibody were added to the mesangial cells as indicated. The concentration of TGFβ1 secreted into the media was quantified (figure 5.19).

These inhibitors did not cause a significant decrease in TGFβ1 secretion in mesangial cells. These results suggest that another mechanism must be involved in inducing TGFβ1 in mesangial cells when apoptotic cells bind.

Figure 5.19: Effect of blocking αvβ3/CD36/TSP-1 on TGFβ1 secretion

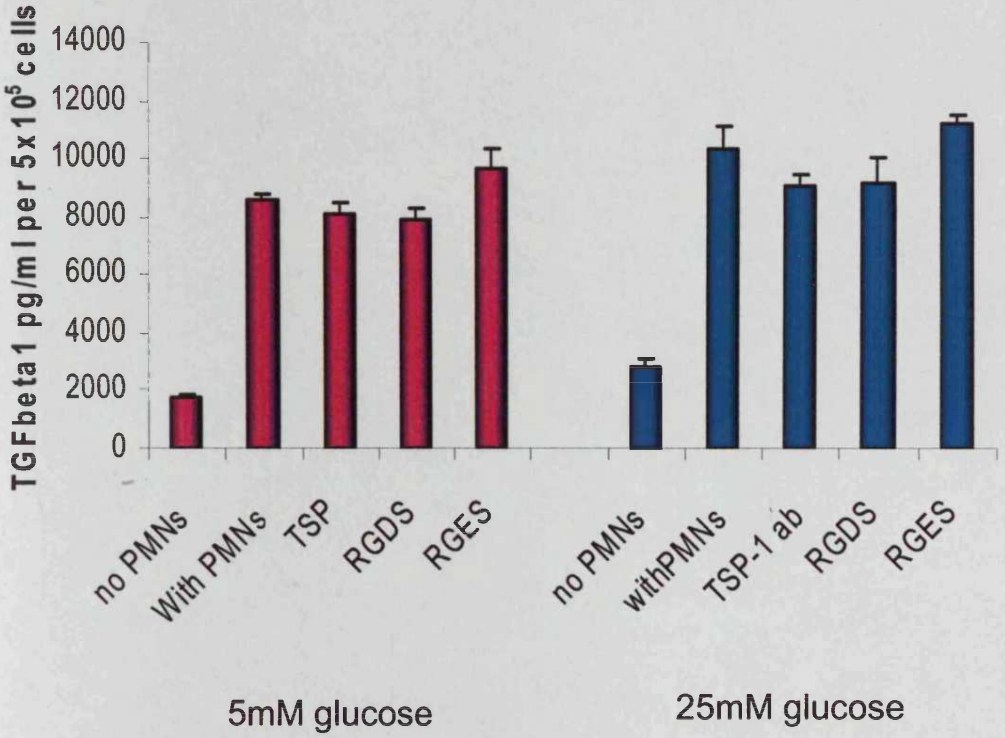

Rat mesangial cells were grown to confluence, followed by growth in serum free media containing 5mM (NG) or 25mM (HG) glucose for 48 hours. 30 minutes before the addition of aged PMNs, the RGES (100μM) peptide, RGDS (100μM) peptide and the TSP-1 neutralising antibody (7μg/ml) were added to mesangial cells, as indicated. After the three hours incubation, the PMNs were washed off and the media changed to NG without FCS for 48 hours. The amount of TGFβ1 secreted into this media was then quantified by ELISA. The mean result of three individual samples is expressed, ± S.E. and * denotes $p < 0.05$.

5.2.8: Involvement of PS receptor

Previous studies have suggested that the PSR although not involved in engulfment may be involved in binding of apoptotic cells. We therefore examined the effect of PLS on apoptotic cell dependent mesangial cell TGF-ß1 production.

The mesangial cells were cultured in 5mM or 25mM glucose for 48 hours, prior to co-culture with aged PMNs. Thirty minutes before co-culture, phospho-L-serine was added to the mesangial cells as indicated. The concentration of TGFβ1 secreted into the medium was quantified (figure 5.20). Addition of PLS together with apoptotic cells significantly reduced TGF-ß1 production by mesangial cells from 10311.21±730.2 pg/ml to 8021.58±648.0 pg/ml, suggesting that this mechanism may be involved in binding of apoptotic cells and TGF-ß1 generation.

Figure 5.20: Effect of blocking PSR on TGFβ1 secretion

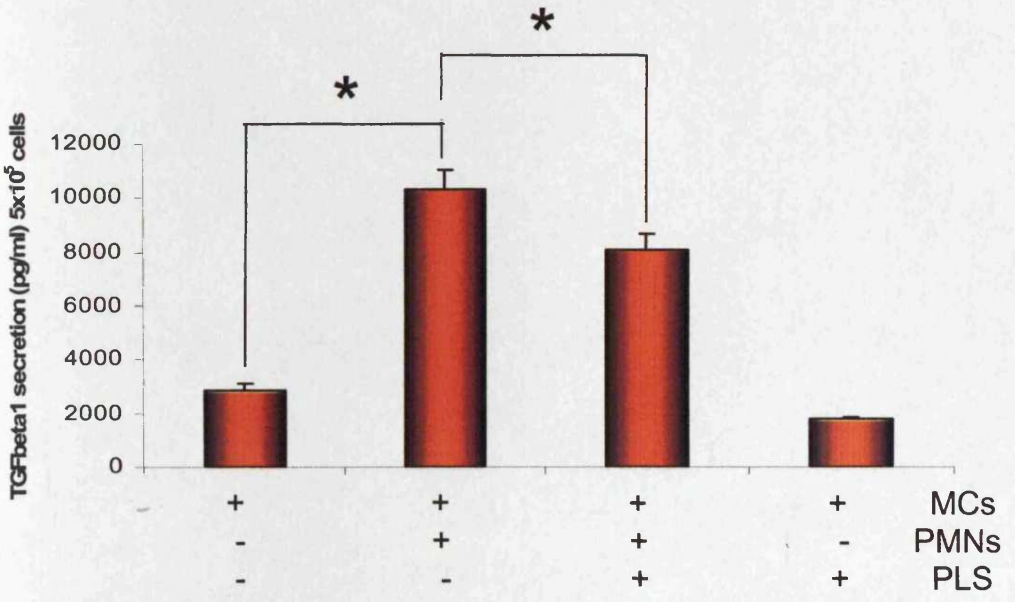

Rat mesangial cells were grown to confluence, followed by growth in serum free medium for 48 hours. 30 minutes before the addition of aged PMNs, 1mM PLS was added to mesangial cells, as indicated. After the three hours incubation, the PMNs were washed off and the media changed to NG without FCS for 48 hours. The amount of TGFβ1 secreted into this media was then quantified by ELISA. The mean result of three individual samples is expressed, ± S.E. and * denotes significance.

5.3: Discussion

Clinical studies and *in vitro* studies have shown that high glucose directly affects mesangial cell function [32, 38, 298]. The fact that mesangial cell loss is a feature of diabetic glomerulosclerosis led me led me to study the effect of high glucose on apoptosis (chapter 3). Apoptotic cells are rarely seen *in vivo* because they are phagocytosed by neighbouring cells or macrophages. Mesangial cells are semi-professional phagocytes and have been shown to phagocytosis apoptotic cells [227, 239] and they have a 'cleansing' role in the glomerulus [227]. I therefore investigated the effect of high glucose on mesangial cell phagocytosis. Aged PMNs were used as a model of apoptotic cells as this chapter investigated handling of apoptotic cells by mesangial cells, not resolution of inflammation.

Mesangial cells cultured in high glucose ingested more apoptotic cells compared to cells cultured in normal glucose. Culturing mesangial cells under high glucose conditions also led to increased apoptosis (chapter 3 results). Therefore, under high glucose conditions, there were fewer healthy mesangial cells but still an increase in cell uptake compared to cells cultured in 5mM glucose. The mesangial cells will be ingesting their non-labelled, apoptotic neighbours as well as the aged neutrophils. This suggests that the differences in apoptotic cell ingestion between cells cultured in normal and high glucose are actually greater.

TGFβ1 plays a pivotal role in diabetic nephropathy (section 1.2.3); mesangial cells cultured under high glucose conditions secrete more TGFβ1 and culturing mesangial cells in high glucose increases their sensitivity to TGFβ1 (chapter 4). The effect of TGFβ1 on phagocytosis was therefore determined. Addition of recombinant TGFβ1

lead to increased ingestion and addition of the TGFβ1 antibody to cells cultured in high glucose lead to a decrease in phagocytosis. The TGFβ1 had to be added at least 48 hours prior to co-culture for this effect. If it was added at the same time as the aged PMNs for 3 hours, this increase in phagocytosis was not seen. In contrast, TGFβ1 added 6 hours prior to co-culture of macrophages with apoptotic neutrophils lead to enhanced phagocytosis [292]. This suggests that a secondary stimulus is required for TGFβ1 induced phagocytosis, i.e., increased expression of molecules involved in phagocytosis. TGFβ1 could affect the expression of αvβ3 or CD36 on the cell surface, or could lead to increased secretion of TSP-1, the bridging molecule.

The two main methods involved in mesangial cell phagocytosis of apoptotic cells are the PS receptor and the αvβ3/CD36/TSP-1 mechanism [239, 250, 257]. The phosphatidylserine receptor is found on the phagocytic cell. It binds to phosphatidylserine on the apoptotic cell. A previous study has shown that apoptotic cells which did not express phosphatidylserine externally were not phagocytosed by macrophages or fibroblasts [242]. In this system, however, the phosphatidylserine receptor was not involved in mesangial cell phagocytosis of apoptotic cells. The αvβ3/CD36/TSP-1 mechanism, however, was involved in mesangial phagocytosis of aged PMNs. In mesangial cells cultured under normal glucose conditions, the RGDS peptide and TSP-1 inhibited ingestion both on their own and also in combination, the maximum decrease in phagocytosis was 30%. In the cells cultured under high glucose conditions, inhibition was only achieved with a combination of TSP-1 antibody and RGDS but still the maximum inhibition was 23%. This may be because high glucose increased expression of the cell surface receptors or molecules involved in phagocytosis, such as CD36, αv, β3 or TSP-1 secretion.

There are limitations to the FACS-based method to quantify phagocytosis. Although trypsin was used to form a single-cell suspension, the PMNs could have been bound to the mesangial cell surface. These PMN-mesangial cell complexes would have been counted as phagocytosed cells because they would have formed large, fluorescent complexes. It time had not been limiting, further experiments could have been carried out to confirm ingestion. Electron microscopy or confocal microscopy techniques could have been used to confirm phagocytosis and other microscopic methods could have been developed to quantify phagocytosis and confirm the FACS results.

Apoptotic fibroblasts have been shown to actively secrete increased amounts of TSP-1 to recruit macrophages and the expression of TSP-1 and its receptor CD36 were also increased on the cell surface [230]. In contrast, apoptotic neutrophils do not secrete TSP-1 [230, 257]. High glucose had no effect on changes in TSP-1 mRNA expression compared to normal glucose over 72 hours but might have caused increased TSP-1 secretion from the cell. Yevdokimova *et al* have shown that TSP-1 expression is increased significantly in cells cultured in high glucose after 5 days compared to cells cultured in normal glucose [298]. However, a commercial TSP-1 ELISA kit is not available to measure the concentration of TSP-1 in the supernatants. The effect of TGFβ1 on TSP-1 mRNA expression could also have been determined.

CD36 expression has been described on a variety of cell types including macrophages, endothelial cells and platelets [299, 300]. Limited investigations have been carried out in the regulation of CD36 expression. Embryonic human fibroblasts had an intracellular pool of CD36 that became expressed on the cell surface after exposure to TSP-1 [301]. Upregulation of surface CD36 may be a consequence of

changes of cell membrane asymmetry that occurs during apoptosis. In monocytes, TGFβ1 has been shown to decrease CD36 mRNA expression and surface protein expression [302-304]. In contrast, in endothelial cells, high glucose has been shown to upregulate CD36 [305] and in subjects with type 2 diabetes, CD36 expression in monocytes is increased [306]. Mesangial cells do not express CD36 although inhibition of αvβ3 and TSP-1 still inhibited phagocytosis, suggesting that mesangial cell phagocytosis of apoptotic neutrophils involves a CD-36 independent, αvβ3/TSP-1 mediated mechanism [257]. FACS analysis was used to study cell surface or cytoplasmic expression of CD36 in mesangial cells. Mesangial cells were negative for CD36 but positive for cell surface expression of αvβ3 and secretion of TSP-1 [257]. To my knowledge, this is the only study that has been published that investigated the expression of CD36 and αvβ3 on the surface of a mesangial cell.

The effect of high glucose and TGFβ1 on αv and β3 expression could therefore be explored. High glucose, via TGFβ1, may be upregulating the expression of these receptors on the cell surface.

Previous studies show conflicting results regarding macrophage ingestion of apoptotic cells and secretion of anti-inflammatory cytokines [247, 254]. *Kurosaka et al* have shown that phagocytosis of cells in the very early stages of apoptosis by macrophages does not induce increased secretion of anti-inflammatory cytokines such as IL-8 and TGFβ1. As the stage of apoptosis advanced, the amount of IL-8 and TGFβ1 secreted by the macrophages increased. They argue that, *in vivo*, apoptotic cells are hardly detected and therefore phagocytosis of apoptotic cells without production of cytokines is occurring in normal tissues [247]. Huynh *et al* showed that apoptotic cell

recognition and clearance by macrophages requires PS exposure on the apoptotic cell and induces TGFβ1 secretion and results in accelerated resolution of inflammation [254].

In this system, binding of mesangial cells to apoptotic cells lead to an increase in TGFβ1 secretion. Addition of FCS increased phagocytosis but did not lead to increased TGFβ1 secretion. Therefore ingestion of cells did not lead to a further increase in TFβ1 secretion, suggesting binding alone was sufficient. Co-culture of mesangial cells with fresh neutrophils lead to an increase in TGFβ1 secretion, and the amount of TGFβ1 secreted was greater in the presence of aged neutrophils. The effect of fresh PMNs could caused by the small amount of apoptotic PMNs present (15% apoptotic cells in freshly isolated neutrophils cultures, compared to 71% apoptotic cells in aged neutrophils cultures, figure in methods section).

There was an increase in latent and active TGFβ1, independent of glucose concentration. ICAM cross-linking was studied because it can increase TGFβ1 secretion in proximal tubular cells [296]. ICAM cross-linking did not induce TGFβ1 secretion in mesangial cells. The effect of inhibiting the αvβ3/CD36/TSP-1 mechanism on TGFβ1 secretion was also studied but this mechanism did not inhibit TGFβ1 secretion either. Inhibition of the PSR using PLS did inhibit TGFβ1 secretion upon binding of apoptotic cells. L-α-phosphatidylcholine (PC) could have been used as a control for PLS. Unlike PLS, PC does not bind to the phosphatidylserine receptor [Witting et al, J Neurochem (2000) 75:1060-1070].

This increase in TGFβ1 secretion was independent of glucose concentration, only binding of apoptotic cells was required for this effect, and it could not be inhibited with the RGDS peptide and the TSP-1 neutralising antibody. It was therefore occurring independently to phagocytosis, via PSR which did not have a role in mesangial cell phagocytosis in this system.

In conclusion, 25mM glucose mediated increased phagocytosis by mesangial cells via TGFβ1 and this is involved the αvβ3/CD36/TSP1 mechanism. Binding of apoptotic cells to mesangial cells induced TGFβ1 secretion via PSR, a mechanism independent of phagocytosis of apoptotic cells.

CHAPTER 6: GENERAL DICUSSION

CHAPTER 6: GENERAL DISCUSSION

Apoptosis is essential for the regulation of development, immune system generation and maintenance of homeostatis in adult tissues. Inappropriate apoptosis can result in diseases such as neurodegenerative syndromes, tumour formation and autoimmune syndromes [307]. Dyregulation of apoptosis is also important in progression of renal diseases such as polycystic kidney disease, glomerulonephritis and diabetic nephropathy [180]. The late phase of diabetic nephropathy is characterised by loss of resident glomerular cells, a process which correlates with the decline in glomerular filtration rate [308]. Numerous studies have implicated hyperglycaemia as a regulator of apoptosis in numerous cell types [264, 268, 309, 310].

In the current study I used numerous different methodological approaches to demonstrate that elevated glucose concentration increases the pro-apoptotic pathway activated by serum deprivation in renal mesangial cells. In addition, I demonstrated enhanced activation of capsase-3 following exposure to glucose.

The data also demonstrate that maintenance of mesangial cells under conditions of elevated glucose leads to augmentation of NFκB inhibition and that this is associated with an alteration in the ratio of Bax:Bcl-2 which favours increased apoptotic cell death. More specifically our data demonstrate a decrease in the expression of the cell survival factor Bcl-2 with no change in the expression of Bax which facilitates apoptosis. In this study I demonstrated that not only is glucose enhanced apoptosis associated with reduced NFκB activation, but that inhibition of NFκB activation with a peptide which prevents NFκB translocation mimics the effects of glucose in

enhancing apoptosis and also down-regulating Bcl-2 expression, thus providing convincing evidence that glucose mediated inhibition of NFκB activity is involved in determination of apoptotic cell fate. This data is consistent with numerous studies which have demonstrated that NFκB is a cell survival factor in mesangial cells [135, 311]. In some cell lines, such as embroyonic kidney cells, NFκB can induce apoptosis [312]. Bcl-2 was able to repress the pro-apoptotic ability of NFκB in these cells by contollong a signalling pathway involving the p65 subunit of NFκB.

Numerous studies have demonstrated that TGF-ß1 mediates many of the effects of glucose on mesangial cell function. Elevated glucose leads to transcriptional activation of TGF-ß1 [276, 277]. Furthermore glucose mediated alteration in mesangial cell function are mediated by autocrine activation of transforming growth factor beta [125]. Glucose also enhances sensitivity of mesangial cells to the effects of TGF-ß by increasing ERK and PKCδ activity [279]. They showed that mesangial cell culture in high glucose lead to increased TGFβ signaling via Smads and this was independent of either production of active TGFβ or TGFβ receptor binding capacity.

The data in this study demonstrates that recombinant TGFβ1 mimics the effects of high glucose and inhibition of NFκB. Inhibition of TGFß1 action using a blocking antibody abrogated 25mM D-glucose enhanced apoptosis, confirming the central role of TGF-ß1 in this response. TGFβ1 mediated and high glucose mediated mesangial cell apoptosis could be inhibited by blocking the action of p38 MAPK. Although I have also confirmed increased generation of bio-active TGF-ß1 in mesangial cells exposed to an elevated concentration of D-glucose, the delayed time course suggests that stimulation of *de novo* synthesis is unlikely to be the mediator of the effects of

elevated ambient glucose on apoptosis, but rather it is likely that this is mediated by enhanced sensitivity to TGF-ß1 signalling.

Apoptosis is considered to be a mechanism by which cells are deleted without damaging surrounding tissues, with clearance occurring by swift recognition and ingestion by phagocytes. Engulfment of apoptotic cells is thought no only to remove them from the tissues but also to provide protections from local damage resulting from release or discharge of injurious or pro-inflammatory content [291].

Furthermore, recent studies have shown that, in addition to its role in removing cells before they undergo lysis, ingestion of apoptotic cells by macrophages actively suppresses production of pro-inflammatory cytokines and chemokines [313, 314]. Intriguingly this suppressive effect was largely inhibited by TGF-ß1 neutralizing antibodies and reproduced by exogenous TGF-ß1. Apoptotic cell clearance is therefore believed to represent a critical process in tissue remodelling and resolution of inflammatory injury.

In this study I examined the effect of elevated glucose concentration on engulfment of apoptotic cells, and defined the mechanism by which this occurs. In addition I examined the functional consequences of interaction between mesangial cells and apoptotic cells with particular emphasis on TGF-ß1 generation, which has been implicated as a critical factor promoting renal injury in diabetes.

The data in this study demonstrates that mesangial cells cultured in high glucose ingest more apoptotic cells. High glucose induced increased secretion of and

sensitivity to TGFβ1 which, in turn, increased phagocytosis of apoptotic cells. Mesangial cell phagocytosis of apoptotic cells involved the αvβ3/CD36/TSP-1 mechanism. Apoptotic cells cultured with mesangial cells also lead to increased TGFβ1 secretion via the PS receptor, a mechanism independent of phagocytosis.

In conclusion we have demonstrated that glucose enhanced mesangial cell apoptosis is mediated by autocrine TGF-ß1 activity, which leads to inhibition of nuclear translocation of NFκB and suppression of Bcl2 expression. Glucose and TGFβ1 also enhanced phagocytosis of apoptotic cells by mesangial cells. Also, mesangial cell contact with apoptotic cells lead to increased production of the anti-inflammatory cytokine, TGFβ1. In the absence of inflammation, this increased TGFβ1 secretion can lead to increased fibrosis within the kidney. The data provide insight in to how alterations in glucose related to diabetes mellitus may influence mesangial cell number and contribute to glomerulosclerosis associated with diabetic nephropathy.

Further work could involve investigating the effect of other apoptotic stimuli, to determine if cell death is augmented by high glucose via a different pathway. Examples are Fas ligand or TNF-α to induce mesangial cell death via the death receptors and caspase-8, rather than caspase-9.

The effects of TGFβ1 on mesangial cell apoptosis could also be studied further. The role of the Smad proteins could be investigated again. Other TGFβ1-mediated pathways could also be investigated, e.g. Erk. Erk MAPK phosphorylates Smad2 via activation of MAPK/Erk kinase kinase 1 (MEKK1) [115]. TGFβ1-induced activation

of Ras/Erk MAPK signalling can induce TGFβ1 expression, thereby amplifying the TGFβ response [315].

Further work on mesangial cell phagocytosis could involve looking for the receptor on the apoptotic cell which binds to TSP-1, forming a bridge with the phagocytic cell. Other work could involve studying the effects of high glucose and TGFβ1 on mesangial cell surface expression of αv, β3 and CD36. The effects of TGFβ1 on TSP-1 mRNA expression and secretion could also be studied.

BMP-7 is a member of the TGFβ superfamily which is able to counteract TGFβ-mediated fibrosis [316], partially by maintaining high levels of matrix metalloprotease-2 [317]. It is the most abundant BMP expressed in the kidney [316]. BMP-7 mediated signalling activates Smad-1, -5 and -8 and does not involve Erk1/2 or p38 [318]. These interact with Smad4 and translocate to the nucleus [316]. Smad6 negatively regulates BMP-7 signalling [316]. Further work could involve investigating the effects of BMP7 on mesangial cell apoptosis, the effect of high glucose on BMP-7 and the effect on BMP-7 of co-culturing mesangial cells with aged PMNs.

CHAPTER 7: BILIOGRAPHY

Bibliography:

1. CRW Edwards, I.B., C Haslett, ER Chilvers. Davidson's Principles and Practice of Medicine. 17th edition.
2. Renal Physiology Volume I.
3. Cameron, Davidson, Grunfeld, Kerr, and Ritz. Oxford Textbook of Clinical Nephrology Volume I.
4. Warrell, Cox, G.W., and Firth. Oxford Textbook of Medicine, 4th Edition.
5. Wolthuis. Mesangial Cell Biology.
6. Johnson, G., and Feehaly. Comprehensive Clinical Nephrology, 2nd edition.
7. Kreisberg, J.I., Venkatachalam, M., and Troyer, D. 1985. Contractile properties of cultured glomerular mesangial cells. *Am J Physiol* 249:F457-463.
8. Dworkin, L.D., Ichikawa, I., and Brenner, B.M. 1983. Hormonal modulation of glomerular function. *Am J Physiol* 244:F95-104.
9. Mene, P., Simonson, M.S., and Dunn, M.J. 1989. Physiology of the mesangial cell. *Physiol Rev* 69:1347-1424.
10. Gutteridge, I.F. 1999. Diabetes mellitus: a brief history, epidemiology, definition and classification. *Clin Exp Optom* 82:102-106.
11. Bell. Diabetes Mellitus, Oxford Textbook of Medicine.
12. Zimmet, P., Alberti, K.G., and Shaw, J. 2001. Global and societal implications of the diabetes epidemic. *Nature* 414:782-787.
13. King, H., Aubert, R.E., and Herman, W.H. 1998. Global burden of diabetes, 1995-2025: prevalence, numerical estimates, and projections. *Diabetes Care* 21:1414-1431.
14. Amos, A.F., McCarty, D.J., and Zimmet, P. 1997. The rising global burden of diabetes and its complications: estimates and projections to the year 2010. *Diabet Med* 14 Suppl 5:S1-85.
15. Glassock, R.J. 2004. The rising tide of end-stage renal disease: what can be done? *Clin Exp Nephrol* 8:291-296.
16. Ansell, Feest, Byrne, and Ahmad. The Renal Association UK Renal Registry. The sixth annual report, December 2003.
17. Fagot-Campagna, A., Narayan, K.M., and Imperatore, G. 2001. Type 2 diabetes in children. *Bmj* 322:377-378.
18. Brosnan, C.A., Upchurch, S., and Schreiner, B. 2001. Type 2 diabetes in children and adolescents: an emerging disease. *J Pediatr Health Care* 15:187-193.
19. Pontiroli, A.E. 2004. Type 2 diabetes mellitus is becoming the most common type of diabetes in school children. *Acta Diabetol* 41:85-90.
20. Dalla Vestra, M., Saller, A., Bortoloso, E., Mauer, M., and Fioretto, P. 2000. Structural involvement in type 1 and type 2 diabetic nephropathy. *Diabetes Metab* 26 Suppl 4:8-14.
21. Ritz. Diabetic Nephropathy in textbook of Nephrology.
22. Thomas, and Viberti. Diabetic Nephropathy, Textbook of Medicine.
23. Bruno, G., Merletti, F., Biggeri, A., Bargero, G., Ferrero, S., Pagano, G., and Cavallo Perin, P. 2003. Progression to overt nephropathy in type 2 diabetes: the Casale Monferrato Study. *Diabetes Care* 26:2150-2155.

24. Gaede, P., Tarnow, L., Vedel, P., Parving, H.H., and Pedersen, O. 2004. Remission to normoalbuminuria during multifactorial treatment preserves kidney function in patients with type 2 diabetes and microalbuminuria. *Nephrol Dial Transplant* 19:2784-2788.
25. White, K.E., and Bilous, R.W. 2000. Type 2 diabetic patients with nephropathy show structural-functional relationships that are similar to type 1 disease. *J Am Soc Nephrol* 11:1667-1673.
26. Osterby, R., Gall, M.A., Schmitz, A., Nielsen, F.S., Nyberg, G., and Parving, H.H. 1993. Glomerular structure and function in proteinuric type 2 (non-insulin-dependent) diabetic patients. *Diabetologia* 36:1064-1070.
27. Drummond, K., and Mauer, M. 2002. The early natural history of nephropathy in type 1 diabetes: II. Early renal structural changes in type 1 diabetes. *Diabetes* 51:1580-1587.
28. White, K.E., and Bilous, R.W. 2004. Structural alterations to the podocyte are related to proteinuria in type 2 diabetic patients. *Nephrol Dial Transplant* 19:1437-1440.
29. Steffes, M.W., Osterby, R., Chavers, B., and Mauer, S.M. 1989. Mesangial expansion as a central mechanism for loss of kidney function in diabetic patients. *Diabetes* 38:1077-1081.
30. Fioretto, P., Steffes, M.W., Brown, D.M., and Mauer, S.M. 1992. An overview of renal pathology in insulin-dependent diabetes mellitus in relationship to altered glomerular hemodynamics. *Am J Kidney Dis* 20:549-558.
31. Mauer, S.M., Steffes, M.W., Ellis, E.N., Sutherland, D.E., Brown, D.M., and Goetz, F.C. 1984. Structural-functional relationships in diabetic nephropathy. *J Clin Invest* 74:1143-1155.
32. Pagtalunan, M.E., Miller, P.L., Jumping-Eagle, S., Nelson, R.G., Myers, B.D., Rennke, H.G., Coplon, N.S., Sun, L., and Meyer, T.W. 1997. Podocyte loss and progressive glomerular injury in type II diabetes. *J Clin Invest* 99:342-348.
33. Sharma, K., and Ziyadeh, F.N. 1995. Hyperglycemia and diabetic kidney disease. The case for transforming growth factor-beta as a key mediator. *Diabetes* 44:1139-1146.
34. White, K.E., Bilous, R.W., Marshall, S.M., El Nahas, M., Remuzzi, G., Piras, G., De Cosmo, S., and Viberti, G. 2002. Podocyte number in normotensive type 1 diabetic patients with albuminuria. *Diabetes* 51:3083-3089.
35. Steffes, M.W., Schmidt, D., McCrery, R., and Basgen, J.M. 2001. Glomerular cell number in normal subjects and in type 1 diabetic patients. *Kidney Int* 59:2104-2113.
36. Mishra, R., Emancipator, S.N., Kern, T., and Simonson, M.S. 2005. High glucose evokes an intrinsic proapoptotic signaling pathway in mesangial cells. *Kidney Int* 67:82-93.
37. Mishra, Emancipator, Kern, and Simonson. 2005. High glucose evokes an intrinsic proapoptotic signalling pathway in mesangial cells. *Kidney International* 67:82-93.
38. Bader, R., Bader, H., Grund, K.E., Mackensen-Haen, S., Christ, H., and Bohle, A. 1980. Structure and function of the kidney in diabetic glomerulosclerosis.

Correlations between morphological and functional parameters. *Pathol Res Pract* 167:204-216.
39. Sedlak, T.W., Oltvai, Z.N., Yang, E., Wang, K., Boise, L.H., Thompson, C.B., and Korsmeyer, S.J. 1995. Multiple Bcl-2 family members demonstrate selective dimerizations with Bax. *Proc Natl Acad Sci U S A* 92:7834-7838.
40. Dalla Vestra, M., Saller, A., Mauer, M., and Fioretto, P. 2001. Role of mesangial expansion in the pathogenesis of diabetic nephropathy. *J Nephrol* 14 Suppl 4:S51-57.
41. Lemley, K.V., Abdullah, I., Myers, B.D., Meyer, T.W., Blouch, K., Smith, W.E., Bennett, P.H., and Nelson, R.G. 2000. Evolution of incipient nephropathy in type 2 diabetes mellitus. *Kidney Int* 58:1228-1237.
42. White, and Bilous. 2004. Structural alterations to the podocytes are related to proteinuria in type 2 diabetic patients. *Nephrol Dial Trasplant* 19:1437-1440.
43. Dalla Vestra, M., Masiero, A., Roiter, A.M., Saller, A., Crepaldi, G., and Fioretto, P. 2003. Is podocyte injury relevant in diabetic nephropathy? Studies in patients with type 2 diabetes. *Diabetes* 52:1031-1035.
44. van Dijk, C., and Berl, T. 2004. Pathogenesis of diabetic nephropathy. *Rev Endocr Metab Disord* 5:237-248.
45. Parving, H.H. 1998. Renoprotection in diabetes: genetic and non-genetic risk factors and treatment. *Diabetologia* 41:745-759.
46. Forsblom, C.M., Kanninen, T., Lehtovirta, M., Saloranta, C., and Groop, L.C. 1999. Heritability of albumin excretion rate in families of patients with Type II diabetes. *Diabetologia* 42:1359-1366.
47. Fogarty, D.G., Rich, S.S., Hanna, L., Warram, J.H., and Krolewski, A.S. 2000. Urinary albumin excretion in families with type 2 diabetes is heritable and genetically correlated to blood pressure. *Kidney Int* 57:250-257.
48. Fioretto, P., Steffes, M.W., Barbosa, J., Rich, S.S., Miller, M.E., and Mauer, M. 1999. Is diabetic nephropathy inherited? Studies of glomerular structure in type 1 diabetic sibling pairs. *Diabetes* 48:865-869.
49. Chase, H.P., Jackson, W.E., Hoops, S.L., Cockerham, R.S., Archer, P.G., and O'Brien, D. 1989. Glucose control and the renal and retinal complications of insulin-dependent diabetes. *Jama* 261:1155-1160.
50. 1995. Effect of intensive therapy on the development and progression of diabetic nephropathy in the Diabetes Control and Complications Trial. The Diabetes Control and Complications (DCCT) Research Group. *Kidney Int* 47:1703-1720.
51. 1993. The effect of intensive treatment of diabetes on the development and progression of long-term complications in insulin-dependent diabetes mellitus. The Diabetes Control and Complications Trial Research Group. *N Engl J Med* 329:977-986.
52. 2000. Retinopathy and nephropathy in patients with type 1 diabetes four years after a trial of intensive therapy. The Diabetes Control and Complications Trial/Epidemiology of Diabetes Interventions and Complications Research Group. *N Engl J Med* 342:381-389.
53. 1998. Intensive blood-glucose control with sulphonylureas or insulin compared with conventional treatment and risk of complications in patients with type 2

diabetes (UKPDS 33). UK Prospective Diabetes Study (UKPDS) Group. *Lancet* 352:837-853.
54. Swidan, S.Z., and Montgomery, P.A. 1998. Effect of blood glucose concentrations on the development of chronic complications of diabetes mellitus. *Pharmacotherapy* 18:961-972.
55. Evans, J.L., Goldfine, I.D., Maddux, B.A., and Grodsky, G.M. 2002. Oxidative stress and stress-activated signaling pathways: a unifying hypothesis of type 2 diabetes. *Endocr Rev* 23:599-622.
56. Ayo, S.H., Radnik, R.A., Glass, W.F., 2nd, Garoni, J.A., Rampt, E.R., Appling, D.R., and Kreisberg, J.I. 1991. Increased extracellular matrix synthesis and mRNA in mesangial cells grown in high-glucose medium. *Am J Physiol* 260:F185-191.
57. Fumo, P., Kuncio, G.S., and Ziyadeh, F.N. 1994. PKC and high glucose stimulate collagen alpha 1 (IV) transcriptional activity in a reporter mesangial cell line. *Am J Physiol* 267:F632-638.
58. Nahman, N.S., Jr., Leonhart, K.L., Cosio, F.G., and Hebert, C.L. 1992. Effects of high glucose on cellular proliferation and fibronectin production by cultured human mesangial cells. *Kidney Int* 41:396-402.
59. McLennan, S.V., Fisher, E.J., Yue, D.K., and Turtle, J.R. 1994. High glucose concentration causes a decrease in mesangium degradation. A factor in the pathogenesis of diabetic nephropathy. *Diabetes* 43:1041-1045.
60. Haneda, M., Koya, D., Isono, M., and Kikkawa, R. 2003. Overview of glucose signaling in mesangial cells in diabetic nephropathy. *J Am Soc Nephrol* 14:1374-1382.
61. Brownlee, M. 2001. Biochemistry and molecular cell biology of diabetic complications. *Nature* 414:813-820.
62. Greene, D.A., Lattimer, S.A., and Sima, A.A. 1987. Sorbitol, phosphoinositides, and sodium-potassium-ATPase in the pathogenesis of diabetic complications. *N Engl J Med* 316:599-606.
63. Mauer, S.M., Steffes, M.W., Azar, S., and Brown, D.M. 1989. Effects of sorbinil on glomerular structure and function in long-term-diabetic rats. *Diabetes* 38:839-846.
64. Engerman, R.L., Kern, T.S., and Larson, M.E. 1994. Nerve conduction and aldose reductase inhibition during 5 years of diabetes or galactosaemia in dogs. *Diabetologia* 37:141-144.
65. Greene, D.A., Arezzo, J.C., and Brown, M.B. 1999. Effect of aldose reductase inhibition on nerve conduction and morphometry in diabetic neuropathy. Zenarestat Study Group. *Neurology* 53:580-591.
66. Studer, R.K., Craven, P.A., and DeRubertis, F.R. 1993. Role for protein kinase C in the mediation of increased fibronectin accumulation by mesangial cells grown in high-glucose medium. *Diabetes* 42:118-126.
67. Koya, D., Jirousek, M.R., Lin, Y.W., Ishii, H., Kuboki, K., and King, G.L. 1997. Characterization of protein kinase C beta isoform activation on the gene expression of transforming growth factor-beta, extracellular matrix components, and prostanoids in the glomeruli of diabetic rats. *J Clin Invest* 100:115-126.

68. Koya, D., Haneda, M., Nakagawa, H., Isshiki, K., Sato, H., Maeda, S., Sugimoto, T., Yasuda, H., Kashiwagi, A., Ways, D.K., et al. 2000. Amelioration of accelerated diabetic mesangial expansion by treatment with a PKC beta inhibitor in diabetic db/db mice, a rodent model for type 2 diabetes. *Faseb J* 14:439-447.
69. Nerlich, A.G., Sauer, U., Kolm-Litty, V., Wagner, E., Koch, M., and Schleicher, E.D. 1998. Expression of glutamine:fructose-6-phosphate amidotransferase in human tissues: evidence for high variability and distinct regulation in diabetes. *Diabetes* 47:170-178.
70. Daniels, M.C., McClain, D.A., and Crook, E.D. 2000. Transcriptional regulation of transforming growth factor beta1 by glucose: investigation into the role of the hexosamine biosynthesis pathway. *Am J Med Sci* 319:138-142.
71. Schleicher, E.D., and Weigert, C. 2000. Role of the hexosamine biosynthetic pathway in diabetic nephropathy. *Kidney Int Suppl* 77:S13-18.
72. Weigert, C., Friess, U., Brodbeck, K., Haring, H.U., and Schleicher, E.D. 2003. Glutamine:fructose-6-phosphate aminotransferase enzyme activity is necessary for the induction of TGF-beta1 and fibronectin expression in mesangial cells. *Diabetologia* 46:852-855.
73. Ha, H., and Lee, H.B. 2001. Oxidative stress in diabetic nephropathy: basic and clinical information. *Curr Diab Rep* 1:282-287.
74. Makita, Z., Radoff, S., Rayfield, E.J., Yang, Z., Skolnik, E., Delaney, V., Friedman, E.A., Cerami, A., and Vlassara, H. 1991. Advanced glycosylation end products in patients with diabetic nephropathy. *N Engl J Med* 325:836-842.
75. Tanji, N., Markowitz, G.S., Fu, C., Kislinger, T., Taguchi, A., Pischetsrieder, M., Stern, D., Schmidt, A.M., and D'Agati, V.D. 2000. Expression of advanced glycation end products and their cellular receptor RAGE in diabetic nephropathy and nondiabetic renal disease. *J Am Soc Nephrol* 11:1656-1666.
76. Forbes, J.M., Thallas, V., Thomas, M.C., Founds, H.W., Burns, W.C., Jerums, G., and Cooper, M.E. 2003. The breakdown of preexisting advanced glycation end products is associated with reduced renal fibrosis in experimental diabetes. *Faseb J* 17:1762-1764.
77. Nakamura, T., Fukui, M., Ebihara, I., Osada, S., Nagaoka, I., Tomino, Y., and Koide, H. 1993. mRNA expression of growth factors in glomeruli from diabetic rats. *Diabetes* 42:450-456.
78. Yamamoto, T., Nakamura, T., Noble, N.A., Ruoslahti, E., and Border, W.A. 1993. Expression of transforming growth factor beta is elevated in human and experimental diabetic nephropathy. *Proc Natl Acad Sci U S A* 90:1814-1818.
79. Sharma, K., and Ziyadeh, F.N. 1994. Renal hypertrophy is associated with upregulation of TGF-beta 1 gene expression in diabetic BB rat and NOD mouse. *Am J Physiol* 267:F1094-1001.
80. Pankewycz, O.G., Guan, J.X., Bolton, W.K., Gomez, A., and Benedict, J.F. 1994. Renal TGF-beta regulation in spontaneously diabetic NOD mice with correlations in mesangial cells. *Kidney Int* 46:748-758.
81. Shankland, S.J., Scholey, J.W., Ly, H., and Thai, K. 1994. Expression of transforming growth factor-beta 1 during diabetic renal hypertrophy. *Kidney Int* 46:430-442.

82. Sharma, and Ziyadeh. 1995. Hyperglycaemia and diabetic kidney disease. The case for transforming growth factor-beta as a key mediator. *Diabetes* 44:1139-1146.
83. Fukami, K., Ueda, S., Yamagishi, S., Kato, S., Inagaki, Y., Takeuchi, M., Motomiya, Y., Bucala, R., Iida, S., Tamaki, K., et al. 2004. AGEs activate mesangial TGF-beta-Smad signaling via an angiotensin II type I receptor interaction. *Kidney Int* 66:2137-2147.
84. Miyazono, K. 2000. Positive and negative regulation of TGF-beta signaling. *J Cell Sci* 113 (Pt 7):1101-1109.
85. ten Dijke, P., and Hill, C.S. 2004. New insights into TGF-beta-Smad signalling. *Trends Biochem Sci* 29:265-273.
86. Xiao, Y.Q., Malcolm, K., Worthen, G.S., Gardai, S., Schiemann, W.P., Fadok, V.A., Bratton, D.L., and Henson, P.M. 2002. Cross-talk between ERK and p38 MAPK mediates selective suppression of pro-inflammatory cytokines by transforming growth factor-beta. *J Biol Chem* 277:14884-14893.
87. Roberts, A.B., Kim, S.J., Noma, T., Glick, A.B., Lafyatis, R., Lechleider, R., Jakowlew, S.B., Geiser, A., O'Reilly, M.A., Danielpour, D., et al. 1991. Multiple forms of TGF-beta: distinct promoters and differential expression. *Ciba Found Symp* 157:7-15; discussion 15-28.
88. MacKay, K., Kondaiah, P., Danielpour, D., Austin, H.A., 3rd, and Brown, P.D. 1990. Expression of transforming growth factor-beta 1 and beta 2 in rat glomeruli. *Kidney Int* 38:1095-1100.
89. Yu, L., Border, W.A., Huang, Y., and Noble, N.A. 2003. TGF-beta isoforms in renal fibrogenesis. *Kidney Int* 64:844-856.
90. Miyazono, K., Olofsson, A., Colosetti, P., and Heldin, C.H. 1991. A role of the latent TGF-beta 1-binding protein in the assembly and secretion of TGF-beta 1. *Embo J* 10:1091-1101.
91. Saharinen, J., Hyytiainen, M., Taipale, J., and Keski-Oja, J. 1999. Latent transforming growth factor-beta binding proteins (LTBPs)--structural extracellular matrix proteins for targeting TGF-beta action. *Cytokine Growth Factor Rev* 10:99-117.
92. Murphy-Ullrich, J.E., and Poczatek, M. 2000. Activation of latent TGF-beta by thrombospondin-1: mechanisms and physiology. *Cytokine Growth Factor Rev* 11:59-69.
93. Daniel, C., Wiede, J., Krutzsch, H.C., Ribeiro, S.M., Roberts, D.D., Murphy-Ullrich, J.E., and Hugo, C. 2004. Thrombospondin-1 is a major activator of TGF-beta in fibrotic renal disease in the rat in vivo. *Kidney Int* 65:459-468.
94. Vodovotz, Y., Chesler, L., Chong, H., Kim, S.J., Simpson, J.T., DeGraff, W., Cox, G.W., Roberts, A.B., Wink, D.A., and Barcellos-Hoff, M.H. 1999. Regulation of transforming growth factor beta1 by nitric oxide. *Cancer Res* 59:2142-2149.
95. Barcellos-Hoff, M.H., and Dix, T.A. 1996. Redox-mediated activation of latent transforming growth factor-beta 1. *Mol Endocrinol* 10:1077-1083.
96. Khalil, N., Corne, S., Whitman, C., and Yacyshyn, H. 1996. Plasmin regulates the activation of cell-associated latent TGF-beta 1 secreted by rat alveolar

macrophages after in vivo bleomycin injury. *Am J Respir Cell Mol Biol* 15:252-259.
97. Yehualaeshet, T., O'Connor, R., Begleiter, A., Murphy-Ullrich, J.E., Silverstein, R., and Khalil, N. 2000. A CD36 synthetic peptide inhibits bleomycin-induced pulmonary inflammation and connective tissue synthesis in the rat. *Am J Respir Cell Mol Biol* 23:204-212.
98. Munger, J.S., Huang, X., Kawakatsu, H., Griffiths, M.J., Dalton, S.L., Wu, J., Pittet, J.F., Kaminski, N., Garat, C., Matthay, M.A., et al. 1999. The integrin alpha v beta 6 binds and activates latent TGF beta 1: a mechanism for regulating pulmonary inflammation and fibrosis. *Cell* 96:319-328.
99. Wang, S., Skorczewski, J., Feng, X., Mei, L., and Murphy-Ullrich, J.E. 2004. Glucose up-regulates thrombospondin 1 gene transcription and transforming growth factor-beta activity through antagonism of cGMP-dependent protein kinase repression via upstream stimulatory factor 2. *J Biol Chem* 279:34311-34322.
100. 23.
101. Yevdokimova, N., Wahab, N.A., and Mason, R.M. 2001. Thrombospondin-1 is the key activator of TGF-beta1 in human mesangial cells exposed to high glucose. *J Am Soc Nephrol* 12:703-712.
102. Poczatek, M.H., Hugo, C., Darley-Usmar, V., and Murphy-Ullrich, J.E. 2000. Glucose stimulation of transforming growth factor-beta bioactivity in mesangial cells is mediated by thrombospondin-1. *Am J Pathol* 157:1353-1363.
103. Yehualaeshet, T., O'Connor, R., Green-Johnson, J., Mai, S., Silverstein, R., Murphy-Ullrich, J.E., and Khalil, N. 1999. Activation of rat alveolar macrophage-derived latent transforming growth factor beta-1 by plasmin requires interaction with thrombospondin-1 and its cell surface receptor, CD36. *Am J Pathol* 155:841-851.
104. Hughes, J., Liu, Y., Van Damme, J., and Savill, J. 1997. Human glomerular mesangial cell phagocytosis of apoptotic neutrophils: mediation by a novel CD36-independent vitronectin receptor/thrombospondin recognition mechanism that is uncoupled from chemokine secretion. *J Immunol* 158:4389-4397.
105. Frazier, W.A. 1987. Thrombospondin: a modular adhesive glycoprotein of platelets and nucleated cells. *J Cell Biol* 105:625-632.
106. Jimenez, B., Volpert, O.V., Crawford, S.E., Febbraio, M., Silverstein, R.L., and Bouck, N. 2000. Signals leading to apoptosis-dependent inhibition of neovascularization by thrombospondin-1. *Nat Med* 6:41-48.
107. Mansfield, P.J., and Suchard, S.J. 1994. Thrombospondin promotes chemotaxis and haptotaxis of human peripheral blood monocytes. *J Immunol* 153:4219-4229.
108. Raugi, G.J., Olerud, J.E., and Gown, A.M. 1987. Thrombospondin in early human wound tissue. *J Invest Dermatol* 89:551-554.
109. Mansfield, P.J., Boxer, L.A., and Suchard, S.J. 1990. Thrombospondin stimulates motility of human neutrophils. *J Cell Biol* 111:3077-3086.
110. Suchard, S.J., Burton, M.J., Dixit, V.M., and Boxer, L.A. 1991. Human neutrophil adherence to thrombospondin occurs through a CD11/CD18-independent mechanism. *J Immunol* 146:3945-3952.

111. Varani, J., Stoolman, L., Wang, T., Schuger, L., Flippen, C., Dame, M., Johnson, K.J., Todd, R.F., 3rd, Ryan, U.S., and Ward, P.A. 1991. Thrombospondin production and thrombospondin-mediated adhesion in U937 cells. *Exp Cell Res* 195:177-182.
112. Silverstein, R.L., and Nachman, R.L. 1987. Thrombospondin binds to monocytes-macrophages and mediates platelet-monocyte adhesion. *J Clin Invest* 79:867-874.
113. Silverstein, R.L., Asch, A.S., and Nachman, R.L. 1989. Glycoprotein IV mediates thrombospondin-dependent platelet-monocyte and platelet-U937 cell adhesion. *J Clin Invest* 84:546-552.
114. Wang, W., Koka, V., and Lan, H.Y. 2005. Transforming growth factor-beta and Smad signalling in kidney diseases. *Nephrology (Carlton)* 10:48-56.
115. Derynck, R., and Zhang, Y.E. 2003. Smad-dependent and Smad-independent pathways in TGF-beta family signalling. *Nature* 425:577-584.
116. Chen, R., Huang, C., Morinelli, T.A., Trojanowska, M., and Paul, R.V. 2002. Blockade of the effects of TGF-beta1 on mesangial cells by overexpression of Smad7. *J Am Soc Nephrol* 13:887-893.
117. Bitzer, M., von Gersdorff, G., Liang, D., Dominguez-Rosales, A., Beg, A.A., Rojkind, M., and Bottinger, E.P. 2000. A mechanism of suppression of TGF-beta/SMAD signaling by NF-kappa B/RelA. *Genes Dev* 14:187-197.
118. Nagarajan, R.P., Chen, F., Li, W., Vig, E., Harrington, M.A., Nakshatri, H., and Chen, Y. 2000. Repression of transforming-growth-factor-beta-mediated transcription by nuclear factor kappaB. *Biochem J* 348 Pt 3:591-596.
119. Iwano, M., Kubo, A., Nishino, T., Sato, H., Nishioka, H., Akai, Y., Kurioka, H., Fujii, Y., Kanauchi, M., Shiiki, H., et al. 1996. Quantification of glomerular TGF-beta 1 mRNA in patients with diabetes mellitus. *Kidney Int* 49:1120-1126.
120. Pfeiffer, A., Middelberg-Bisping, K., Drewes, C., and Schatz, H. 1996. Elevated plasma levels of transforming growth factor-beta 1 in NIDDM. *Diabetes Care* 19:1113-1117.
121. Wolf, Sharma, Chen, Ericksen, and Ziyadeh. 1992. high glucose-induced proliferation in mesangial cells is reversed by autocrine TGF-beta. *Kidney International* 42.
122. Ziyadeh, F.N., Sharma, K., Ericksen, M., and Wolf, G. 1994. Stimulation of collagen gene expression and protein synthesis in murine mesangial cells by high glucose is mediated by autocrine activation of transforming growth factor-beta. *J Clin Invest* 93:536-542.
123. Wolf, G., Sharma, K., Chen, Y., Ericksen, M., and Ziyadeh, F.N. 1992. High glucose-induced proliferation in mesangial cells is reversed by autocrine TGF-beta. *Kidney Int* 42:647-656.
124. Hoffman, B.B., Sharma, K., and Ziyadeh, F.N. 1998. Potential role of TGF-beta in diabetic nephropathy. *Miner Electrolyte Metab* 24:190-196.
125. same as 122.
126. Wolf, G., Mueller, E., Stahl, R.A., and Ziyadeh, F.N. 1993. Angiotensin II-induced hypertrophy of cultured murine proximal tubular cells is mediated by endogenous transforming growth factor-beta. *J Clin Invest* 92:1366-1372.

127. Choi, M.E., Kim, E.G., Huang, Q., and Ballermann, B.J. 1993. Rat mesangial cell hypertrophy in response to transforming growth factor-beta 1. *Kidney Int* 44:948-958.
128. Yamamoto, Nakamura, Noble, Ruoslahti, and Border. 1993. Expression of TGF-beta is elevated in human and experimental diabetic nephropathy. *Am J Physiol* 267:F1094-1001.
129. Yoshioka, K., Takemura, T., Murakami, K., Okada, M., Hino, S., Miyamoto, H., and Maki, S. 1993. Transforming growth factor-beta protein and mRNA in glomeruli in normal and diseased human kidneys. *Lab Invest* 68:154-163.
130. Suzuki, S., Ebihara, I., Tomino, Y., and Koide, H. 1993. Transcriptional activation of matrix genes by transforming growth factor beta 1 in mesangial cells. *Exp Nephrol* 1:229-237.
131. Hong, S.W., Isono, M., Chen, S., Iglesias-De La Cruz, M.C., Han, D.C., and Ziyadeh, F.N. 2001. Increased glomerular and tubular expression of transforming growth factor-beta1, its type II receptor, and activation of the Smad signaling pathway in the db/db mouse. *Am J Pathol* 158:1653-1663.
132. Isono, M., Chen, S., Hong, S.W., Iglesias-de la Cruz, M.C., and Ziyadeh, F.N. 2002. Smad pathway is activated in the diabetic mouse kidney and Smad3 mediates TGF-beta-induced fibronectin in mesangial cells. *Biochem Biophys Res Commun* 296:1356-1365.
133. Ziyadeh, F.N., Hoffman, B.B., Han, D.C., Iglesias-De La Cruz, M.C., Hong, S.W., Isono, M., Chen, S., McGowan, T.A., and Sharma, K. 2000. Long-term prevention of renal insufficiency, excess matrix gene expression, and glomerular mesangial matrix expansion by treatment with monoclonal antitransforming growth factor-beta antibody in db/db diabetic mice. *Proc Natl Acad Sci U S A* 97:8015-8020.
134. Barkett, M., and Gilmore, T.D. 1999. Control of apoptosis by Rel/NF-kappaB transcription factors. *Oncogene* 18:6910-6924.
135. Kochlatyi, S., Gibbons, N., and Mattana, J. 2002. Extracellular matrix oxidation modulates survival, NF-kappaB translocation, and MAPK activity in mesangial cells. *Exp Mol Pathol* 73:191-197.
136. Carter, B.D., Kaltschmidt, C., Kaltschmidt, B., Offenhauser, N., Bohm-Matthaei, R., Baeuerle, P.A., and Barde, Y.A. 1996. Selective activation of NF-kappa B by nerve growth factor through the neurotrophin receptor p75. *Science* 272:542-545.
137. Grilli, M., Pizzi, M., Memo, M., and Spano, P. 1996. Neuroprotection by aspirin and sodium salicylate through blockade of NF-kappaB activation. *Science* 274:1383-1385.
138. Massy, Z.A., Guijarro, C., O'Donnell, M.P., Kim, Y., Kashtan, C.E., Egido, J., Kasiske, B.L., and Keane, W.F. 1999. The central role of nuclear factor-kappa B in mesangial cell activation. *Kidney Int Suppl* 71:S76-79.
139. Ghosh, S., May, M.J., and Kopp, E.B. 1998. NF-kappa B and Rel proteins: evolutionarily conserved mediators of immune responses. *Annu Rev Immunol* 16:225-260.
140. Baldwin, A.S., Jr. 1996. The NF-kappa B and I kappa B proteins: new discoveries and insights. *Annu Rev Immunol* 14:649-683.

141. Guijarro, C., and Egido, J. 2001. Transcription factor-kappa B (NF-kappa B) and renal disease. *Kidney Int* 59:415-424.
142. Fan, C., Yang, J., and Engelhardt, J.F. 2002. Temporal pattern of NFkappaB activation influences apoptotic cell fate in a stimuli-dependent fashion. *J Cell Sci* 115:4843-4853.
143. Han, S.H., Yea, S.S., Jeon, Y.J., Yang, K.H., and Kaminski, N.E. 1998. Transforming growth factor-beta 1 (TGF-beta1) promotes IL-2 mRNA expression through the up-regulation of NF-kappaB, AP-1 and NF-AT in EL4 cells. *J Pharmacol Exp Ther* 287:1105-1112.
144. Sovak, M.A., Arsura, M., Zanieski, G., Kavanagh, K.T., and Sonenshein, G.E. 1999. The inhibitory effects of transforming growth factor beta1 on breast cancer cell proliferation are mediated through regulation of aberrant nuclear factor-kappaB/Rel expression. *Cell Growth Differ* 10:537-544.
145. Arsura, M., Wu, M., and Sonenshein, G.E. 1996. TGF beta 1 inhibits NF-kappa B/Rel activity inducing apoptosis of B cells: transcriptional activation of I kappa B alpha. *Immunity* 5:31-40.
146. Monteleone, G., Mann, J., Monteleone, I., Vavassori, P., Bremner, R., Fantini, M., Del Vecchio Blanco, G., Tersigni, R., Alessandroni, L., Mann, D., et al. 2004. A failure of transforming growth factor-beta1 negative regulation maintains sustained NF-kappaB activation in gut inflammation. *J Biol Chem* 279:3925-3932.
147. Lallemand, F., Mazars, A., Prunier, C., Bertrand, F., Kornprost, M., Gallea, S., Roman-Roman, S., Cherqui, G., and Atfi, A. 2001. Smad7 inhibits the survival nuclear factor kappaB and potentiates apoptosis in epithelial cells. *Oncogene* 20:879-884.
148. Schiffer, M., Bitzer, M., Roberts, I.S., Kopp, J.B., ten Dijke, P., Mundel, P., and Bottinger, E.P. 2001. Apoptosis in podocytes induced by TGF-beta and Smad7. *J Clin Invest* 108:807-816.
149. Cobb, M.H., and Goldsmith, E.J. 1995. How MAP kinases are regulated. *J Biol Chem* 270:14843-14846.
150. Frasch, S.C., Nick, J.A., Fadok, V.A., Bratton, D.L., Worthen, G.S., and Henson, P.M. 1998. p38 mitogen-activated protein kinase-dependent and -independent intracellular signal transduction pathways leading to apoptosis in human neutrophils. *J Biol Chem* 273:8389-8397.
151. Graves, J.D., Draves, K.E., Craxton, A., Saklatvala, J., Krebs, E.G., and Clark, E.A. 1996. Involvement of stress-activated protein kinase and p38 mitogen-activated protein kinase in mIgM-induced apoptosis of human B lymphocytes. *Proc Natl Acad Sci U S A* 93:13814-13818.
152. Kawasaki, H., Morooka, T., Shimohama, S., Kimura, J., Hirano, T., Gotoh, Y., and Nishida, E. 1997. Activation and involvement of p38 mitogen-activated protein kinase in glutamate-induced apoptosis in rat cerebellar granule cells. *J Biol Chem* 272:18518-18521.
153. Wilmer, W.A., Dixon, C.L., and Hebert, C. 2001. Chronic exposure of human mesangial cells to high glucose environments activates the p38 MAPK pathway. *Kidney Int* 60:858-871.

154. Tsiani, E., Lekas, P., Fantus, I.G., Dlugosz, J., and Whiteside, C. 2002. High glucose-enhanced activation of mesangial cell p38 MAPK by ET-1, ANG II, and platelet-derived growth factor. *Am J Physiol Endocrinol Metab* 282:E161-169.
155. Igarashi, M., Wakasaki, H., Takahara, N., Ishii, H., Jiang, Z.Y., Yamauchi, T., Kuboki, K., Meier, M., Rhodes, C.J., and King, G.L. 1999. Glucose or diabetes activates p38 mitogen-activated protein kinase via different pathways. *J Clin Invest* 103:185-195.
156. Yu, L., Hebert, M.C., and Zhang, Y.E. 2002. TGF-beta receptor-activated p38 MAP kinase mediates Smad-independent TGF-beta responses. *Embo J* 21:3749-3759.
157. Kummer, J.L., Rao, P.K., and Heidenreich, K.A. 1997. Apoptosis induced by withdrawal of trophic factors is mediated by p38 mitogen-activated protein kinase. *J Biol Chem* 272:20490-20494.
158. same as 157.
159. Nakagami, H., Morishita, R., Yamamoto, K., Yoshimura, S.I., Taniyama, Y., Aoki, M., Matsubara, H., Kim, S., Kaneda, Y., and Ogihara, T. 2001. Phosphorylation of p38 mitogen-activated protein kinase downstream of bax-caspase-3 pathway leads to cell death induced by high D-glucose in human endothelial cells. *Diabetes* 50:1472-1481.
160. Teramoto, T., Kiss, A., and Thorgeirsson, S.S. 1998. Induction of p53 and Bax during TGF-beta 1 initiated apoptosis in rat liver epithelial cells. *Biochem Biophys Res Commun* 251:56-60.
161. Ono, K., and Han, J. 2000. The p38 signal transduction pathway: activation and function. *Cell Signal* 12:1-13.
162. Cahill, M.A., Peter, M.E., Kischkel, F.C., Chinnaiyan, A.M., Dixit, V.M., Krammer, P.H., and Nordheim, A. 1996. CD95 (APO-1/Fas) induces activation of SAP kinases downstream of ICE-like proteases. *Oncogene* 13:2087-2096.
163. Cardone, M.H., Salvesen, G.S., Widmann, C., Johnson, G., and Frisch, S.M. 1997. The regulation of anoikis: MEKK-1 activation requires cleavage by caspases. *Cell* 90:315-323.
164. Carter, A.B., Knudtson, K.L., Monick, M.M., and Hunninghake, G.W. 1999. The p38 mitogen-activated protein kinase is required for NF-kappaB-dependent gene expression. The role of TATA-binding protein (TBP). *J Biol Chem* 274:30858-30863.
165. Steller, H. 1995. Mechanisms and genes of cellular suicide. *Science* 267:1445-1449.
166. Jacobson, M.D., Weil, M., and Raff, M.C. 1997. Programmed cell death in animal development. *Cell* 88:347-354.
167. Raff, M.C. 1992. Social controls on cell survival and cell death. *Nature* 356:397-400.
168. Ashkenazi, A., and Dixit, V.M. 1998. Death receptors: signaling and modulation. *Science* 281:1305-1308.
169. Arends, M.J., and Wyllie, A.H. 1991. Apoptosis: mechanisms and roles in pathology. *Int Rev Exp Pathol* 32:223-254.
170. Banki, K., Hutter, E., Gonchoroff, N.J., and Perl, A. 1999. Elevation of mitochondrial transmembrane potential and reactive oxygen intermediate levels

are early events and occur independently from activation of caspases in Fas signaling. *J Immunol* 162:1466-1479.
171. Zheng, T.S., Schlosser, S.F., Dao, T., Hingorani, R., Crispe, I.N., Boyer, J.L., and Flavell, R.A. 1998. Caspase-3 controls both cytoplasmic and nuclear events associated with Fas-mediated apoptosis in vivo. *Proc Natl Acad Sci U S A* 95:13618-13623.
172. Thornberry, N.A., and Lazebnik, Y. 1998. Caspases: enemies within. *Science* 281:1312-1316.
173. Hengartner, M.O. 2000. The biochemistry of apoptosis. *Nature* 407:770-776.
174. Gross, A., McDonnell, J.M., and Korsmeyer, S.J. 1999. BCL-2 family members and the mitochondria in apoptosis. *Genes Dev* 13:1899-1911.
175. Savill, J. 1999. Regulation of glomerular cell number by apoptosis. *Kidney Int* 56:1216-1222.
176. Martin, S.J., Reutelingsperger, C.P., McGahon, A.J., Rader, J.A., van Schie, R.C., LaFace, D.M., and Green, D.R. 1995. Early redistribution of plasma membrane phosphatidylserine is a general feature of apoptosis regardless of the initiating stimulus: inhibition by overexpression of Bcl-2 and Abl. *J Exp Med* 182:1545-1556.
177. Enari, M., Sakahira, H., Yokoyama, H., Okawa, K., Iwamatsu, A., and Nagata, S. 1998. A caspase-activated DNase that degrades DNA during apoptosis, and its inhibitor ICAD. *Nature* 391:43-50.
178. Cohen, G.M. 1997. Caspases: the executioners of apoptosis. *Biochem J* 326 (Pt 1):1-16.
179. Thompson, C.B. 1995. Apoptosis in the pathogenesis and treatment of disease. *Science* 267:1456-1462.
180. Savill, J., Mooney, A., and Hughes, J. 1996. What role does apoptosis play in progression of renal disease? *Curr Opin Nephrol Hypertens* 5:369-374.
181. Ortiz, A., Ziyadeh, F.N., and Neilson, E.G. 1997. Expression of apoptosis-regulatory genes in renal proximal tubular epithelial cells exposed to high ambient glucose and in diabetic kidneys. *J Investig Med* 45:50-56.
182. Kang, B.P., Frencher, S., Reddy, V., Kessler, A., Malhotra, A., and Meggs, L.G. 2003. High glucose promotes mesangial cell apoptosis by oxidant-dependent mechanism. *Am J Physiol Renal Physiol* 284:F455-466.
183. Rosen, A., and Casciola-Rosen, L. 1999. Autoantigens as substrates for apoptotic proteases: implications for the pathogenesis of systemic autoimmune disease. *Cell Death Differ* 6:6-12.
184. Savill, J., and Johnson, R.J. 1995. Glomerular remodelling after inflammatory injury. *Exp Nephrol* 3:149-158.
185. Kang, B.P., Urbonas, A., Baddoo, A., Baskin, S., Malhotra, A., and Meggs, L.G. 2003. IGF-1 inhibits the mitochondrial apoptosis program in mesangial cells exposed to high glucose. *Am J Physiol Renal Physiol* 285:F1013-1024.
186. Schultz, D.R., and Harrington, W.J., Jr. 2003. Apoptosis: programmed cell death at a molecular level. *Semin Arthritis Rheum* 32:345-369.
187. Martinou, J.C. 1999. Apoptosis. Key to the mitochondrial gate. *Nature* 399:411-412.

188. Adams, J.M., and Cory, S. 1998. The Bcl-2 protein family: arbiters of cell survival. *Science* 281:1322-1326.
189. Hockenbery, D., Nunez, G., Milliman, C., Schreiber, R.D., and Korsmeyer, S.J. 1990. Bcl-2 is an inner mitochondrial membrane protein that blocks programmed cell death. *Nature* 348:334-336.
190. Xiang, J., Chao, D.T., and Korsmeyer, S.J. 1996. BAX-induced cell death may not require interleukin 1 beta-converting enzyme-like proteases. *Proc Natl Acad Sci U S A* 93:14559-14563.
191. Pastorino, J.G., Chen, S.T., Tafani, M., Snyder, J.W., and Farber, J.L. 1998. The overexpression of Bax produces cell death upon induction of the mitochondrial permeability transition. *J Biol Chem* 273:7770-7775.
192. Finucane, D.M., Bossy-Wetzel, E., Waterhouse, N.J., Cotter, T.G., and Green, D.R. 1999. Bax-induced caspase activation and apoptosis via cytochrome c release from mitochondria is inhibitable by Bcl-xL. *J Biol Chem* 274:2225-2233.
193. Wang, X. 2001. The expanding role of mitochondria in apoptosis. *Genes Dev* 15:2922-2933.
194. Martinou, J.C., Desagher, S., and Antonsson, B. 2000. Cytochrome c release from mitochondria: all or nothing. *Nat Cell Biol* 2:E41-43.
195. Kluck, R.M., Bossy-Wetzel, E., Green, D.R., and Newmeyer, D.D. 1997. The release of cytochrome c from mitochondria: a primary site for Bcl-2 regulation of apoptosis. *Science* 275:1132-1136.
196. Li, P., Nijhawan, D., Budihardjo, I., Srinivasula, S.M., Ahmad, M., Alnemri, E.S., and Wang, X. 1997. Cytochrome c and dATP-dependent formation of Apaf-1/caspase-9 complex initiates an apoptotic protease cascade. *Cell* 91:479-489.
197. Liu, X., Kim, C.N., Yang, J., Jemmerson, R., and Wang, X. 1996. Induction of apoptotic program in cell-free extracts: requirement for dATP and cytochrome c. *Cell* 86:147-157.
198. Zou, H., Henzel, W.J., Liu, X., Lutschg, A., and Wang, X. 1997. Apaf-1, a human protein homologous to C. elegans CED-4, participates in cytochrome c-dependent activation of caspase-3. *Cell* 90:405-413.
199. Marsden, V.S., O'Connor, L., O'Reilly, L.A., Silke, J., Metcalf, D., Ekert, P.G., Huang, D.C., Cecconi, F., Kuida, K., Tomaselli, K.J., et al. 2002. Apoptosis initiated by Bcl-2-regulated caspase activation independently of the cytochrome c/Apaf-1/caspase-9 apoptosome. *Nature* 419:634-637.
200. Adams, J.M. 2003. Ways of dying: multiple pathways to apoptosis. *Genes Dev* 17:2481-2495.
201. Yang, B., Johnson, T.S., Thomas, G.L., Watson, P.F., Wagner, B., Furness, P.N., and El Nahas, A.M. 2002. A shift in the Bax/Bcl-2 balance may activate caspase-3 and modulate apoptosis in experimental glomerulonephritis. *Kidney Int* 62:1301-1313.
202. Reed, J.C. 1997. Double identity for proteins of the Bcl-2 family. *Nature* 387:773-776.
203. Kelekar, A., and Thompson, C.B. 1998. Bcl-2-family proteins: the role of the BH3 domain in apoptosis. *Trends Cell Biol* 8:324-330.

204. Oltvai, Z.N., Milliman, C.L., and Korsmeyer, S.J. 1993. Bcl-2 heterodimerizes in vivo with a conserved homolog, Bax, that accelerates programmed cell death. *Cell* 74:609-619.
205. Antonsson, B., and Martinou, J.C. 2000. The Bcl-2 protein family. *Exp Cell Res* 256:50-57.
206. Boise, L.H., Minn, A.J., Noel, P.J., June, C.H., Accavitti, M.A., Lindsten, T., and Thompson, C.B. 1995. CD28 costimulation can promote T cell survival by enhancing the expression of Bcl-XL. *Immunity* 3:87-98.
207. von Freeden-Jeffry, U., Solvason, N., Howard, M., and Murray, R. 1997. The earliest T lineage-committed cells depend on IL-7 for Bcl-2 expression and normal cell cycle progression. *Immunity* 7:147-154.
208. Krajewski, S., Tanaka, S., Takayama, S., Schibler, M.J., Fenton, W., and Reed, J.C. 1993. Investigation of the subcellular distribution of the bcl-2 oncoprotein: residence in the nuclear envelope, endoplasmic reticulum, and outer mitochondrial membranes. *Cancer Res* 53:4701-4714.
209. Zhu, W., Cowie, A., Wasfy, G.W., Penn, L.Z., Leber, B., and Andrews, D.W. 1996. Bcl-2 mutants with restricted subcellular location reveal spatially distinct pathways for apoptosis in different cell types. *Embo J* 15:4130-4141.
210. Fang, W., Rivard, J.J., Mueller, D.L., and Behrens, T.W. 1994. Cloning and molecular characterization of mouse bcl-x in B and T lymphocytes. *J Immunol* 153:4388-4398.
211. Wolter, K.G., Hsu, Y.T., Smith, C.L., Nechushtan, A., Xi, X.G., and Youle, R.J. 1997. Movement of Bax from the cytosol to mitochondria during apoptosis. *J Cell Biol* 139:1281-1292.
212. Hsu, Y.T., Wolter, K.G., and Youle, R.J. 1997. Cytosol-to-membrane redistribution of Bax and Bcl-X(L) during apoptosis. *Proc Natl Acad Sci U S A* 94:3668-3672.
213. Schendel, S.L., Montal, M., and Reed, J.C. 1998. Bcl-2 family proteins as ion-channels. *Cell Death Differ* 5:372-380.
214. Vander Heiden, M.G., Chandel, N.S., Williamson, E.K., Schumacker, P.T., and Thompson, C.B. 1997. Bcl-xL regulates the membrane potential and volume homeostasis of mitochondria. *Cell* 91:627-637.
215. Shimizu, S., Narita, M., and Tsujimoto, Y. 1999. Bcl-2 family proteins regulate the release of apoptogenic cytochrome c by the mitochondrial channel VDAC. *Nature* 399:483-487.
216. Huang, D.C., Adams, J.M., and Cory, S. 1998. The conserved N-terminal BH4 domain of Bcl-2 homologues is essential for inhibition of apoptosis and interaction with CED-4. *Embo J* 17:1029-1039.
217. Goping, I.S., Gross, A., Lavoie, J.N., Nguyen, M., Jemmerson, R., Roth, K., Korsmeyer, S.J., and Shore, G.C. 1998. Regulated targeting of BAX to mitochondria. *J Cell Biol* 143:207-215.
218. Jurgensmeier, J.M., Xie, Z., Deveraux, Q., Ellerby, L., Bredesen, D., and Reed, J.C. 1998. Bax directly induces release of cytochrome c from isolated mitochondria. *Proc Natl Acad Sci U S A* 95:4997-5002.

219. Vekrellis, K., McCarthy, M.J., Watson, A., Whitfield, J., Rubin, L.L., and Ham, J. 1997. Bax promotes neuronal cell death and is downregulated during the development of the nervous system. *Development* 124:1239-1249.
220. Boise, L.H., Gonzalez-Garcia, M., Postema, C.E., Ding, L., Lindsten, T., Turka, L.A., Mao, X., Nunez, G., and Thompson, C.B. 1993. bcl-x, a bcl-2-related gene that functions as a dominant regulator of apoptotic cell death. *Cell* 74:597-608.
221. Miyashita, T., and Reed, J.C. 1995. Tumor suppressor p53 is a direct transcriptional activator of the human bax gene. *Cell* 80:293-299.
222. Adams, J.M., and Cory, S. 2002. Apoptosomes: engines for caspase activation. *Curr Opin Cell Biol* 14:715-720.
223. Wang, C.Y., Mayo, M.W., Korneluk, R.G., Goeddel, D.V., and Baldwin, A.S., Jr. 1998. NF-kappaB antiapoptosis: induction of TRAF1 and TRAF2 and c-IAP1 and c-IAP2 to suppress caspase-8 activation. *Science* 281:1680-1683.
224. Algeciras-Schimnich, A., Barnhart, B.C., and Peter, M.E. 2002. Apoptosis-independent functions of killer caspases. *Curr Opin Cell Biol* 14:721-726.
225. Tamatani, M., Che, Y.H., Matsuzaki, H., Ogawa, S., Okado, H., Miyake, S., Mizuno, T., and Tohyama, M. 1999. Tumor necrosis factor induces Bcl-2 and Bcl-x expression through NFkappaB activation in primary hippocampal neurons. *J Biol Chem* 274:8531-8538.
226. Dixon, E.P., Stephenson, D.T., Clemens, J.A., and Little, S.P. 1997. Bcl-Xshort is elevated following severe global ischemia in rat brains. *Brain Res* 776:222-229.
227. Savill, J., Smith, J., Sarraf, C., Ren, Y., Abbott, F., and Rees, A. 1992. Glomerular mesangial cells and inflammatory macrophages ingest neutrophils undergoing apoptosis. *Kidney Int* 42:924-936.
228. Krieser, R.J., and White, K. 2002. Engulfment mechanism of apoptotic cells. *Curr Opin Cell Biol* 14:734-738.
229. Lauber, K., Blumenthal, S.G., Waibel, M., and Wesselborg, S. 2004. Clearance of apoptotic cells: getting rid of the corpses. *Mol Cell* 14:277-287.
230. Moodley, Y., Rigby, P., Bundell, C., Bunt, S., Hayashi, H., Misso, N., McAnulty, R., Laurent, G., Scaffidi, A., Thompson, P., et al. 2003. Macrophage recognition and phagocytosis of apoptotic fibroblasts is critically dependent on fibroblast-derived thrombospondin 1 and CD36. *Am J Pathol* 162:771-779.
231. Devitt, A., Moffatt, O.D., Raykundalia, C., Capra, J.D., Simmons, D.L., and Gregory, C.D. 1998. Human CD14 mediates recognition and phagocytosis of apoptotic cells. *Nature* 392:505-509.
232. Scott, R.S., McMahon, E.J., Pop, S.M., Reap, E.A., Caricchio, R., Cohen, P.L., Earp, H.S., and Matsushima, G.K. 2001. Phagocytosis and clearance of apoptotic cells is mediated by MER. *Nature* 411:207-211.
233. Hanayama, R., Tanaka, M., Miwa, K., Shinohara, A., Iwamatsu, A., and Nagata, S. 2002. Identification of a factor that links apoptotic cells to phagocytes. *Nature* 417:182-187.
234. Nauta, A.J., Daha, M.R., van Kooten, C., and Roos, A. 2003. Recognition and clearance of apoptotic cells: a role for complement and pentraxins. *Trends Immunol* 24:148-154.

235. Brown, S., Heinisch, I., Ross, E., Shaw, K., Buckley, C.D., and Savill, J. 2002. Apoptosis disables CD31-mediated cell detachment from phagocytes promoting binding and engulfment. *Nature* 418:200-203.
236. Somersan, S., and Bhardwaj, N. 2001. Tethering and tickling: a new role for the phosphatidylserine receptor. *J Cell Biol* 155:501-504.
237. Savill, J., Hogg, N., Ren, Y., and Haslett, C. 1992. Thrombospondin cooperates with CD36 and the vitronectin receptor in macrophage recognition of neutrophils undergoing apoptosis. *J Clin Invest* 90:1513-1522.
238. Stern, M., Savill, J., and Haslett, C. 1996. Human monocyte-derived macrophage phagocytosis of senescent eosinophils undergoing apoptosis. Mediation by alpha v beta 3/CD36/thrombospondin recognition mechanism and lack of phlogistic response. *Am J Pathol* 149:911-921.
239. Cortes-Hernandez, J., Fossati-Jimack, L., Carugati, A., Potter, P.K., Walport, M.J., Cook, H.T., and Botto, M. 2002. Murine glomerular mesangial cell uptake of apoptotic cells is inefficient and involves serum-mediated but complement-independent mechanisms. *Clin Exp Immunol* 130:459-466.
240. Mutsaers, S.E., Bishop, J.E., McGrouther, G., and Laurent, G.J. 1997. Mechanisms of tissue repair: from wound healing to fibrosis. *Int J Biochem Cell Biol* 29:5-17.
241. Heidenreich, S., Sato, T., Schmidt, M., August, C., Timmerman, J.J., van Es, L.A., and Daha, M.R. 1997. Induction of mesangial interleukin-6 synthesis by apoptotic U937 cells and monocytes. *Kidney Int* 52:318-328.
242. Fadok, V.A., de Cathelineau, A., Daleke, D.L., Henson, P.M., and Bratton, D.L. 2001. Loss of phospholipid asymmetry and surface exposure of phosphatidylserine is required for phagocytosis of apoptotic cells by macrophages and fibroblasts. *J Biol Chem* 276:1071-1077.
243. Hoffmann, P.R., deCathelineau, A.M., Ogden, C.A., Leverrier, Y., Bratton, D.L., Daleke, D.L., Ridley, A.J., Fadok, V.A., and Henson, P.M. 2001. Phosphatidylserine (PS) induces PS receptor-mediated macropinocytosis and promotes clearance of apoptotic cells. *J Cell Biol* 155:649-659.
244. Fadok, V.A., Bratton, D.L., Rose, D.M., Pearson, A., Ezekewitz, R.A., and Henson, P.M. 2000. A receptor for phosphatidylserine-specific clearance of apoptotic cells. *Nature* 405:85-90.
245. Li, M.O., Sarkisian, M.R., Mehal, W.Z., Rakic, P., and Flavell, R.A. 2003. Phosphatidylserine receptor is required for clearance of apoptotic cells. *Science* 302:1560-1563.
246. Krahling, S., Callahan, M.K., Williamson, P., and Schlegel, R.A. 1999. Exposure of phosphatidylserine is a general feature in the phagocytosis of apoptotic lymphocytes by macrophages. *Cell Death Differ* 6:183-189.
247. Kurosaka, K., Takahashi, M., Watanabe, N., and Kobayashi, Y. 2003. Silent cleanup of very early apoptotic cells by macrophages. *J Immunol* 171:4672-4679.
248. Arur, S., Uche, U.E., Rezaul, K., Fong, M., Scranton, V., Cowan, A.E., Mohler, W., and Han, D.K. 2003. Annexin I is an endogenous ligand that mediates apoptotic cell engulfment. *Dev Cell* 4:587-598.
249. Cortez-Hernandez, Fossati-Jimack, Carugati, Potter, Walport, Cook, and Botto. 2002. Murine glomerular mesangial cell uptake of apoptotic cells is inefficient

and and involves serum-mediated but complementindependent mechanisms. *Clin Exp Immunol* 130:459-466.
250. Hoffman, deCathelineau, Ogden, Leverrier, Bratton, Daleke, Ridley, Fadok, and Henson. 2001. PS induces receptor-mediated macropinocytosis and promotes clearance of apoptotic cells. *JCB* 1555.
251. Voll, R.E., Herrmann, M., Roth, E.A., Stach, C., Kalden, J.R., and Girkontaite, I. 1997. Immunosuppressive effects of apoptotic cells. *Nature* 390:350-351.
252. Fadok, V.A., Bratton, D.L., Konowal, A., Freed, P.W., Westcott, J.Y., and Henson, P.M. 1998. Macrophages that have ingested apoptotic cells in vitro inhibit proinflammatory cytokine production through autocrine/paracrine mechanisms involving TGF-beta, PGE2, and PAF. *J Clin Invest* 101:890-898.
253. Huynh, M.L., Fadok, V.A., and Henson, P.M. 2002. Phosphatidylserine-dependent ingestion of apoptotic cells promotes TGF-beta1 secretion and the resolution of inflammation. *J Clin Invest* 109:41-50.
254. Lan, e.a. 2002. Phosphatidylserine-dependent ingestion of apoptotic cells promotes TGFbeta1 secretion and the resolution of inflammation. *JCI* 109:41-50.
255. Kurosaka, K., Watanabe, N., and Kobayashi, Y. 2002. Potentiation by human serum of anti-inflammatory cytokine production by human macrophages in response to apoptotic cells. *J Leukoc Biol* 71:950-956.
256. Meagher, L.C., Savill, J.S., Baker, A., Fuller, R.W., and Haslett, C. 1992. Phagocytosis of apoptotic neutrophils does not induce macrophage release of thromboxane B2. *J Leukoc Biol* 52:269-273.
257. al, H.e. 1997. Human glomerular mesangial cell phagocytosis of apoptotic neutrophils. *Journal of Immunology* 158:4389-4397.
258. Haugland. Handbook of Fluorescent Probes and Research Products, 9th edition.
259. Wilson, and Walker. Principles and Techniques of Practical Biochemistry, 5th edition.
260. Fraser, D., Brunskill, N., Ito, T., and Phillips, A. 2003. Long-term exposure of proximal tubular epithelial cells to glucose induces transforming growth factor-beta 1 synthesis via an autocrine PDGF loop. *Am J Pathol* 163:2565-2574.
261. Brown, P.D., Wakefield, L.M., Levinson, A.D., and Sporn, M.B. 1990. Physicochemical activation of recombinant latent transforming growth factor-beta's 1, 2, and 3. *Growth Factors* 3:35-43.
262. Cai, L., Li, W., Wang, G., Guo, L., Jiang, Y., and Kang, Y.J. 2002. Hyperglycemia-induced apoptosis in mouse myocardium: mitochondrial cytochrome C-mediated caspase-3 activation pathway. *Diabetes* 51:1938-1948.
263. Moley, K.H., Chi, M.M., Knudson, C.M., Korsmeyer, S.J., and Mueckler, M.M. 1998. Hyperglycemia induces apoptosis in pre-implantation embryos through cell death effector pathways. *Nat Med* 4:1421-1424.
264. Fine, E.L., Horal, M., Chang, T.I., Fortin, G., and Loeken, M.R. 1999. Evidence that elevated glucose causes altered gene expression, apoptosis, and neural tube defects in a mouse model of diabetic pregnancy. *Diabetes* 48:2454-2462.
265. Baumgartner-Parzer, S.M., Wagner, L., Pettermann, M., Grillari, J., Gessl, A., and Waldhausl, W. 1995. High-glucose--triggered apoptosis in cultured endothelial cells. *Diabetes* 44:1323-1327.

266. Mizutani, M., Kern, T.S., and Lorenzi, M. 1996. Accelerated death of retinal microvascular cells in human and experimental diabetic retinopathy. *J Clin Invest* 97:2883-2890.
267. Delaney, C.L., Russell, J.W., Cheng, H.L., and Feldman, E.L. 2001. Insulin-like growth factor-I and over-expression of Bcl-xL prevent glucose-mediated apoptosis in Schwann cells. *J Neuropathol Exp Neurol* 60:147-160.
268. Hall, J.L., Matter, C.M., Wang, X., and Gibbons, G.H. 2000. Hyperglycemia inhibits vascular smooth muscle cell apoptosis through a protein kinase C-dependent pathway. *Circ Res* 87:574-580.
269. Wu, M., Lee, H., Bellas, R.E., Schauer, S.L., Arsura, M., Katz, D., FitzGerald, M.J., Rothstein, T.L., Sherr, D.H., and Sonenshein, G.E. 1996. Inhibition of NF-kappaB/Rel induces apoptosis of murine B cells. *Embo J* 15:4682-4690.
270. Van Antwerp, D.J., Martin, S.J., Kafri, T., Green, D.R., and Verma, I.M. 1996. Suppression of TNF-alpha-induced apoptosis by NF-kappaB. *Science* 274:787-789.
271. Wang, C.Y., Guttridge, D.C., Mayo, M.W., and Baldwin, A.S., Jr. 1999. NF-kappaB induces expression of the Bcl-2 homologue A1/Bfl-1 to preferentially suppress chemotherapy-induced apoptosis. *Mol Cell Biol* 19:5923-5929.
272. al, Y.e. 2002. A shift in the Bax/Bcl2 balance may activate caspase-3 and modulate apoptosis in experimental glomerulonephritis. *Kidney Int* 62:1301-1313.
273. Osterby, R., Schmitz, A., Nyberg, G., and Asplund, J. 1998. Renal structural changes in insulin-dependent diabetic patients with albuminuria. Comparison of cases with onset of albuminuria after short or long duration. *Apmis* 106:361-370.
274. Baker, A.J., Mooney, A., Hughes, J., Lombardi, D., Johnson, R.J., and Savill, J. 1994. Mesangial cell apoptosis: the major mechanism for resolution of glomerular hypercellularity in experimental mesangial proliferative nephritis. *J Clin Invest* 94:2105-2116.
275. Sugiyama, H., Kashihara, N., Makino, H., Yamasaki, Y., and Ota, A. 1996. Apoptosis in glomerular sclerosis. *Kidney Int* 49:103-111.
276. Hoffman, B.B., Sharma, K., Zhu, Y., and Ziyadeh, F.N. 1998. Transcriptional activation of transforming growth factor-beta1 in mesangial cell culture by high glucose concentration. *Kidney Int* 54:1107-1116.
277. Isono, M., Mogyorosi, A., Han, D.C., Hoffman, B.B., and Ziyadeh, F.N. 2000. Stimulation of TGF-beta type II receptor by high glucose in mouse mesangial cells and in diabetic kidney. *Am J Physiol Renal Physiol* 278:F830-838.
278. al, D.e. 2000. Transcriptional regulation of TGFb1 by glucose. *Am J Med Sci* 319:138-142.
279. Hayashida, T., Poncelet, A.C., Hubchak, S.C., and Schnaper, H.W. 1999. TGF-beta1 activates MAP kinase in human mesangial cells: a possible role in collagen expression. *Kidney Int* 56:1710-1720.
280. Hayashida, T., and Schnaper, H.W. 2004. High ambient glucose enhances sensitivity to TGF-beta1 via extracellular signal--regulated kinase and protein kinase Cdelta activities in human mesangial cells. *J Am Soc Nephrol* 15:2032-2041.
281. Ravanti, L., Hakkinen, L., Larjava, H., Saarialho-Kere, U., Foschi, M., Han, J., and Kahari, V.M. 1999. Transforming growth factor-beta induces collagenase-3

expression by human gingival fibroblasts via p38 mitogen-activated protein kinase. *J Biol Chem* 274:37292-37300.
282. Isono, M., Cruz, M.C., Chen, S., Hong, S.W., and Ziyadeh, F.N. 2000. Extracellular signal-regulated kinase mediates stimulation of TGF-beta1 and matrix by high glucose in mesangial cells. *J Am Soc Nephrol* 11:2222-2230.
283. Edlund, S., Landstrom, M., Heldin, C.H., and Aspenstrom, P. 2002. Transforming growth factor-beta-induced mobilization of actin cytoskeleton requires signaling by small GTPases Cdc42 and RhoA. *Mol Biol Cell* 13:902-914.
284. Bhowmick, N.A., Ghiassi, M., Bakin, A., Aakre, M., Lundquist, C.A., Engel, M.E., Arteaga, C.L., and Moses, H.L. 2001. Transforming growth factor-beta1 mediates epithelial to mesenchymal transdifferentiation through a RhoA-dependent mechanism. *Mol Biol Cell* 12:27-36.
285. Sowa, H., Kaji, H., Yamaguchi, T., Sugimoto, T., and Chihara, K. 2002. Activations of ERK1/2 and JNK by transforming growth factor beta negatively regulate Smad3-induced alkaline phosphatase activity and mineralization in mouse osteoblastic cells. *J Biol Chem* 277:36024-36031.
286. Engel, M.E., McDonnell, M.A., Law, B.K., and Moses, H.L. 1999. Interdependent SMAD and JNK signaling in transforming growth factor-beta-mediated transcription. *J Biol Chem* 274:37413-37420.
287. Dai, C., Yang, J., and Liu, Y. 2003. Transforming growth factor-beta1 potentiates renal tubular epithelial cell death by a mechanism independent of Smad signaling. *J Biol Chem* 278:12537-12545.
288. blank.
289. Yoo, J., Ghiassi, M., Jirmanova, L., Balliet, A.G., Hoffman, B., Fornace, A.J., Jr., Liebermann, D.A., Bottinger, E.P., and Roberts, A.B. 2003. Transforming growth factor-beta-induced apoptosis is mediated by Smad-dependent expression of GADD45b through p38 activation. *J Biol Chem* 278:43001-43007.
290. Negulescu, O., Bognar, I., Lei, J., Devarajan, P., Silbiger, S., and Neugarten, J. 2002. Estradiol reverses TGF-beta1-induced mesangial cell apoptosis by a casein kinase 2-dependent mechanism. *Kidney Int* 62:1989-1998.
291. Haslett, C. 1999. Granulocyte apoptosis and its role in the resolution and control of lung inflammation. *Am J Respir Crit Care Med* 160:S5-11.
292. Ren, Y., and Savill, J. 1995. Proinflammatory cytokines potentiate thrombospondin-mediated phagocytosis of neutrophils undergoing apoptosis. *J Immunol* 154:2366-2374.
293. Wolf, G., and Ziyadeh, F.N. 1999. Molecular mechanisms of diabetic renal hypertrophy. *Kidney Int* 56:393-405.
294. Licht, R., Jacobs, C.W., Tax, W.J., and Berden, J.H. 1999. An assay for the quantitative measurement of in vitro phagocytosis of early apoptotic thymocytes by murine resident peritoneal macrophages. *J Immunol Methods* 223:237-248.
295. Sato, Y., Okada, F., Abe, M., Seguchi, T., Kuwano, M., Sato, S., Furuya, A., Hanai, N., and Tamaoki, T. 1993. The mechanism for the activation of latent TGF-beta during co-culture of endothelial cells and smooth muscle cells: cell-type specific targeting of latent TGF-beta to smooth muscle cells. *J Cell Biol* 123:1249-1254.

296. Zhang, X.L., Selbi, W., de la Motte, C., Hascall, V., and Phillips, A. 2004. Renal proximal tubular epithelial cell transforming growth factor-beta1 generation and monocyte binding. *Am J Pathol* 165:763-773.
297. Clayton, A., Evans, R.A., Pettit, E., Hallett, M., Williams, J.D., and Steadman, R. 1998. Cellular activation through the ligation of intercellular adhesion molecule-1. *J Cell Sci* 111 (Pt 4):443-453.
298. Pesce, C., Menini, S., Pricci, F., Favre, A., Leto, G., DiMario, U., and Pugliese, G. 2002. Glomerular cell replication and cell loss through apoptosis in experimental diabetes mellitus. *Nephron* 90:484-488.
299. Huh, H.Y., Lo, S.K., Yesner, L.M., and Silverstein, R.L. 1995. CD36 induction on human monocytes upon adhesion to tumor necrosis factor-activated endothelial cells. *J Biol Chem* 270:6267-6271.
300. Swerlick, R.A., Brown, E.J., Xu, Y., Lee, K.H., Manos, S., and Lawley, T.J. 1992. Expression and modulation of the vitronectin receptor on human dermal microvascular endothelial cells. *J Invest Dermatol* 99:715-722.
301. Stomski, F.C., Gani, J.S., Bates, R.C., and Burns, G.F. 1992. Adhesion to thrombospondin by human embryonic fibroblasts is mediated by multiple receptors and includes a role for glycoprotein 88 (CD36). *Exp Cell Res* 198:85-92.
302. Draude, G., and Lorenz, R.L. 2000. TGF-beta1 downregulates CD36 and scavenger receptor A but upregulates LOX-1 in human macrophages. *Am J Physiol Heart Circ Physiol* 278:H1042-1048.
303. Han, J., Hajjar, D.P., Tauras, J.M., Feng, J., Gotto, A.M., Jr., and Nicholson, A.C. 2000. Transforming growth factor-beta1 (TGF-beta1) and TGF-beta2 decrease expression of CD36, the type B scavenger receptor, through mitogen-activated protein kinase phosphorylation of peroxisome proliferator-activated receptor-gamma. *J Biol Chem* 275:1241-1246.
304. Yevodokimova. 2001. TSP-1 is the key activator of mesangial cells exposed to high glucose. *JASN.*
305. Farhangkhoee, H., Khan, Z.A., Barbin, Y., and Chakrabarti, S. 2005. Glucose-induced up-regulation of CD36 mediates oxidative stress and microvascular endothelial cell dysfunction. *Diabetologia* 48:1401-1410.
306. Sampson, M.J., Davies, I.R., Braschi, S., Ivory, K., and Hughes, D.A. 2003. Increased expression of a scavenger receptor (CD36) in monocytes from subjects with Type 2 diabetes. *Atherosclerosis* 167:129-134.
307. Fischer, U., and Schulze-Osthoff, K. 2005. New approaches and therapeutics targeting apoptosis in disease. *Pharmacol Rev* 57:187-215.
308. Lei, K., Nimnual, A., Zong, W.X., Kennedy, N.J., Flavell, R.A., Thompson, C.B., Bar-Sagi, D., and Davis, R.J. 2002. The Bax subfamily of Bcl2-related proteins is essential for apoptotic signal transduction by c-Jun NH(2)-terminal kinase. *Mol Cell Biol* 22:4929-4942.
309. Fiordaliso, F., Leri, A., Cesselli, D., Limana, F., Safai, B., Nadal-Ginard, B., Anversa, P., and Kajstura, J. 2001. Hyperglycemia activates p53 and p53-regulated genes leading to myocyte cell death. *Diabetes* 50:2363-2375.
310. Du, X., Stocklauser-Farber, K., and Rosen, P. 1999. Generation of reactive oxygen intermediates, activation of NF-kappaB, and induction of apoptosis in

human endothelial cells by glucose: role of nitric oxide synthase? *Free Radic Biol Med* 27:752-763.

311. Furusu, A., Nakayama, K., Xu, Q., Konta, T., Sugiyama, H., and Kitamura, M. 2001. Expression, regulation, and function of inhibitor of apoptosis family genes in rat mesangial cells. *Kidney Int* 60:579-586.
312. Grimm, S., Bauer, M.K., Baeuerle, P.A., and Schulze-Osthoff, K. 1996. Bcl-2 down-regulates the activity of transcription factor NF-kappaB induced upon apoptosis. *J Cell Biol* 134:13-23.
313. McDonald, P.P., Fadok, V.A., Bratton, D., and Henson, P.M. 1999. Transcriptional and translational regulation of inflammatory mediator production by endogenous TGF-beta in macrophages that have ingested apoptotic cells. *J Immunol* 163:6164-6172.
314. al, F.e. 1998. Macrophages that have ingested apoptotic cells in vitro inhibit proinflammatory cytokine production through autocrine/paracrine mechanisms involving TGF-beta, PGE2, and PAF. *JCI* 101.
315. Poncelet, A.C., de Caestecker, M.P., and Schnaper, H.W. 1999. The transforming growth factor-beta/SMAD signaling pathway is present and functional in human mesangial cells. *Kidney Int* 56:1354-1365.
316. Patel, S.R., and Dressler, G.R. 2005. BMP7 signaling in renal development and disease. *Trends Mol Med.*
317. Wang, S., and Hirschberg, R. 2003. BMP7 antagonizes TGF-beta -dependent fibrogenesis in mesangial cells. *Am J Physiol Renal Physiol* 284:F1006-1013.
318. Wang, S., and Hirschberg, R. 2004. Bone morphogenetic protein-7 signals opposing transforming growth factor beta in mesangial cells. *J Biol Chem* 279:23200-23206.